# The age-related reduction in adrenergic response as a limitation of cardiac function in old age

Thesis submitted in accordance with the requirements for the degree of Doctor of Philosophy at the University of Leeds

By

Luke Andrew Howlett

Faculty of Biological Sciences

School of Biomedical Sciences

University of Leeds

October 2022

# Declarations

Some elements of this thesis have been published, submitted for publication, or presented in a conference.

## Publications

Howlett, L.A. and Lancaster, M.K. (2021). Reduced cardiac response to the adrenergic system is a key limiting factor for physical capacity in old age. *Experimental Gerontology*, 150, p. 111339.

Howlett, L.A., Jones, S.A., Lancaster, M.K. (2022). Pharmacy and Exercise as Complimentary Partners for Successful Cardiovascular Ageing. *Current Vascular Pharmacology.* 20 (3), p. 284 – 302.

Howlett, L.A., Kirton, H.M., Al-Owais, M.M., Steele, D. and Lancaster, M.K. (2022). Action potential responses to changes in stimulation frequency and isoproterenol in rat ventricular myocytes. *Physiological Reports.* 10 (2), p.e15166.

## Conferences

Howlett, L.A., Kirton, H., Yang, Z., Al-Owais, M.M., Steele, D., Lancaster, M.K. (2021). Ventricular myocyte action potential responses to adrenergic stimulation and changes in rate. (ePoster). Physiology 2021 (online). The Physiological Society.

Howlett, L.A., Kirton, H., Yang, Z., Al-Owais, M.M., Steele, D., Lancaster, M.K. (2021). The age-related reduction in adrenergic response as a limitation of cardiac function in old age. (ePoster). University of Leeds Postgraduate Symposium, Leeds, UK.

The candidate confirms that the work submitted is his own and that appropriate credit has been given where reference has been made to the work of others.

# Acknowledgements

Firstly, I would like to extend thanks to my supervisors: Dr Matthew Lancaster and Dr Al Benson for their support throughout the project. Specifically, I would like to thank Matthew for helping me develop as a scientist, rapidly bringing me up to speed in the world of cellular cardiology and inspiring a passion for electrophysiology within me. Al, thank you for helping introduce a computational aspect to the project and for making the models easy to navigate for a non-computational student.

I am very grateful to Dr Derek Steele, Dr Hannah Kirton and Dr Zhaokang Yang for allowing me a continuous flow of cardiomyocytes, vital to the project. Hannah and Zhaokang, your continual cooperation and support has been fundamental to the project and to my experimental competence.

I am also grateful to the University of Leeds and the demonstrator studentship which has funded my time here and allowed me the opportunity to obtain demonstrating experience whilst studying for a PhD.

Thanks also to my family and friends who have supported me throughout many cross-country moves to achieve my goals. I am especially grateful to my grandparents Vernon and Veronica Wiseman; you have been persistent cheerleaders of everything I have pursued, and I could not have asked for better role-models.

Most importantly, thank you to my wife and best friend Charlotte. Without your constant support and devotion and willingness to pick me up, I would absolutely never have gotten this far and made such great memories along the way.

# Abstract

A reduction in the efficacy of the beta-adrenergic receptor (βAR) signalling response is thought to be a key component of the reduction in cardiac reserve in old age. However, evidence is far from unanimous regarding dynamic changes in $\beta_1$AR and immediate signalling with ageing. Therefore, changes in downstream effector mechanisms may be responsible for a significant component of the reduced adrenergic response seen in advanced age. At the myocyte level, $\beta_1$AR signalling heavily controls action potential (AP) repolarisation during stress and this, in part, facilitates the ability to follow higher cardiac rates. A large body of evidence has demonstrated that AP repolarisation is prolonged in old age and whilst its response to adrenergic stimulation has been postulated to be reduced in old age, little physiologically relevant evidence exists. This project aimed to: assess the influence of age on ventricular myocyte AP form and response to adrenergic stimulation, explore potential key components responsible for the duration of the AP and thus set minimal stable cycle length of the heart during exercise and finally to modify a recent computational electrophysiological adult rat heart model (Leeds Rat (LR) model) to recreate the AP and AP response to adrenergic stimulation observed in this work and others.

Whole-cell patch-clamp investigations on adult (3 months of age) and old (22 – 23 months of age) ventricular myocytes from male Wistar rat hearts found time to achieve 90 % full repolarisation ($APD_{90}$) prolonged (29 %) in old rats compared with adult rats. Peak L-type $Ca^{2+}$ channel (LTCC) current remained similar with ageing, however the influence of chromanol 293b-sensitive current on late AP repolarisation reduced in old rats compared with adult rats during adrenergic stimulation. Other measures of chromanol 293b-sensitive current (51 - 99 %) alongside the response to adrenergic stimulation also reduced in old rats compared with adult rats. Similarly with ageing, inward rectifying $K^+$ channel ($I_{K1}$) current reduced (> 95 %). Conversely, rapid delayed rectifying $K^+$ channel ($I_{Kr}$) current was greater in old rats compared with adult rats (235 – 467 %) during adrenergic stimulation. Finally, the modified LR (mLR) model was able to reproduce ventricular myocyte APD from adult rats comparable to experimental data at a range of pacing frequencies during basal and adrenergic stimulation conditions.

This work provides novel reference values for future electrophysiological and computational studies alongside the foundation for the development of a computational old rat heart model which will aid understanding of the loss of cardiac reserve in old age. This work also highlights the need for further AP and ion channel investigations at elevated pacing frequencies that more closely emulate a physiological exercise response.

# Table of Contents

# List of Figures and Tables

## Figures

# Tables

# Abbreviations

| | |
|---|---|
| **$\alpha_1$** | Alpha 1 adrenergic receptor |
| **$\alpha_2$** | Alpha 2 adrenergic receptor |
| **AC** | Adenylyl cyclase |
| **ADP** | Adenosine diphosphate |
| **AgCl** | Silver chloride |
| **AKAP** | A-kinase anchoring protein |
| **ANOVA** | Analysis of variance |
| **ANS** | Autonomic nervous system |
| **AP** | Action potential |
| **APD** | Action potential duration |
| **$APD_{25}$** | Time to 25% action potential repolarisation |
| **$APD_{50}$** | Time to 50% action potential repolarisation |
| **$APD_{75}$** | Time to 75% action potential repolarisation |
| **$APD_{90}$** | Time to 90% action potential repolarisation |
| **$APD_{100}$** | Time to 100% action potential repolarisation |
| **ATP** | Adenosine triphosphate |
| **AV** | Atrioventricular |
| **$Ba^+$** | Barium |
| **$BaCl_2$** | Barium chloride |
| **BCL** | Basic cycle length |
| **BIN1** | Bridging integrator-1 |
| **BSA** | Bovine serum albumin |
| **βAR** | Beta adrenergic receptor |

| | |
|---|---|
| **$\beta_1$AR** | Beta 1 adrenergic receptor |
| **$\beta_2$AR** | Beta 2 adrenergic receptor |
| **$\beta_3$AR** | Beta 3 adrenergic receptor |
| **$Ca^{2+}$** | Calcium |
| **$CaCl_2$** | Calcium chloride |
| **CAMKII** | Calcium/ calmodulin-dependent protein kinase II |
| **cAMP** | 3', 5' - Cyclic adenosine monophosphate |
| **CICR** | Calcium-induced calcium release |
| **Cm** | Capacitance |
| **CO** | Cardiac output |
| **CVD** | Cardiovascular disease |
| **DAD** | Delayed-afterdepolarisation |
| **dd$H_2O$** | De-ionised water |
| **DMSO** | Dimethyl sulfoxide |
| **EAD** | Early-afterdepolarisation |
| **ECM** | Extracellular matrix |
| **EDV** | End-diastolic volume |
| **EGTA** | Ethylene glycol-bis(β-aminoethyl ether)-N,N,N′,N′-tetraacetic acid |
| **ERG** | Ether-à-go-go-Related Gene |
| **GDP** | Guanosine diphosphate |
| **$G_i$ protein** | G-inhibitory protein |
| **GPCR** | G-protein receptor |
| **GRK** | G-protein receptor kinase |
| **$G_s$ protein** | G-stimulatory protein |

| | |
|---|---|
| **GTP** | Guanosine triphosphate |
| **HCN** | Hyperpolarisation-activated cyclic nucleotide-gated channels |
| **HERG** | Human Ether-à-go-go-Related Gene |
| **HR** | Heart rate(s) |
| **I** | Current |
| **$I_f$** | Funny current |
| **$I_{Kr}$** | Rapid delayed rectifying potassium channel |
| **$I_{Ks}$** | Slow delayed rectifying potassium channel |
| **$I_{Kur}$** | Ultra-rapid delayed rectifying potassium channel |
| **$I_{K1}$** | Inward rectifying potassium channel |
| **$IP_3$** | Inositol triphosphate |
| **$I_{ss}$** | Steady-state potassium channel |
| **$I_{to}$** | Transient outward channel |
| **JP2** | Junctophilin 2 |
| **$K^+$** | Potassium ion |
| **$K_{ATP}$** | ATP-sensitive potassium channel |
| **KCl** | Potassium chloride |
| **KCNE1** | Beta subunit for $Ik_s$ |
| **KCNQ1** | Alpha subunit for $Ik_s$ |
| **$KHCO_3$** | Potassium bicarbonate |
| **$KH_2PO_4$** | Potassium monophosphate |
| **KOH** | Potassium hydroxide |
| **LR** | Leeds Rat (Model) |
| **LTCC** | L-type calcium channel |

| | |
|---|---|
| **LV** | Left ventricle/ ventricular |
| **$M_2$** | Muscarinic type two receptor |
| **$MgCl_2$** | Magnesium chloride |
| **$MgSO_4$-$7H_2O$** | Magnesium sulfate heptahydrate |
| **mLR** | Modified Leeds Rat Model |
| **mRNA** | Messenger ribonucleic acid |
| **n** | Denotes cell number |
| **N** | Denotes animal number |
| **$Na^+$** | Sodium |
| **NaCl** | Sodium chloride |
| **$NaHCO_3$** | Sodium bicarbonate |
| **$NaH_2PO_4$** | Sodium monophosphate |
| **NaOH** | Sodium hydroxide |
| **NCX** | Sodium-calcium exchanger |
| **PDE** | Phosphodiesterase |
| **PKA** | Protein kinase A |
| **PKC** | Protein kinase C |
| **PLC** | Phospholipase C |
| **PLN** | Phospholamban |
| **PNS** | Parasympathetic nervous system |
| **RV** | Right ventricle/ ventricular |
| **RYR2** | Ryanodine type 2 receptor |
| **SAN** | Sino-atrial node |
| **SD** | Standard deviation |

| | |
|---|---|
| **SEM** | Standard error of the mean |
| **SERCA2a** | Sarcoplasmic/endoplasmic reticulum calcium ATPase |
| **SNS** | Sympathetic nervous system |
| **SR** | Sarcoplasmic reticulum |
| **SV** | Stroke volume |
| **$Tn_c$** | Troponin C |
| **$Tn_i$** | Troponin I |
| **T-tubule** | Transverse tubule |
| **$\dot{V}O_{2max}$** | Maximum rate of oxygen consumption |

# Chapter 1: Introduction

## 1.1 The Impact of Ageing

Ageing is associated with many physiological changes that limit organ function and in turn, whole-body function (Niccoli and Partridge, 2012; Santulli and Iaccarino, 2013). After maturation, ageing coincides with miniscule adaptations, which over a life span, may accumulate to moderate or large-scale alterations and increase overall disease risk (Niccoli and Partridge, 2012; Santulli and Iaccarino, 2013). In research, adults are defined as ≥ 18 years of age and aged or old individuals are ≥ 65 years of age in humans (Tellez et al., 2011). In rat models, adults are defined as approximately 3 - 6 months of age and aged or old individuals are defined as approximately ≥ 20 - 24 months of age; commonly acknowledged to represent the equivalent of adult and old age in humans (Tellez et al., 2011).

Advanced age is associated with increased inflammation, a loss of regenerative cells, poorer regenerative capacity, neurodegeneration, changes in hormone regulation and reduced immune responses (Niccoli and Partridge, 2012; Barnes et al., 1982; Fleg et al., 1985). The underlying mechanisms of age-related alterations are not completely clear due to the wide variety of factors involved. Interest in ageing-related research has increased in recent years in response to the declining health span: lifespan ratio (Ferrara et al., 2014; Mathers et al., 2015). Concern exists regarding the greater percentage of older individuals predicted in society in the coming years. By 2038, approximately a quarter of the UK population is predicted to be over 65 years of age compared with just one in six in 1998 according to the *Office for National Statistics* (Randall, 2017). This may be problematic for healthcare providers as an older population will increase demand on already strained services.

### 1.1.1 Age-Related Deterioration of the Heart

Amongst the vast number of age-related changes, changes in heart structure and function present a key figure in the ageing phenomenon. Throughout a lifespan the heart undergoes continual adaptation with ‘normal ageing’ alongside the typical influences of lifestyle and environment (De Lucia et al., 2018; Ferrara et al., 2014; Maron and Pelliccia, 2006). These changes can be physiological as well as

pathological. Physiological adaptation normally consists of improved or maintained efficiency and function, whilst reductions in function and increased risk of abnormality and disease are the hallmark of pathological adaptation (Pluim et al., 2000; Steenman and Lande, 2017). For example, exercise training, dependent on modality, can stimulate physiological increases in wall thickness and cavity size of both atria and ventricles to enhance myocardial performance and efficiency in response to volume and pressure overload (Morganroth et al., 1975; Weiner and Baggish, 2012; Maron and Pelliccia, 2006). Conversely, poor vascular health, sedentariness, hypertension and disease may contribute to persistent high diastolic filling pressure, whereby stimulation of mechanotransduction and neuro-hormonal mechanisms caused by repeated myocardial wall stretch or load can trigger pathological increases in wall thickness (Shimizu and Minamino, 2016). Normal ageing is essentially a gradual development toward a pathological state. Whilst age-related changes do not cause pathology, it can increase the risk of its onset. At global organ level, ageing is associated with reductions in contractile velocity, early diastolic filling, myocardial relaxation, maximum heart rate (HR) and response to stress, cardiac reserve and automaticity (Parashar et al., 2016; Roh et al., 2016; Stratton et al., 2003; Keller and Howlett, 2016; De Lucia et al., 2018; Ferrara et al., 2014). Ageing is also linked to myocardial hypertrophy, predominantly via increases in ventricular wall thickness as well as increased fibrosis from modifications in extracellular matrix (ECM) (Trial and Cieslik, 2018). At a cellular level, the aged heart shows a reduction in myocyte density, sino-atrial node (SAN) function, intracellular calcium ($Ca^{2+}$) release and sequestration, action potential (AP) repolarisation and adrenergic signalling (Liu et al., 2000; Jiang and Narayanan, 1990; Saeed et al., 2018; Moghtadaei et al., 2016; Strait and Lakatta, 2012; Keller and Howlett, 2016; De Lucia et al., 2018; Ferrara et al., 2014; Rengo et al., 2012; Spadari et al., 2018; Santulli and Iaccarino, 2016). Increases in cell size, type 1 collagen deposition and arrhythmia risk are also common age-related cellular augmentations (Lakatta, 1993; Meschiari et al., 2017).

The above-mentioned changes prevalent with advanced age can significantly impede function, increase cardiovascular disease (CVD) risk and lower the threshold for CVD occurrence (Mathers et al., 2015). The prevalence of CVD in society may, in part, underlie mounting interest in age-related and age-disease interaction research. Cardiovascular disease is a leading cause of mortality globally, accounting for

approximately 45 % of all European deaths and amounting to costs of an estimated €210 billion per year (Wilkins et al., 2017). Cardiovascular disease rates have actually dropped slightly in recent years after rapid inclines over previous decades prior to the 21st century (Andersson and Vasan, 2018; Wilkins et al., 2017). However, high levels of drug and alcohol abuse, inactivity and obesity, prevalent in young adults may lead to a future rise in CVD-related incidents (Andersson and Vasan, 2018). Irrespective of its potential relevance to CVD, ageing alone is a significant issue in global health. As a result of the numerous age-related cardiac alterations, performance of daily activities, overall physical activity and exercise can become constrained due to reductions in the dynamic range of cardiac output (CO) and thus weakened ability to respond to increments in cardiorespiratory demand (Stratton et al., 1992; Stratton et al., 1994). This can severely limit health and quality of life in old individuals (Ferrara et al., 2014; Najafi et al., 2016). In 2015 approximately 5 % of the UK population reported difficulty in the performance of a minimum of one essential daily activity (stairclimbing or dressing) (Wittenberg et al., 2018). Further, physical capacity and mobility is believed to become impaired by a degree of 11 – 30 % in the last quarter of lifespan when compared with young adults (< 30 years of age) (Ferrucci et al., 2016; Rikli and Jones, 1998; Milanović et al., 2013).

## 1.2 Influence of Ageing on HR: Alterations in the Rate Aspect of CO

At the global level, factors contributing to autonomic innervation, contractility, diastolic filling, afterload, HR and stroke volume (SV) have all been implicated in the age-related reduction of CO and the reduction of its dynamic range (Vincent, 2008; Roh et al., 2016; Parashar et al., 2016). Basal HR is controlled by the autonomic nervous system (ANS) alongside intrinsic mechanisms. When subject to stress or increases in stress intensity the sympathetic nervous system (SNS) is predominantly responsible for HR modulation. Modulation of HR by the SNS under stress is attained through augmenting components of the coupled clock mechanism, understood to facilitate SAN cell function (Lakatta et al., 2010). Research investigating the influence of ageing on HR has found that resting HR is largely unaffected by advancing age despite declining intrinsic HR as a result of a compensatory increase in ANS control (Moghtadaei et al., 2016; Strait and Lakatta, 2012; Christou and Seals, 2008).

However, HR performance during exercise is understood to deteriorate (Carter et al., 2003; Flaatten et al., 2018). Poorer maximum HR, HR recovery and response to adrenergic stimulus are hallmark age-related changes in myocardial function and in part explain the loss of CO provision during exercise (Carter et al., 2003; Flaatten et al., 2018). Restricted HR performance and attrition of maximum CO with ageing may be a result of changes, partially, in the SAN coupled clock mechanism and its relationship to the adrenergic signalling mechanism (Liu et al., 2014; Christou and Seals, 2008).

## 1.3 Influence of Ageing on SV: Alterations in the Inotropic Aspect of CO

As mentioned previously SV is a major contributor to CO and has unsurprisingly been implicated in its age-associated reduction (Vincent, 2008; Roh et al., 2016; Parashar et al., 2016). Stroke volume has been suggested to have equal or even greater responsibility than HR for adjusting CO response to exercise and changes in exercise intensity, particularly during strenuous exercise bouts in old age (Stratton et al., 2003; Roh et al., 2016). One study in humans reported a reduction in CO of approximately 21 – 25 % and a reduction of 25 – 41 % in maximal oxygen uptake ($\dot{V}O_{2max}$) in aged (~ 63 years of age) compared with young adults (~ 27 years of age) (Ogawa et al., 1992). This study found reduced oxygen extraction and maximum HR were responsible for approximately half of the decrease in $\dot{V}O_{2max}$, with the age-related decline in SV alone responsible for the other half (Ogawa et al., 1992). Furthermore, the decreased SV in aged adults was also displayed to account for ~ 66 % of the loss in CO with ageing, whilst only ~ 25 % was related to a drop in maximum HR (Ogawa et al., 1992). This suggests SV and associated inotropic changes may have the dominant role in the age-related loss of CO range and physical capacity.

Changes in SV or ventricular contractility at the cellular level with ageing are very complex and implicate a number of mechanisms in the age-related deterioration of ventricular function and thus CO reserve during exercise, with adrenergic signalling response a prominent mechanism involved (Fares and Howlett, 2010; Feridooni et al., 2015; Ferrara et al., 2014; Fields et al., 2016). However the underlying mechanism is not currently clear (Tanaka and Seals, 2008). At the global functioning level, age-related modifications of SV are less unanimous than the limitations in HR described

previously (Fleg et al., 1985; Ogawa et al., 1992; Rodeheffer et al., 1984; Roh et al., 2016; Stratton et al., 1994). Some research has stated resting SV and SV response to maximal (running, cycling) exercise does not change with age in humans (21 - 96 years of age) (Fleg et al., 1995; Feridooni et al., 2015; Fleg et al., 1994). Whilst a further study, this time investigating the response to isoproterenol, in young (24 - 32 years of age) and old (60 – 82 years of age) humans also yielded a statistically similar change in SV between age groups (Stratton et al., 1992). In contrast, one study found resting SV significantly declines in humans with ageing (19 - 32 years of age vs 45 - 58 years of age) and appears to vary with gender (male: ~ 20 % vs female: ~ 10 %) (Nio et al., 2017). This reduction in SV coincided with a decrease in resting CO (male: ~ 18 % vs female: ~ 11 %) and unchanged resting HR (Nio et al., 2017). The reduction of resting SV in ageing was also supported in another study, which reported a reduction of ~ 18 % in old (≥ 65 years of age) compared with young adults (21 - 34 years of age) (Fujimoto et al., 2012). A further study reported reductions of 25 % and 10 % in CO and SV during peak exercise respectively in ageing humans (≤ 40 vs ≥ 60 years of age) (Agostoni et al., 2017). Such changes in maximal cardiac parameters have been documented elsewhere in literature (Tanaka and Seals, 2008).

One study investigating age-related changes in cardiac function and response to maximal supine cycling exercise found aged humans (> 60 vs 18 - 32 years of age), exhibited reduced basal SV index (~ 21 %), cardiac index (~ 22 %) and end-diastolic volume (EDV; ~ 21 %) index compared with their younger counterparts (Stratton et al., 1994). The response to exercise in HR (old: 105 % vs young: 166 %) and cardiac index (old: 135 % vs young: 189 %) decreased with ageing (Stratton et al., 1994). Conversely, SV index response to exercise remained statistically similar with ageing (young: 6 % vs old: 14 %) (Stratton et al., 1994). This might be indicative of HR limitation as primarily responsible for poorer CO responses in aged populations. However previous literature has suggested SV changes in aged individuals are predominantly modulated by the *Frank-Starling mechanism* as opposed to SNS and adrenergic mechanisms (Nakou et al., 2016; Cheitlin, 2003; Ferrara et al., 2014). Therefore, this would suggest that aged hearts depend more greatly on diastolic filling to facilitate improved CO during response to stress. This phenomenon may be supported in the findings of the above study (Stratton et al., 1994) which reported a significantly greater EDV index response (~ 8 %) in aged (> 60 years of age) compared

with young (18 - 32 years of age) humans (~ -10 %) (Stratton et al., 1994). The paradoxical alterations evidenced by positive and negative changes yielded in old and young subjects respectively may aid the validation of this suggested change in modulatory mechanisms. The underlying mechanism explaining this shift in CO provision is not clear. However, age-related changes in HR have been postulated to, in part, influence compensatory changes in SV to reduce the deficit of declining CO with age (Rodeheffer et al., 1984). The change in the mechanism modulating CO response to stress and exercise may also be a clear sign of the age-related breakdown of efficient adrenergic signalling (Howlett and Lancaster, 2021).

In support of the above notion, a study investigated age-related cardiac function in humans (28 - 72 years of age) at rest and during maximal cycling exercise, with and without adrenergic blockade (Fleg et al., 1994). During rest, participants subject to adrenergic blockade exhibited reduced HR and cardiac index and increased EDV index compared with the control group (Fleg et al., 1994). Interestingly, during exercise, younger subjects in the adrenergic blockade group displayed greater reductions in HR compared with old adrenergic blockade counterparts (Fleg et al., 1994). Greater increments in SV index and EDV index were also displayed in young compared with old in the adrenergic blockade group (Fleg et al., 1994). Such changes appear to mimic common age-related limitations in cardiac function described in literature (Parashar et al., 2016; Roh et al., 2016; Stratton et al., 2003; Keller and Howlett, 2016; De Lucia et al., 2018; Ferrara et al., 2014). The apparent loss of blocking sensitivity may indeed indicate a loss of efficiency in adrenergic modulation of CO-related components with ageing.

## 1.4 Excitation-Contraction Coupling

Excitation-contraction coupling is a process that involves the transduction of muscle contraction from electrical activity. This process relies on efficient activation and function of ion channels, enzymes, proteins, transporters, and myofilament synergy in response to AP propagation.

### 1.4.1 Excitation-Contraction Coupling in the Young Healthy Heart

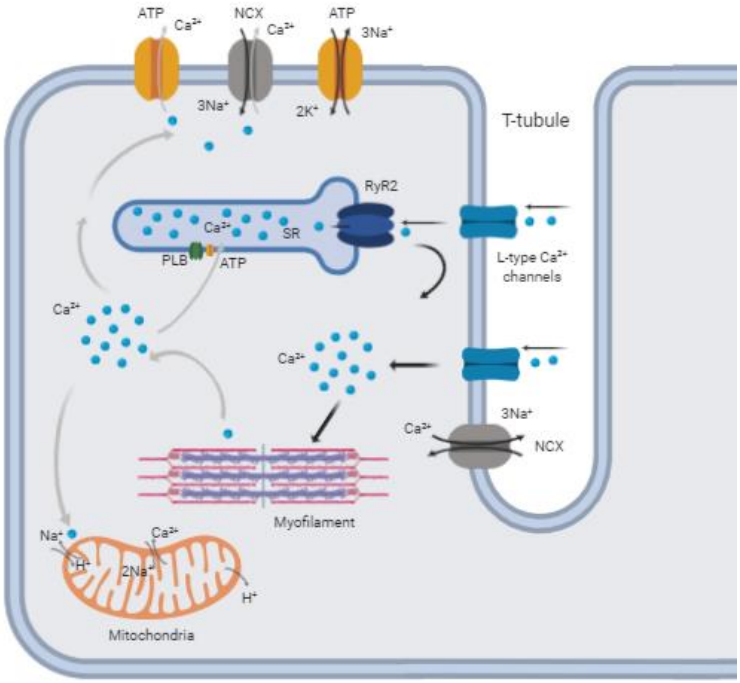


Figure 1. Normal excitation-contraction coupling in a ventricular myocyte (adapted from Bers (2002)) (Bers, 2002). Solid black arrows display normal excitation-contraction coupling during contraction, whilst solid grey arrows reflect relaxation. Image created with BioRender.

The heart relies on excitation-contraction coupling to meet cardiovascular demands (figure 1). In ventricular myocytes at rest, this process begins with the opening of L-type $Ca^{2+}$ channels (LTCC) after depolarisation triggered by an AP (Mayourian et al., 2018a). L-type $Ca^{2+}$ channels allow $Ca^{2+}$ to enter the cell, triggering instantaneous $Ca^{2+}$ release from the sarcoplasmic reticulum (SR) via ryanodine type 2 receptors (RyR2), dramatically increasing intracellular $Ca^{2+}$ and facilitating $Ca^{2+}$ binding to troponin C ($Tn_c$) (Bers, 2002; Mayourian et al., 2018a). This stimulates a change in myofilament complex and leads to troponin I ($Tn_i$) exposing actin binding sites, where myosin heads utilise myosin adenosine tri-phosphatase (ATPase) to bind to actin sites and move the thin filament (Gambardella et al., 2017). Adenosine tri-phosphate (ATP) hydrolysis supplies the energy to facilitate the subsequent sarcomere shortening, which instigates muscle contraction (Mayourian et al., 2018a). Muscle relaxation occurs during reductions in intracellular $Ca^{2+}$, leading to the unbinding of $Ca^{2+}$ and $Tn_c$ (Gambardella et al., 2017). The intracellular $Ca^{2+}$ reduction occurs through several different pathways: activation of sarco/endoplasmic reticulum ATPase (SERCA2a),

activation of sodium-calcium exchange units (NCX) and activation of sarcolemmal $Ca^{2+}$ ATPase (Bers, 2002) (figure 1). This excitation-contraction coupling process can be altered by stressors such as age and exercise as well as disease (Gambardella et al., 2017; Bers, 2002; Xiao et al., 1994).

## 1.4.2 Age-related Changes in Excitation-Contraction Coupling

### 1.4.2.1 SAN

Table 1. Sino atrial node changes with ageing (Behar and Yaniv, 2017; Boyett et al., 2000; Choudhury et al., 2015; Christou and Seals, 2008; Huang et al., 2007; Jones et al., 2004; Larson et al., 2013; Liu et al., 2014; Moghtadaei et al., 2016; Stuart et al., 2018; Tellez et al., 2011). Table adapted and reprinted from (Howlett and Lancaster, 2021). ↑ Indicates an increase; ↔ indicates no change; ↓ indicates a reduction.

| SAN | | |
|---|---|---|
| Global | Cellular | Subcellular |
| Basal HR ↔ | Basal APD ↑ | $I_f$ Current Density ↓ |
| Intrinsic HR ↓ | Intrinsic AP Firing ↓ | LTCC Response to Stress ↔ |
| Maximum HR ↓ | Maximum AP Firing ↓ | $I_f$ Current Response to Stress ↔ |
| HR Response to Stress ↓ | $Ca^{2+}$ Transient Magnitude ↓ | T-Type $Ca^{2+}$ Current Response to Stress ↔ |
| | $Ca^{2+}$ Transient Duration ↑ | RyR2 Expression ↓ |
| | CICR ↓ | SERCA2a Expression ↑↓ |
| | | HCN2 and HCN4 ↓ |
| | | $Connexin_{43}$ expression ↓ |

Existing literature has shown significant reductions in SAN recovery velocity (27 %) in aged compared with adult mice (23 vs 3 months of age) (Moghtadaei et al., 2016) alongside large age-related (2 - 3 vs 21 - 24 vs 28+ months of age) decreases in funny current ($I_f$) density (34 – 52 %) (Larson et al., 2013). Deterioration of $I_f$ current with ageing has been linked with remodelling of hyperpolarisation-activated cyclic nucleotide-gated (HCN) channels (Huang et al., 2007; Larson et al., 2013) with studies

in aged rats (30 months of age vs 1 month of age) demonstrating a decline in HCN2 (~ 51 %) and HCN4 (61 %) expression (Huang et al., 2007; Larson et al., 2013), which has been associated with declining intrinsic HR (Larson et al., 2013; Liu et al., 2014). Such alterations in the most prominent HCN isoforms in the heart (Zhang et al., 2009) may prolong diastolic depolarisation, influence $Ca^{2+}$ transient dynamics and in turn, action potential duration (APD). In addition, the amalgamation of: wide-scale reductions in $connexin_{43}$ (> 90 %), alterations in collagen deposition, gap junction remodelling and the disparity in declining SAN cell number with increased SAN hypertrophy throughout ageing may disturb the velocity and efficiency of signal conduction velocity, by impairing SAN impulse drive, increasing risk of pacemaker dysfunction and arrhythmogenesis in aged individuals (Jones et al., 2004; Lakatta, 1993; Meschiari et al., 2017; Jones et al., 2007; Larson et al., 2013; Fontes et al., 2012; Howlett and Lancaster, 2021). It is also plausible that disturbed signal conduction velocity may limit exercising HR (Lakatta, 1993; Meschiari et al., 2017).

Remodelling of SAN cells with advancing age can also be associated with changes in LTCC, RyR2, SERCA2a and phospholamban (PLN) alongside phosphorylation by protein kinase A (PKA) during adrenergic stimulation (Jones et al., 2007; Liu et al., 2014; Larson et al., 2013). Previous studies have found significant reductions in LTCC expression (20 – 45 %) (Jones et al., 2007) in ageing guinea pigs (1 vs 18 vs 28 vs 38 months of age). Decreased LTCC expression in SAN cells adversely affect intracellular $Ca^{2+}$ influx, which may be linked to the impaired $Ca^{2+}$ cycling associated with ageing (Roh et al., 2016), by contributing to reduced $Ca^{2+}$-induced $Ca^{2+}$ release (CICR) from the SR.

Further studies investigating the coupled clock mechanism in ageing have often reported deteriorated $Ca^{2+}$ release units and altered $Ca^{2+}$ transporters (Roh et al., 2016). A study on ageing mice (2 - 4 vs 20 - 27 months of age) found reductions of 38 % and 23 % in CICR and $Ca^{2+}$ transient amplitude in old compared with young adult mice respectively (Liu et al., 2014). This study also yielded concomitant increases in $Ca^{2+}$ transient duration (57 %) in aged compared with young adult mice (Liu et al., 2014). These findings have been supported in other studies (Table 1) (Behar and Yaniv, 2017; Choudhury et al., 2015). The above changes may be partly responsible for the increased APD in SAN cells associated with advanced age (Tellez et al., 2011; Boyett et al., 2000; Howlett and Lancaster, 2021). Such changes in $Ca^{2+}$ cycling are

considered to be a result of RyR2 and SERCA2a remodelling, where reductions in expression of approximately 90 % and 30 % have been observed in aged mice SAN cells (3 vs 24 months of age) respectively (Liu et al., 2014). Abundance of SAN RyR2 mRNA has also been found to reduce in old rats (25 months of age vs 3 months of age) (~ 5-fold) (Tellez et al., 2011). However, in contrast to the previous study (Liu et al., 2014), this study displayed a 10 % increase in SAN SERCA2a mRNA in aged rats (Tellez et al., 2011).

Respective inhibition of $Ca^{2+}$ release units and $Ca^{2+}$ transporters with selective blocking agents within SAN cells has also been found to alter with ageing (Liu et al., 2014). Selective block of RyR2 in adult mice has been found to achieve an approximate 60 % reduction in spontaneous SAN beating rate compared with > 90 % in aged mice (Liu et al., 2014). Aged mice showed a similarly increased sensitivity to SERCA2a block, exhibiting SAN beating rate abnormalities or a complete reduction compared with a 38 % beating rate reduction in adult mice (Liu et al., 2014). An increase in selective blocking sensitivity could demonstrate a greater reliance on SERCA2a in old age and may reflect a greater vulnerability to rate-dependent limitations.

The combined literature discussed above describe several components of the SAN coupled clock mechanism as casualties of the ageing phenomenon and appear to support a shift in the functional range of many key components. These changes may underlie the declining upper limit in HR range, contributing to poorer responses to stress which are likely amplified by less efficient adrenergic signalling.

#### 1.4.2.2 Atria

A study investigating LTCC changes in ageing canine (2 - 2.5 years of age vs > 8 years of age) left atria (2000 ms cycle length) found decreased AP plateau potential (~ 48 %) and increased time to 90 % repolarisation ($APD_{90}$) (~ 6 %) in aged canines compared with young canines (Gan et al., 2013). Peak LTCC current reduced by approximately 43 % in old canines compared with young canines and was accompanied by an approximate 50 – 55 % decrease in $Ca_v1.2$ mRNA and protein (Gan et al., 2013). The reductions in LTCC structure and function support the age-related decrease in AP plateau potential and increased $APD_{90}$. However, such changes in AP waveform may also be contributed to by changes in rectifying potassium ($K^+$)

currents and changes in $Ca^{2+}$: $K^{+}$ channel ratios. Similarly, a study investigating human right atrial LTCC changes with ageing (young: < 55 years of age vs middle aged: 55 - 75 years of age vs old: > 75 years of age) displayed reduced peak LTCC current (50 %) as well as delayed fast (~ 31 %) and slow (~ 39 %) inactivation of the LTCC current (Herraiz et al., 2013). This study also reported a reduction in SR $Ca^{2+}$ content (~ 28 %) in old compared with young adults (Herraiz et al., 2013). The reduced SR $Ca^{2+}$ content and delayed LTCC inactivation is likely a result of age-related reductions in SERCA2a, evidenced in this study through declining protein levels in aged compared with young adults (Herraiz et al., 2013). The degradation of LTCC, SR content and SERCA2a depict a declining ability within atrial myocytes to cycle $Ca^{2+}$. Such changes coupled with negative AP waveform alterations in the atria, likely contribute to myocardial performance limitations during stress or exercise as well as increased arrhythmia risk with advancing age, particularly due to the increased workload of the atria because of the age-related modifications in myocardial filling and pressure (Ai, 2015).

#### 1.4.2.3 Ventricles

Table 2. Ventricular changes with ageing (Agostoni et al., 2017; Christou and Seals, 2008; Feridooni et al., 2015; Fleg et al., 1995; Fleg et al., 1994; Fujimoto et al., 2012; Jiang and Narayanan, 1990; Josephson et al., 2002; Lim et al., 1999; Liu et al., 2000; Moghtadaei et al., 2016; Nio et al., 2017; Ogawa et al., 1992; Pan et al., 2016; Slack et al., 2001; Strait and Lakatta, 2012; Stratton et al., 1992; Stratton et al., 1994; Walker et al., 1993; Welsh et al., 2002; Xiao et al., 1994; Xu and Narayanan, 1998; Zhou et al., 1998; Zhu et al., 2005). Table adapted and reprinted from (Howlett and Lancaster, 2021). ↑ Suggests an increase; ↔ suggests no change; ↓ suggests a reduction.

| Ventricle | | |
|---|---|---|
| Global | Cellular | Subcellular |
| Basal SV ↓↔ | APD ↑ | LTCC Peak Current ↑↓↔ |
| SV Response to Stress ↓↔ | AP Amplitude ↓ | LTCC Current Inactivation ↓ |
| EDV ↓ | $Ca^{2+}$ Spark Magnitude ↓ | LTCC current Response to Stress ↓ |
| CO ↓ | $Ca^{2+}$ Spark duration ↓ | NCX Expression ↓ |
| | $Ca^{2+}$ Frequency ↑ | RyR2 Expression ↔ |
| | $Ca^{2+}$ Transient Response to Stress ↓↔ | SERCA2a Expression ↓↔ |
| | Contractile Response to Stress ↓↔ | PLN Expression ↑↔ |
| | SR $Ca^{2+}$ Loading ↓ | SERCA2a : PLN Ratio ↓ |
| | | $Tn_i$ Expression ↓ |

Existing research, though mixed, generally suggests raw peak LTCC current increases with age, but such increases are offset by age-related myocyte hypertrophy; thus values relative to cell capacitance remain similar, whilst channel inactivation is slower in old age (Table 2) (Zhou et al., 1998; Josephson et al., 2002; Howlett and Lancaster, 2021). A study in rats (young: 3 months of age vs adult: 6 - 8 months of age vs old: 24 months of age) found peak LTCC current increased (94 – 104 %) in old compared with adult and young rat ventricles (Josephson et al., 2002). This study also found slower (137 %) LTCC inactivation in old compared with young rats (Josephson et al., 2002). The age-related LTCC changes in this study were linked to alterations in gating, whereby open probability and channel availability were greater in aged rats (Josephson et al., 2002). Such changes support the age-related prolongation of APD (Zhou et al., 1998) and compensate for poorer diastolic filling by aiding prolonged contractions. In contrast, another study using rat ventricles demonstrated age-related (6 vs > 27 months of age) reductions in peak LTCC current (14 – 15 %) whilst slow LTCC inactivation reduced once more (Liu et al., 2000). This study also yielded an increase in basal $APD_{90}$ (54 %) and a reduction in AP amplitude (9 %) in old compared with young rats (Liu et al., 2000). A further study found unchanged peak LTCC currents, when normalised to cell size, and similarly reported slower LTCC inactivation rates in old (21 - 25 months of age) compared with young (2 - 3 months of age) rat ventricles (Walker et al., 1993). The contrasting literature in age-related

peak LTCC current changes creates difficulty in interpretation. Differences in species and strain (Wistar vs Fisher vs Long-Evans), alongside patch-clamp technique may, in part, explain the mixed findings. For instance, the use of single channel techniques in one study may lead to an overestimation or underestimation of values, as the current density relative to the area of membrane subject to the patch-clamp cannot be accounted for (Josephson et al., 2002). The age-associated increase (43 %) in active $Ca^{2+}$ channels per patched membrane may also support this (Josephson et al., 2002). The overall suggested maintenance of LTCC peak current with ageing described above, when coupled with the hallmark reduction in contractility in advanced age, could be indicative of a loss in coupling efficiency and lead to a disparity in $Ca^{2+}$ entry and CICR in old age. On the other hand, the unanimous agreement of poorer LTCC inactivation in research has highlighted its potential involvement in basal age-related APD prolongation (Zhou et al., 1998). Combined, this could trigger vulnerability under stress and vulnerability to arrhythmia development.

Further investigations in ventricular intracellular $Ca^{2+}$ cycling have displayed reductions in $Ca^{2+}$ spark magnitude (~ 5 %) and duration (~ 6 %) but enhanced spark frequency (~ 91 %) in old compared with adult rats (24 vs 6 months of age) (Zhu et al., 2005). Age-related changes in RyR2 gating, evidenced by increased channel open probability (157 %) and decreased average open (~ 76 %) time in aged rats support these changes (Zhu et al., 2005). This study also found a significant age-related reduction in SR $Ca^{2+}$ loading (~ 30 %) (Zhu et al., 2005). No changes in PLN and RyR2 expression were found, yet SERCA2a expression demonstrated a significant decrease in aged compared with adult rats (Zhu et al., 2005). Despite a lack of age-related changes in RyR2 expression, aged hearts exhibited greater sensitivity to increasing extracellular $Ca^{2+}$ concentrations. Together, this may support the previous suggestion of a breakdown in LTCC: RyR2 coupling and such aberrant $Ca^{2+}$ handling likely becomes problematic when stress / demand requires an upregulation in function. In another study, no differences were found in RyR2, SERCA2a and PLN expression between young (6 - 8 months of age) and old (26 - 28 months of age) rat ventricles (Xu and Narayanan, 1998). Conversely, a study using mice (5 vs 24 vs 34 months of age), found significantly reduced NCX expression (37 – 58 %), significantly increased PLN expression (158 – 340 %) and unchanged SERCA2a expression in aged (24 months of age) and senescent (34 months of age) left ventricular (LV) tissue compared

with adult (5 months of age) counterparts (Lim et al., 1999). Overall, the SERCA2a: PLN ratio was reduced in old and senescent mice ventricles by 68 – 69 % (Lim et al., 1999). In terms of whole-heart function, this study highlighted an age-related impairment in myocardial relaxation, but maintained contractility (Lim et al., 1999). In this study the reduction in relaxation was evident from increased LV end-diastolic pressure and increased $Ca^{2+}$ transient duration (Lim et al., 1999). Whilst a further study in ageing mice (3 vs 6 vs 12 vs 18 vs 24 months of age) demonstrated no changes in SERCA2a expression, PLN or calsequestrin between old and young ventricles (Slack et al., 2001). Such age-related remodelling in SERCA2a: PLN balance is linked to impaired relaxation through the associated prolongation of $Ca^{2+}$ transient and subsequent decay (Lim et al., 1999).

Research focusing on the myofilament complex within ageing ventricles is scarce. One of the only studies to our knowledge investigating age-related $Tn_i$ changes was completed in mice (Pan et al., 2016). This study found reductions in $Tn_i$ protein and mRNA levels (30 – 40 %; 25 – 30 %) in aged compared with young mice ventricles (18 vs 3 months of age) (Pan et al., 2016). Similarly, a study in humans (25 – 79 years of age) reported a 7 – 8-fold reduction of $Tn_i$ concentration in old (> 35 years of age) compared with young human LV (< 35 years of age) (Welsh et al., 2002). Reductions in $Tn_i$ can negatively affect myocyte relaxation and significantly contribute to diastolic function impairments, which are known to occur in old individuals (Pan et al., 2016).

Overall, age-related changes in ventricular LTCC suggest peak current likely remains unchanged whilst inactivation slows with increasing age (Table 2). Calcium transient frequency increases, whilst transient duration and magnitude both decline throughout ageing and is in-line with age-related remodelling of RyR2 gating. In addition, SERCA2a: PLN ratio as well as $Tn_i$ levels deteriorate in old age compared with young or adult ventricles. Such changes describe an age-related deterioration of efficient intracellular $Ca^{2+}$ cycling, including $Ca^{2+}$ influx, CICR, $Ca^{2+}$ removal, SR loading and myofilament relaxation, which likely, in part, explain widely documented prolongation of APD and myocyte contraction and increased risk of $Ca^{2+}$-induced injury. This array of age-related excitation-contraction coupling changes potentially demonstrate the remodelling required to maintain and protect adequate basal cardiac function. Such changes in basal function likely, in part, occur at the expense of a

constrained dynamic range and therefore contribute to limitations in rate and contractile function response during adrenergic stimulation.

#### 1.4.2.4 Myocyte Ultrastructure

Remodelling within ultrastructural components such as transverse tubules (T-tubules) may exacerbate the remodelling of $Ca^{2+}$ handling and other components of excitation-contraction coupling discussed above (Cheah and Lancaster, 2015a). Interest in ultrastructural changes in age and disease has risen to help explain $Ca^{2+}$ cycling alterations. This has resulted in increased investigation of T-tubules (figure 2). Transverse-Tubules represent a "headquarters" for excitation-contraction coupling and are susceptible to remodelling when subject to disease, documented widely in heart failure (Manfra et al., 2017). Remodelling has also been found to occur with ageing (Kong et al., 2018). Changes in T-Tubule structure with age have a marked impact on $Ca^{2+}$ transients and thus myocardial contractility due to their relationship with LTCC and the SR (figure 2). Structural modifications are characterised by re-organisation, reduced density and increased dilatation (Manfra et al., 2017). Transverse-tubules function through enabling propagation of APs through these micro-domains. Age-related changes in T-Tubules have been implicated in decrements in $Ca^{2+}$ handling, most notably, compromised $Ca^{2+}$ current (Kong et al., 2018). As understanding of T-Tubules has become greater, interest has increased in junctophilin2 (JP2) and bridging integrator-1 (BIN1). Junctophilin2 anchors the sarcolemma to the SR, which helps both form and maintain the dyads within the T-Tubules (Manfra et al., 2017). Downregulations in JP2 are associated with T-tubular alterations and subsequently, impaired cardiac function and increased arrhythmia risk (Manfra et al., 2017). Junctophilin2 has been further implicated in the localisation of RyR2 clusters and LTCC, evident from RyR2 hyperactivity during JP2 downregulation, whilst upregulation coincides with inhibition of $Ca^{2+}$ sparks (Manfra et al., 2017). Bridging integrator1 like JP2, has a role in the formation and maintenance of dyads. Collectively, BIN1 isoforms are involved in cell proliferation; T-Tubule growth and micro-domain formulation via membrane folding (Manfra et al., 2017). In particular, BIN1 aids the localisation of LTCC and RyR2 to the dyad (Hong et al., 2010). According to existing literature (Zhou and Hong, 2017), a fall in BIN1 coincides with increased arrhythmia risk as well as contractile impairments.

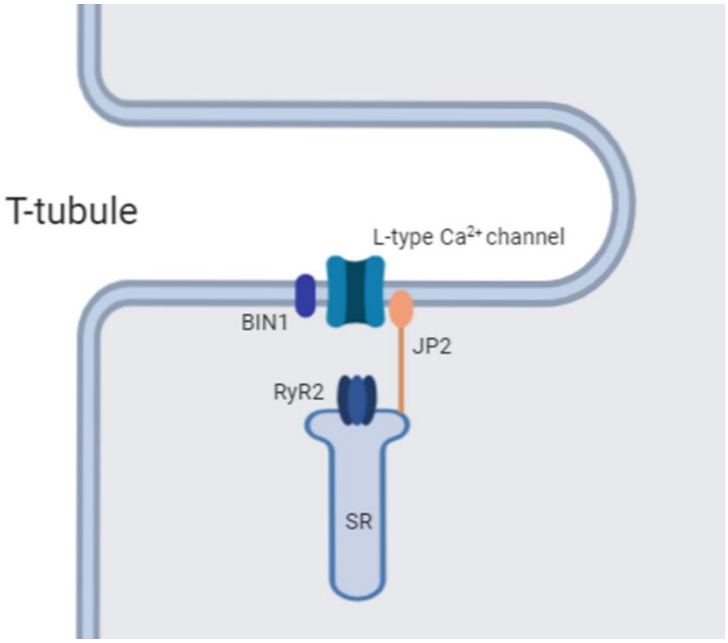


Figure 2. Transverse tubule (T-tubule) structure.

Some evidence exists revealing cardiomyocyte ultra-structure changes in aged mice (24 months of age) compared with young (6 months of age) evident from reductions in LV JP2, BIN-1 and T-tubule expression (57 %, 63 %, 18 %) (Cheah and Lancaster, 2015b). This reduction was associated with concomitant decrements in $Ca^{2+}$ transient kinetics (36 % increase in time to peak) (Cheah and Lancaster, 2015b). Such findings have important ramifications for the ageing population as greater understanding of influential cardiac markers can lead to advances in therapeutic strategies and even prevention. So far, T-Tubule and JP2 restoration can be achieved in heart failure models through the use of beta adrenergic receptor (βAR) blockers and also phosphodiesterase inhibitors (PDE; PDE5) (Chen et al., 2012; Huang et al., 2016). Though, this was observed in response to damage induced by myocardial infarction, thus it remains to be seen whether the more gradual cardiac deterioration associated with age rather than the abrupt insult of infarction, will obtain beneficial results from such interventions. Given the benefits of exercise intervention in the $beta_1$ adrenergic receptor ($\beta_1$AR) mechanism and the reversal of age-associated desensitisation, the effect of exercise training on T-Tubular domains may provide valuable responses, although this is yet to be studied.

## 1.5 Sympathetic Activity and Ageing

Neuro-hormonal alterations have been established as a major contributor to the ageing phenomenon and this has led to investigation of the adrenergic response to adrenergic receptor stimulation. Ageing coincides with chronic increased levels of circulating epinephrine and norepinephrine in the heart, which are responsible for changes in HR, contractility and relaxation upon onset of adrenergic stimulation through binding to $\beta_1$AR, triggering a signalling cascade (Farrell and Howlett, 2008; Spadari et al., 2018; Xiao et al., 1994). Increased age-associated sympathetic activity is, in part, caused by reduced plasma clearance, increased post-synaptic nerve-terminal catecholamine spill-over and poorer uptake (De Lucia et al., 2018; Ferrara et al., 2014; Howlett and Lancaster, 2021). Aged individuals have been shown to have basal epinephrine and norepinephrine levels approximately 95 % and 21 – 40 % greater than young adults respectively (Barnes et al., 1982; Fleg et al., 1985; Howlett and Lancaster, 2021). Upon exercise, aged individuals display almost an 11-fold increase in norepinephrine in contrast to a 7-fold increase elicited by young adults (Barnes et al., 1982; Fleg et al., 1985; Howlett and Lancaster, 2021). Epinephrine responses are also greater in aged populations compared with young adults, although by a less exaggerated magnitude (11 vs 10-fold increases) (Barnes et al., 1982; Fleg et al., 1985; Howlett and Lancaster, 2021). Chronic catecholamine elevation is suggested to lead to the chronic desensitisation of $\beta_1$AR and abrogate the adrenergic response (Moghtadaei et al., 2016; Strait and Lakatta, 2012; Nakou et al., 2016; Rodeheffer et al., 1984), impairing the dynamic range of CO (Ferrara et al., 2014; Spadari et al., 2018), contributing to limitations in cardiac contraction, relaxation and exercise tolerance in older age (Roh et al., 2016; Stratton et al., 1992; Stratton et al., 1994; Navaratnarajah and Jackson, 2017). The greater relative catecholamine response in aged individuals demonstrates a compensatory move to provide cardiac augmentation by overcoming the heightened basal sympathetic activity. This suggests the increase in catecholamine stimulus remains robust in old age and points toward a loss of tissue response and supports investigation of $\beta_1$AR signalling to explain age-associated CO reserve and exercise capacity limitations. Chronic increased sympathetic activity is generally considered to compensate for age-related limitations in HR, SV and CO developed through multifaceted cardiac remodelling (Rodeheffer et al., 1984; Fares and Howlett, 2010).

## 1.6 Adrenergic Response

As previously mentioned, (see section 1.2) the ANS is responsible for modulating cardiac function in response to stress and is also a major influencer of basal function. The ANS can be separated into two subsystems, the parasympathetic nervous system (PNS) and the SNS. The PNS alongside intrinsic cardiac mechanisms, is responsible for cardiac function in basal conditions and for withdrawal upon stress onset. The PNS influences HR more so than contractility according to research, but is able to reduce CO through direct innervation of the vagus nerve or via the binding of acetylcholine to Muscarinic ($M_2$) receptors leading to G-protein inhibitory actions and a decrease in adenyl cyclase (AC) activity (Gordan et al., 2015; Harvey and Belevych, 2003). In contrast the SNS is responsible for augmenting cardiac function in response to stress, facilitating elevations in CO to satisfy increased cardiorespiratory demand. Under stress, the SNS typically modulates chronotropy, lusitropy, dromotropy and inotropy through innervation by sympathetic nerves or through activation of adrenergic receptors during neurotransmitter or hormone binding.

### 1.6.1 Adrenergic Receptors

Table 3. Adrenergic receptors and their roles (De Lucia et al., 2018; Ferrara et al., 2014; Garcia and Boehning, 2017; Giovannitti Jr et al., 2015; Madamanchi, 2007; O'Connell et al., 2014; Skeberdis, 2004).

| **Alpha (α) Receptors** | | **Beta (β) Receptors** | | |
|---|---|---|---|---|
| $\alpha_1$ | $\alpha_2$ | $\beta_1$ | $\beta_2$ | $\beta_3$ |
| Myocyte hypertrophy | Blood pressure modulation | Myocyte inotropy | Smooth muscle dilation | Thermogenesis |
| Myocyte inotropy | Heart rate modulation | Myocyte chronotropy | Myocyte inotropy | Lipolysis |
| | | Myocyte lusitropy | Cell survival | |
| | | Cardiac reserve | | |

Adrenergic receptors are a class of G-protein-coupled receptors (GPCR). Various types of adrenergic receptor exist and can be broadly categorised into alpha (α) and beta (β) type receptors (Table 3). Adrenergic receptors are coupled to specific G-proteins which facilitate their intended function. Alpha receptors can then be separated into $\alpha_1$ and $\alpha_2$ and further, $\alpha_{1a}$, $\alpha_{1b}$, $\alpha_{1d}$, $\alpha_{2a}$, $\alpha_{2b}$ and $\alpha_{2c}$ subtypes. $Alpha_1$ receptors are coupled to $G_q$-proteins, which aid phospholipase C/ inositol triphosphate/ protein kinase C (PLC/ $IP_3$/ PKC) signalling. $Alpha_1$ receptors are prominent in smooth muscle and mediate vasoconstriction. However, in the heart $\alpha_1$ receptors influence myocyte hypertrophy as well as myocyte inotropy through a role in intracellular $Ca^{2+}$ regulation, although the true extent of this in the heart is currently unknown (O'Connell et al., 2014; Garcia and Boehning, 2017). $Alpha_2$ receptors are coupled to $G_i$-proteins and are predominantly found on pre-synaptic terminals of postganglionic sympathetic neurons as well as smooth muscle and serve to reduce norepinephrine release by inhibiting AC. Stimulation of $\alpha_2$ receptors can cause blood pressure and HR to decrease and $\alpha_2$ agonists are commonly used in anaesthesia (Giovannitti Jr et al., 2015).

Similarly, βARs can be separated into $\beta_1$AR, beta 2 adrenergic receptor ($\beta_2$AR) and beta 3 adrenergic receptor ($\beta_3$AR) subtypes. $Beta_1$ receptors are the most prominent adrenergic receptor in the heart and are coupled to $G_s$-proteins responsible for modulating many cardiac functions using the AC/ cyclic adenosine monophosphate (cAMP)/ PKA pathway amongst others. $Beta_1$ receptors account for almost 80 % of all adrenergic receptors in the heart and modulate cardiac chronotropy, inotropy and lusitropy under stimulation, augmenting CO (Madamanchi, 2007; Ferrara et al., 2014). $Beta_2$ receptors account for approximately 20 – 25 % of adrenergic receptors located in the heart (Madamanchi, 2007; Ferrara et al., 2014). Like their $\beta_1$AR counterparts, $\beta_2$ARs are coupled to $G_s$-proteins, but are also coupled to $G_i$-proteins and therefore have stimulatory and inhibitory influence on the AC/ cAMP/ PKA pathway (Ferrara et al., 2014). These receptors have significant roles in smooth muscle, airway dilation, cardiac inotropy and cell survival (Ferrara et al., 2014). Finally, $\beta_3$ARs are also coupled to $G_s$-proteins and are involved predominantly in lipolysis and thermogenesis in adipose tissue via similar $G_s$-protein pathways as $\beta_1$AR and $\beta_2$AR but are historically suggested to have little influence on cardiac function, due to little presence (Ferrara et al., 2014; Skeberdis, 2004; De Lucia et al., 2018). More recent research,

however, has suggested a link between $\beta_3$ARs and ventricular contractility, although whether this is positive or negative is highly debated (Skeberdis, 2004; De Lucia et al., 2018).

### 1.6.2 $\beta_1$AR Mechanism

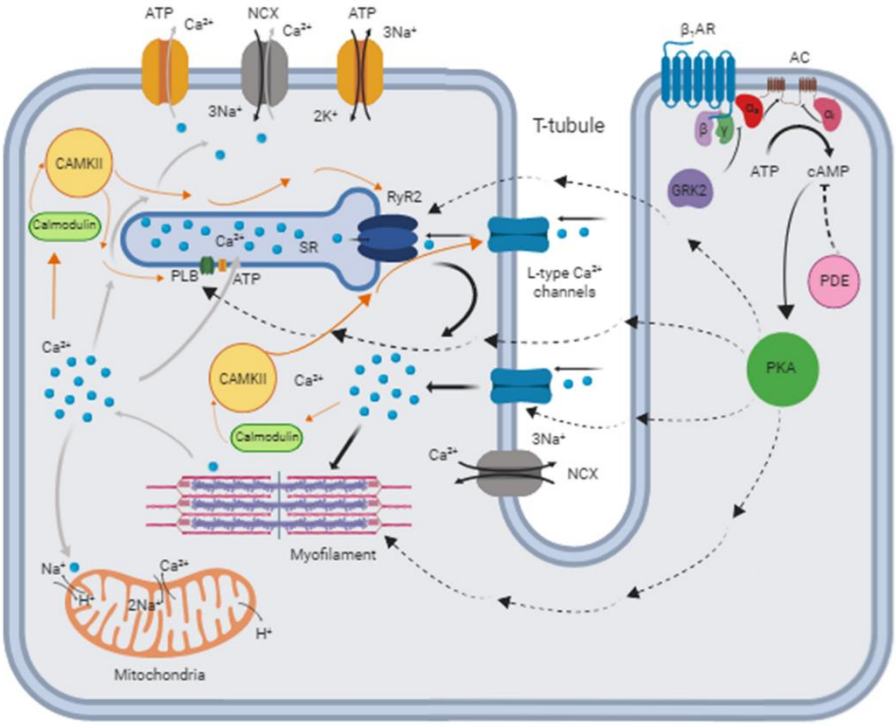


Figure 3. Excitation-contraction coupling and $\beta_1$AR signalling within a ventricular myocyte during $\beta_1$AR stimulation (adapted from Bers, 2002) (Bers, 2002; Behar et al., 2016; Chen-Izu et al., 2000; Ferrara et al., 2014; Fink et al., 2001; Kuschel et al., 1999; Layland et al., 2005; Pare et al., 2005; Rochais et al., 2004; Skeberdis, 2004). Solid black arrows display normal excitation-contraction coupling during contraction, whilst solid grey arrows reflect relaxation. Dashed arrows represent phosphorylation during adrenergic stimulation mechanism. Orange arrows display effect of $Ca^{2+}$/ calmodulin-dependent protein kinase (CaMKII) phosphorylation during adrenergic stimulation. Image created with BioRender.

Increases in CO in response to stress are facilitated largely by $\beta_1$AR stimulation (Najafi et al., 2016). At the onset of stress, epinephrine is released from the adrenal medulla by chromaffin cells (~ 80 %) and by sympathetic nerve terminals to a lesser extent (Gordan et al., 2015; McCorry, 2007; Ferrara et al., 2014; Howlett and Lancaster, 2021). Norepinephrine is released by mostly postganglionic sympathetic neurons as well as the adrenal medulla (~20 %) (Gordan et al., 2015; McCorry, 2007; Ferrara et al., 2014; Howlett and Lancaster, 2021). These catecholamines bind to $\beta_1$AR, triggering a signalling cascade. $G_s$-proteins are dissociated into α and β-gamma (γ) activated subunits as a result of increased transfer of guanosine diphosphate (GDP) for guanosine triphosphate (GTP) (Skeberdis, 2004). Binding between the α subunits and AC, facilitate transformation of ATP to cAMP, stimulating the activation of cAMP-dependent PKA, triggering downstream phosphorylation via A-kinase anchoring protein (AKAP) complexes (figure 3) (Skeberdis, 2004; Fink et al., 2001; Howlett and Lancaster, 2021). In response to stimulation, PKA phosphorylates LTCC and RyR2, elevating intracellular $Ca^{2+}$ entry (116 %) and SR $Ca^{2+}$ release (133 %) respectively (Pare et al., 2005; Saucerman and McCulloch, 2006; Chen-Izu et al., 2000; Kuschel et al., 1999; Xiao et al., 1994; Howlett and Lancaster, 2021). Phosphorylation of slow delayed rectifying $K^+$ channels ($I_{Ks}$) by PKA, counterbalances the increased $Ca^{2+}$ channel activity, reducing APD (Jeevaratnam et al., 2018; Sampson and Kass, 2010). Protein kinase A also phosphorylates PLN, which attenuates its inhibition of SERCA2a, enhancing cytosolic $Ca^{2+}$ removal and SR $Ca^{2+}$ loading (Saucerman and McCulloch, 2006; Howlett and Lancaster, 2021). Calcium removal is further enhanced through increased NCX activation as a response to increasing $Ca^{2+}$ in the cytosol (Behar et al., 2016; Ferrara et al., 2014). Moreover, PKA phosphorylates $Tn_i$ and PDE, weakening myofilament $Ca^{2+}$ sensitivity and increasing local cAMP modulation and thus spatio-temporal signalling respectively (Kuschel et al., 1999; Saucerman and McCulloch, 2006; Rochais et al., 2004; Layland et al., 2005). In SAN cells, the PKA signalling cascade elevates $I_f$ density through directly stimulating HCN channels, whilst $K^+$ permeability has been suggested to decline during adrenergic stimulation, making diastolic depolarisation potentials less negative (Fujita et al., 2017; Pinnell et al., 2007; Howlett and Lancaster, 2021). Finally, $\beta_1$AR signalling-induced elevations in intracellular $Ca^{2+}$, trigger additional phosphorylation of many of the above effectors (LTCC, RyR2, PLN) through increased $Ca^{2+}$/

calmodulin-dependent protein kinase II (CAMKII) involvement (Behar et al., 2016; Ferrara et al., 2014; Howlett and Lancaster, 2021).

Together, the above changes augment chronotropy, inotropy and lusitropy in the heart. Chronotropic increments occur as a result of SAN-related changes in $I_f$ and $K^+$ permeability leading to increased AP firing (Fujita et al., 2017; Pinnell et al., 2007; Howlett and Lancaster, 2021). Elevated $Ca^{2+}$ entry and release from the SR instigates improved inotropy (135 %) (Pare et al., 2005; Saucerman and McCulloch, 2006; Chen-Izu et al., 2000; Kuschel et al., 1999; Xiao et al., 1994; Howlett and Lancaster, 2021), whilst lusitropy is increased through augmented $Ca^{2+}$ sequestration and SR $Ca^{2+}$ loading alongside accelerated $Ca^{2+}$ removal from the troponin complex (Saucerman and McCulloch, 2006; Kuschel et al., 1999; Howlett and Lancaster, 2021).

### 1.6.3 $\beta_1$AR Mechanism of Desensitisation

$Beta_1$ adrenergic receptor desensitisation can be described as the normal protective mechanism required to prevent harmful effects of $\beta_1$AR overstimulation which may lead to $Ca^{2+}$ overload, cell death and arrythmia (Najafi et al., 2016). $Beta_1$ adrenergic receptor desensitisation is also used simultaneously to describe the age-associated loss of adrenergic response in cardiac function. These two considered definitions might be better described as transient and chronic $\beta_1$AR desensitisation or degradation (figure 4; figure 5). Transient $\beta_1$AR desensitisation is understood to occur as a result of excess $\beta_1$AR stimulation, which causes G-protein receptor kinases (GRK; $GRK_2$, $GRK_5$) to become activated by PKA and transferred to transmembrane areas via β-γ G-protein subunit interactions (Ferrara et al., 2014; Najafi et al., 2016). G-protein receptor kinases phosphorylate $\beta_1$AR and prevent G-protein coupling by facilitating the binding of β-arrestin proteins (Ferrara et al., 2014; Najafi et al., 2016; Howlett and Lancaster, 2021). This process mediates further $\beta_1$AR signalling (figure 4). Transient $\beta_1$AR desensitisation can occur within a duration of minutes or hours (Rajagopal and Shenoy, 2018; De Lucia et al., 2018; Ferrara et al., 2014; Howlett and Lancaster, 2021).

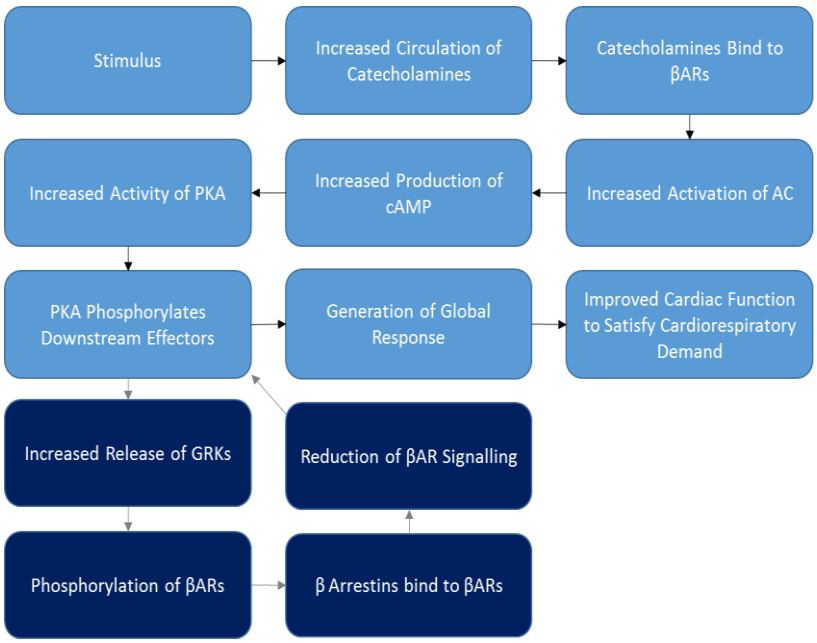


Figure 4. Schematic displaying an example of transient desensitisation of $\beta_1$AR signalling (De Lucia et al., 2018; Ferrara et al., 2014; Najafi et al., 2016; Rajagopal and Shenoy, 2018).

Chronic overstimulation of $\beta_1$AR known to occur in heart disease and ageing as a result of increased sympathetic activity causes the $\beta_1$AR mechanism and its mechanism of desensitisation to deteriorate (Ferrara et al., 2014; Najafi et al., 2016). Chronic $\beta_1$AR overstimulation can cause $\beta_1$AR internalisation and degradation during this process, which can lead to a loss in receptor density (~ 11 – 37 %) and response to downstream effector signalling during $\beta_1$AR stimulation (10 – 20-fold) (figure 5) (Ferrara et al., 2014; Najafi et al., 2016; Davies et al., 1996; Narayanan and Derby, 1982; White et al., 1994). The time period that this degradation occurs over is unknown, however it is widely accepted $\beta_1$AR mechanism-related decrements are prevalent in over 65-year-old humans, or 20 - 24+ month old rodent equivalents (Rajagopal and Shenoy, 2018; De Lucia et al., 2018; Ferrara et al., 2014). The physiological mechanism involved varies between disease and ageing despite similarities in sympathetic activity and $\beta_1$AR response. Most notably, heart failure coincides with greater GRK presence, whereas evidence suggests GRK activity does not increase with age and there is also no evidence in existing literature to suggest increases in $G_i$-proteins are responsible for altered adrenergic response in ageing (Santulli and Iaccarino, 2013; De Lucia et al., 2018). Such findings have guided further

exploration to elsewhere in the $\beta_1$AR pathway and to all its associated components outside of the immediate mechanism of transient desensitisation.

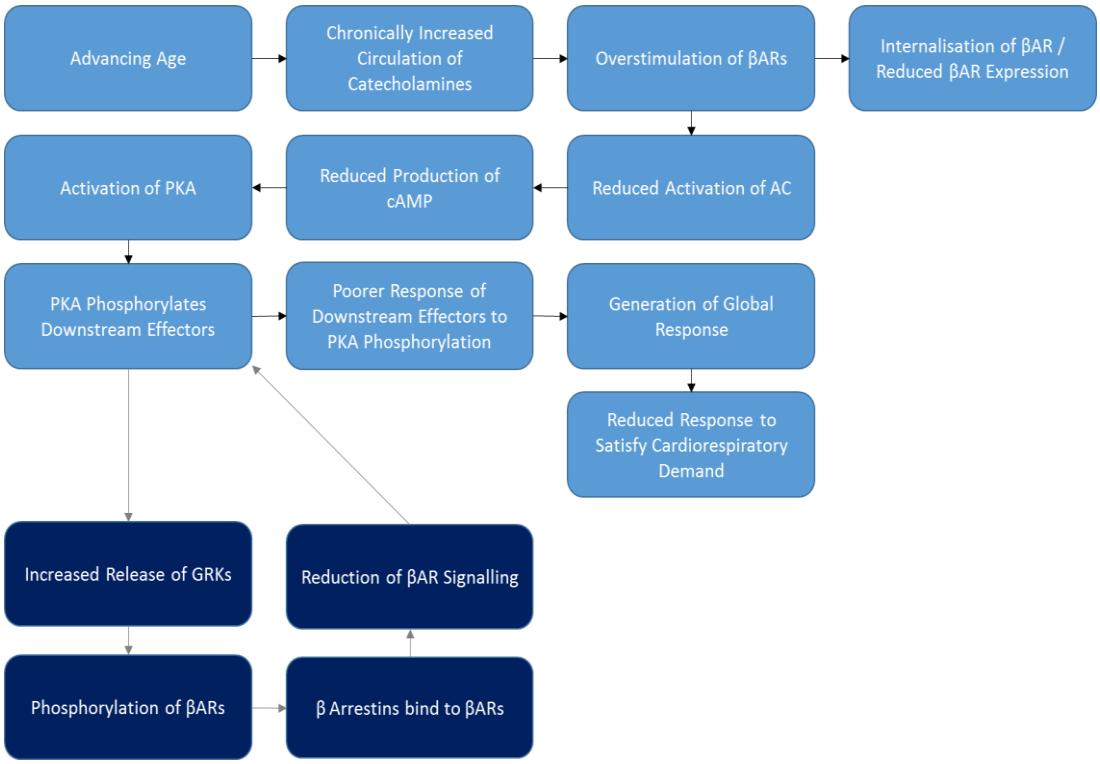


Figure 5. Schematic displaying an example of chronic desensitisation of $\beta_1$AR signalling (Davies et al., 1996; De Lucia et al., 2018; Ferrara et al., 2014; Najafi et al., 2016; Narayanan and Derby, 1982; Rajagopal and Shenoy, 2018; Santulli and Iaccarino, 2013; White et al., 1994).

## 1.6.4 Age-Related Changes in the $\beta_1$AR Mechanism

### 1.6.4.1 Alterations in the $\beta_1$AR and Early Signalling

Beta adrenergic receptors have been an extensive area of interest in research since their discovery in 1948 (Ahlquist, 1948; Wachter and Gilbert, 2012), yet studies investigating age-related differences in adrenergic response and the $\beta_1$AR mechanism independent of co-morbidities and disease are scarce. In the ageing heart, a specific βAR subtype ratio has not been quantified (Ferrara et al., 2014). However, age-related alterations in the βAR response appear to result from selective $\beta_1$AR and downstream

activity downregulation, as $\beta_2$ARs are known to maintain expression density, with alterations limited to the uncoupling of its signalling pathway (Wachter and Gilbert, 2012). Literature investigating adrenergic response in old compared with adult ventricular tissue is mixed, likely as a result of differences in methodology, species, gender, age and confounding presence of disease (Akashi et al., 2015; Chouabe et al., 2004; Ferrara et al., 2014; Fields et al., 2016; Golf et al., 1985; Liu et al., 1993; Molina et al., 2016). However, $\beta_1$AR expression and activity are widely accepted to remain the same or decrease with ageing (Abrass and Scarpace, 1981; Davies et al., 1996; Narayanan and Derby, 1982; Narayanan and Tuckler, 1986; White et al., 1994). The lack of unanimous findings has led to the increase in interest of effector components involved in or affected by downstream signalling to explain the age-related loss of CO reserve.

Early research investigating βAR expression failed to identify any age-related alterations (Abrass and Scarpace, 1981; Narayanan and Derby, 1982). Despite a lack of age-associated changes in expression, one of these early studies indicated βAR-catecholamine affinity was reduced by 10 – 20-fold, and downstream signalling (AC) response to agonist stimulation (old: 20 – 50 % increase vs young: 3-fold increase) were reduced in old (24 - 25 months of age) compared with young (3 - 4 months of age) rat hearts (Narayanan and Derby, 1982). Later research, in contrast, found $\beta_1$AR expression reduced in old age (Ungerer et al., 1993; White et al., 1994). Reductions in $\beta_1$AR expression of approximately 31 – 43 % alongside a 3 – 4-fold reduction in response to stimulation were reported in these studies (Ungerer et al., 1993; White et al., 1994). Differences in these earlier findings are likely related to the use of dissimilar methodologies, whereby different species, gender and age cohorts were tested, whilst some studies failed to specify βAR subtype (Abrass and Scarpace, 1981; Howlett and Lancaster, 2021).

As mentioned previously, GRK activity appears to be differently involved in the ageing $\beta_1$AR mechanism (section 1.6.3). G-protein receptor kinases have been suggested as disruption mediators of βAR function in mouse models of heart failure, where GRK inhibition improves inotropic reserve and $\beta_1$AR response (De Lucia et al., 2018; Koch et al., 1995). Yet its role in the ageing heart is controversial (De Lucia et al., 2018). It has been speculated that while an extreme cardiac event such as a myocardial infarction may cause an increase in $GRK_2$ activity and an increase in

catecholamine circulation; the less abrupt myocardial insult provided by age-related chronic sympathetic and βAR overstimulation may not be adequate to alter $GRK_2$ synthesis (De Lucia et al., 2018). One study found that whilst increasing age is associated with decreased $\beta_1$AR and AC activity, concomitant alterations are not observed in GRKs and therefore likely do not contribute to βAR maladaptation (Xiao et al., 1998). However, whether more intricate GRK changes occur with age, not measured in this study such as in location or regional signalling, requires future investigation.

Research has shown AC activity (predominantly $AC_5$ and $AC_6$) in response to stimulation by isoproterenol and forskolin reduces by $\sim \geq 50$ % and 63 % respectively in aged (24 months of age) compared with young adult (3 months of age) rats (Farrell and Howlett, 2008; Scarpace et al., 1991; Tobise et al., 1994; Narayanan and Derby, 1982). Aged rats also display a significantly decreased cAMP production during isoproterenol (> 40 %) and forskolin stimulation (> 25 %) as a result (Farrell and Howlett, 2008). This can trigger downregulation of PKA signalling, casting considerable effects on downstream effectors through altered phosphorylation and eventual blunting of contractile augmentation (Fields et al., 2016; Liu et al., 2014; Tobise et al., 1994; Roh et al., 2016; Howlett and Lancaster, 2021). An age-related decrease in the cAMP/ PKA signalling pathway may cause reduced intracellular $Ca^{2+}$ influx, reduced $Ca^{2+}$ sequestration, altered signal compartmentalisation efficiency and prolonged APD underlying some of the detrimental ageing effects related to relaxation, contractility and exercise response (Ferrara et al., 2014; Santulli and Iaccarino, 2016; Roh et al., 2016; Fields et al., 2016; Liu et al., 2014; Tobise et al., 1994).

Tight regulation of local cAMP levels in the heart is essential for efficient spatio-temporal signalling which facilitates the correct functioning of the heart, particularly in response to stress. The impact of recognised global reductions in cAMP has been discussed above and it may lead to significant detriments in cardiac performance. This likely also impacts PDE expression and activity, responsible for modulating local cAMP levels. Some evidence does exist showing a decrease in the gene expression of certain PDE isoforms (PDE 1A, 1B, 2A, 3B and 4A) in the aorta of middle-aged rats (Han et al., 2018). Little is known of the impact of this in relation to ageing and adrenergic response. Little is also known regarding whether this age-associated

reduction in certain PDE isoforms is a cardioprotective attempt to maintain depleting cAMP levels or whether the reduction in cAMP/ PKA signalling causes PDE downregulation (Han et al., 2018; Canepari et al., 1994; Nakano et al., 2017). Age-related changes in the control of spatio-temporal adrenergic signalling could well be indicative of regional heterogeneity in cardiac decrements.

As mentioned previously (see section 1.6.2.) CAMKII has a role in the normal $\beta_1$AR signalling mechanism. However, CAMKII has also been suggested to have a role in the reduction of phosphorylation and effector response to adrenergic stimulation with ageing (Xu and Narayanan, 1998; Feridooni et al., 2015). Under adrenergic stimulation, CAMKII along with PKA becomes activated and is involved in phosphorylating key $Ca^{2+}$ cycling components such as RyR2, LTCC and PLN (Behar et al., 2016; Ferrara et al., 2014). However, similar to cAMP and PKA, phosphorylation by CAMKII reduces in old age (Ferrara et al., 2014; Roh et al., 2016). This has led to the implication of CAMKII in the RyR2-related increased $Ca^{2+}$ spark frequency and reduced $Ca^{2+}$ spark duration and amplitude in ageing (Xu and Narayanan, 1998; Zhu et al., 2005). This pathway therefore may potentially contribute to age-associated cardiac limitations during exercise (Feridooni et al., 2015; Ferrara et al., 2014; Roh et al., 2016; Xu and Narayanan, 1998).

### 1.6.4.2 Alterations in Downstream Signalling and Effectors

Adrenergic stimulation of normal healthy SAN cells improves coupling of membrane and $Ca^{2+}$ clocks to modulate cardiac function and provide an increase in HR (Liu et al., 2014; Fujita et al., 2017). In aged hearts, the coupling of adrenergic signalling to the coupled clock mechanism has been suggested to be compromised due to diminished components of the signalling process (Spadari et al., 2018). In support, research investigating SAN response to adrenergic stimulus in ageing SAN cells has shown reduced HR response in mice (~ 50 %) and humans (~ 40 %) (Table 1) (Francis Stuart et al., 2018; Christou and Seals, 2008). However, literature investigating age-related alterations in components of SAN cell membrane and $Ca^{2+}$ clock mechanisms have been predominantly focused on changes in basal function, with little evidence available on age-related adrenergic response in these components, particularly concerning the $Ca^{2+}$ clock. One study has found adrenergic responses (1 µM isoproterenol) in HR, $I_f$, LTCC current and T-type $Ca^{2+}$ current are preserved in mice

SAN cells with increasing age (2 – 3, 21 – 24, and > 32 months of age) (Larson et al., 2013). Though significant reductions in intrinsic HR, maximum HR, intrinsic AP firing rate and maximum AP firing rate in aged mice compared with adult mice were found in this study (Larson et al., 2013). However, this study, as with many studies investigating adrenergic response, used a sole saturating (1μM) concentration of isoproterenol. This may not reflect changes existing elsewhere within the adrenergic response curve during the superfusion of more physiological doses.

Research involving age-related remodelling of excitation-contraction coupling in ventricular myocytes has similarly dwelled on changes in basal function, however, a study in ageing rats (2 vs 6 - 8 vs 24 months of age) found an age-associated decrease in contractility and $Ca^{2+}$ transient (20 %) response to adrenergic stimulus (Xiao et al., 1994). This supports previous findings of poorer contractile adrenergic response with ageing (Davies et al., 1996). The concentration of adrenergic stimulus (norepinephrine) required to produce half maximal effect increased by 213 % in the aged compared with young rats in the study above (Xiao et al., 1994). In this study, concomitant reductions in LTCC current response to adrenergic stimulation with ageing (~ 50 – 200 %) were suggested to be responsible for the loss of adrenergic-induced contractility and $Ca^{2+}$ cycling (Xiao et al., 1994). The increased level of adrenergic stimulation required to produce a substantial effect in old compared with young ventricles supports the theory of desensitisation within adrenergic signalling with ageing, with the isoproterenol response curve appearing to shift rightward.

Research has reported no age-related changes in PLN phosphorylation by PKA in rat ventricles (6 vs 12 vs 28 months of age) (Jiang and Narayanan, 1990). The influence of PLN phosphorylation by PKA on cytosolic $Ca^{2+}$ removal is also unaffected by age (Jiang and Narayanan, 1990). Yet an age-related decline in SR $Ca^{2+}$ uptake (35 – 50 %) does exist, likely as a result of alterations in SERCA2a (Jiang and Narayanan, 1990). Although during phosphorylation by PKA, aged rat ventricles have been found to exhibit greater relative responses in SR $Ca^{2+}$ uptake compared with young rat ventricles (Jiang and Narayanan, 1990). However overall SR $Ca^{2+}$ uptake in old rat ventricles was found to not surpass uptake by young rat ventricles without PKA influence (Jiang and Narayanan, 1990). This may suggest changes in SR $Ca^{2+}$ uptake with ageing might be influenced greater by SERCA2a expression or function than by altered PKA phosphorylation during adrenergic stimulation. It might be that age-

related losses in SERCA2a or other components of $Ca^{2+}$ sequestration, despite an upregulation in phosphorylation through maintained relief of PLN inhibition during adrenergic stimulation, cause SR $Ca^{2+}$ cycling range to become limited. The main contributor is difficult to establish since both appear to be heavily involved and similarly constructed studies are few.

In another study, significant reductions in CAMKII levels (50 %) were observed in overall ventricular tissue as well as specifically in the SR within aged rat ventricles (6 - 8 months of age vs 26 - 28 months of age) (Xu and Narayanan, 1998). Phosphorylation by CAMKII, a key enzyme involved in excitation-contraction coupling (or just $Ca^{2+}$ cycling/ maximising phosphorylation of key excitation-contraction coupling components) during adrenergic stimulation, is reduced significantly in SERCA (40 %), RyR2 (25 %) and PLN (25 %) with ageing (Xu and Narayanan, 1998). A reduction in these proteins appear to further suggest altered SR $Ca^{2+}$ cycling in response to stress with increasing age, evidenced by poorer SR $Ca^{2+}$ uptake in response to calmodulin, stimulated during adrenergic agonist superfusion (30 – 40 %) (Xu and Narayanan, 1998).

Overall, the existing literature concerning age-related changes in excitation-contraction coupling response to adrenergic stimulation suggest intracellular $Ca^{2+}$ influx, CICR and SR $Ca^{2+}$ loading deteriorate with ageing (Table 2). This is likely a result of age-related reductions in expression and phosphorylation of key excitation-contraction coupling components, though some controversy exists. Previous literature presents a common theme of poorer response to adrenergic stimulation and apparent loss of sensitivity in its signalling, which may partially explain the age-associated loss in cardiac performance under stress. However there remains a great deal unknown regarding the age-related alterations of the components within the adrenergic mechanism.

## 1.7 AP

Action potentials are responsible for excitation of cardiomyocytes and make up the first step of myocyte contraction (Bers, 2002; Pinnell et al., 2007). Action potentials within the heart are generated by pacemaker cells within the SA node (Pinnell et al., 2007). From the SAN, APs propagate to the rest of the heart systematically exciting myocytes and facilitating the transduction of electrical impulses to mechanical

contractions (Pinnell et al., 2007). The Atrioventricular (AV) node and bundle of his and purkinje fibers also provide secondary and tertiary pacemakers respectively. Action potentials are the product of ion channel activity and alterations in ion movement can dramatically influence AP waveform (Bers, 2002; Grant, 2009; Pinnell et al., 2007). Action potentials are a key area of focus in arrhythmogenesis, ageing and disease, providing information on excitatory remodelling, the mechanisms of which it arrives and how it may translate into mechanical impairments (Feridooni et al., 2015; Gan et al., 2013; Herraiz et al., 2013; Li et al., 2004; Liu et al., 2000; Ocorr et al., 2007; Sorrentino et al., 2016).

### 1.7.1 AP Waveform

Action potentials within the heart exist in a variety of waveforms depending on their regional location (Molina et al., 2016; Pandit et al., 2001; Natali et al., 2002). Differences in AP waveform are largely a result of variations in the key ion channels that make up and contribute to its formation. Action potential differences also provide the heterogeneity of excitation across the heart needed to develop a coordinated muscular contraction. Action potentials are typically described and categorised by changes in certain phases of its waveform (figure 6). Action potentials are generally considered to contain five phases (0 - 4) which follow the order of phase four, phase zero, phase one, phase two and finally phase three. Phase four of the AP reflects resting membrane potential, whilst phase zero reflects rapid depolarisation (Wei et al., 2020; Grant, 2009; Grunnet, 2010). Phases one, two and three describe the early repolarisation, plateau, and late repolarisation phases of the AP, respectively (Wei et al., 2020; Grant, 2009; Grunnet, 2010).

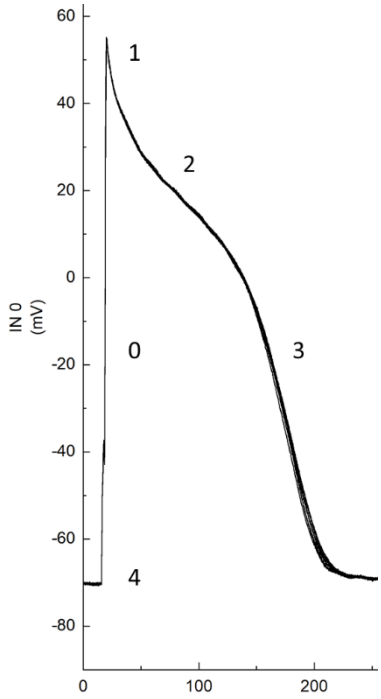


Figure 6. Recording of an AP from a Wistar rat demonstrating the AP phases. Phase 4: resting membrane potential. Phase 0: depolarisation. Phase 1: early repolarisation. Phase 2: plateau. Phase 3: late repolarisation.

However, APs emitted by the SAN consist of different phases and (see figure 7) are characterised by their slow depolarisation (Wei et al., 2020; Grant, 2009; Grunnet, 2010). Action potentials within the SAN begin with early depolarisation during phase four, where $I_f$ through HCN channels are active. As the membrane potential becomes less negative during this slow early depolarisation, T-type and LTCC become active (Wei et al., 2020; Grant, 2009; Grunnet, 2010). This leads to phase zero, where LTCC conductance is increased, allowing increasing $Ca^{2+}$ influx to depolarise the cell. In SAN cells, phase one and two are missing, with phase three solely reflecting repolarisation through increased conductance of outward $K^+$ channel currents, returning towards initial resting membrane potential. Action potentials of the AV node follow very similar waveforms to SAN cells and rely on the same ion channel movement.

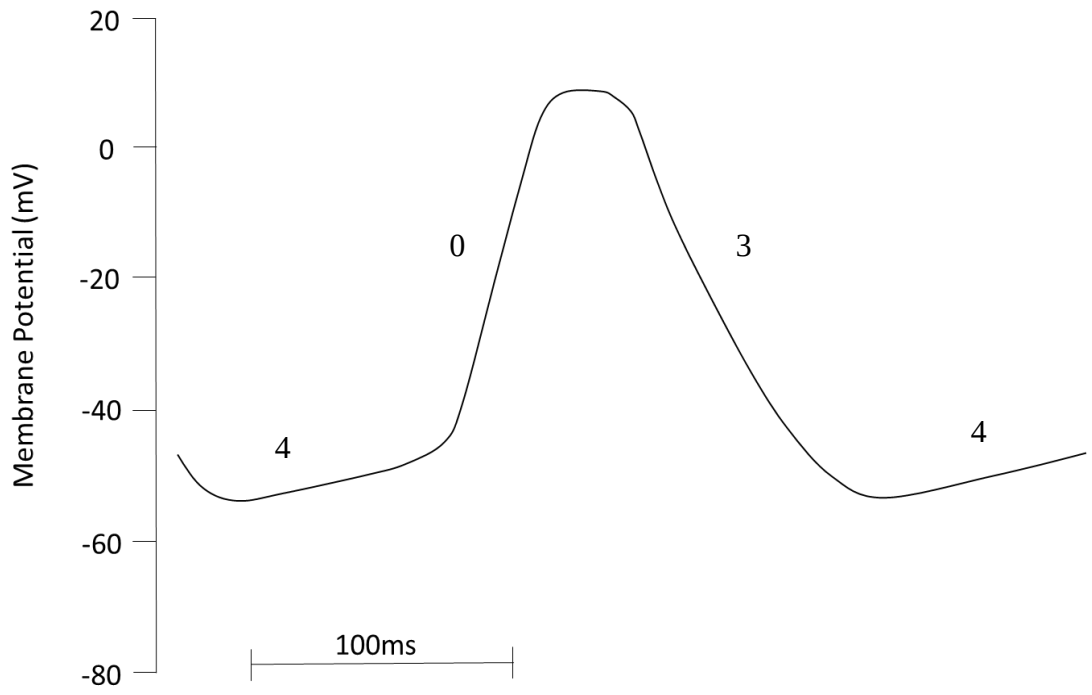


Figure 7. Schematic drawing of a SAN myocyte AP demonstrating the SAN AP phases. Phase 4: pacemaker potential. Phase 0: depolarisation. Phase 3: repolarisation.

Ventricular myocytes (see figure 8) begin with phase four reflecting the resting potential, which is more negative than pacemaker cells, whilst phase zero entails a rapid depolarisation via activation of fast sodium ($Na^+$) channels (Wei et al., 2020; Grant, 2009; Grunnet, 2010). Immediately following rapid depolarisation, early repolarisation occurs briefly through transient outward $K^+$ currents (phase one) before the increased conductance of LTCC triggers a plateau (phase two) (Grunnet, 2010). As LTCC inactivate, outward $K^+$ channels increase in conductance and facilitate repolarisation (phase three) toward resting membrane potential. Action potentials exhibited by the atria, his bundle and purkinje fibres are very similar, although atrial APs are characterised by a greater 'notch' in waveform after depolarisation during phase one due to greater transient outward current, and also a shorter phase two plateau due to smaller LTCC current (figure 8) (Grunnet, 2010). Action potentials of purkinje fibres and his bundle also have a prominent AP notch, alongside greater time to 50 % repolarisation ($APD_{50}$) and $APD_{90}$ and more negative AP plateau (Boyden et al., 2010) compared with ventricular APs, as a result of differences in rectifying $K^+$ currents

(reduced HERG, ERG, KCNQ1 and KCNE1) and LTCC (reduced $Ca_v1.2$; increased $Ca_v1.3$) (Dun and Boyden, 2008; Haissaguerre et al., 2016).

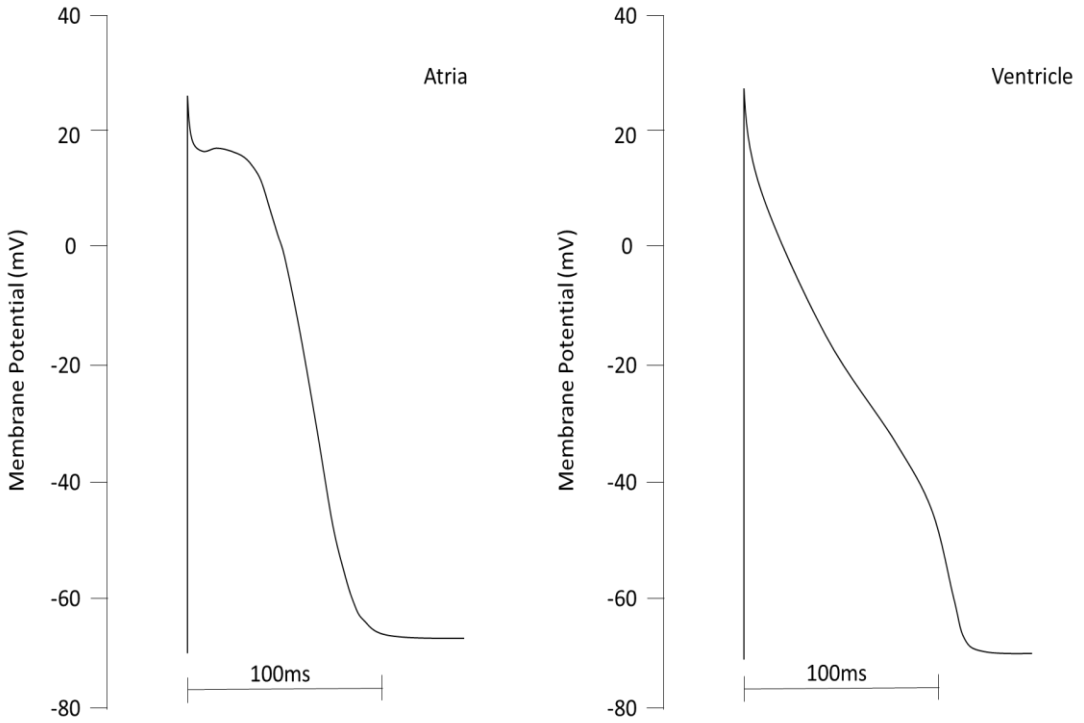


Figure 8. Schematic drawings of atrial (left) and ventricular (right) myocyte APs.

## 1.7.2 Changes in AP Repolarisation with Ageing

Cardiomyocyte repolarisation can be observed during phase 1 and 3 of the AP waveform and is also influenced by phase 2. Phase 3 specifically is responsible for the return to resting membrane potential. Action potential repolarisation is integral to cardiac function and controls APD at rest and during response to stress. Repolarisation of the AP prevents prolonged depolarising inward currents using myocyte repolarisation reserve, where outward $K^+$ channels increase in conductance to make membrane potentials more negative. Alterations in myocyte repolarisation or repolarisation reserve can cause APD prolongation and arrhythmogenesis (Grunnet, 2010).

Age-related changes in the later phases of the AP are vital when considering cardiac reserve and exercise tolerance. A prolongation in repolarisation time or efficiency may impede the heart's ability to manipulate diastolic intervals to facilitate increases in rate and contractility, leading to events such as early or delayed after-depolarisations (EADs; DADs), arrhythmias or cell death (Ocorr et al., 2007; Keating et al., 2001). This has facilitated increased interest in cardiac repolarisation kinetics to explain APD prolongation and the inability to maintain CO reserve with advancing age (Feridooni et al., 2015).

Existing literature suggests a reduced rate of myocardial repolarisation and potentially repolarisation reserve occurs with ageing (Feridooni et al., 2015). This is true of the atria and ventricles, with significant elevations $APD_{50}$ and $APD_{90}$ observed in dog and rat (6 – 38 %) (Huang et al., 2006; Feridooni et al., 2015; Gan et al., 2013; Liu et al., 2014; Liu et al., 2000; Waldeyer et al., 2009; Feridooni et al., 2017). Increased repolarisation duration is understood to develop throughout ageing, as a mechanism to prevent pathological contractile function and maintain CO (Janczewski et al., 2002; Sorrentino et al., 2016). By increasing APD, inotropic support is provided through a prolonged contraction as a result of modified intracellular $Na^+$ and $Ca^{2+}$ load through LTCC and NCX (reverse mode), however, at the cost of chronotropic reserve (Sorrentino et al., 2016). This ultimately enhances susceptibility to exercise limitation and intolerance (Sorrentino et al., 2016). Understanding key changes in excitation-contraction coupling, is vital in unveiling the underlying mechanism of the reduced adrenergic response in aged individuals.

A cross-sectional study by Liu et al. (Liu et al., 2000) found old rats (27 months of age) demonstrated increased APD ($APD_{90}$; 35 %) compared with adult rats (6 months of age) (Liu et al., 2000). Similarly, increased $APD_{90}$ has been displayed in dogs with ageing (4 - 7 vs 10 - 13 y) (Liu et al., 2000; Sorrentino et al., 2016). Greater changes were found in a study using rat ventricles, displaying control $APD_{50}$ (> 2.5-fold) and $APD_{75}$ (> 4.2-fold) to be significantly prolonged in aged (24 months of age) compared with young (3 months of age) counterparts (Capasso et al., 1983a). Similar age-related (2 - 3 vs 24 - 25 months of age) increments in $APD_{50}$ (> 2.2-fold) and $APD_{75}$ (1.9-fold) in rat ventricles have been reported elsewhere in research (Walker et al., 1993). Surprisingly, APD response to adrenergic stimulation has been comparatively far less reported. The available evidence generally demonstrates APD shortening to

magnitudes of approximately 7 – 43 % with adrenergic stimulation in adult subjects (Kang et al., 2017; Stuart et al., 2018; Wang and Fitts, 2017; Wang and Fitts, 2020). Although response to adrenergic stimulation is widely considered to become poorer in old age, little evidence exists. Whilst it is reasonable to expect this, given the wide scale age-related changes within the $\beta_1$AR mechanism, some studies have suggested ventricular APD response to adrenergic stimulation is in fact preserved in aged rodent hearts (Francis Stuart et al., 2018; Farrell and Howlett, 2007).

To date no studies to our knowledge have investigated ventricular APD responses to adrenergic stimulation at a physiological frequency and temperature with respect to ageing. Therefore, the unequivocal mechanisms by which APs become altered with increasing age is currently not understood and future physiologically relevant studies are warranted, particularly those with a focus on factors controlling repolarisation.

### 1.7.3 Repolarising $K^+$ Channels

Ventricular repolarisation is widely known to be modulated by adrenergic signalling through the $\beta_1$AR mechanism. When coupled with the suggested reduction in repolarisation reserve with age, the logical progression is an increased investigation of potential attributing $K^+$ channels. Alterations in these channels may be fundamental in reducing dynamic capacity and repolarisation reserve and in turn, the ability to achieve stable CO at higher exercise intensities. Channels such as the inward rectifying $K^+$ channel ($I_{K1}$), transient outward channel ($I_{to}$), ultra-rapid, rapid and slow delayed rectifying $K^+$ channels ($I_{Kur}$, $I_{Kr}$, $I_{Ks}$) and ATP-sensitive $K^+$ channels ($K_{ATP}$) all influence AP repolarisation to some extent. It is the combination of the above channels which make up the repolarisation reserve (Grunnet, 2010) combined with LTCC that modulate the direction and magnitude of changes in repolarisation and APD.

A study by Walker, Lakatta and Houser (Walker et al., 1993) found old rat ventricles (21 - 25 months of age) exhibited reduced peak $I_{to}$ density (~ 29 – 31 %) compared with young adult rat ventricular cardiomyocytes (2 - 3 months of age) (Walker et al., 1993). In support, a reduction in $I_{to}$ current (~ 25 – 41 %) has been observed in rat LV myocyte investigations during normal ageing and ageing with spontaneous hypertension (3 vs 18 months of age) (Cerbai et al., 1994). Age-related decreases in $I_{to}$ density (~ > 50 %) have also been reported in rat right ventricular (RV) myocytes (2 vs 6 vs 18 months of age) (Chouabe et al., 2004). However an age-related increase

in peak $I_{to}$ current (39 – 64 %) and activation alongside unchanged inactivation was displayed in one study investigating old (27 - 28 months of age) vs adult (6 months of age) rat ventricular myocytes (Liu et al., 2000). Differences in external bath solution (presence of $Na^+$) and concurrent utilisation of barium ($Ba^{2+}$) alongside differences in experimental temperatures (room temperature vs physiological temperature) between the above studies may explain some of the variation in outcome. Differences in experimental outcomes may have also resulted from differences in rat strain and the analysis of various ventricular regions due to heterogeneity of AP waveform and $K^+$ channel current expression (Chouabe et al., 2004). Transient outward current response to adrenergic stimulation in ageing has not yet been investigated in literature.

Although $I_{to}$ has been implicated in cardiac ageing, the mixed literature above may suggest other repolarising $K^+$ channels might contribute more greatly to the cardiac ageing phenomenon (Yang and Nerbonne, 2016). It is unlikely $I_{Kur}$ plays a role in the declining ventricular response to stress, as negligible protein expression levels exist in the ventricles in comparison to the atria (Ravens and Cerbai, 2008), though this might be species-dependent. However $I_{Kr}$ and $I_{Ks}$ are far more prominent in ventricular tissues and contribute to the latter phase of ventricular myocyte AP repolarisation, influencing $APD_{50}$ - $APD_{90}$ – known to alter with age - greater (Feridooni et al., 2015). The contribution of $I_{Kr}$ to APD in resting states is initially far greater (~ 86 %) than contributions of $I_{Ks}$ (Banyasz et al., 2014; Kang et al., 2017). Yet upon adrenergic stimulation this contribution reverses, with $I_{Ks}$ providing a greater magnitude of response which is further amplified with increases in isoproterenol dose (10 nM = ~ 22; 30 nM = ~ 64 %) (Banyasz et al., 2014). This indicates $I_{Ks}$ may be more responsible, in part, for the reduced myocardial response to stimulation with increasing age (Kang et al., 2017). Studies investigating $I_{Ks}$ in relation to ageing are few. Available literature has found a reduction (67 %) in KCNQ1 (gene code for $I_{Ks}$ channel) in aged (5 weeks) compared with young (1 week) drosophila, whilst KCNQ1 knockdown displayed increased APD, decreased stress tolerance and rhythmicity (tachyarrhythmias, asystole) and a higher failure rate (70 – 80 %) (Banyasz et al., 2014; Wessells and Bodmer, 2007; Nishimura et al., 2011; Ocorr et al., 2007). Such changes reflect the well-known age-related cardiac decrements and support further $I_{Ks}$ investigation in ageing models (Nishimura et al., 2011; Ocorr et al., 2007). The effect of ageing on ventricular $I_{Ks}$ structure and function in larger, more commonly used

animal models (rat, guinea-pig, rabbit, dog, human) is currently unknown and yet to be investigated. Moreover, the impact of ageing on $I_{Ks}$ response to adrenergic stimulation has also not been investigated to our knowledge.

Other channels such as $K_{ATP}$ and $I_{K1}$ have also been theorised to be influenced by ageing (Liu et al., 2000; Bao et al., 2013; Yang et al., 2016). However studies investigating $I_{K1}$ have documented unchanged or enhanced peak and steady-state channel density (24 – 46 %) alongside inactivation (34 – 47 %) with increasing age (Walker et al., 1993; Liu et al., 2000). Such findings do not correlate with the typical AP changes in old age, as an increase in $I_{K1}$ theoretically would reduce APD due to increased influence on late phase AP and resting membrane potential hyperpolarisation, enhancing AP repolarisation and contractile velocity. This has been shown in transgenic mice, whereby upregulated $I_{K1}$ induced reductions in time to 75 % repolarisation ($APD_{75}$) (25 – 30 %), $APD_{90}$ (60 %) and QT intervals (26 – 45 %) (Li et al., 2004). Therefore, whilst age-related alterations exist in $I_{K1}$, other rectifying currents are suspected to display greater involvement in age-induced AP modulations. On the other hand, $K_{ATP}$ currents have been found to reduce (45 %) with advanced age (Bao et al., 2013). The ATP sensitive $K^+$ channel currents are involved in phase 2 and 3 of the AP, but activate predominantly under stress; indicating specific $K_{ATP}$ current changes may contribute to the reduced response to exercise and adrenergic stimulation (Yang et al., 2016).

## 1.8 Species Differences

Species differences represent a major consideration for the interpretation of existing literature as well as study design within the field of cardiac physiology, particularly for the investigation of AP repolarisation. Specifically, rat cardiomyocyte APs – much like those of mouse cardiomyocytes – are significantly shorter than human cardiomyocyte APs, as well as cardiomyocyte APs of other species commonly used in similar research such as guinea pig, rabbit and dog (Varró et al., 1993; Árpádffy-Lovas et al., 2022). The considerable inter-species differences in APD are facilitated by contrasting ion channel expression and current densities, particularly involving ion channels that have a role in the modulation of repolarisation (Varró et al., 1993; Árpádffy-Lovas et al., 2022). This creates difficulty when translating findings from smaller mammals - such as rats - to humans (Árpádffy-Lovas et al., 2022).

Rat cardiomyocyte APs are characterised by rapid phase 1 repolarisation and no discernible AP plateau due to greater $I_{to}$ current compared with other species (Varró et al., 1993). Further, rat ventricular myocytes exhibit a reduced magnitude of $I_{K1}$ current compared to other mammals such as guinea pig and rabbit (Varró et al., 1993) though its block has a greater influence on APD compared with dogs and humans (Árpádffy-Lovas et al., 2022). Historically, rat ventricular myocytes have been shown to demonstrate little rectifying $K^+$ current with limited influences on the modulation of AP repolarisation which can present difficulties in the reliable measurement of such currents during experimentation (Varró et al., 1993; Joukar, 2021; Regan et al., 2005; Pond et al., 2000; Tande et al., 1990), though recent studies may indicate these currents are more relevant to repolarisation in the rat ventricle than first thought and have hinted at a potentially greater role for rectifier $K^+$ currents such as $I_{Ks}$ particularly during adrenergic stress and in turn ageing within this species (Wang and Fitts, 2020; Olgar et al., 2022). How these recent findings may compare or translate to humans as well as other species with cardiac AP morphology more closely related to humans, is unknown. Conversely, recent research has continued to demonstrate the limited role of $I_{Kr}$ in the rat heart (Wang and Fitts, 2020; Árpádffy-Lovas et al., 2022) providing a significant contrast to its understood prominent role in human cardiomyocyte repolarisation (Árpádffy-Lovas et al., 2022; Joukar, 2021), further compounding the difficulty of obtaining reliable measurements of some repolarising $K^+$ currents within this species. Moreover, recent research has highlighted further inter-species differences with the influence of $I_{Kur}$ on AP repolarisation and in turn APD shown to be far greater in rats than dogs and humans (Árpádffy-Lovas et al., 2022).

Put simply, the main difficultly, established by some existing literature is the difficulty in translating the findings from rats to humans, particularly in relation to AP repolarisation due to the differences in $K^+$ channel expression, $K^+$ current densities and the relative influence currents such as $I_{to}$, $I_{Kur}$, $I_{Kr}$ and $I_{Ks}$ have on the modulation of repolarisation within myocytes of their respective species (Joukar, 2021; Árpádffy-Lovas et al., 2022).

Further difficulty in the translation of findings in the rat heart to the human heart may exist in the electrophysiological responses to adrenergic stimulation and ageing, where ionic responses and in turn, AP responses to adrenergic stimulation in adult and old hearts may also demonstrate inter-species differences. However in the absence of

further evidence, this is speculation. Although the difference in balance of repolarising currents will likely provide different balances of the impact of age-related changes in specific currents, even though the age-related prolongation of the AP and repolarisation in general is a conserved phenomenon observed across species including humans and rats (Huang et al., 2006; Feridooni et al., 2015; Gan et al., 2013; Liu et al., 2014; Liu et al., 2000; Waldeyer et al., 2009; Feridooni et al., 2017; Reardon and Malik, 1996; Rabkin et al., 2016), though the balance of currents may differ in terms of those involved. Therefore, the animal models chosen for the electrical investigations of the heart should be thoroughly considered, for the reasons described above, in order to obtain electrophysiological findings that are meaningful and have the capacity to effectively improve our understanding of the heart and its response to adrenergic stress, ageing and disease.

Typically, the use of rats and mice for investigations exploring the potential of pharmacological therapies on the modulation of cardiac repolarisation are not considered appropriate due to the issues discussed above regarding the translation of findings from rodents to humans resulting from inter-species differences in $K^+$ channel expression and function (Árpádffy-Lovas et al., 2022; Joukar, 2021; Varró et al., 1993). However rat models do provide value outside of investigations on the electrical safety of drugs for human use. Rat models have been used extensively for the investigation of ageing phenomena and continue to play a role in cardiac ageing research as well as general cardiac electrophysiology investigations (Josephson et al., 2002; Liu et al., 2000; Walker et al., 1993; Farrell and Howlett, 2008; Scarpace et al., 1991; Tobise et al., 1994; Narayanan and Derby, 1982; Olgar et al., 2022; Wang and Fitts, 2020). This is largely because rats are a mammalian species that are readily available and less costly than larger animals, easy to handle and have the potential to succumb to similar cardiac disorders as humans (Joukar, 2021). Moreover, many of the identified ion channels present in humans, are indeed present in rats, albeit in varied amounts or varied function (Joukar, 2021). Further, the lifestyle of rats can easily be controlled unlike humans to avoid external interferences that may affect disease and co-morbidity development, which are extremely useful qualities in ageing research. Rats also have a significantly reduced lifespan compared with humans and many other mammals used in cardiovascular research (Tellez et al., 2011), presenting a convenient model for ageing investigations and the extensive use of rat models in

similar research historically also allows for effective comparisons to be made with ease with evidence from the literature.

## 1.9 Computational Modelling

In biomedical science, computational modelling allows an interdisciplinary approach to be taken by scientists with the aim of expediting scientific progress towards the greater understanding of a particular mechanism or the targeting of new therapies. The benefit of computational models is that they provide a completely different perspective, often at much faster speeds, with the same goals of laboratory research: testing hypotheses and exploring whole systems as well as various layers of a system. A key benefit, likely enhancing the demand of computational presence in many laboratories is the ability to assimilate a wide variety of relevant and disparate findings that better reflect an entire physiological system or process (Brodland, 2015; Niederer and Smith, 2012). Left solely to experimental work, it becomes very difficult to bring fragmented results key to the same topic together to improve whole system knowledge, which can lead to more information but less understanding (Brodland, 2015; Niederer and Smith, 2012).

Computational models typically work by extracting mathematical model equivalents of specific mechanisms, often relating to global organ and cellular level processes, and using the ever-growing data processing and storage power of computers to perform simulations (Brodland, 2015). Key existing relevant biophysical findings can be incorporated to generate very complex and specific models. Comparisons are then frequently made between laboratory data and computational data to help validate the computational model (Brodland, 2015; Niederer and Smith, 2012). Ultimately, the end goal is to develop a robust computational model capable of simulating complex and intricate experiments at speed, which can help provide predictive information for future investigations. The cycle of validating against laboratory data then continues perpetually (Niederer and Smith, 2012). Great value lies in the ability of a model to perform numerous simulations, replacing money, time, and resource consuming laboratory experiments in order to highlight the most important investigations required to be performed in the laboratory for the greatest benefit. It is also a valuable tool in helping to reduce the use of animals in research.

### 1.9.1 Computational Modelling in Cardiac Physiology

Computational modelling has grown rapidly in cardiac physiology after the work of Hodgkin and Huxley (Hodgkin and Huxley, 1952; Hodgkin and Huxley, 1952b; Hodgkin and Huxley, 1952a; Hodgkin and Huxley, 1952c; Hodgkin and Huxley, 1952) was modified to apply to cardiac APs (Noble, 1962). Since then, the development of computational models and the demand for such has increased phenomenally, with use widespread today (Brodland, 2015).

Computational modelling is an incredibly important tool in electrophysiology and the evaluation of the intricacies of cardiac excitation and its coupling to contractile changes (Mayourian et al., 2018b). Numerous models exist in varying complexities, because of the variations in tissues used and protocol complexity in the laboratory (Heijman et al., 2011; Pandit et al., 2001; Pathmanathan and Gray, 2018; Fink et al., 2011). However, it is as a result of the varied nature of laboratory investigations as well as the inherent heterogeneity of species and cells, that developing a robust computational model is increasingly difficult (Niederer and Smith, 2012). Laboratory experiments in cellular cardiology are notorious for utilising vast arrays of set-ups, particularly in electrophysiology, which differ in pacing frequency, intracellular and extracellular solutions, animal species and strains, drug interventions, patch-clamp type and so on. This is often troublesome for end-point comparisons between laboratory studies never mind for the development of computational models. The absence of uniformity in laboratory investigation findings even amongst those using similar animal species forces computational model development to then rely on extracting data where possible from simply the available data. Given the heterogeneity of cardiomyocyte cell function amongst species this can make the validation of computational models incredibly difficult.

Developing complex, physiologically relevant, and accurate models of rats is vital in helping extract the full benefits of computational modelling and utilising their full predictive capacity can be extremely beneficial for the area of cardiac physiology. Many computational models cannot simulate myocyte function at the full physiological range of stress and do not include the full range of ion channels. Though, in recent years, a greater interest in the accurate modelling of the $\beta_1$AR signalling control of myocytes has been generated (Heijman et al., 2011; Saucerman et al., 2003). However, whilst this previous work has granted attention to a full range of isoproterenol doses, these models do not account for adrenergic responses, particularly

in APs, at more physiological frequencies (Saucerman et al., 2003). Furthermore, developing computational models to investigate heart disease has received a great deal of attention, whilst ageing has yielded far less attention (Niederer and Smith, 2012). Generating computational models capable of reflecting electrophysiological rate and adrenergic dependency as well as aged heart characteristics could dramatically increase potential therapeutic targets.

In the past few years, a computational rat model has been developed in our laboratory with this view in mind (Stevenson-Cocks, 2019). Generating good reference data for electrophysiological responses to physiological stressors such as adrenergic stimulation and ageing will aid model validation and eventually lead to the improvement in understanding of the age-related loss in the dynamic range of CO. Translating basic results to human tissue models will also go some way to understanding the cardiac ageing problem in the wider context and help considerably where experiments are difficult.

## 1.10 Objectives of the Work

Changes in sympathetic modulation of the heart are suggested to have a key role in the ageing phenomenon (Ferrara et al., 2014; Fleg et al., 1994; Fares and Howlett, 2010; De Lucia et al., 2018). This has led to extensive research of the $\beta_1$AR mechanism (Fares and Howlett, 2010; De Lucia et al., 2018; Xiao et al., 1994). Electrical changes induced by adrenergic stimulation are mediated, in part, by repolarisation of the AP through alterations in $Ca^{2+}$ and $K^+$ currents, which in turn, facilitate changes in contractility (Jeevaratnam et al., 2018; Sampson and Kass, 2010). Action potential repolarisation is widely considered to become slower with age (Feridooni et al., 2015) and it has also been postulated that the cardiac response to adrenergic stimulation becomes narrower (Stratton et al., 1992; Stratton et al., 1994; Feridooni et al., 2015; Ferrara et al., 2014), though very limited physiologically relevant evidence exists regarding changes to adrenergic response of AP repolarisation. Recent literature has heavily implicated $I_{Ks}$ in the modulation AP repolarisation during adrenergic stimulation (Banyasz et al., 2014), suggesting a potential role for $I_{Ks}$ in relation to the age-related decline of cardiac response to stress. However, myocyte repolarisation is considerably influenced by the balance of $Ca^{2+}$ and $K^+$ handling (Jeevaratnam et al., 2018; Sampson and Kass, 2010; Banyasz et al., 2014; Banyasz et al., 2011). Previous

data from this laboratory as well as existing literature, has shown the deterioration and significant remodelling of $Ca^{2+}$ and $K^{+}$ channels as well as many downstream signalling components of the $\beta_1$AR mechanism with ageing (Xiao et al., 1994; Cheah and Lancaster, 2015b; Jones et al., 2007; Walker et al., 1993; Liu et al., 2000; Bao et al., 2013; Josephson et al., 2002; Lim et al., 1999; Zhu et al., 2005; Xu and Narayanan, 1998). A great deal of literature to date however has focused on age-related changes to such elements associated with the $\beta_1$AR mechanism in basal conditions, or under conditions of adrenergic stimulation that are not physiologically relevant. Age-related decline in such components involved in the $\beta_1$AR mechanism, particularly those involved in repolarisation, may underlie in part, the cardiac decrements in aged populations and help explain the loss of cardiac reserve and physical capacity in old age.

Furthermore, the demand for computational modelling in biomedical science and in turn cardiology has grown considerably in recent years, particularly in human-based investigations, as they provide an invaluable predictive tool (Winslow et al., 2012; Niederer et al., 2019). However, physiologically relevant computational models of the heart based on the most common models used in basic science (rodents) are not particularly abundant (Stevenson-Cocks, 2019). Aiding the development of a robust rat computational model - recently developed in our lab (Stevenson-Cocks, 2019) - through incorporating key information on how rat ventricular myocytes function under the varied and combined stress of adrenergic stimulation, increased rate and ageing will be an invaluable tool in future cellular cardiology investigations.

The hypotheses of this project were:

1. Basal APD is prolonged in aged rats and this prolongation exists irrespective of activation frequency changes. It was also hypothesised that APD response to adrenergic stimulation is reduced in old rats and this is potentiated by increases in activation frequency.
2. Peak basal LTCC current is similar between adult and old hearts when normalised to cell size, whilst peak current response to adrenergic stimulation is reduced.

3. Peak $I_{Ks}$ tail current response to adrenergic stimulation is reduced in aged hearts compared with adult hearts and this is reflected in a loss of influence on APD.
4. $I_{Ks}$, $I_{Kr}$ and $I_{K1}$ current response to adrenergic stimulation is blunted in old age, with $I_{Ks}$ current most affected. Further, it was hypothesised that during control conditions $I_{Ks}$ current is reduced whilst $I_{Kr}$ and $I_{K1}$ is unaffected in old age.

The aims of this project were:

1. To assess the influence of age on AP form and response of ventricular myocytes to adrenergic stimulation.
2. To investigate key components of the AP that may be responsible for the duration of the AP and thus set minimal stable cycle length of the heart during exercise.
3. To further develop and use a computational electrophysiological rat heart model recently developed in our lab to test the relative influence of observed changes in ionic currents along with those documented by others with the view to facilitate the future generation of an aged heart model capable of recreating the AP and AP response to adrenergic stimulation observed in this work and others.

# Chapter 2: Materials and Methods

## 2.1 Experimental Animals and Cardiomyocyte Isolation

### 2.1.1 Experimental Animals

Adult (3 months of age) and old (22 - 23 months of age) male Wistar rats were housed in the Animal Unit, Faculty of Biological Sciences, University of Leeds. Animals were situated in environmentally controlled rooms subject to 12-hour light: dark cycles with food and water provided ad libitum. All rats used in this study were either 3 months of age (adult: 146 – 215 g) or 22 – 23 months of age (old: 306 – 448 g weight), at time of sacrifice. Adult rats were sacrificed by concussion of the brain by striking the cranium, followed by cervical dislocation, whilst old rats were sacrificed using rising $CO_2$ exposure in accordance with Schedule One methods stated in the Animals (Scientific Procedures) Act, 1986 and approved by the University of Leeds ethics committee.

A rat model was used for the duration of this project as rats are a mammalian species that were readily available and have been widely used for the study of ageing and age-related electrophysiological cardiac remodelling which is beneficial for relatively easy comparison to historical literature (Josephson et al., 2002; Liu et al., 2000; Walker et al., 1993; Farrell and Howlett, 2008; Scarpace et al., 1991; Tobise et al., 1994; Narayanan and Derby, 1982; Olgar et al., 2022). As mentioned in section 1.8, in the absence of availability of larger mammal species, rats present a useful alternative for the study of cardiac ageing due to their expedited ageing compared with other mammals, as well as their low cost, ease of handling and ability to control interferences of external factors throughout an entire lifespan (Joukar, 2021). In addition, rats are prone to similar cardiovascular disorders as humans and are also host to similar ion channels as humans, though their function and influence on repolarisation varies (Joukar, 2021). More specifically, a male rat model was used throughout this project largely due to greater availability, whilst the greater catalogue of relevant evidence in male rats from similar research increased the ease of comparison to large quantities of literature. However the extension of such research to females is important and requires further investigation directly evaluating sex-specific

age-related cardiac remodelling to better understand cardiac ageing within the entire human species.

### 2.1.2 Cardiomyocyte Isolation

Ventricular myocytes of adult male Wistar rats were isolated in part by the researcher and in part by another research group (Dr Z. Yang, Dr H. Kirton, Dr D. Steele.). Hearts were obtained from rats, euthanized by methods explained above (section 2.1.1.1) and immediately placed in rat isolation solution ($Ca^{2+}$-free). Excised hearts were rapidly cannulated via the aorta and perfused using the Langendorff approach at a constant flow rate of 3.5 – 4 mls per minute. Old rat hearts were placed initially in cardioplegic solution for approximately 5 minutes prior to the transfer onto the Langendorff apparatus. This approach was necessitated by changes to operating environment due to COVID-19 restrictions. Hearts were perfused at 37°C, using retrograde constant flow, with rat perfusion solution containing 750 µM calcium chloride ($CaCl_2$) for several minutes until blood was removed. Hearts were then perfused in rat $Ca^{2+}$ buffer solution containing 100 µM ethylene glycol-bis(β-aminoethyl ether)-N,N,N′,N′-tetraacetic acid (EGTA) for approximately 3 minutes. Hearts were perfused further with rat enzyme containing solution (~ 8 - 13 minutes). All solutions perfused via Langendorff methods were bubbled with oxygen (100%; BOC). Next, both left and right rat ventricles were removed just below the valve annulus, dissected, finely chopped, placed in a conical flask, and gently shaken at 37°C (500 - 550 oscillations/ minute) in 4 ml of rat enzyme (collagenase and protease) containing solution for 5-minute intervals using a temperature-controlled water bath (Grant Instruments) with attached shaker (Stuart Scientific, Keison Products). After, myocytes were filtered through nylon gauze (200 µm) into a falcon tube (15 ml graduated, CELLSTAR, Greiner Bio-One) and centrifuged (500 rpm x 45 - 60 s) (Rotina 46R, Hettich Zentrifugen) to remove supernatant. Myocytes were washed once more and re-suspended in rat perfusion solution containing 750 µM $CaCl_2$, stored at room temperature and used within 6 - 8 hours. Leftover heart tissue was placed back into a conical flask and shaken in rat enzyme containing solution for a further 5 minutes. This process was repeated a maximum of 5 times or until remaining heart tissue turned pale in colour. Myocytes were assessed regularly under a microscope (CK2, Olympus) throughout the agitation process to ensure a high yield of quiescent rectangular striated myocytes with limited myocytes exhibiting spontaneous activity.

## 2.2 Electrophysiology Recordings

Cellular electrophysiology is the study of biological tissues with the aim to measure changes in current and / or voltage in order to understand the associated electrical properties and their response to manipulation (Penner, 1995). This manipulation can entail changes to internal and external environment as well as electrical and pharmaceutical alterations to tissues. Cellular electrophysiology can be performed on a number of different tissues and pursued through various modalities such as: sharp electrode, whole-cell, cell-attached, inside-out, outside-out and perforated patch-clamp (Sakmann and Neher, 1984; Penner, 1995). Throughout this project, ventricular myocytes were the sole tissue of interest, whilst whole-cell patch-clamp was used for all current-clamp, voltage-clamp and AP-clamp studies.

### 2.2.1 Electrophysiology Set Up

Normal rat Tyrode solution super-fused isolated ventricular myocytes placed in a 2 ml perfusion bath on the platform (Gibraltar, Burleigh) of a microscope (Olympus BX51). The microscope was held on an anti-vibration table within a Faraday cage to reduce electrical interference and noise. Tyrode solution perfused myocytes at a rate of 3 ml per minute (Fujisawa et al., 2000) via a peristaltic valve assembly (cF-8VS valve assembly, Cell MicroControls) and flow controller (cFlow Flow Controller, Cell MicroControls). Perfusion bath temperature was maintained at 37 ± 1°C (NBD TC2 Bip Temperature Controller, Cell MicroControls). Myocytes were allowed 5 minutes to settle after transfer into the perfusion bath. Myocytes were stimulated by glass pipettes filled with physiological pipette solution, unless otherwise stated, placed over a silver chloride (AgCl) coated silver wire electrode fitted to a headstage (CV203BU, Axon Instruments, Molecular Devices). The AgCl electrode was placed in bleach (Domestos) for at least 30 minutes weekly to re-introduce/ maintain the AgCl coating, rinsed with deionised water (dd$H_2O$) and air-dried before use. The headstage was moved along x, y and z axes via a micro manipulator using joystick and piezo motor controls (PCS-6000, Exfo, Burleigh). A low-noise amp meter (AxoPatch 200B integrating patch-clamp, Axon CNS, Molecular Devices) was used to measure electrical activity of myocytes. A data acquisition system (pCLAMP 9.0 software; Digidata 1440A, Axon CNS, Molecular Devices) was used to digitise all electrophysiological data within Clampex (Version 10.7). Glass pipettes were pulled

from borosilicate glass capillary tubes (1.5 mm O.D x 1.16 mm I.D, Harvard Apparatus) using a two-stage pipette puller (PIP5, Heka). Low resistance glass pipettes were used for all whole-cell patch-clamp experiments (4-8 MΩ) in order to optimise access resistance (Armstrong and Gilly, 1992).

### 2.2.2 Whole-Cell Patch-Clamp

The performance of the whole-cell patch-clamp technique required the gentle application of a glass pipette filled with physiological solution to the surface of a myocyte membrane. A small amount of positive pressure (via syringe) was applied upon approach and upon contact with the myocyte membrane. Once contact was made between the myocyte membrane and the glass pipette, brief gentle negative pressure was produced via suction to achieve gigaseal formation (1 GΩ). A further rapid brief suction applied to the membrane enabled whole-cell configuration through the rupturing of a piece of membrane and subsequent mixing with pipette solution. During this process, several key factors were adhered to. Prior to myocyte membrane contact, the pipette voltage offset was set to zero to attenuate the sum of liquid potentials. Liquid junction potential was calculated as ~ 7 mV, though this was not adjusted for. Upon gigaseal formation, capacitance was compensated to remove capacitance from the glass pipette, minimise noise and reduce voltage delay during recording. Finally series resistance was considered and compensated for (≥ 80 %) (Armstrong and Gilly, 1992).

When a single electrode system is used during patch-clamp as opposed to two electrode systems, current is applied and measured in the same electrode. This can cause voltage drop and impair the ability to maintain or rapidly inject sufficient current to obtain a set voltage during voltage-clamp experiments (Armstrong and Gilly, 1992). This problem can also impact current-clamp experiments by harming the current input required to induce a voltage change. Issues arising as a result of series resistance and capacitance can be dampened, though not negated, by using low resistance pipettes, achieving a stable series resistance, monitoring series resistance throughout and also by performing compensation (Armstrong and Gilly, 1992).

### 2.2.3 Current-Clamp

All current-clamp experiments adhered to the electrophysiology set up outlined previously (section 2.2.1). Action potentials, evoked by 2 ms (~ 1.5 nA) current pulses, were achieved in current-clamp mode using standard whole-cell patch-clamp techniques (Axopatch-200B amplifier, Axon Instruments; pCLAMP 9.0 software, Molecular Devices). In whole-cell mode, after gigaseal formation and membrane rupture, APs were recorded (1 - 2 minutes), via repeated sweep sequences, at pre-determined experimental frequencies separated by a period of pre-conditioning (30 - 90 s). All experimental drugs were administered at the same flow rate defined for Tyrode superfusion (section 2.2.1). Action potentials were recorded at the same pre-determined frequencies once more after a specified period which enabled full drug equilibration. When multiple experimental drugs were administered, adequate washout time was allowed prior to introduction of further drugs. After termination of a patch-clamp session for all myocytes, the perfusion bath was completely removed and washed 3 times in normal Tyrode solution before patching new cells. Action potential signals were sampled at 5000 KHz after low-pass filtering at 1 KHz. Three – five steady-state AP traces for each separate experimental group or experimental intervention in each cell were averaged and analysed using Clampfit 10.7 software. Action potential variables: $APD_{25}$, $APD_{50}$, $APD_{75}$, $APD_{90}$ and $APD_{100}$, defined as the time for the AP to return to 25, 50, 75, 90 and 100 % of the diastolic voltage after the peak of the initial upstroke, were measured in each averaged AP (figure 9). Most current-clamp experiments also included measurement of upstroke velocity (rate of AP depolarisation from onset to peak), diastolic membrane potential (membrane potential recorded during diastolic interval) and AP amplitude (difference between peak membrane potential achieved during depolarisation and diastolic membrane potential). These steps were repeated for all current-clamp experiments.

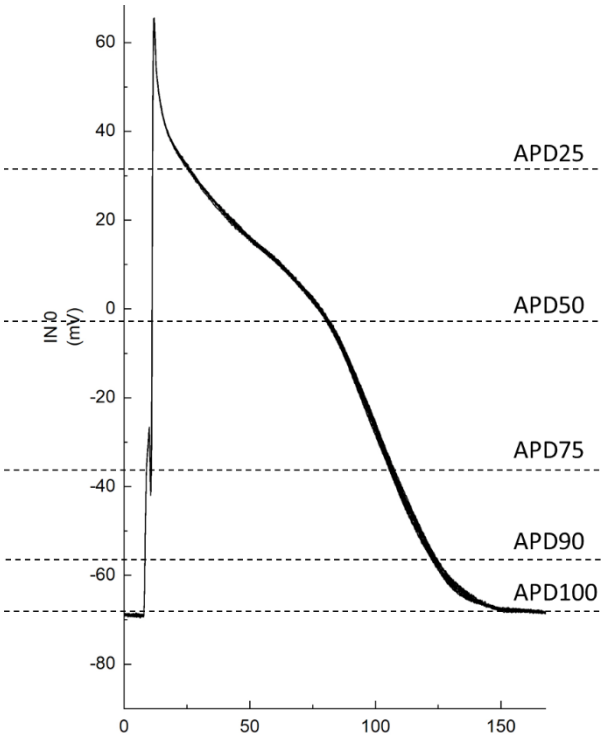


Figure 9. AP recording from a Wistar rat displaying APD variable breakdown.

### 2.2.4 Voltage-Clamp

All voltage-clamp experiments adhered to the electrophysiology set up outlined previously (section 2.2.1). After achievement of whole-cell configuration, ventricular myocytes were stimulated using pre-determined voltage-clamp protocols involving depolarising square test pulses from a specified holding potential. Several voltage-clamp recordings were obtained for each experimental condition or experimental intervention and later averaged during analysis using Clampfit software. Pre-conditioning periods of 1 - 2 minutes were allowed prior to all recordings. Once more, experimental drugs were administered at the same flow rate defined for Tyrode superfusion (section 2.2.1). Recordings were repeated after specified durations which enabled full drug equilibration and washout periods were allowed prior to further drug superfusion. Voltage-clamp signals were sampled at 5000 KHz after low-pass filtering at 1 KHz. All voltage-clamp data was normalised to cell capacitance (I / Cm) to prevent cell size bias. Cell capacitance was calculated using 10 mV square pulses. These steps were repeated for all voltage-clamp experiments.

### 2.2.5 AP-Clamp

All AP-clamp experiments adhered to the electrophysiology set up outlined previously (section 2.2.1). Using whole-cell patch-clamp techniques (Axopatch-200B amplifier, Axon Instruments; pCLAMP 9.0 software, Molecular Devices), APs were evoked by 2 ms pulses initially in current-clamp mode. Action potentials were stimulated at 1 Hz via repeated sweep sequences for approximately 3 minutes to achieve steady state. The steady-state AP was recorded prior to switching to voltage-clamp mode. After switching to voltage-clamp mode, the cells own steady-state AP provided the command voltage for further cell recording (Banyasz et al., 2014; Banyasz et al., 2011). The initial recording should display zero current and represent a baseline prior to adding ion channel blockers. Specific ion channel blockers were applied sequentially (Banyasz et al., 2014; Banyasz et al., 2011) at the same flow rate defined for Tyrode superfusion (section 2.2.1). Adequate equilibration times and, where necessary, washout times were adhered to for all drugs used during experiments. After the application of each blocker, compensatory currents were elicited and recorded (Banyasz et al., 2014; Banyasz et al., 2011). Compensatory currents were subtracted from the baseline current or the previous compensatory current during later offline analysis, revealing the contribution of each ion channel during the cells own AP (Banyasz et al., 2014; Banyasz et al., 2011). All current data was normalised to cell capacitance (I / Cm) to prevent cell size bias. After cessation of all recordings for each myocyte, the perfusion bath was completely removed and washed 3 times in normal Tyrode solution before patching new cells. Action potential signals were sampled at 5000 KHz after low-pass filtering at 1 KHz. All AP-clamp recordings were analysed using Clampfit 10.7 software.

## 2.3 Computational Modelling

Computational modelling allows the scientific investigation of a chosen system through computer-based simulations using a combination of mathematics, physics and computational science resources (Brodland, 2015). As described in chapter 1 (section 1.8), relevant data is incorporated into computational models, which then perform simulations that can be compared with existing laboratory evidence and allow equally for model validation and experimental prediction (Brodland, 2015; Niederer and Smith, 2012). Computational modelling can help alleviate many of the numerous

necessary experiments and enable the faster realisation of vital experiments in research.

### 2.3.1 Computational Model Structure

This study used a computational model recently developed within our laboratory (Stevenson-Cocks, 2019). This Model (the Leeds Rat (LR) model), based on previous works by Gattoni and Colman (Stevenson-Cocks, 2019; Colman et al., 2017; Colman, 2019; Gattoni et al., 2016), was designed to replicate the rat ventricular myocyte AP. For the works in this project, the LR model underwent modification. Full methodology entailing model modifications, model structure, model variants and simulation protocols for all computational experiments are explained in chapter 7).

## 2.4 Statistical analysis

All data presented as mean ± standard error of the mean (SEM). Statistical analyses were completed using IBM statistics 26 software (SPSS Inc., Chicago, IL). The number of cells tested denoted by n and number of animals denoted by N throughout. The specifics of each data analyses and statistical comparison are described within the relevant results sections. Briefly, mixed analysis of variance (ANOVA) was used for comparison of all current-clamp, voltage-clamp and AP-clamp experiment data between adult and old hearts. Bonferroni post-hoc analyses were used for all experiments. All relevant statistical assumptions were met unless otherwise stated. Statistical significance set at $p < 0.05$. Confidence intervals were calculated using the formulae SEM x 1.96 for data involved in computational model development. Microsoft Excel (2016) was used to store, organise, and process all quantitative data. Origin 2018b was used to generate all experimental figures. Microsoft Word (2016) was used to produce all tables. All non-experimental figures were created using Microsoft PowerPoint (2016) and BioRender.

## 2.5 Experimental Drugs and Solutions

### 2.5.1 Extracellular Solutions

All materials purchased from Sigma unless otherwise stated. All molarity of solutions expressed in mM unless otherwise stated.

**Cardioplegic solution** Contained Glucose 277.5, KCl 30, $NaHCO_3$ 25 and Mannitol 34.3. Cardioplegic solution was placed in 50 ml falcon tubes and stored at -20°C until use. For each use, one 50 ml tube was defrosted overnight at 4°C and then placed in dry ice ready for use.

**Rat Isolation Solution ($Ca^{2+}$-free)** Contained NaCl 130, KCl 5.4, $MgCl_2$ 1.4 (Fluka), $NaH_2PO_4$ 0.4 (Acros Organics), HEPES 10, Glucose 10, Taurine 20, Creatine 10. The solution pH was titrated to 7.3 using NaOH (1 M) (BDH Laboratory Supplies) via a pH meter (SevenCompact, Toledo). Solution was stored at 0 - 4°C and used within 1 week.

**Rat Enzyme Containing Solution** Contained $Ca^{2+}$-free rat isolation solution (50 ml) with BSA (50 mg), protease (5 mg) and collagenase (50 mg) (type 2 Worthington, 0.1 mg/ml). Solution was prepared fresh for each use, stored at 37°C during use and discarded immediately after.

**Rat Calcium Buffer Solution** Contained 100 µM EGTA in $Ca^{2+}$ free rat isolation solution. Solution was stored at 0 - 4°C and used within 1 week.

**Rat Perfusion Solution** Contained 750 µM $CaCl_2$ in $Ca^{2+}$ free rat isolation solution. Solution was stored at 0 - 4°C and used within 1 week.

**Normal Rat Tyrode Solution** Contained NaCl 136, KCl 4, $MgCl_2$ 2, $CaCl_2$ 1, HEPES 10, Glucose 10. Tyrode solution pH was adjusted to 7.4 using NaOH (1 M). Solution was stored at 0 - 4°C and used within 1 week.

### 2.5.2 Intracellular Solutions

**Physiological Pipette Solution** Contained KCl 135, EGTA 10, HEPES 10, glucose 5. Solution pH was titrated to 7.2 using KOH (1 M) (Alfa Aesar). Solution was added to 5 ml vials and stored at -20°C. Upon use, vials were defrosted, stored at room temperature, and used within 4 days.

### 2.5.3 Experimental Drugs

**Isoproterenol** Is a non-selective βAR agonist. Isoproterenol was prepared as a 1 mM stock in $ddH_2O$ and stored at -20°C in 1ml Eppendorf vials for a maximum of 3 months. Upon use, vials were defrosted at room temperature, diluted with normal rat or mouse Tyrode to 5 nM, 100 nM or 1 µM concentrations and used within 6 hours.

**Chromanol 293b** Is a blocker of the $I_{Ks}$ current. Chromanol 293b (Tocris Bioscience) was prepared as a 6 mM stock solution in 0.5 ml dimethyl sulfoxide (DMSO) and stored at -20°C in Eppendorf vials for a maximum of 3 months. Upon use vials were defrosted at room temperature, diluted with 100 ml normal rat Tyrode and stirred thoroughly with gentle heating to 37°C. This provided a 30 µM chromanol 293b in 0.5 % DMSO solution ready for use. Combined chromanol 293b and isoproterenol solutions were made following the same procedure mentioned above with isoproterenol added to achieve the desired isoproterenol concentration (5 nM, 100 nM) in 30 µM chromanol 293b. Solutions were used within 6 hours.

**E4031** Is a selective blocker of the $I_{Kr}$ current. E4031 was prepared as a 1 mM stock solution in $ddH_2O$ and stored at -20°C in Eppendorf vials for a maximum of 3 months. Upon use, vials were defrosted at room temperature, diluted with normal rat Tyrode solution to achieve a 1 µM solution ready for use. In AP-clamp experiments, E4031 (1 µM) was combined with Chromanol 239B (30 µM) to adhere to the required sequential block. Furthermore, in the same experiments, the further addition of 100 nM isoproterenol created the combined isoproterenol and blocker solution.

**Barium chloride** Is a selective blocker of the $I_{K1}$ current. Barium chloride (Brand details) was prepared as a 1 mM stock solution in $ddH_2O$ and stored at -20°C in Eppendorf vials for a maximum of 3 months. Upon use, vials were defrosted at room temperature, diluted with normal rat Tyrode solution to achieve a 50 µM solution ready for use. In AP-clamp experiments, $BaCl_2$ (50 µM) was combined with Chromanol 239B (30 µM) and E4031 (1 µM) to adhere to the required sequential block. Furthermore, in the same experiments, the further addition of 100 nM isoproterenol created the combined isoproterenol and blocker solution.

# Chapter 3: Effects of Ageing on APD Responses to Adrenergic Stimulation and Changes in Activation Frequency in Rat Ventricular Myocytes

## 3.1 Introduction

The cardiac AP is understood to have an important role in excitation-contraction coupling, providing the link between electrical activity and its transduction to a global contraction. Action potentials are commonly measured in research investigating arrhythmogenesis, disease and cardiac ageing, to improve understanding of the link between changes in excitation and its translation to the decline or limitation in global mechanical function (Liu et al., 2000; Gan et al., 2013; Herraiz et al., 2013; Feridooni et al., 2015; Sorrentino et al., 2016; Li et al., 2004). Research has implicated AP repolarisation as a key component of the ageing phenomenon which may, in part, explain the limitation in cardiac reserve (Feridooni et al., 2015).

Action potential repolarisation is widely accepted to become compromised with age, by prolonging APD (Feridooni et al., 2015). The prolongation in APD is considered to help maintain contractility by providing inotropic support at the expense of chronotropic reserve (Janczewski et al., 2002; Capasso et al., 1983a). Existing research has frequently displayed increased $APD_{50}$ and $APD_{90}$ to magnitudes ranging between 6 - 38 % in old compared with adult rat and dog models (Liu et al., 2000; Liu et al., 2014; Gan et al., 2013; Feridooni et al., 2015; Huang et al., 2006; Waldeyer et al., 2009; Feridooni et al., 2017), with some evidence indicating even greater prolongation of $APD_{50\text{-}90}$ between ~ 100 – 300 % in old compared with adult hearts (Capasso et al., 1983a; Walker et al., 1993). In humans, advanced age is associated with prolonged QT interval (Reardon and Malik, 1996; Rabkin et al., 2016). Such prolongation of repolarisation in old age may have significant consequences for overall cardiac function and may constrict the repolarisation reserve. This may limit the AP shortening typically required to cope with the onset of stress and the associated increased demand

for greater CO. Indeed, a poorer response to adrenergic stimuli is widely considered to occur with ageing, contributing to age-related limitations in cardiac reserve (Ferrara et al., 2014). Despite this common standpoint however, very little evidence exists demonstrating age-related losses in AP response to adrenergic stimulation. In fact, some evidence suggests adrenergic response is maintained (Farrell and Howlett, 2007; Stuart et al., 2018). However, the downregulation of several components directly and indirectly involved in the $\beta_1$AR mechanism cascade, acknowledged to develop with ageing, may support the deterioration of the AP response to adrenergic stimulation (Ferrara et al., 2014; Farrell and Howlett, 2007). This is because alterations in $Ca^{2+}$ and $K^+$ channels have been implicated in the deteriorating $\beta_1$AR mechanism and are responsible, in part, for modulating the balance of AP depolarisation and repolarisation (Stuart et al., 2018; Feridooni et al., 2017; Janczewski et al., 2002; Jeevaratnam et al., 2017; Lakatta and Sollott, 2002).

In experimental settings, APs are typically measured at a fixed activation frequency reflecting a fixed HR (Banyasz et al., 2014; Bao et al., 2013; Kang et al., 2017). This is also common practice in studies which have investigated the impact of isoproterenol in isolated cells, where a single and sometimes saturating dose of the adrenergic stimulant is used (Sala et al., 2017; Stuart et al., 2018; Kang et al., 2017; Wang and Fitts, 2017). Whilst this provides some information on adrenergic response, often it is not a good approximation of a normal physiological response. Onset of adrenergic stimuli such as exercise, usually upregulates both activation frequency and contractility in order to provide enhanced CO (Ogawa et al., 1992; Fujita et al., 2017; Lakatta et al., 2010; Liu et al., 2014; Roh et al., 2016; Stratton et al., 2003). Therefore, measurements taken at one frequency, miss out on potential changes occurring at greater frequencies and the respective interaction with contractile changes provided by adrenergic stimulation. The use of a single or saturating dose also risks changes in sensitivity to be undiscovered. Furthermore, the fixed activation frequencies often used, are much lower than physiological resting HR's of the animal model being used (Liu et al., 2000; Gan et al., 2013; Farrell and Howlett, 2007; Banyasz et al., 2014; Cerbai et al., 1994; Bao et al., 2013; Kang et al., 2017; Natali et al., 2002; Sala et al., 2017). Such low activation rates are used due to the increased stability that it provides and thus enables greater manipulation of other factors, such as the administration of drugs or the changing of extracellular solutions. It may be that information obtained

at low activation rates is transferable to physiologically relevant rates, however this requires evidence throughout a range of activation frequencies and has not yet been established.

To date, no studies have assessed the AP response to varying doses of adrenergic stimuli at a range of physiological frequencies in old compared with adult hearts. Therefore, the initial objective of this research project was to measure AP responses to isoproterenol superfusion at increasing doses, as well as changes in activation frequency separately and combined in adult and old rat ventricular myocytes. This would allow the quantification of cellular excitatory responses to changes in rate and contractility in adult and old hearts, and help to confirm whether a decline in AP response to adrenergic stimulation exists alongside well documented age-related basal APD prolongation. Isoproterenol was chosen as a result of the intended focus on APD changes in response to βAR signalling as opposed to the combined βAR and αAR signalling provided by epinephrine and norephinephrine.

## 3.2 Methods

### 3.2.1 Specific Experimental Procedures

Steady-state APs of adult (3 months of age) and old (22 - 23 months of age) male Wistar rat ventricular myocytes (adult, n = 26; old, n = 22) were recorded via repeated sweep sequences at various frequencies (1, 2, 4, 6 Hz) during normal rat Tyrode superfusion and after isoproterenol superfusion at different doses (5 nM, 100 nM, 1 μM). Five minutes separated the introduction of the first isoproterenol dose (5 nM) and the recording of subsequent AP traces (Harding et al., 1988; Lim et al., 1999; Johnson et al., 2012). Two minutes separated the introduction of each further isoproterenol dose (100 nM, 1 μM) and their subsequent respective AP recordings (Wang and Fitts, 2020; Wang and Fitts, 2017). Steady-state AP data (3 – 5 traces) were averaged in each cell at each frequency before and after each isoproterenol dose: $APD_{25}$, $APD_{50}$, $APD_{75}$, $APD_{90}$, $APD_{100}$, upstroke velocity, AP amplitude and diastolic membrane potential were subsequently measured. All cell data was then averaged per heart and compared between adult (N = 12) and old (N = 12) rats. Elements of the data were also used for comparisons to computational simulation findings (chapter 7).

### 3.2.2 Specific Statistical Analyses

A Mixed ANOVA was performed on all AP data to provide comparison between adult (3 months of age) and old (22 – 23 months of age) rat hearts across all pacing frequencies (1 – 6 Hz) and isoproterenol doses (5 nM; 100 nM; 1 μM). In cases where variables violated the assumption of approximate normal distribution, data transformations (log 10) were used. Data transformations (log 10) were performed on $APD_{25}$, $APD_{50}$, $APD_{75}$, $APD_{90}$ and $APD_{100}$ and in all cases satisfied the assumption of approximate normal distribution. Where assumptions of sphericity were violated, the Huynh Feldt correction was used. Where assumptions of homogeneity were violated (AP amplitude; $APD_{25}$; upstroke velocity), Tamhane's T2 was used. In variables where the assumption of no significant outliers was violated (AP amplitude; upstroke velocity), data Winsorization was performed (Kwak and Kim, 2017; Liao et al., 2016). In both cases, data Winsorization of these significant outliers did not significantly alter the outcome of the mixed ANOVA compared with non-Winsorized data. All other mixed ANOVA assumptions were met.

## 3.3 Results

### 3.3.1 Brief Summary of Recordings

Current-clamp recordings at 1 – 6 Hz pacing frequencies and 5 nM - 1 μM isoproterenol doses were successfully collected in adult (N = 12; n = 26) and old rat ventricular myocytes (N = 12; n = 22). Similar recordings were successfully achieved for a greater range of pacing frequencies (1 – 10 Hz) in adult rat ventricular myocytes (Howlett et al., 2022) enabling the behaviour of ventricular myocyte AP's and their response to isoproterenol to be studied across a full range of physiological pacing frequencies in the rat. However, ventricular myocytes were unable to maintain pacing at 10 Hz for the duration required to obtain successful recordings in old rats. Myocytes were able to maintain pacing more successfully at 8 Hz in the old rat, though yielded considerably less data compared with 6 Hz pacing. Average access resistance was 22 ± 1.0 MΩ. Average cell capacitance was 142 ± 9.6 pF in adult rats and 158 ± 10.6 pF in old rats. An unpaired t-test found no significant difference in cell capacitance between adult and old rats ($p = 0.301$). Examples of raw recordings are shown in figure 10. Figure 10 A and B shows an initial prolongation in APD in response to increasing pacing frequency followed by shortening at higher pacing frequencies that more closely reflect physiologically relevant rat HR (6 Hz). Figure 10 C shows a

prolongation of AP plateau and late AP repolarisation in old rats. Moreover, figure 10 D – G shows mild – moderate isoproterenol-induced APD shortening in adult and old rats at the most commonly used pacing frequency in research (1 Hz) and the most physiologically relevant pacing frequency used in this study (6 Hz). In this example, the isoproterenol-induced APD shortening appears slightly blunted in old rats particularly at increased pacing, though a shortening effect is still visible. Also, visually, the APD remodelling that occurs in response to changes in pacing was observed in both adult and old rats, though the AP phases most impacted appear slightly different in this example.

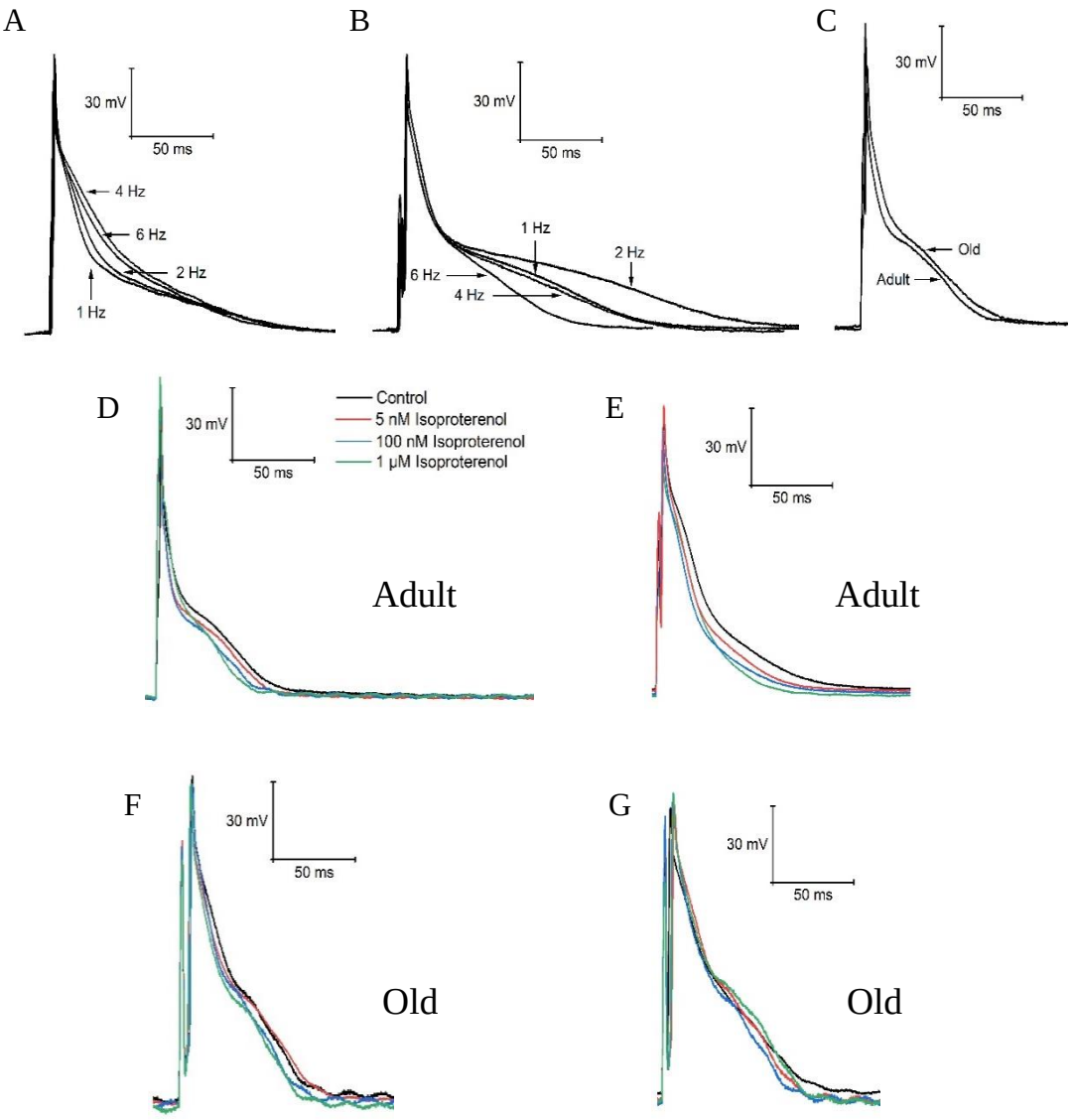


Figure 10. Example overlaid APs from typical electrophysiological recordings of adult and old rat ventricular myocytes illustrating the effects of varied pacing frequency and isoproterenol stimulation. (A) AP traces during 1 – 6 Hz pacing in adult rats. (B) AP traces during 1 – 6 Hz pacing in old rats. (C) AP traces during 1 Hz pacing comparing adult and old rats. (D) Adult rat AP traces during isoproterenol stimulation (5 nM, 100 nM, 1 μM) at 1 Hz. (E) Adult rat AP traces during isoproterenol stimulation at 6 Hz. (F) Old rat AP traces during isoproterenol stimulation at 1 Hz. (G) Old rat AP traces during isoproterenol stimulation at 6 Hz.

### 3.3.2 $APD_{25}$ / Early AP Repolarisation

Significant main effects were found in $APD_{25}$ with isoproterenol superfusion ($p = 0.025$) and changes in pacing frequency ($p < 0.001$). No significant main ageing effects ($p = 0.985$) or interactions between ageing, isoproterenol and pacing frequency ($p > 0.115$) were found. Post hoc analyses revealed $APD_{25}$ was prolonged during 1 μM isoproterenol superfusion compared with 100 nM isoproterenol superfusion (figure 11 A - D) ($p = 0.005$). In addition, $APD_{25}$ was prolonged at 6 Hz pacing compared with 1 – 4 Hz; 4 Hz pacing compared with 1 – 2 Hz and 2 Hz pacing compared with 1 Hz (figure 11 C - E) ($p < 0.02$).

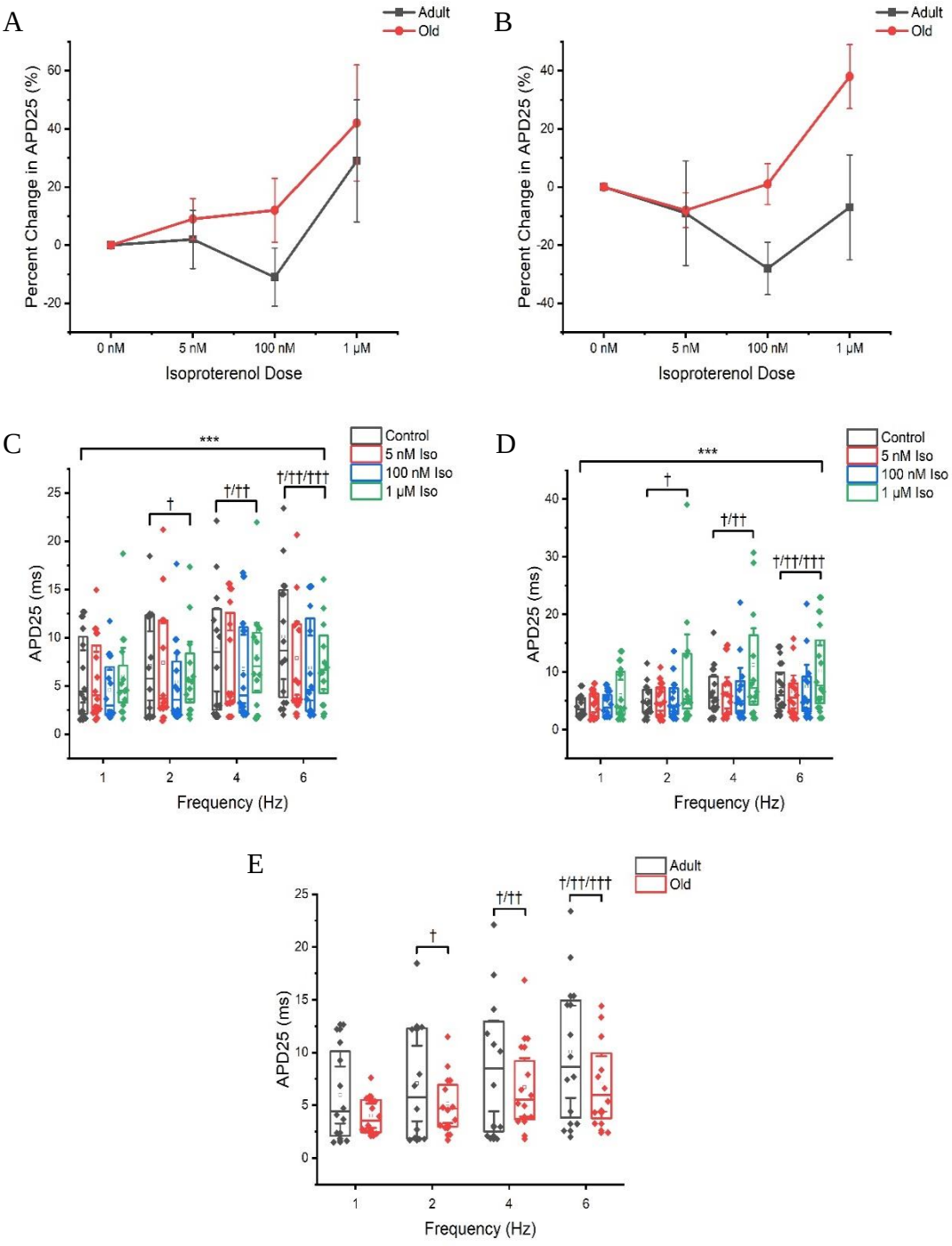
A
Adult
Old
Percent Change in APD25 (%)
60
40
20
0
-20
0 nM
5 nM
100 nM
1 µM
Isoproterenol Dose
B
Adult
Old
Percent Change in APD25 (%)
40
20
0
-20
-40
0 nM
5 nM
100 nM
1 µM
Isoproterenol Dose
C
***
†
†/††
†/††/†††
Control
5 nM Iso
100 nM Iso
1 µM Iso
APD25 (ms)
25
20
15
10
5
0
1
2
4
6
Frequency (Hz)
D
***
†
†/††
†/††/†††
Control
5 nM Iso
100 nM Iso
1 µM Iso
APD25 (ms)
40
30
20
10
0
1
2
4
6
Frequency (Hz)
E
†
†/††
†/††/†††
Adult
Old
APD25 (ms)
25
20
15
10
5
0
1
2
4
6
Frequency (Hz)

Figure 11. Plots demonstrating the average isoproterenol responses per animal at 1 Hz (A) and 6 Hz pacing (B) (SEM error bars), alongside the combined responses to varied pacing (1 – 6 Hz) and levels of adrenergic stimulation (5 nM, 100 nM, 1 μM isoproterenol) in early AP repolarisation ($APD_{25}$) in adult (C) and old (D) rats. (E) Comparative adult and old APD responses across the range of pacing frequencies under control conditions. *** Indicates a significant difference between 1 μM and 100 nM isoproterenol. † Indicates a significant difference compared with 1 Hz. †† Indicates a significant difference compared with 2 Hz. ††† Indicates a significant difference compared with 4 Hz. Box plots display mean (open square), median (solid middle line), upper, and lower quartiles (solid upper and lower lines) and confidence intervals (error bars).

### 3.3.3 $APD_{50}$ / AP Plateau

No significant ageing effects ($p = 0.816$) or ageing interactions with isoproterenol or pacing frequency ($p = 0.326$) were observed in $APD_{50}$, though the results showed a trend toward greater $APD_{50}$ shortening in adult rats during 5 – 100 nM isoproterenol stimulation compared with control conditions and a trend toward $APD_{50}$ prolongation at 1 μM isoproterenol stimulation in old rats (figure 12 A – D) ($p = 0.071$; partial $eta^2 = 0.112$). However significant main effects were yielded in isoproterenol ($p = 0.001$), pacing frequency ($p = < 0.001$) and isoproterenol*pacing frequency interaction ($p = 0.038$). Post hoc analyses found: $APD_{50}$ was shortened during 100 nM isoproterenol stimulation compared with control at 1 - 6 Hz (figure 12 C – D) ($p < 0.05$). Meanwhile, 5 nM isoproterenol stimulation only shortened $APD_{50}$ compared with control during 1 Hz pacing (figure 12 C – D) ($p < 0.02$). However, 1 μM isoproterenol stimulation prolonged $APD_{50}$ compared with 100 nM at 1 - 6 Hz (figure 12 C – D) ($p < 0.03$). Pacing at 2 – 6 Hz prolonged $APD_{50}$ compared with 1 Hz during 5 nM, 100 nM and 1 μM isoproterenol stimulation (figure 12 C – D) ($p < 0.01$) but not during control conditions (figure 12 E).

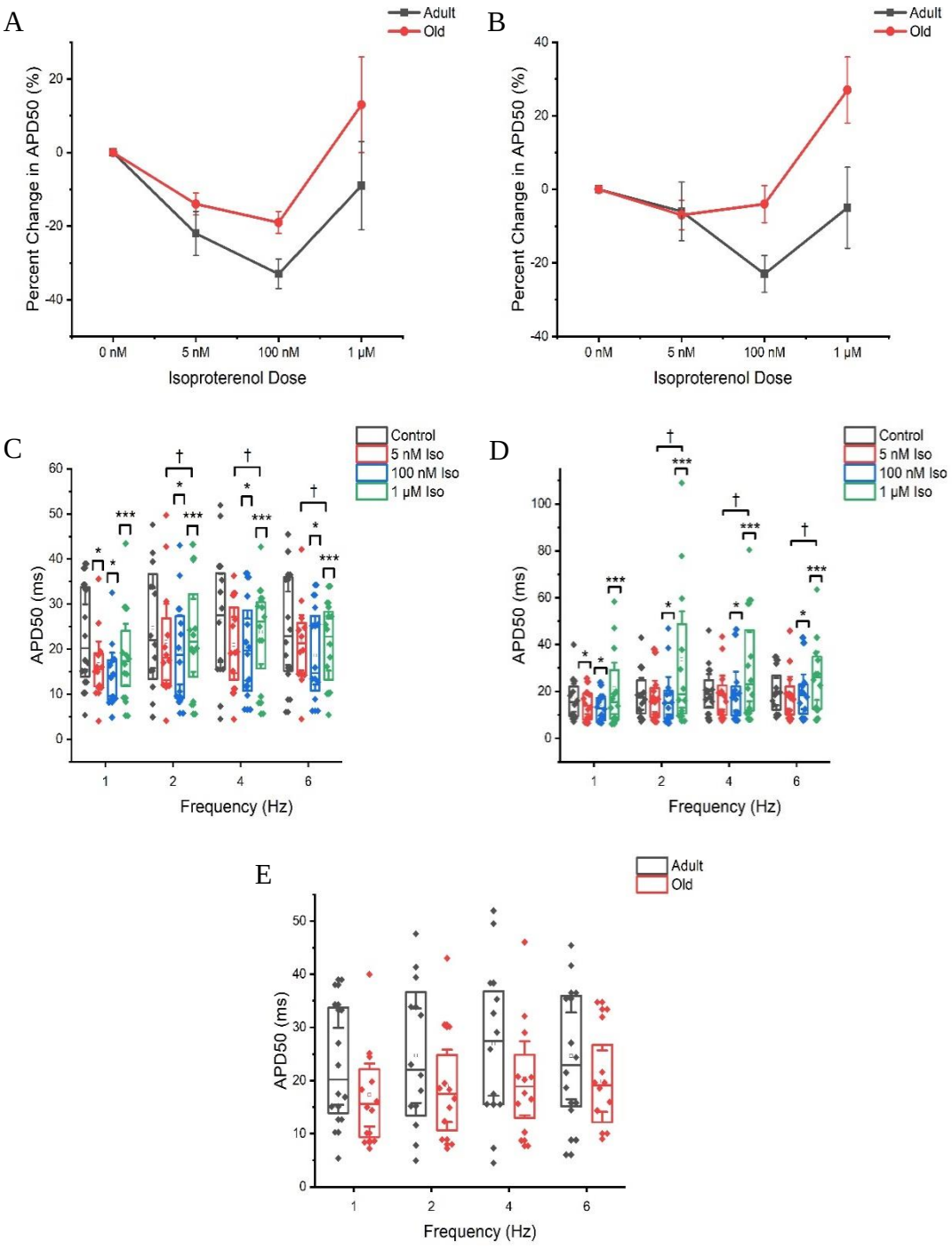
A
Adult
Old
Percent Change in APD50 (%)
20
0
-20
-40
0 nM
5 nM
100 nM
1 μM
Isoproterenol Dose
B
Adult
Old
Percent Change in APD50 (%)
40
20
0
-20
-40
0 nM
5 nM
100 nM
1 μM
Isoproterenol Dose
C
Control
5 nM Iso
100 nM Iso
1 μM Iso
APD50 (ms)
60
50
40
30
20
10
0
1
2
4
6
Frequency (Hz)
D
Control
5 nM Iso
100 nM Iso
1 μM Iso
APD50 (ms)
100
80
60
40
20
0
1
2
4
6
Frequency (Hz)
E
Adult
Old
APD50 (ms)
50
40
30
20
10
0
1
2
4
6
Frequency (Hz)

Figure 12. Plots demonstrating the average isoproterenol responses per animal at 1 Hz (A) and 6 Hz pacing (B) (SEM error bars), alongside the combined responses to varied pacing (1 – 6 Hz) and levels of adrenergic stimulation (5 nM, 100 nM, 1 μM isoproterenol) in AP plateau ($APD_{50}$) in adult (C) and old (D) rats. (E) Comparative adult and old APD responses across the range of pacing frequencies under control conditions. * Indicates a significant difference compared with control. *** Indicates a significant difference between 1 μM and 100 nM isoproterenol. † Indicates a significant difference compared with 1 Hz. Box plots display mean (open square), median (solid middle line), upper, and lower quartiles (solid upper and lower lines) and confidence intervals (error bars).

### 3.3.4 $APD_{75}$ / Late AP Repolarisation

No significant interactions between ageing and pacing frequency were found in $APD_{75}$ ($p = 0.502$). Similarly, there were no significant effects of ageing ($p = 0.106$; partial $eta^2 = 0.114$) or ageing interactions with isoproterenol ($p = 0.077$; partial $eta^2 = 0.108$) observed, though the results showed a trend toward $APD_{75}$ prolongation in old rats compared with adult rats alongside a trend toward greater isoproterenol-induced $APD_{75}$ shortening in adult rats compared with old rats (figure 13 A – E). Significant differences were found in $APD_{75}$ with isoproterenol superfusion ($p = 0.001$) and changes in pacing frequency ($p < 0.001$) as well as a significant interaction between isoproterenol and pacing frequency ($p = 0.008$). Post hoc analyses show 100 nM isoproterenol stimulation shortened $APD_{75}$ compared with control at all pacing frequencies (figure 13 A – D) ($p < 0.05$). Superfusion of 5 nM and 1 μM isoproterenol shortened $APD_{75}$ compared with control only at 1 Hz pacing (figure 13 C – D) ($p < 0.01$). Similarly at 1 Hz pacing, $APD_{75}$ shortened during 100 nM isoproterenol stimulation compared with 5 nM (figure 13 C - D) ($p = 0.001$). Post hoc analyses also showed $APD_{75}$ was prolonged during 2 – 6 Hz pacing compared with 1 Hz at 100 nM and 1 μM isoproterenol stimulation (figure 13 C -D) ($p < 0.02$). Similarly, 2 – 4 Hz pacing prolonged $APD_{75}$ compared with 1 Hz at 5 nM isoproterenol stimulation ($p < 0.002$); while $APD_{75}$ shortened during 6 Hz pacing compared with 4 Hz at 5 nM and 100 nM isoproterenol stimulation (figure 13 C – D) ($p < 0.02$). No significant pacing effects were observed in $APD_{75}$ during control conditions (figure 13 E).

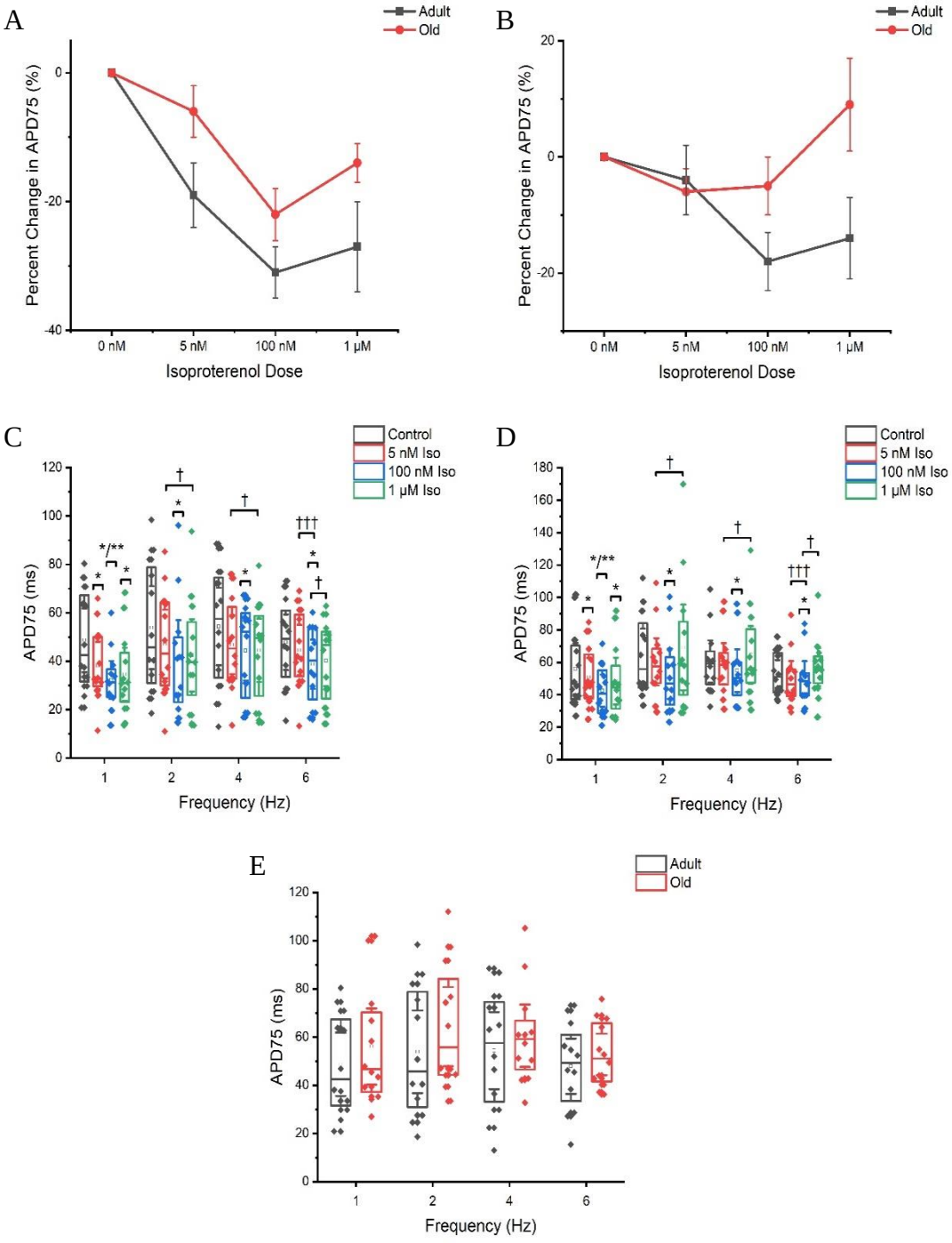
A
Adult
Old
Percent Change in APD75 (%)
0
-20
-40
0 nM
5 nM
100 nM
1 μM
Isoproterenol Dose
B
Adult
Old
Percent Change in APD75 (%)
20
0
-20
0 nM
5 nM
100 nM
1 μM
Isoproterenol Dose
C
Control
5 nM Iso
100 nM Iso
1 μM Iso
APD75 (ms)
120
100
80
60
40
20
0
*/**
*
*
†
*
†
*
†
†††
*
†
1
2
4
6
Frequency (Hz)
D
Control
5 nM Iso
100 nM Iso
1 μM Iso
APD75 (ms)
180
160
140
120
100
80
60
40
20
0
*/**
*
*
†
*
†
*
†
†††
*
†
1
2
4
6
Frequency (Hz)
E
Adult
Old
APD75 (ms)
120
100
80
60
40
20
0
1
2
4
6
Frequency (Hz)

Figure 13. Plots demonstrating the average isoproterenol responses per animal at 1 Hz (A) and 6 Hz pacing (B) (SEM error bars), alongside the combined responses to varied pacing (1 – 6 Hz) and levels of adrenergic stimulation (5 nM, 100 nM, 1 μM isoproterenol) in late AP repolarisation ($APD_{75}$) in adult (C) and old (D) rats. (E) Comparative adult and old APD responses across the range of pacing frequencies under control conditions. * Indicates a significant difference compared with control. ** Indicates a significant difference compared with 5 nM isoproterenol. † Indicates a significant difference compared with 1 Hz. ††† Indicates a significant difference compared with 4 Hz. Box plots display mean (open square), median (solid middle line), upper, and lower quartiles (solid upper and lower lines) and confidence intervals (error bars).

### 3.3.5 $APD_{90}$ / Late AP Repolarisation

The results show significant $APD_{90}$ main effects in ageing ($p = 0.034$), isoproterenol ($p < 0.001$) and pacing frequency ($p < 0.001$), alongside a significant isoproterenol*pacing frequency interaction (p 0.006) (figure 14 A – E). Post hoc analyses show $APD_{90}$ was prolonged in old rats compared with adult rats (figure 14 C – E) ($p = 0.034$). Post hoc analyses also found $APD_{90}$ shortened during 100 nM – 1 μM isoproterenol stimulation compared with control at 1 - 2 Hz pacing and compared with 5 nM stimulation at 1 Hz pacing (figure 14 A – D) ($p < 0.05$). 100 nM isoproterenol stimulation also shortened $APD_{90}$ compared with control at 4 – 6 Hz pacing (figure 14 A – D) ($p < 0.02$). Under control conditions and 5 nM isoproterenol stimulation: 2 Hz pacing prolonged $APD_{90}$ compared with 1 Hz (figure 14 C – E) ($p < 0.005$), 6 Hz pacing shortened $APD_{90}$ compared with 2 - 4 Hz (figure 14 C – E) ($p < 0.02$). During 100 nM and 1μM isoproterenol stimulation, 2 - 4 Hz pacing prolonged $APD_{90}$ compared with 1 Hz (figure 14 C – D) ($p < 0.001$). During 100 nM isoproterenol stimulation, 6 Hz pacing shortened $APD_{90}$ compared with 1 Hz (figure 14 C – D) ($p = 0.002$). No significant isoproterenol*ageing or pacing frequency*ageing interactions were observed ($p = 0.233$; $p = 0.373$).

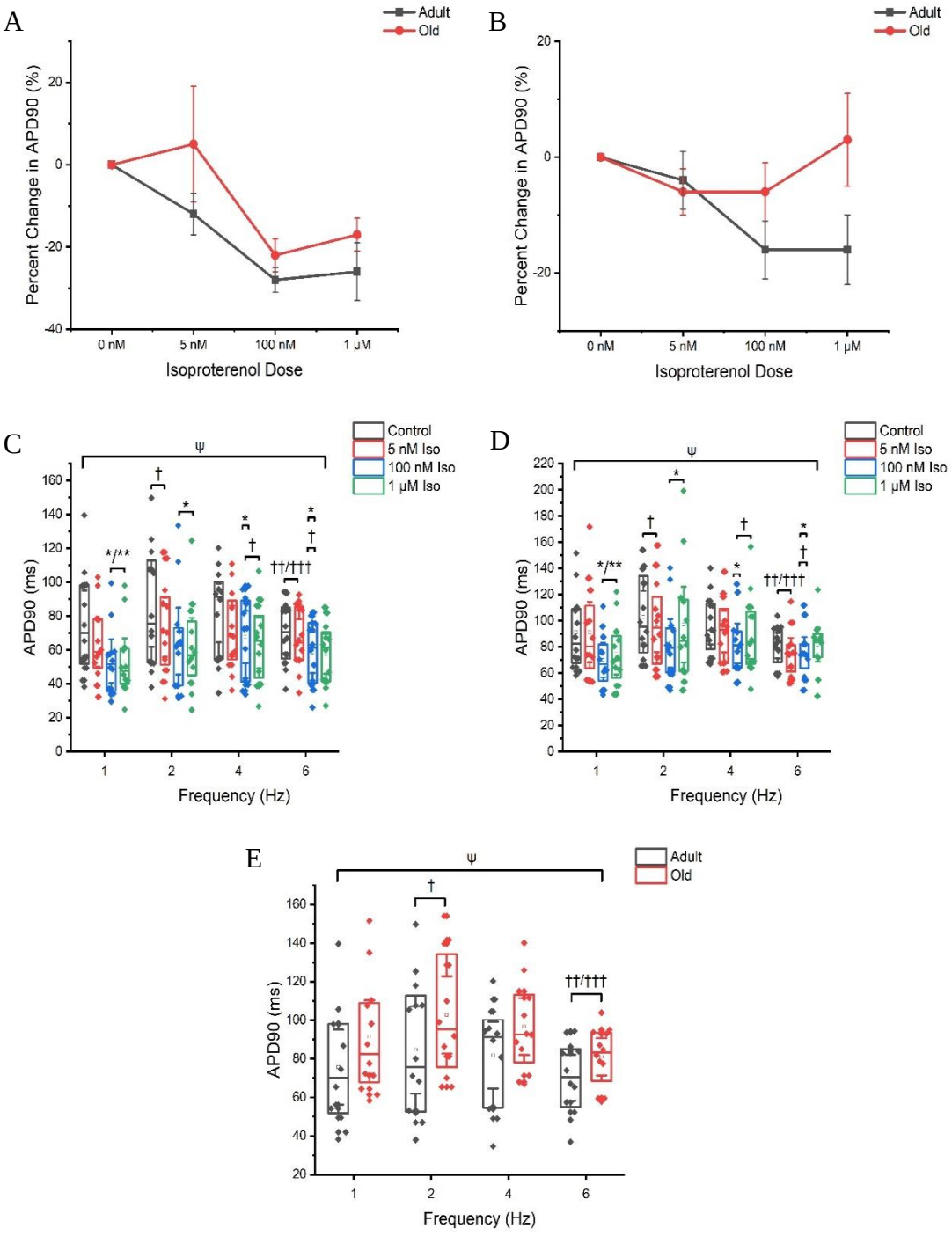
A
Adult
Old
Percent Change in APD90 (%)
20
0
-20
-40
0 nM
5 nM
100 nM
1 μM
Isoproterenol Dose
B
Adult
Old
Percent Change in APD90 (%)
20
0
-20
0 nM
5 nM
100 nM
1 μM
Isoproterenol Dose
C
Control
5 nM Iso
100 nM Iso
1 μM Iso
ψ
†
*
*
†
*
†
*/**
††/†††
APD90 (ms)
160
140
120
100
80
60
40
20
0
1
2
4
6
Frequency (Hz)
D
Control
5 nM Iso
100 nM Iso
1 μM Iso
ψ
*
†
*
†
†
*
*/**
††/†††
APD90 (ms)
220
200
180
160
140
120
100
80
60
40
20
0
1
2
4
6
Frequency (Hz)
E
Adult
Old
ψ
†
††/†††
APD90 (ms)
160
140
120
100
80
60
40
20
1
2
4
6
Frequency (Hz)

Figure 14. Plots demonstrating the average isoproterenol responses per animal at 1 Hz (A) and 6 Hz pacing (B) (SEM error bars), alongside the combined responses to varied pacing (1 – 6 Hz) and levels of adrenergic stimulation (5 nM, 100 nM, 1 μM isoproterenol) in late AP repolarisation ($APD_{90}$) in adult (C) and old (D) rats. (E) Comparative adult and old APD responses across the range of pacing frequencies under control conditions. Ψ Indicates a significant difference between adult and old rats. * Indicates a significant difference compared with control. ** Indicates a significant difference compared with 5 nM isoproterenol. † Indicates a significant difference compared with 1 Hz. †† Indicates a significant difference compared with 2 Hz. ††† Indicates a significant difference compared with 4 Hz. Box plots display mean (open square), median (solid middle line), upper, and lower quartiles (solid upper and lower lines) and confidence intervals (error bars).

### 3.3.6 $APD_{100}$ / Late AP Repolarisation

A Mixed ANOVA revealed significant main effects in $APD_{100}$ with isoproterenol ($p < 0.001$) and pacing frequency ($p < 0.001$) and a significant interaction between isoproterenol and pacing frequency ($p = 0.01$). The results yielded no significant ageing interactions or overall ageing effects, despite a trend toward $APD_{100}$ prolongation in old compared with adult rats ($p = 0.051$; partial $eta^2 = 0.162$). 100 nM – 1 μM isoproterenol stimulation shortened $APD_{100}$ compared with control at 1 – 4 Hz pacing ($p < 0.04$), whilst 100 nM isoproterenol stimulation alone shortened $APD_{100}$ at 6 Hz pacing ($p = 0.017$) (figure 15 A – D). 100 nM isoproterenol stimulation also shortened $APD_{100}$ compared with 5 nM at 1 Hz pacing only (figure 15 A – D) ($p < 0.01$). Post hoc analyses showed during 100 nM – 1 μM isoproterenol stimulation, 2 – 4 Hz pacing prolonged $APD_{100}$ compared with 1 Hz (figure 15 C – D) ($p < 0.04$). Significant reductions in $APD_{100}$ at 6 Hz pacing compared with 1 – 4 Hz ($p < 0.005$) during control conditions and 5 nM isoproterenol stimulation ($p < 0.01$) and compared with 2 – 4 Hz pacing during 100 nM and 1 μM isoproterenol stimulation were also observed ($p < 0.03$) (figure 15 A – E).

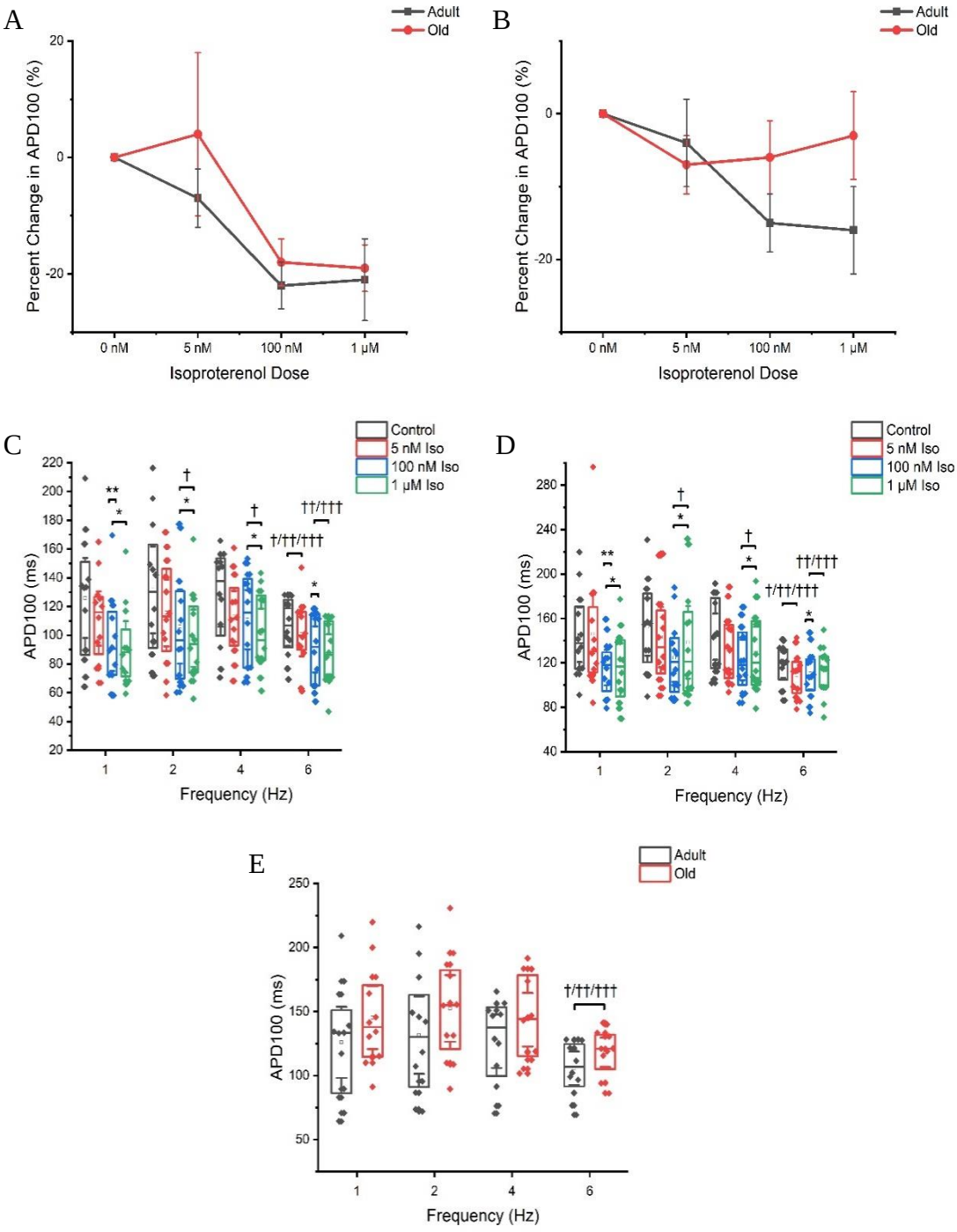
A
Adult
Old
Percent Change in APD100 (%)
20
0
-20
0 nM
5 nM
100 nM
1 μM
Isoproterenol Dose
B
Adult
Old
Percent Change in APD100 (%)
0
-20
0 nM
5 nM
100 nM
1 μM
Isoproterenol Dose
C
Control
5 nM Iso
100 nM Iso
1 μM Iso
APD100 (ms)
Frequency (Hz)
D
Control
5 nM Iso
100 nM Iso
1 μM Iso
APD100 (ms)
Frequency (Hz)
E
Adult
Old
APD100 (ms)
Frequency (Hz)

Figure 15. Plots demonstrating the average isoproterenol responses per animal at 1 Hz (A) and 6 Hz pacing (B) (SEM error bars), alongside the combined responses to varied pacing (1 – 6 Hz) and levels of adrenergic stimulation (5 nM, 100 nM, 1 μM isoproterenol) in late AP repolarisation ($APD_{100}$) in adult (C) and old (D) rats. (E) Comparative adult and old APD responses across the range of pacing frequencies under control conditions. * Indicates a significant difference compared with control. ** Indicates a significant difference compared with 5 nM isoproterenol. † Indicates a significant difference compared with 1 Hz. †† Indicates a significant difference compared with 2 Hz. ††† Indicates a significant difference compared with 4 Hz. Box plots display mean (open square), median (solid middle line), upper, and lower quartiles (solid upper and lower lines) and confidence intervals (error bars).

### 3.3.7 AP Amplitude

A mixed ANOVA found ageing yielded no significant effect on AP amplitude ($p = 0.644$). There were also no significant main effects for isoproterenol ($p = 0.073$) or isoproterenol*ageing ($p = 0.073$) interactions in AP amplitude, though a trend toward increased AP amplitude with high (100 nM) and saturating doses (1 μM) of isoproterenol in adult rats existed and showed a moderate to large effect (partial $eta^2 = 0.100$). No significant frequency*ageing or isoproterenol*frequency*ageing interactions in AP amplitude ($p = 0.513$; $p = 0.377$) were observed. However, a mixed ANOVA found AP amplitude was greater at 100 nM – 1 μM isoproterenol compared with control during 6 Hz pacing ($p < 0.04$). Under control conditions, AP amplitude was reduced at 6 Hz compared with 1 – 4 Hz pacing (table 4) ($p < 0.003$). AP amplitude was reduced at 4 Hz compared with 1 – 2 Hz pacing ($p < 0.003$). Similarly, AP amplitude was reduced at 2 Hz compared with 1 Hz pacing ($p < 0.003$). During 5 nM isoproterenol superfusion, AP amplitude was reduced at 4 - 6 Hz compared with 1 - 2 Hz pacing (table 4) ($p < 0.04$). During 100 nM isoproterenol stimulation, AP amplitude was reduced at 6 Hz compared with 1 – 2 Hz pacing ($p < 0.003$). AP amplitude was reduced at 4 Hz compared with 1 Hz pacing (table 4) ($p < 0.03$). During superfusion of a saturating isoproterenol dose (1 μM), AP amplitude was reduced at 4 Hz compared with 2 Hz pacing (table 4) ($p = 0.003$).

Table 4. Impact of pacing frequency and adrenergic stimulation on AP amplitude in adult and old rats. Data presented as mean (± SEM). * Indicates a significant difference compared with control. † Indicates a significant difference compared with 1 Hz. †† Indicates a significant difference compared with 2 Hz. ††† Indicates a significant difference compared with 4 Hz.

| Frequency (Hz) | | Control (mV) | | 5 nM Iso (mV) | | 100 nM Iso (mV) | | 1 μM Iso (mV) | |
|---|---|---|---|---|---|---|---|---|---|
| 1 | Adult | 118 | (4.6) | 112 | (2.3) | 119 | (2.5) | 116 | (4.5) |
| | Old | 117 | (1.6) | 113 | (1.2) | 113 | (1.6) | 114 | (1.7) |
| 2 | Adult | 113† | (4.4) | 111 | (2.6) | 118 | (3.8) | 117 | (3.3) |
| | Old | 112† | (1.7) | 112 | (1.6) | 112 | (1.9) | 112 | (1.8) |
| 4 | Adult | 107†/†† | (4.1) | 109†/†† | (3.4) | 115† | (2.8) | 114†† | (3.0) |
| | Old | 1.8†/†† | (2.5) | 110†/†† | (1.6) | 110† | (1.9) | 110†† | (1.8) |
| 6 | Adult | 101†/††/††† | (3.2) | 107†/†† | (3.7) | 112*/†/†† | (3.7) | 112* | (4.0) |
| | Old | 106†/††/††† | (2.0) | 109†/†† | (1.7) | 107*/†/†† | (2.3) | 108* | (2.3) |

### 3.3.8 Diastolic Membrane Potential

Diastolic membrane potential was more negative at 5 nM – 1 μM isoproterenol stimulation compared with control conditions (table 5) ($p < 0.01$). No other significant effects were found in diastolic membrane potential.

Table 5. Impact of pacing frequency and adrenergic stimulation on diastolic membrane potential in adult and old rats. Data presented as mean (± SEM). * Indicates a significant difference compared with control.

| Frequency (Hz) | | Control (mV) | | 5 nM Iso (mV)* | | 100 nM Iso (mV)* | | 1 μM Iso (mV)* | |
|---|---|---|---|---|---|---|---|---|---|
| 1 | Adult | -71 | (1.0) | -73 | (1.2) | -74 | (1.5) | -76 | (1.5) |
| | Old | -71 | (1.5) | -73 | (1.7) | -74 | (1.8) | -75 | (1.7) |
| 2 | Adult | -71 | (1.0) | -74 | (1.4) | -75 | (1.6) | -76 | (1.6) |
| | Old | -71 | (1.5) | -73 | (1.7) | -74 | (2.0) | -75 | (1.9) |
| 4 | Adult | -71 | (1.5) | -75 | (1.6) | -75 | (1.5) | -78 | (1.6) |
| | Old | -71 | (1.6) | -73 | (1.7) | -74 | (2.0) | -75 | (1.8) |
| 6 | Adult | -71 | (2.0) | -74 | (1.5) | -76 | (1.6) | -77 | (1.7) |
| | Old | -72 | (1.7) | -74 | (1.7) | -74 | (2.1) | -75 | (1.8) |

### 3.3.9 Upstroke Velocity

Upstroke velocity was significantly greater at 1 Hz compared with 6 Hz pacing ($p = 0.034$) and significantly greater at 2 Hz compared with 4 Hz pacing (table 6) ($p < 0.04$).

Table 6. Impact of pacing frequency and adrenergic stimulation on upstroke velocity in adult and old rats. Data presented as mean (± SEM). † Indicates a significant difference compared with 1 Hz. †† Indicates a significant difference compared with 2 Hz.

| Frequency (Hz) | | Control (mV/ms) | | 5 nM Iso (mV/ms) | | 100 nM Iso (mV/ms) | | 1 μM Iso (mV/ms) | |
|---|---|---|---|---|---|---|---|---|---|
| 1 | Adult | 120 | (15.7) | 99 | (10.4) | 116 | (14.3) | 105 | (13.6) |
| | Old | 120 | (5.3) | 108 | (5.5) | 103 | (5.1) | 103 | (7.2) |
| 2 | Adult | 102 | (13.4) | 94 | (9.2) | 120 | (12.5) | 107 | (9.1) |
| | Old | 112 | (4.5) | 111 | (8.7) | 100 | (5.9) | 96 | (6.9) |
| 4†† | Adult | 94 | (12.7) | 95 | (8.6) | 101 | (9.9) | 102 | (7.6) |
| | Old | 105 | (7.4) | 97 | (5.0) | 98 | (6.6) | 89 | (6.2) |
| 6† | Adult | 80 | (9.4) | 91 | (9.9) | 110 | (12.0) | 112 | (12.4) |
| | Old | 101 | (6.7) | 102 | (8.4) | 92 | (6.9) | 85 | (7.2) |

## 3.4 Discussion

The aim of this study was to measure the effect of ageing on AP responses to adrenergic stimulation at increasing doses of a βAR agonist, as well as changes in activation frequency separately and combined in rat ventricular myocytes.

The main findings of this study were: APD was significantly prolonged (29 %) only during late repolarisation ($APD_{90}$) in old compared with adult rats. No other significant age-related effects or interactions were yielded from the data in this study, however, there was a trend toward prolonged $APD_{75}$ (28 %) and $APD_{100}$ (21 %) in old compared with adult rats, as well as a trend toward greater $APD_{50\text{-}75}$ shortening in adult rats in response to isoproterenol superfusion compared with old rats ($APD_{50}$ = -12 - 26 % vs

-7 - +47 %; $APD_{75}$ = -14 – 23 % vs -14 - +2 %). Isoproterenol predominantly shortened both the AP plateau and late AP repolarisation independent of pacing frequency. Meanwhile diastolic membrane potential became more negative (3 – 6 %) with the introduction of isoproterenol. Lastly, increasing pacing frequency caused early AP repolarisation to become prolonged (27 – 55 %), while $APD_{50-100}$ demonstrated initial prolongation with increased pacing frequency, before shortening at the highest pacing frequency. In $APD_{50-75}$ this was observed during isoproterenol superfusion only, whilst in $APD_{90-100}$ this effect was also observed independent of the presence of isoproterenol. AP amplitude and upstroke velocity declined with increased pacing frequency (AP amplitude = 2 – 6 %; upstroke velocity = 4 – 12 %), though at the highest pacing frequency, isoproterenol superfusion offset some of the decline in AP amplitude through increasing AP amplitude by 7 %.

### 3.4.1 Age-Related Changes in the Ventricular Myocyte AP

The significant prolongation of $APD_{90}$ in old rats compared with adult rats in this study was an expected finding in line with previous literature which has also reported age-related prolongation of late AP repolarisation (Feridooni et al., 2015; Capasso et al., 1983b; Wei et al., 1984; Jullien et al., 1989; Liu et al., 2000; Abete et al., 1996; Bao et al., 2013; Strait and Lakatta, 2012; Zhou et al., 1998; Barbieri et al., 1994), with the magnitude of change reported (29 %) also providing similarities to some existing studies (10 - 54 %) (Liu et al., 2000; Huang et al., 2006; Barbieri et al., 1994), re-affirming the current understanding that old hearts (rat hearts) exhibit prolonged ventricular APs, with late AP repolarisation particularly affected. However, the lack of significant age-related changes elsewhere within the AP waveform was a somewhat unexpected observation. Previous studies have shown an age-related prolongation in the AP plateau (Capasso et al., 1983a; Walker et al., 1993), yet in this study, $APD_{50}$ in old rats was consistently more brief compared with adult rats except during the highest isoproterenol dose, though this was not statistically significant, a finding similarly reported by another research group (Liu et al., 2000), the mechanism for this is unclear. In addition, similar numerical differences were observed in early AP repolarisation ($APD_{25}$) in this study. Focusing solely on late repolarisation, figure 13 - 15 shows, though in the absence of statistical significance, a trend toward prolonged $APD_{75}$ and $APD_{100}$ in old rats compared with adult rats, further establishing the late phase of AP repolarisation as a potentially key area of age-related AP change. Together, the

significant prolongation of $APD_{90}$ and the observed trends towards prolongation elsewhere in late AP repolarisation alongside the shortening of early AP repolarisation and AP plateau in old rats is potentially indicative of significant roles for $Ca^{2+}$ and $K^{+}$ channels in the loss of exercise tolerance and cardiac reserve in old age either through age-related deterioration of these currents or a remodelling of the balance between them.

Unlike a great deal of previous literature (Banyasz et al., 2014; Bao et al., 2013; Kang et al., 2017; Sala et al., 2017; Stuart et al., 2018; Wang and Fitts, 2017; Barbieri et al., 1994), this study investigated both the influence of multiple pacing frequencies as well as multiple doses of isoproterenol, allowing greater insight into ventricular AP behaviour that is potentially more closely aligned with a typical physiological response to exercise in adult and old rat hearts. Therefore, it was most surprising that no rate-dependent significant differences were yielded in APD between adult and old rats. This is likely a result of only small-moderate effects on APD between age groups, alongside the observation that adult and old rats exhibit almost identical APD response patterns to elevations in activation frequency across the frequencies investigated in this study (1 – 6 Hz) (figures 11 - 15). The lack of APD findings in rat ventricular myocytes at pacing frequencies greater than 1 Hz makes both comparison to existing literature and the identification of the underlying mechanism difficult. However, the similar influence of pacing at 1 – 6 Hz on APD in adult and old rats, may perhaps lead to the suggestion that electrophysiological remodelling of myocytes is not key to the aged phenotype. Yet, this would disregard the initial and arguably most important finding of this study, where, as previously explained, old hearts were unable to achieve or maintain pacing at 8 - 10 Hz compared with adult hearts (Howlett et al., 2022). Therefore, conversely, this may indeed indicate that electrophysiological changes, at the myocyte level, have a significant role in the reduced ability of the old heart to maintain a high HR. Furthermore, this highlights the difficulty of undertaking electrophysiological recordings in old hearts at activation frequencies within the physiological range of the test species, but also highlights the importance of performing further studies at increased pacing to be able to tell the full story of cardiac ageing.

The lack of significant differences in adrenergic response in ventricular myocytes between adult and old rats was another interesting finding despite a trend toward

greater isoproterenol-induced $APD_{50-75}$ shortening in adult rats compared with old rats. This was a particularly surprising finding since previous literature has frequently pointed toward the existence of $\beta_1$AR de-sensitisation and suggested this loss in adrenergic sensitivity plays a role in the loss of cardiac reserve in old age (Ferrara et al., 2014; De Lucia et al., 2018; Spadari et al., 2018), whilst the findings of this study appear to suggest that the adrenergic response may be maintained in old age.

Some existing literature has indeed similarly reported no significant age-related changes in adrenergic response in rats and mice at lower frequencies (Farrell and Howlett, 2007; Stuart et al., 2018), though with one study reporting isoproterenol-induced prolongations in $APD_{90}$ in both adult and old rats (Farrell and Howlett, 2007). However, in these studies the use of different animal strains and species as well the utilisation of a sole saturating dose of isoproterenol (Farrell and Howlett, 2007; Stuart et al., 2018) likely underlies the differences to the findings of this study given the observed heterogeneity of the APD response to 1 μM isoproterenol compared with lower more physiological doses in figure 11 - 15. Elsewhere, previous studies have routinely found reductions in chronotropic and inotropic responses to adrenergic stimulation in old rat hearts (Abrass et al., 1982; Xiao et al., 1994; Jiang et al., 1993) though to our knowledge others are yet to have investigated age-related remodelling of the adrenergic response in rat heart excitation, particularly during greater activation frequencies.

Despite the lack of statistically significant differences in APD response to adrenergic stimulation between adult and old rats, it should be noted that the rat heart has a reduced contractile reserve compared with other larger mammals like humans (Endoh, 2004; Feridooni et al., 2015), therefore it should be considered that the existence of smaller changes in adrenergic responses between adult and old rat hearts may reflect greater or more severe influence in humans should similar findings be obtained due to the much greater contrast in HR / SV / CO between basal and maximal exercise and overall capacity for upregulation in function. However, there are understood foundational differences in the expression and function in ion channels contributing to AP repolarisation between rats and humans which may increase the difficulty of such translation between rats and humans (Árpádffy-Lovas et al., 2022; Varró et al., 1993; Joukar, 2021). Further cross-species investigation is required to better understand the

ramifications of age-related rat heart remodelling on humans, particularly regarding the loss of exercise tolerance in old age.

The existence of a trend toward greater AP shortening during AP plateau and late AP repolarisation phases in response to adrenergic stimulation in adult rats compared with old rats potentially signifies the importance of LTCC and repolarising $K^+$ channels above other currents in the cardiac ageing phenomenon, specifically regarding the inability in obtaining and maintaining elevated CO in response to exercise. Further, this is consistent when the difference in APD between adult and old rats is considered with changes in pacing from that equivalent to a basal rat HR (4 Hz) (Carnevali and Sgoifo, 2014; Farmer and Levy, 1968) to the most physiologically relevant condition utilised in this study (6 Hz pacing with 5 nM or 100 nM isoproterenol) which emulates, to a limited extent, the conditions of an exercising rat heart. In this study, adult rat ventricular myocytes displayed remodelling of $APD_{25}$, $APD_{50}$, $APD_{75}$ and $APD_{90}$ during physiological (5 nM) and near maximal (100 nM) (Wang and Fitts, 2017) adrenergic stimulation at 6 Hz compared with 4 Hz pacing of greater magnitudes than old rat ventricular myocytes ($AP_{25}$: Adult = 9 – 21 % vs Old = 1 – 12 %; $AP_{50}$: Adult = 20 – 31 % vs Old = 2 – 6 %; $AP_{75}$: Adult = 18 – 29 % vs Old = 17 %; $AP_{90}$: Adult = 19 – 28 % vs Old = 22 %) with the greatest age-related difference in simulated exercise response occurring in AP plateau. Though in this study the pacing frequencies most closely emulating a physiological exercising rat HR have been curtailed slightly due to difficulties in successfully pacing old myocytes at high frequencies. Similar (slightly increased magnitude) isoproterenol-induced changes were observed when 8 – 10 Hz pacing was used under identical adrenergic stimulation compared with 4 Hz (Howlett et al., 2022) which more closely represents the HR of a rat undertaking strenuous or heavy intensity exercise (Brooks and White, 1978; Bolter and Atkinson, 1988; Barnard et al., 1974; Wisløff et al., 2001).

The lack of multiple statistically significant findings despite a number of clear numerical differences between adult and old rat hearts and trends towards statistical significance demonstrated in the data (figure 11 - 15) may be a result of a number of factors. Firstly, it may simply indicate that the old rat heart is capable of maintaining a robust and effective response to increased pacing and adrenergic stimulation. However this seems unlikely in the wider context outside of the results shown in this study at 1 – 6 Hz pacing given the inability to pace old rat hearts at the full range of

pacing frequencies emulating a physiological response to exercise as would occur in-vivo in the same manner that was demonstrated in our previous work in adult rats under identical testing conditions (Howlett et al., 2022). It may suggest the existence of a more gradual age-related deterioration, which would be better studied by incorporating middle-aged and senescent groups to this investigation, or simply it might be that age-related remodelling of APD and response to varied stress is less distinctive between adult and old hearts when measured at greater intensities when the AP is more abbreviated than at lower intensities (Farrell and Howlett, 2007). Thus, whilst differences in average responses indeed exist which may have a clinical effect, they are smaller and less clear and less likely to reflect a statistically significant change. Also, these findings may indicate that intrinsic function and adrenergic signalling are equally responsible for age-related remodelling with neither demonstrating greater responsibility, evidenced by the significant ageing main effect highlighting the prolongation in $APD_{90}$ without further interaction with pacing and adrenergic stimulation beyond the limitation in pacing at frequencies > 6 Hz. Equally, the influence of APD heterogeneity (Clark et al., 1993; Watanabe et al., 1983) should be considered as a contributing factor which could be better studied in future by separating the commonly used homogenous pool of ventricular cells into specific regions and layers.

### 3.4.2 Impact of Adrenergic Stimulation and Activation Frequency on AP Repolarisation in Adult and Old Rats

APD shortening in response to near maximal (100 nM) adrenergic stimulation in AP plateau and late AP repolarisation was an expected finding which has been previously reported in existing literature in adult rats (Wang and Fitts, 2017; Kamada et al., 2019). However, this study, suggests that such an adrenergic response remains visible across a range of activation frequencies (1 – 6 Hz) and highlights the AP plateau and late AP repolarisation phases of the AP as key players in facilitating a response to adrenergic stimulation. In turn, this further cements LTCC and repolarising $K^+$ channels as potential key components in the investigation the cardiac ageing phenomenon.

Interestingly, a physiological dose (5 nM) of isoproterenol only significantly shortened $APD_{50\text{-}75}$ during 1 Hz pacing (figure 12 - 13). This shows that the myocyte response to adrenergic stimulation has an element of rate-dependency. However, given that ventricular myocytes in this study were most sensitive to adrenergic stimulation

at a synthetic pacing frequency rather than those of physiological relevance, it likely reveals little information about the true response to exercise in the rat heart. This observed rate-dependency in adrenergic response may be due to the increases in physiological concentration of adrenergic stimulus during increases in exercise intensity in-vivo (Zouhal et al., 2008), meaning during periods of high demand or emulated high demand (> 1 Hz pacing) a 5 nM dose of isoproterenol is not adequate to significantly shorten APD.

Conversely, early AP repolarisation and AP plateau were prolonged during supramaximal / saturating doses of isoproterenol (1 μM) compared with near maximal doses (100 nM) in rat ventricular myocytes, though figure 11 and figure 12 show this is far more prominent in old rats compared with adult rats. In general, figure 11 - 12 depicts a trend toward mild isoproterenol-induced shortening / maintenance of $APD_{25-50}$ during physiological (5 nM) and near maximal (100 nM) adrenergic stimulation (Wang and Fitts, 2017). However, when a saturating dose is applied (1 μM), particularly in old rats, a radical directional change occurs, with AP shortening switching to considerable prolongation. This may indicate a limit to $I_{to}$ response to adrenergic stimulation or a shift in balance between $I_{to}$ current and LTCC current. Research has typically reported mixed $I_{to}$ current findings with ageing (Fu et al., 2013; Liu et al., 2000; Walker et al., 1993), whilst little information regarding the response to isoproterenol in rats exist (van der Heyden et al., 2006), though a reduction has been reported in rabbits (Zhengrong et al., 2011). Given that the APD prolongation stimulated by a saturating dose of isoproterenol becomes negligible and disappears later on in the AP waveform, it could be speculated that the prolongation may occur as a protective measure to help maintain myocyte contraction during periods of elevated HR. This may explain why the greatest prolongation in response to 1 μM isoproterenol was observed in old rats, as old rats in this study exhibited faster early AP repolarisation and faster AP plateau relative to adult rats.

The early AP repolarisation response in ventricular myocytes to variations in pacing frequency in this study may be a result of changes in $I_{to}$ during periods of higher demand or stress. Existing literature suggests $I_{to}$ current declines as activation frequency is elevated across a similar range of frequencies (0.2 – 5 Hz) (Shigematsu et al., 1997; Josephson et al., 1984). Meanwhile the AP plateau response to increased pacing may be indicative of rate-dependent changes in LTCC current as well as an

indirect impact of $I_{to}$ current modulations. Little information exists regarding the rate-dependent remodelling of the LTCC current and separate studies investigating LTCC current at fixed frequencies between 0.1 and 2.5 Hz have displayed a range of current magnitudes (Xiao et al., 1994; Liu et al., 2000; Sakatani et al., 2006; Walker et al., 1993; Jourdon and Feuvray, 1993; Scamps et al., 1990; Meszaros et al., 1997; Vizgirda et al., 2002; Zhou et al., 1998).

Moreover, the initial prolongation in late AP repolarisation before shortening at the highest activation frequency in this study may be reflective of a rate-dependent balance in LTCC current and repolarising $K^+$ ($I_{Ks}$, $I_{Kr}$, $I_{K1}$) currents to facilitate an increase in impulse conduction without compromising contractile function during increased demand. Such currents have not yet been investigated, to our knowledge, at pacing frequencies similar to physiological HR in rats, though the development of the onion peeling technique (Banyasz et al., 2011; Banyasz et al., 2014; Chen-Izu et al., 2012) may expedite research in this area.

Overall, such rate-dependent changes in APD were expected as a result of our previous work (Howlett et al., 2022) which demonstrated in adult rat ventricular myocytes that an adrenergic response is still visible and also that a significant pacing-related shortening of late AP repolarisation occurs beyond 6 Hz. Such findings are supported by limited similar existing literature utilising activation frequencies that emulate basal and exercising rat HR (Wang and Fitts, 2017; Shigematsu et al., 1997; Hardy et al., 2018; Fauconnier et al., 2003).

However, although similar rate-dependent APD changes in rat ventricular myocytes were observed in the study performed by Shigematsu et al. compared with this study, some important points must be considered (Shigematsu et al., 1997). The work by Shigematsu et al. indeed reported rate-dependent prolongations in APD with increases in pacing frequency from 0.2 – 5 Hz in rat ventricular myocytes, largely attributable to the aforementioned rate-dependent decreases in $I_{to}$ current, evidenced by the amelioration of this rate-dependent APD prolongation with $I_{to}$ block (Shigematsu et al., 1997). Though interestingly, the rate-dependent prolongation of APD was not observed when the experiment was repeated in rat papillary muscle (Shigematsu et al., 1997). Because different electrophysiological techniques were used, with whole-cell patch-clamp used in the original measurements - which included similar EGTA

content in the pipette solution to this study – and sharp-electrode electrophysiology in the latter experiment, it was concluded that rate-dependent APD prolongation might have been masked by changes in NCX current with increasing pacing frequency and might be influenced by the chelation of intracellular $Ca^{2+}$ with EGTA in the pipette solution (Shigematsu et al., 1997).

The main implication for the work carried out in this chapter is that the above study may indicate that rate-dependent changes measured using electrophysiological techniques that do not interfere so greatly with the intracellular milieu and do not chelate intracellular $Ca^{2+}$ may provide results that are somewhat different to the findings presented in this chapter and may call into question the potential physiological relevance of findings laid out section 3.3.1 and beyond. Whilst this is a legitimate concern for the interpretation of the work in this chapter, the differences in rate-dependent APD responses in the rat ventricle described by Shigematsu et al. may have been influenced by differences in ventricular regions tested as well as simply inserting electrodes into the cell membrane and the isolation of cells may artificially alter intracellular $Ca^{2+}$ due to the impact of removing electrotonic and buffering effects from neighbouring cells. Nevertheless, the stability provided by the level of intracellular $Ca^{2+}$ buffering through the use of EGTA in the pipette solution permitted the ability to pace ventricular myocytes at pacing frequencies more closely reflecting physiological HRs of the test species under control and adrenergic stimulation conditions in this chapter and in our previous work (Howlett et al., 2022). Equally the main focus of the work in this chapter as well as the overall project, was to uncover electrophysiological and adrenergic signalling changes in ventricular myocytes with ageing and the conditions were identical during the collection of data in both adult and old rats. Though, indeed, further research using non-invasive techniques that alter the intracellular milieu to a lesser extent is required to corroborate the findings laid out in this work and facilitate the better understanding of the true physiological responses of ventricular myocytes to emulated exercise. When considering the physiological relevance of in-vitro electrophysiological data from rat ventricular myocytes, it is also reasonable to note that the response to physiological adrenergic stimulation as may occur in-vivo under the influence of epinephrine and norepinephrine may differ from the responses recorded during the experiments in this chapter where the primary focus was on βAR stimulation and specifically $\beta_1$AR signalling.

The response in old rats to a full range of pacing emulating physiological stress is unknown and requires further study. Whilst our previous work led to the expectation of similar results in this study, the rate-dependent changes observed were initially surprising given previous literature has indeed reported stepwise reductions in APD with increases in pacing frequency (Huang et al., 2006) which admittedly aligns with the logical progression that APD would reduce as the diastolic interval becomes narrower with elevated pacing (Liu et al., 1993). Though the study by Huang et al. was performed in atrial myocytes rather than ventricular myocytes and likely influences the differences in findings (Huang et al., 2006). Such differences may also be linked to the understood irregular cardiac force-frequency / rate-dependency in rats compared with other mammals (Endoh, 2004; Carmeliet, 2006).

### 3.4.3 Impact of Adrenergic Stimulation and Activation Frequency on AP Amplitude, Diastolic Membrane Potential and Upstroke Velocity in Adult and Old Rats

This study's findings on other components of the AP waveform demonstrate a lack of age-related change, in agreement with existing literature (Feridooni et al., 2015), alongside a shift toward more negative diastolic membrane potentials with the introduction of isoproterenol and the maintenance of diastolic membrane potentials with variations in activation frequency. Further the results demonstrate reductions in both AP amplitude and upstroke velocity as activation frequency was increased, which was slightly offset at the highest pacing frequency in response to adrenergic stimulation in the case of AP amplitude.

The reasons underlying the hyperpolarising diastolic membrane potential response to adrenergic stimulation but not elevations in pacing frequency are not abundantly clear and further study is required focusing on such AP changes alongside ion current balance at these greater activation frequencies. However, the hyperpolarisation of diastolic membrane potential in rat ventricular myocytes was an expected finding and is in line with our previous work as well as some existing literature (Crumbie, 2016; Farrell and Howlett, 2007). It is thought that such hyperpolarisation is a result of isoproterenol-induced increases in $K^+$ channel conductance (Crumbie, 2016; Gadsby, 1983). However, the $K^+$ channel which primarily dictates diastolic membrane potential ($I_{K1}$) has been observed to provide a mixed response to adrenergic stimulation in previous studies (Chiamvimonvat et al., 2017).

The AP amplitude and upstroke velocity changes in this study were equally expected and were in line with our previous work. Existing literature separately investigating AP amplitude and upstroke velocity responses to pacing (Ravens and Wettwer, 1998; Attwell et al., 1981; Verkerk et al., 2012) and AP amplitude responses to adrenergic stimulation support the findings of this study (Verkerk et al., 2012; Wang et al., 2009). However, few studies exclusively investigating changes in rats exist and findings overall in existing literature are limited to lower pacing frequencies, with only a fraction investigating changes towards 4 - 5 Hz (Verkerk et al., 2012; Attwell et al., 1981). The mechanism underlying such changes in AP amplitude is likely related to changes in $Na^+$ current and the subsequent response to stress (Wang et al., 2009; King et al., 2013; Liu et al., 1999).

## 3.5 Conclusion

The findings of this study demonstrate $APD_{90}$ prolongs in rat ventricular myocytes with age, highlighting the importance of late AP repolarisation in age-related remodelling. In addition, this study revealed interesting findings in relation to the existence of an adrenergic response in old ventricular myocytes at a range of pacing frequencies, some of which emulate physiological rat HR, despite a trend toward blunted isoproterenol-induced shortening of the AP plateau and late AP repolarisation when compared with adult myocytes. Further interesting findings were revealed in relation to APD responses to elevations in pacing frequency. This study demonstrated firstly that old rat ventricular myocytes could not (on this occasion) maintain pacing at frequencies emulating heavy exercising rat HR in the same way it has been shown to be possible in adult rats. Secondly, across the measured pacing frequencies (1 – 6 Hz), both adult and old rats demonstrated similar rate-dependent AP repolarisation. The underlying mechanisms explaining the findings of this study are not currently clear, though it is likely that changes in LTCC and repolarising $K^+$ currents and their subsequent responses to (emulated) exercise stress alongside the influence of intracellular $Ca^{2+}$ buffering via the presence of EGTA in the pipette solution contribute to such observations. The varied nature of the electrophysiological responses to ageing, activation frequency and adrenergic stimulation in ventricular myocytes within this study highlight the need for further similar studies which also incorporate ion channel investigations alongside varied electrophysiological techniques to help

clarify the age-related remodelling of the exercise response in the rat heart to help better understand the mechanisms responsible for the loss of exercise tolerance in the elderly. Nonetheless, this study provides novel electrophysiological reference values in adult and old rat ventricular myocytes in response to varied stress emulating, in part, responses to exercise more closely reflecting physiologically relevant in-vivo responses. This work creates the foundation for further comparative studies potentially investigating disease and for the generation or development of computational electrophysiological rat heart models.

# Chapter 4: Effects of Ageing on the LTCC and its Response to Isoproterenol in Rat Ventricular Myocytes

## 4.1 Introduction

Alterations in cellular $Ca^{2+}$ homeostasis have a significant role in both disease and ageing. Due to the integral role of $Ca^{2+}$ in the transduction of excitation to myocyte contraction, it has a large history of research. Maladaptation in intracellular $Ca^{2+}$ handling can increase risk of arrhythmia, impair contractility and limit CO.

Research investigating ageing-related changes in cellular $Ca^{2+}$ homeostasis has identified numerous changes in aged hearts compared with adult hearts (Zhou et al., 1998; Josephson et al., 2002; Liu et al., 2000; Walker et al., 1993; Xiao et al., 1994; Zhu et al., 2005; Cheah and Lancaster, 2015a). Such changes typically involve changes in the fluxes and kinetics of $Ca^{2+}$ transporters, $Ca^{2+}$ release units and $Ca^{2+}$ channels. Studies investigating LTCC have yielded mixed results. Reductions in peak LTCC current have been found in atrial preparations in humans and dogs with ageing (50 %, 43 %) (Gan et al., 2013; Herraiz et al., 2013). Whereas, some ventricular preparations have suggested peak LTCC current increases (94 – 100 %) in aged compared with adult hearts in rats (Josephson et al., 2002). However, some contradictory evidence suggests peak LTCC current reduces (14 – 15 %) in rat ventricular myocytes (Liu et al., 2000). Whilst several other studies have reported unchanged peak LTCC current with ageing in rat ventricles (Walker et al., 1993; Xiao et al., 1994; Larson et al., 2013). Evidence in LTCC expression also has displayed mixed responses to ageing (Gan et al., 2013; Walton et al., 2015). Despite mixed findings in peak LTCC current, age-related research in LTCC inactivation appears unanimous. Inactivation of LTCC has been found to become slower (31 – 137 %) in aged human and rat hearts (Herraiz et al., 2013; Josephson et al., 2002; Liu et al., 2000; Walker et al., 1993). Notwithstanding mixed findings, peak LTCC current is generally understood to remain unchanged relative to cell size, whilst LTCC current inactivation slows with advancing age (Josephson et al., 2002; Walker et al., 1993; Zhou et al.,

1998; Xiao et al., 1994; Herraiz et al., 2013; Larson et al., 2013; Liu et al., 2000; Howlett and Lancaster, 2021).

The alterations in LTCC described above may support age-related AP prolongation and are likely responsible, in part, for prolonged contractions associated with advanced age. Declining LTCC inactivation speed may prolong AP depolarisation and impede efficient repolarisation by rectifying $K^+$ currents and will have an impact on intracellular $Ca^{2+}$ and sustained NCX flux. It is possible, the preservation of normal healthy APD relies on the balance or ratio between such $Ca^{2+}$ and $K^+$ currents whereby small differences in age-related alterations in both currents significantly impact APD. The adrenergic response of LTCC is also an important component which may be influential in the age-related development of CO limitation. However age-related LTCC research has predominantly measured changes in basal function. The limited available findings on adrenergic response suggest adrenergic LTCC response is either preserved or markedly reduced (~ 50 – 200 %) in old hearts compared with adult hearts (Larson et al., 2013; Xiao et al., 1994). According to one study, significantly greater doses of adrenergic stimuli (~ 213 %) were required in old compared with adult hearts, to achieve half maximal effects (Xiao et al., 1994). This might indicate a significant loss of sensitivity to $\beta_1$AR stimulation.

Overall, existing literature appears to implicate a loss in basal LTCC current inactivation speed in age-related AP prolongation, whilst any alterations in adrenergic response in the LTCC may contribute to the declining overall adrenergic response and cardiac reserve. However very little evidence exists on LTCC response to adrenergic stimulation in old compared with adult hearts. Therefore, the aim of the work in this chapter was to assess the influence of ageing on LTCC peak current and its response to adrenergic stimulation.

## 4.2 Methods

### 4.2.1 Specific Experimental Procedures

Peak inward $Ca^{2+}$ currents were measured in adult (3 months of age) and old (22 - 23 months of age) male Wistar rat ventricular myocytes (adult, n = 36; old, n = 13) in voltage-clamp mode. Membrane currents were stimulated using the voltage sequence displayed in figure 16 at a frequency of 1 Hz. Each voltage sequence began with a -80

mV holding potential before a pre-pulse to -50 mV to remove sodium currents, then $Ca^{2+}$ currents were measured during 10 mV steps from -50 mV to +10 mV. Approximately 5 recordings were achieved during normal rat Tyrode superfusion after a period of pre-conditioning (1 - 2 minutes) and following 100 nM isoproterenol. Isoproterenol was superfused for 5 minutes prior to recording (Harding et al., 1988; Lim et al., 1999; Johnson et al., 2012). All cell data was then averaged per heart and peak current was compared between adult (N = 6) and old (N = 6) rats.

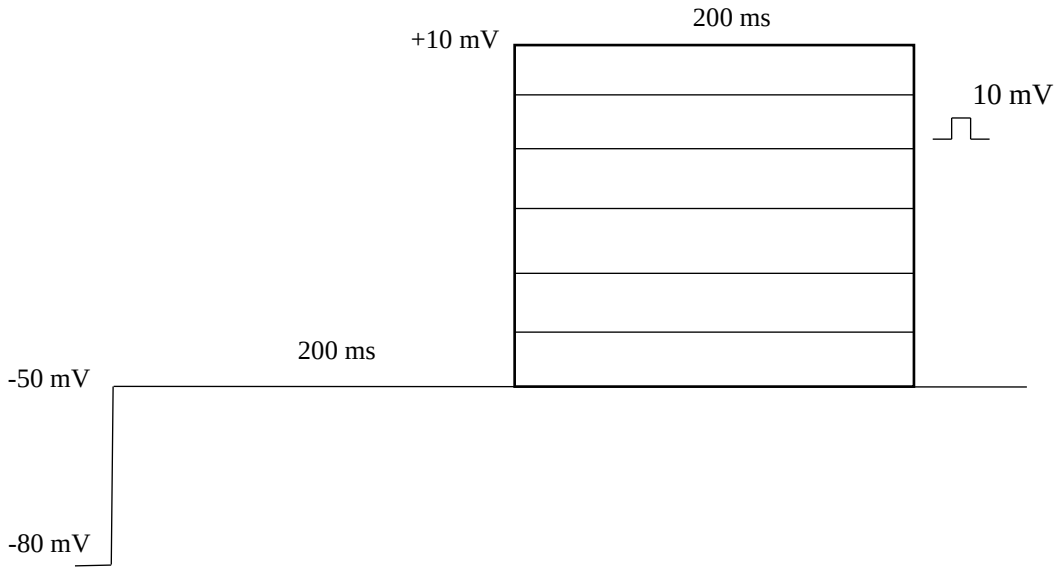


Figure 16. Schematic drawing of the voltage-clamp protocol used to determine peak inward $Ca^{2+}$ currents in rats.

### 4.2.2 Specific Statistical Analyses

A Mixed ANOVA was performed on all LTCC current data to provide comparison between adult (3 months of age) and old (22 – 23 months of age) rat hearts during control conditions and during 100 nM isoproterenol stimulation at 1 Hz pacing. Where assumptions of sphericity were violated, the Huynh Feldt correction was used. All other mixed ANOVA assumptions were met.

## 4.3 Results

### 4.3.1 Brief Summary of Recordings

Voltage-clamp recordings during control conditions and conditions of isoproterenol stimulation (100 nM) were successfully collected in adult (N = 6; n = 36) and old rats (N = 6; n = 13). Average access resistance was 24 ± 1.2 MΩ. Average cell capacitance was 150 ± 7.5 pF in adult rats and 171 ± 5.8 pF in old rats. An unpaired t-test found no significant difference in cell capacitance between adult and old rats (p = 0.066). Examples of raw recordings are shown in figure 17.

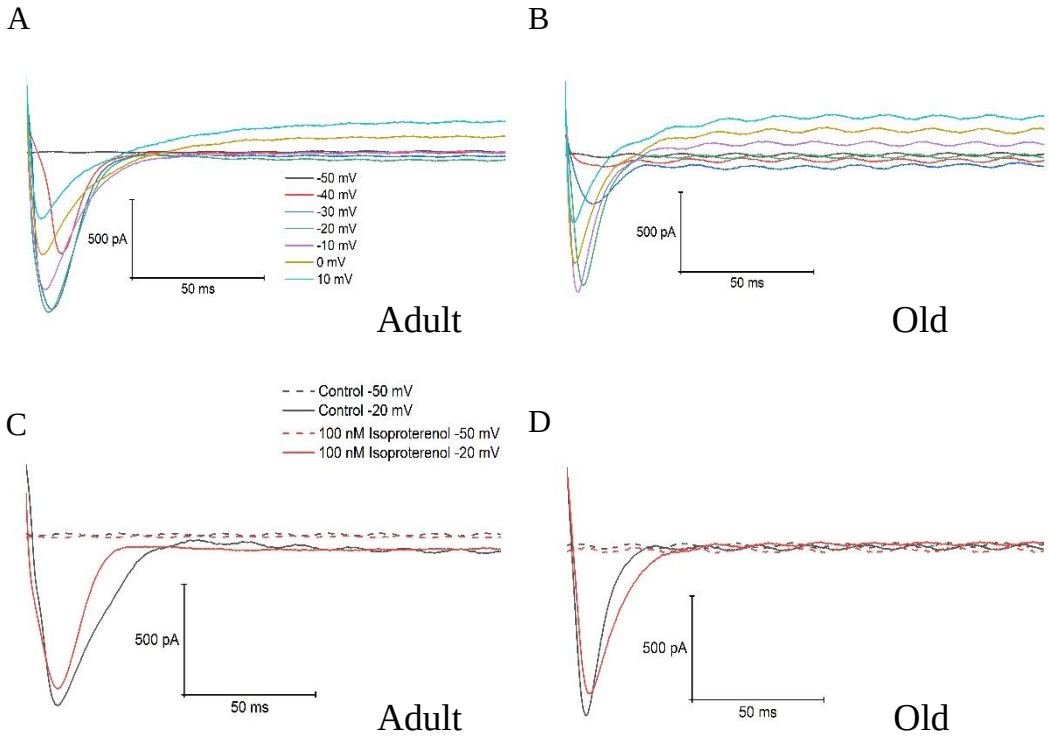


Figure 17. Example overlaid ventricular myocyte LTCC current traces illustrating typical recordings acquired during control conditions in adult (A) and old rats (B) at 1 Hz pacing alongside a typical response to adrenergic stimulation (100 nM isoproterenol) in adult (C) and old rats (D).

### 4.3.2 Peak LTCC Current

A mixed ANOVA found ageing and isoproterenol yielded no significant effects or interactions on peak LTCC current in rat ventricular myocytes (figure 18 A – B). However, the data displayed a trend toward reduced peak LTCC current in old rats

compared with adult rats (figure 18 A – B; figure 19) ($p = 0.239$; partial $eta^2 = 0.136$). Similarly, there was a trend toward reduced LTCC current during isoproterenol stimulation compared with control conditions in old rats (figure 18 A – B); figure 19) ($p = 0.184$; partial $eta^2 = 0.169$).

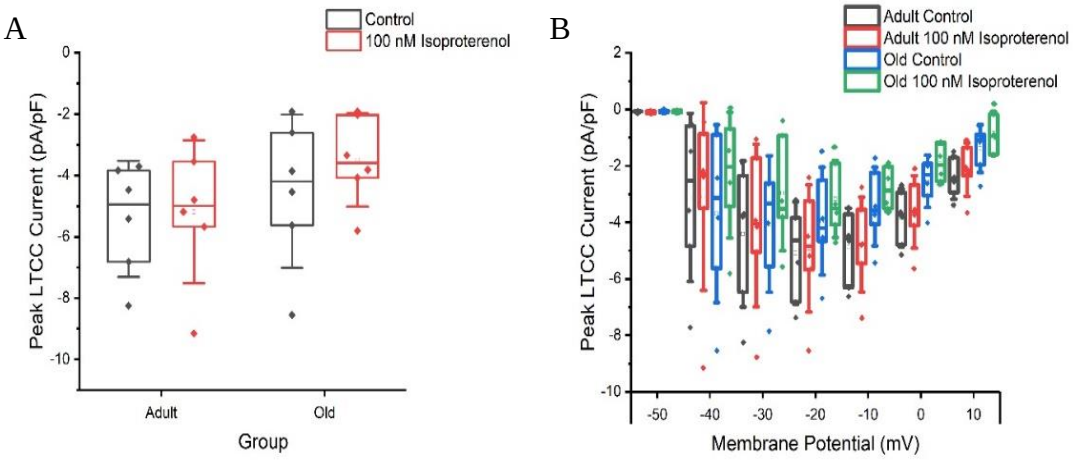


Figure 18. Influence of ageing on LTCC current and response to adrenergic stimulation (100 nM isoproterenol). Plots demonstrate overall peak LTCC current (A) alongside peak LTCC current at membrane potentials of -50 – 10 mV. Box plots display mean (open square), median (solid middle line), upper, and lower quartiles (solid upper and lower lines) and confidence intervals (error bars).

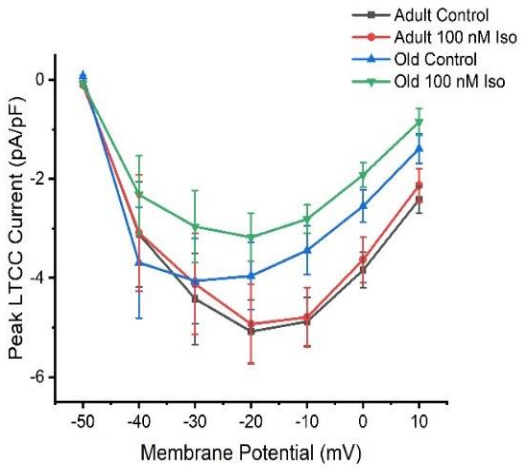


Figure 19. Average peak LTCC current during control conditions and during 100 nM isoproterenol stimulation in adult and old rat ventricular myocytes. (SEM error bars).

## 4.4 Discussion

The aim of this study was to measure the effect of ageing on peak LTCC current and its response to adrenergic stimulation in rat ventricular myocytes. The main findings of this study were: ageing did not significantly alter peak LTCC current, though the data showed a trend toward a reduction in peak current in old rats compared with adult rats (29 %). The superfusion of isoproterenol also did not significantly alter peak LTCC current, yet there was a trend toward a reduction in LTCC current during isoproterenol compared with control conditions in old rats.

Despite the trend toward age-related reductions in peak current, the results of this study appear to suggest that ageing has little impact on peak LTCC current. The findings regarding age-related changes in peak current in this study were somewhat expected given the mixed literature surrounding this subject (Zhou et al., 1998; Liu et al., 2000; Walker et al., 1993; Xiao et al., 1994; Josephson et al., 2002). When existing literature is considered as a whole, typically, LTCC appears to remain similar between adult and old hearts. Relatively speaking, commonly reported age-related increases in current are normally explained as changes in raw LTCC current which are diminished when myocyte cell size is accounted for as a result of hypertrophy associated with ageing (Zhou et al., 1998; Walker et al., 1993; Xiao et al., 1994). Though little relative change on average in LTCC peak current has been reported in previous research, an age-related slowing of LTCC current inactivation has been frequently demonstrated (Zhou et al., 1998; Liu et al., 2000; Walker et al., 1993; Josephson et al., 2002). Such findings typically imply that though peak current yields little change, net $Ca^{2+}$ entry is greater in aged hearts, which contributes to the prolongation of the AP and may facilitate, in part, the impaired cardiac contractility linked with old age, particularly since buffering excess intracellular $Ca^{2+}$ has been shown to attenuate the associated AP prolongation (Zhou et al., 1998). Whilst inactivation was not measured on this occasion, the LTCC findings of this study likely underpin the statistically similar $APD_{50}$ outcomes in adult and old rats in the previous chapter. Equally, the observed trend toward an age-related reduction in peak LTCC current may explain the trend toward the shortened AP plateau in old rat ventricular myocytes in the previous chapter. However, this is speculation in the absence of measured LTCC kinetics and

repolarising $K^+$ channel currents which both could possibly underlie such APD changes.

The findings regarding age-related changes in peak LTCC current response to adrenergic stimulation in this study were more surprising. The results of this study appear to suggest that ageing has little impact on the adrenergic response of peak LTCC current. The lack of isoproterenol-induced increase in LTCC current in rat ventricular myocytes overall was also a surprising outcome. Such findings are somewhat contradictory to previous findings in this area. Previously, LTCC current has been found to increase significantly in response to adrenergic stimulation (Xiao et al., 1994; Sakatani et al., 2006; Şengül Ayan et al., 2020; Scamps et al., 1990; Katsube et al., 1996; Vizgirda et al., 2002; Zhou et al., 1998). Increases in LTCC current have also been reported in old rat ventricular myocytes, though at a considerably reduced magnitude compared with adult rats (~65 % vs 116 %) (Xiao et al., 1994). This may suggest that, though an ageing impact is considered to occur, LTCC current is still capable of providing a significant current response to adrenergic stimulation contrary to the findings of this study.

Although the rat ventricular myocyte LTCC current response to adrenergic stimulation is largely at odds with the typical response to adrenergic stress defined in the literature, some studies have demonstrated variability in response level (Xiao et al., 1994; Sakatani et al., 2006; Şengül Ayan et al., 2020; Scamps et al., 1990; Katsube et al., 1996; Vizgirda et al., 2002; Zhou et al., 1998). The mechanisms underlying the differences in findings are unclear, however, differences in pacing frequency, pipette solution, bath solution, type and dose of adrenergic stimulant as well as variations in voltage sequence and the presence of ion blockers may contribute to these differences. As a result of the differences in LTCC current response to isoproterenol in adult rat ventricular myocytes outlined in the work in this chapter compared with much of the related existing literature, the interpretation of such results in regards to age-related remodelling may be complicated. Therefore, there exists a need for future research to be carried out using conditions that are more favourable for the demonstration of a significant adrenergic response in LTCC current in rat ventricular myocytes as shown in a number of previous studies to better understand the age-related remodelling of ventricular myocytes that may underlie, in part, the AP prolongation and overall loss of cardiac response to exercise associated in the elderly.

Though our findings related to LTCC current response to adrenergic stimulation contradict the findings of similar studies (Xiao et al., 1994; Sakatani et al., 2006; Şengül Ayan et al., 2020; Scamps et al., 1990; Katsube et al., 1996; Vizgirda et al., 2002; Zhou et al., 1998), they may partially help to explain the lack of age-related differences in AP plateau response to adrenergic stimulation in the previous chapter. For example, the observed maintenance of adult rat ventricular myocyte LTCC current during isoproterenol superfusion, coupled with the trend toward an isoproterenol-induced reduction of LTCC current in old rat ventricular myocytes provides support to the similarly reported trend toward reduced adrenergic response in $APD_{50-75}$ in old rats the previous chapter. However, it is possible changes in channel inactivation coupled with isoproterenol-induced changes in repolarising $K^+$ channel currents contribute significantly to such APD responses displayed in the previous chapter.

The occurrence of peak LTCC current at more negative potentials than typically demonstrated in previous literature must also be considered during the interpretation of $Ca^{2+}$ current findings from rat ventricular myocytes recorded in this study. Figure 18b and figure 19 shown in section 4.3.2 suggest peak LTCC current was exhibited at membrane potentials of -20 mV. This is in contrast to previous studies which highlight that peak myocyte LTCC current is typically exhibited at membrane potentials between -10 mV and 0 mV (Xiao et al., 1994; Sakatani et al., 2006; Şengül Ayan et al., 2020; Scamps et al., 1990; Katsube et al., 1996; Vizgirda et al., 2002; Zhou et al., 1998). It could be that LTCC current peaked at more negative membrane potentials in this study as a result of interference or contamination from other ion currents due to the sole reliance on the voltage sequence to measure peak LTCC current as opposed to the additional use of LTCC or other ion channel blockers to confirm the observations as LTCC current or changes in LTCC current. Such differences may also have resulted from impairments to voltage control due to changes in resistance throughout testing. However, the use of similar voltage sequences to determine LTCC current have been used widely in the literature and should prevent contamination from $Na^+$ currents. Further, although the access resistance was a little higher than typically desired for similar measurements and may limit settling time, series resistance compensation would help compensate this and access resistance was monitored throughout all experiments with any significant deviations resulting in cell discard. The findings demonstrating peak LTCC current at more negative membrane potentials

is more likely attributable, at least in part, to the lack of measurement adjustment for calculated liquid junction potential – as is quite common. Although this may not account for the entire magnitude of deviation, the calculated liquid junction potential does account for approximately 7 mV, meaning peak LTCC current from rat ventricular myocytes measured in this study likely occurs more toward -10 mV and in turn toward membrane potentials more commonly identified in the literature (Xiao et al., 1994; Sakatani et al., 2006; Şengül Ayan et al., 2020; Scamps et al., 1990; Katsube et al., 1996; Vizgirda et al., 2002; Zhou et al., 1998). Perhaps future similar investigations involving LTCC current to further pursue the intended goals of this chapter would benefit from the performance of studies including selective LTCC recording conditions, whereby alternative extracellular solutions and ion current blockers might be used as confirmatory measures of individual LTCC current alongside the investigation of LTCC inactivation kinetics.

Age-related literature investigating other elements involved in the cycling of $Ca^{2+}$ that are important in determining contractile modulations has demonstrated that the ageing heart is associated with the greater frequency of spontaneous $Ca^{2+}$ releases at rest and reduced magnitude of $Ca^{2+}$ transients as a result of RyR2 remodelling, supported by increased RyR2 leak (Feridooni et al., 2015; Zhu et al., 2005). These changes reflect the typical development of aberrant $Ca^{2+}$ cycling in old age and may indicate a potential breakdown in the coupling of $Ca^{2+}$ entry to SR $Ca^{2+}$ release (if LTCC current is also maintained) which provides a potential substrate for contractile impairments common with advanced age. Age-related remodelling in factors controlling myocyte inotropy are coupled with the reduction in SERCA2a: PLN ratio (68%), which is detrimental to myocyte relaxation through associated slower $Ca^{2+}$ sequestration (Lim et al., 1999). Taken together, misalignment of $Ca^{2+}$ entry and CICR alongside poorer cytosolic $Ca^{2+}$ sequestration and increased RyR2 leak may lead to the problems with SR $Ca^{2+}$ content/ load documented in ageing hearts (Xu and Narayanan, 1998; Jiang and Narayanan, 1990; Feridooni et al., 2015). Though some evidence suggests it is predominantly alterations in SR $Ca^{2+}$ release function and not SR $Ca^{2+}$ content and diastolic $Ca^{2+}$ levels that underlie impaired Ca transients in advanced age (Howlett et al., 2006). Meanwhile, relatively little evidence on the adrenergic response in $Ca^{2+}$ handling with advanced age exists, however existing literature has shown SR $Ca^{2+}$ uptake magnitude in response to adrenergic stimulation reduces (35 - 50%) with

advanced age (Lim et al., 1999; Jiang and Narayanan, 1990; Zhu et al., 2005; Xiao et al., 1994). The changes in intrinsic function and adrenergic response of components responsible for efficient $Ca^{2+}$ handling, may collectively significantly contribute to the age-related loss of cardiac reserve and exercise tolerance and facilitate the transformation of the heart from a youthful to an older more vulnerable phenotype, though future studies are required (Feridooni et al., 2015; Fares and Howlett, 2010).

Studies investigating LTCC current thus far have typically been limited to observations at pacing frequencies ≤ 2.5 Hz (Xiao et al., 1994; Liu et al., 2000; Sakatani et al., 2006; Walker et al., 1993; Jourdon and Feuvray, 1993; Scamps et al., 1990; Meszaros et al., 1997; Vizgirda et al., 2002; Zhou et al., 1998). Observations from these studies performed at 0.1 – 2.5 Hz pacing show little in the way of a rate-dependency in LTCC current, though further data is required from studies investigating LTCC changes with modulations in activation frequency in the same experiment (Xiao et al., 1994; Liu et al., 2000; Sakatani et al., 2006; Walker et al., 1993; Jourdon and Feuvray, 1993; Scamps et al., 1990; Meszaros et al., 1997; Vizgirda et al., 2002; Zhou et al., 1998). Though such investigations have been performed at activation frequencies considerably lower than rates that might be considered physiologically relevant in the rat, these findings may provide some insight to the ionic changes responsible for the remodelling of APD in response to physiological pacing however, similar studies in old subjects are required.

## 4.5 Conclusion

The results of this study suggest peak LTCC current and its response to adrenergic stimulation are not significantly remodelled with ageing. This may highlight the potential greater importance of repolarising $K^+$ channels in the modulation of APD in old age and in turn the cardiac ageing phenomenon. The underlying mechanisms of the results in this study are unclear, however the findings of this work are partially corroborated by numerous previous studies. However, it is clear, from the results of this study and the findings of existing literature, that greater study is required investigating LTCC behaviour at physiologically relevant pacing frequencies as well greater study of LTCC current and channel kinetics using more selective LTCC recording conditions, particularly those that favour a significant adrenergic response as reported previously in order to better understand the true age-related changes in

excitation-contraction coupling and in turn the mechanisms underlying the loss of exercise tolerance and the overall decline in cardiac function.

# Chapter 5: Effects of Ageing on $I_{Ks}$, its Involvement in AP Repolarisation and the Response to Isoproterenol in Rat Ventricular Myocytes

## 5.1 Introduction

The $I_{Ks}$ current is a widely recognised contributor to AP repolarisation (Banyasz et al., 2014; Feridooni et al., 2015). Originally, $I_{Ks}$ was understood to have a much smaller role in AP repolarisation compared with $I_{Kr}$ (Banyasz et al., 2014; Kang et al., 2017). However, recent years have found introduction of adrenergic stimuli (5 nM - 1 μM Isoproterenol) dramatically amplifies $I_{Ks}$ current (22 – 66 %) disproportionately compared with responses elicited in $I_{Kr}$ current flux, leading to the acknowledgement of a greater role for $I_{Ks}$ in AP repolarisation during adrenergic stress (Banyasz et al., 2014; Wang and Fitts, 2020).

In response to adrenergic stimuli, $I_{Ks}$ is understood to be directly activated through the phosphorylation of the KCNQ1: KCNE1 complex and targeting protein yotiao (splice variant of AKAP9) by the AC/ cAMP/ PKA pathway (Terrenoire et al., 2005; Chen and Kass, 2011). Greater control of $I_{Ks}$ during increased sympathetic activation as a result of adrenergic stimulation, is enabled through the development of macromolecular complexes involving the above components as well as phosphatase-1 and PDE4D3 (Banyasz et al., 2014; Chen and Kass, 2011; Terrenoire et al., 2005). This complex allows spatiotemporally sensitive control of $I_{Ks}$, capable of graded APD shortening in response to increasing adrenergic stimulation (Chen and Kass, 2011; Terrenoire et al., 2005). Shortening of APD through increased $I_{Ks}$ current however, is dependent on concomitant $Ca^{2+}$ current response to adrenergic stimuli (Jeevaratnam et al., 2018; Sampson and Kass, 2010). Thus, the true APD response may depend on the ratio between the two currents.

As previously mentioned, alterations in AP repolarisation are considered to have a vital role in the age-related decline of cardiac reserve (Feridooni et al., 2015). The

slow delayed rectifying $K^+$ current, is key in modulating this APD response and has in turn led to investigation of its influence in this ageing phenomenon (Banyasz et al., 2014; Chen and Kass, 2011; Feridooni et al., 2015; Ocorr et al., 2007; Terrenoire et al., 2005). A reduction in this current could disturb the balance with LTCC current and impair AP shortening in response to increased activation rate and contractility which may also limit repolarisation reserve and potentially constrict overall cardiac reserve.

The limited evidence available in this area has found a decline in KCNQ1 (67%) density in drosophila models (Ocorr et al., 2007). A further study has found knockout of this gene triggers similar detriments to the ageing phenomenon (Nishimura et al., 2011; Ocorr et al., 2007). Such detriments included prolonged APD, increased risk of HF (70 – 80 %), poor rhythmicity and poorer tolerance to stress (Nishimura et al., 2011; Ocorr et al., 2007; Banyasz et al., 2014; Wessells and Bodmer, 2007). More recently, one study found basal $I_{Ks}$ current decreased in old rats (~ 50 %) (24 months of age) compared with adult rats (8 months of age) (Olgar et al., 2022). Conversely, a recent study in guinea pigs reported no age-related changes in basal $I_{Ks}$ current, however significant differences were yielded in $I_{Ks}$ current response to adrenergic stimulation, with an increase (~ 20 – 40 %) observed in adult (1 – 3 months of age) ventricular myocytes and a decrease (~ 15 – 35 %) observed in old (≥ 24 months of age) ventricular myocytes (Zou et al., 2021). Interestingly, no studies to date have investigated $I_{Ks}$ current response to $\beta_1$AR signalling in ageing rat hearts.

Highlighting the influence of $I_{Ks}$ in the ageing heart and improving understanding of any potential place that it may have in the deteriorating $\beta_1$AR mechanism, may facilitate the development of therapeutic intervention for age-related arrhythmogenesis as well as other symptoms of the ageing phenomenon. The aim of these experiments were firstly, to assess the effect of ageing on $I_{Ks}$ tail current and the response to adrenergic stimulus. The second aim was to assess the impact of ageing on the influence of $I_{Ks}$ on APD during control and adrenergic stimulation conditions.

## 5.2 Methods

### 5.2.1 Specific Experimental Procedures

Peak membrane tail currents were measured in adult (3 months of age) and old (22 - 23 months of age) male Wistar rat ventricular myocytes (adult, n = 19; old, n = 17) in

voltage-clamp mode. Membrane currents were stimulated using the voltage sequence displayed in figure 20 at a frequency of 0.1 Hz (Sun et al., 2001; Wang and Fitts, 2020). Three-second test pulses were used to allow for activation of $I_{Ks}$ currents and deactivation of other repolarising currents (Bosch et al., 1998; Jost et al., 2007; Wang and Fitts, 2020). A frequency of 0.1 Hz was used to allow for full deactivation of $I_{Ks}$ after test pulses (Sun et al., 2001; Wang and Fitts, 2020). A holding potential of -40 mV was utilised to remove sodium currents. Membrane current recordings were taken with and without adding potent $I_{Ks}$ blocker chromanol 293b (30 µM) to the bath solution. Recordings were repeated with isoproterenol (100 nM) superfusion, each time with and without chromanol 293b. Chromanol 293b and isoproterenol were administered to ventricular myocytes for 2- and 5-minute periods prior to recording respectively (Harding et al., 1988; Lim et al., 1999; Johnson et al., 2012). Three-minute periods were provided for washout of chromanol 293b with Tyrode solution prior to isoproterenol superfusion (Ding et al., 2002; Harding et al., 1988; Lim et al., 1999; Johnson et al., 2012). The combined chromanol 293b and isoproterenol dose was superfused for 2 minutes prior to recording. Two – Three recordings were achieved for each stage of the experiment. An average was calculated of separate recordings for each stage of the experiment during analysis using Clampfit software. The difference in peak tail current amplitude induced by chromanol 293b with and without isoproterenol were defined as $I_{Ks}$ peak tail currents. Peak membrane $I_{Ks}$ tail currents during control and in response to isoproterenol superfusion were compared. All cell data was then averaged per heart and compared between adult (N = 10) and old (N = 10) rats.

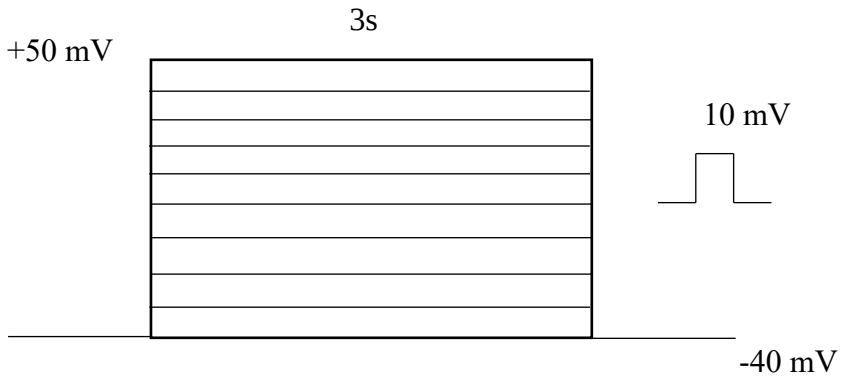


Figure 20. Schematic drawing of the voltage-clamp protocol used to determine peak $I_{Ks}$ tail currents.

Steady-state APs of adult (3 months of age) and old (22 - 23 months of age) male Wistar rat ventricular myocytes (adult, n = 31; old, n = 15) were recorded via repeated sweep sequences at 0.5 Hz to allow for activation and deactivation of $I_{Ks}$ current (Liu and Antzelevitch, 1995). Action potentials were recorded during super fusion of normal rat Tyrode, chromanol 293b (30 μM), isoproterenol (100 nM) and finally during combined superfusion of chromanol 293b and isoproterenol. Previous findings suggest chromanol 293b blocks $I_{Ks}$ at doses ranging from 100 nM – 100 μM, with an IC50 appearing to occur at 1 - 3 μM (Fujisawa et al., 2000; Sun et al., 2001). A 30 μM dose was used in accordance with previous $I_{Ks}$-related literature (Wang and Fitts, 2020). Two minutes of chromanol 293b superfusion were allowed before AP recordings were obtained to enable equilibration of the drug followed by a 3-minute washout period with normal rat Tyrode (Ding et al., 2002). Five minutes were allowed for isoproterenol superfusion prior to AP recordings to ensure drug equilibration (Harding et al., 1988; Lim et al., 1999; Johnson et al., 2012). Recordings of combined isoproterenol and chromanol 293b responses followed a further 2-minute superfusion. Steady-state AP data (3 – 5 traces) were averaged in each cell at each experimental stage (Tyrode, chromanol 293b, isoproterenol, combined chromanol 293b and isoproterenol) and $APD_{25}$, $APD_{50}$, $APD_{75}$, $APD_{90}$, $APD_{100}$, diastolic membrane potential and AP amplitude were calculated. The involvement of $I_{Ks}$ was calculated as the difference in each variable between the presence and absence of chromanol 293b. The involvement of $I_{Ks}$ was then compared between control and isoproterenol

conditions. All cell data was then averaged per heart and compared between adult (N = 10) and old (N = 10) rats.

### 5.2.2 Specific Statistical Analyses

A mixed ANOVA was performed on all data to provide comparison between adult and old hearts during all conditions (control; chromanol 293b; 100 nM isoproterenol; 100 nM isoproterenol + chromanol 293b) and subsequently to provide comparison between the relative change in all variables induced by chromanol 293b superfusion in adult and old hearts during control and isoproterenol conditions. In cases where variables violated the assumption of approximate normal distribution, data transformations (log 10) were used. Data transformation (log 10) was performed on $APD_{25}$, $APD_{50}$, $APD_{75}$, $APD_{90}$ and $APD_{100}$ in the original AP data and also on $APD_{75}$, $APD_{90}$ and $APD_{100}$ in the relative AP change data. In all cases the assumption of approximate normal distribution was satisfied. Where assumptions of sphericity were violated, the Huynh Feldt correction was used. Where the assumption of no significant outliers was violated ($APD_{75}$; $APD_{90}$; diastolic membrane potential in the relative AP data), data Winsorization was performed (Kwak and Kim, 2017; Liao et al., 2016). In all cases except $APD_{90}$, data Winsorization did not significantly alter the outcome of the mixed ANOVA compared with non-Winsorized data. In the case of $APD_{90}$, data Winsorization revealed a significant ageing*isoproterenol interaction ($p = 0.035$; partial $eta^2 = 0.223$) that was not highlighted in the non-Winsorized data ($p = 0.073$; partial $eta^2 = 0.167$). All other mixed ANOVA assumptions were met.

## 5.3 Results

### 5.3.1 Brief Summary of Recordings

Unfortunately, after reviewing a number of rat ventricular myocyte recordings yielded from voltage-clamp investigations described in section 5.2.1, peak $I_{Ks}$ tail currents could not be accurately and reliably analysed and in turn quantified as a result of significant variations in current recordings. Peak absolute $I_{Ks}$ currents measured at the end of the depolarising pulses immediately prior to repolarising to -40 mV holding potentials were also unable to be accurately and reliably analysed and quantified as a result of significant variations in current recordings. Therefore, the decision was made

to refrain from the presentation of such values and to solely focus on the impact of chromanol 293b on AP variables for the remainder of this chapter.

Current-clamp recordings during control conditions; chromanol 293b superfusion; 100 nM isoproterenol superfusion and during both 100 nM isoproterenol and chromanol 293b) superfusion at 0.5 Hz pacing were successfully collected in adult (N = 10; n = 31) and old rats (N = 10; n = 15). The percentage change induced by chromanol 293b was also then calculated and compared between adult and old rats during control conditions as well as conditions of isoproterenol stimulation. Average access resistance was 28 ± 1.6 MΩ. Average cell capacitance was 126 ± 8.2 pF in adult rats and 170 ± 13.6 pF in old rats. An unpaired t-test revealed cell capacitance was significantly greater in old rats compared with adult rats ($p = 0.018$).

As a result of the previously explained inability to reliably quantify both peak absolute $I_{Ks}$ current and peak $I_{Ks}$ tail current in our experiments combined with the lack of other confirmatory experiments and further, the findings of existing literature that point towards potentially contaminating effects of other repolarising $K^+$ channel currents ($I_{to}$ and $I_{Kur}$) key to AP repolarisation during block by chromanol 293b at the concentration used in this experiment (Du et al., 2003; Sun et al., 2001; Árpádffy-Lovas et al., 2022), the findings yielded from the above current-clamp experiments cannot be attributed solely to $I_{Ks}$ current with absolute certainty. Therefore, the influence of chromanol 293b on the AP variables studied in this chapter are, for the remainder of this work, considered as chromanol 293b-sensitive current influences.

Examples of raw recordings are shown in figure 21. Figure 21 shows chromanol 293b-sensitive current maintains a significant influence on APD in adult and old rats. However visually, the influence of chromanol 293b-sensitive current on late AP repolarisation appears to increase with the introduction of isoproterenol compared with control in adult rats, an effect not observed in old rats where the influence of chromanol 293b-sensitive current on late AP repolarisation seems to remain relatively constant. This suggests chromanol 293b-sensitive current response to adrenergic stimulation may be affected by ageing in this example.

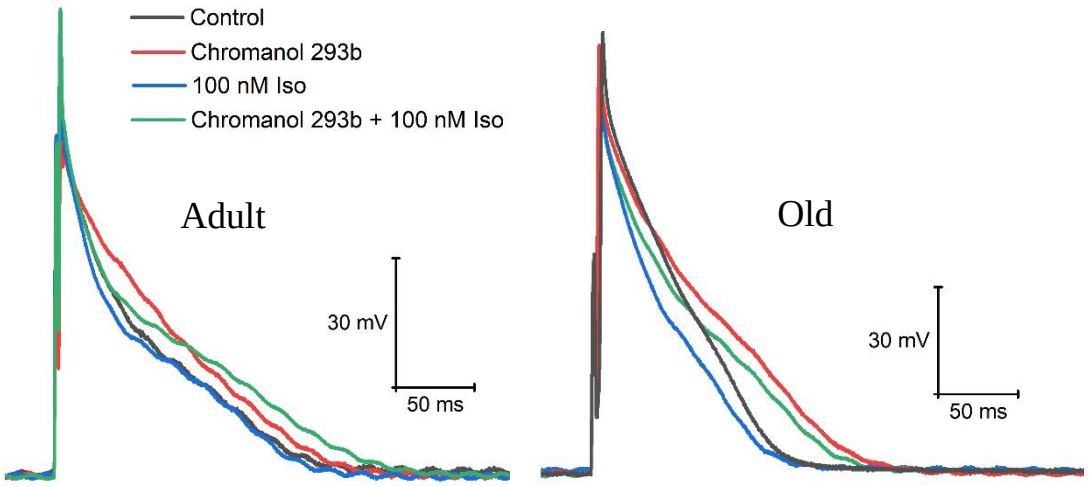


Figure 21. Example overlaid adult (left) and old (right) rat ventricular myocyte current-clamp traces illustrating AP changes induced by chromanol 293b superfusion during control and adrenergic stimulation conditions at 0.5 Hz pacing.

### 5.3.2 Influence of Chromanol 293b on the Rat Ventricular Myocyte AP

#### 5.3.2.1 Early AP Repolarisation and AP Plateau / $APD_{25-50}$

The results indicate $APD_{25-50}$ was shortened in old compared with adult rats ($p < 0.05$). A significant interaction between ageing and condition (control, chromanol 293b, isoproterenol, combined chromanol 293b and isoproterenol) was also identified with $APD_{50}$ becoming shortened during isoproterenol alone alongside combined chromanol 293b and isoproterenol stimulation in old rats compared with adult rats ($p < 0.01$). However, there was no significant interaction between condition and ageing in $APD_{25}$ (figure 22).

$APD_{25}$ was prolonged during chromanol 293b superfusion compared with control conditions ($p = 0.001$) and was also prolonged during combined chromanol 293b and isoproterenol stimulation compared with both control and isoproterenol conditions ($p < 0.001$). In adult and old rats, $APD_{50}$ was prolonged during chromanol 293b and combined chromanol 293b and isoproterenol superfusion compared with control conditions ($p < 0.05$). $APD_{50}$ was also prolonged during combined chromanol 293b and isoproterenol superfusion compared with isoproterenol superfusion in adult and

old rats ($p < 0.001$). However, in old rats, $APD_{50}$ was shortened during isoproterenol superfusion compared with chromanol 293b ($p < 0.001$) (figure 22).

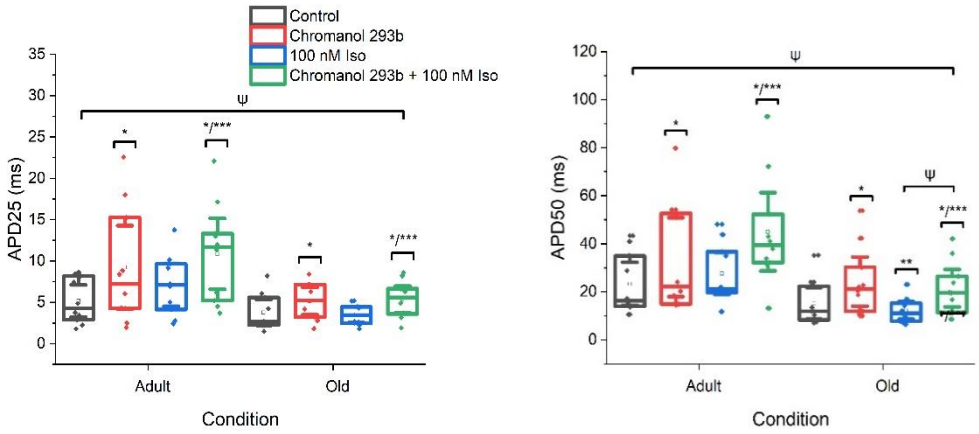


Figure 22. Influence of chromanol 293b on early AP repolarisation ($APD_{25}$) and AP plateau ($APD_{50}$) in adult and old rat ventricular myocytes during control conditions and adrenergic stimulation. Ψ Indicates a significant difference between adult and old rats. * Indicates a significant difference compared with control conditions. ** Indicates a significant difference compared with chromanol 293b. *** Indicates a significant difference compared with isoproterenol. Box plots display mean (open square), median (solid middle line), upper, and lower quartiles (solid upper and lower lines) and confidence intervals (error bars).

### 5.3.2.2 Late AP Repolarisation / $APD_{75\text{-}100}$

The results yielded no significant main effect for ageing in $APD_{75\text{-}100}$, though a significant ageing*condition interaction was observed in $APD_{75\text{-}90}$ ($p < 0.03$) (figure 23).

Post hoc analyses found in adult rats: $APD_{75\text{-}90}$ was prolonged during chromanol 293b and combined chromanol 293b and isoproterenol superfusion compared with control conditions ($p < 0.04$). Furthermore, $APD_{75\text{-}90}$ was prolonged during combined chromanol 293b and isoproterenol superfusion compared with chromanol 293b in adult rats ($p < 0.02$) but was also prolonged during combined chromanol 293b and

isoproterenol superfusion compared with isoproterenol in adult and old rats ($p < 0.002$).

In old rats, $APD_{75}$ was prolonged during chromanol 293b and combined chromanol 293b and isoproterenol superfusion compared with control conditions ($p < 0.03$), whilst $APD_{90}$ was prolonged only during chromanol 293b superfusion compared with control conditions ($p < 0.001$). In addition, $APD_{75-90}$ was shortened during isoproterenol compared with chromanol 293b in old rats ($p < 0.001$) (figure 23).

Meanwhile a mixed ANOVA found $APD_{100}$ was prolonged during chromanol 293b and combined chromanol 293b and isoproterenol superfusion compared with control conditions ($p < 0.003$). $APD_{100}$ was shortened during isoproterenol compared with chromanol 293b ($p = 0.005$) but was prolonged by combined chromanol 293b and isoproterenol superfusion compared with isoproterenol superfusion alone ($p < 0.001$) (figure 23).

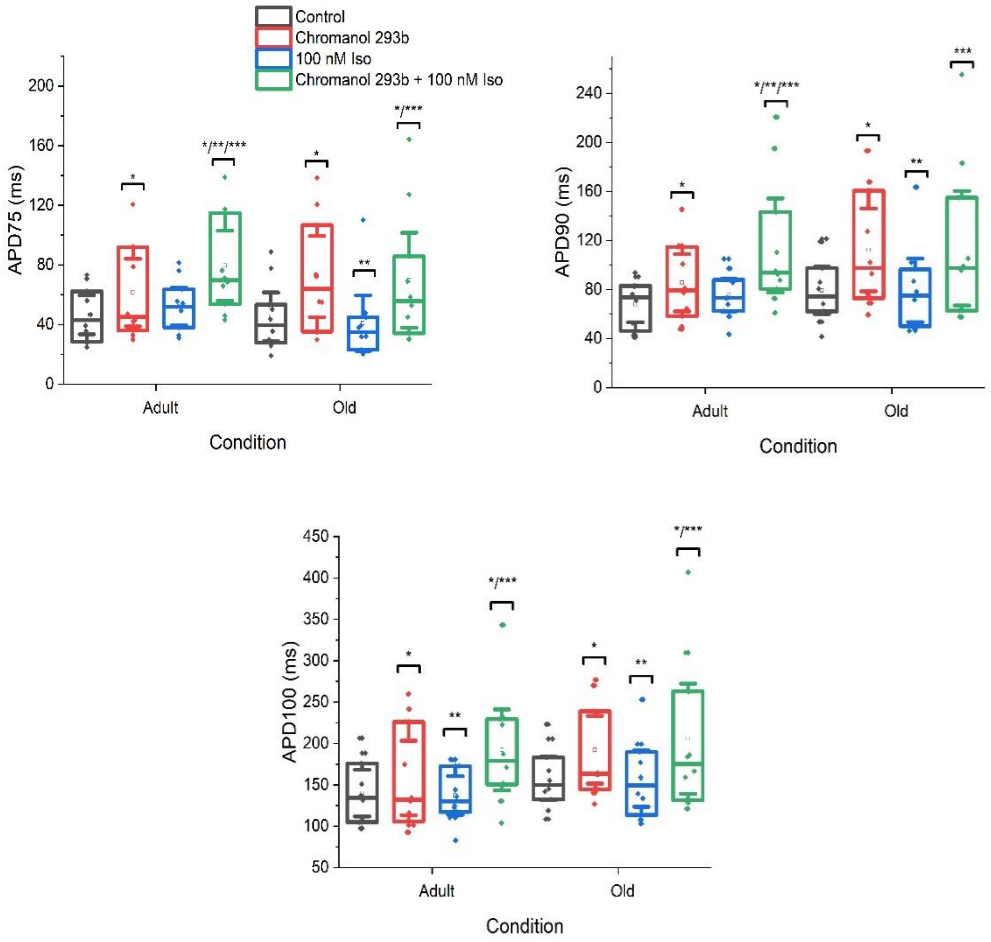


Figure 23. Influence of chromanol 293b on late AP repolarisation ($APD_{75\text{-}100}$) in adult and old rat ventricular myocytes during control conditions and adrenergic stimulation. * Indicates a significant difference compared with control conditions. ** Indicates a significant difference compared with chromanol 293b. *** Indicates a significant difference compared with isoproterenol. Box plots display mean (open square), median (solid middle line), upper, and lower quartiles (solid upper and lower lines) and confidence intervals (error bars).

### 5.3.2.3 AP Amplitude and Diastolic Membrane Potential

A mixed ANOVA revealed no significant main effects on AP amplitude. However, the results show a trend toward reduced AP amplitude in old compared with adult rats ($p = 0.079$; partial $eta^2 = 0.162$). A significant main effect in condition for diastolic membrane potential was identified ($p = 0.024$), however post hoc analyses yielded no pairwise differences (table 7).

Table 7. Influence of chromanol 293b on AP amplitude and diastolic membrane potential in adult and old rats during control conditions and adrenergic stimulation. Data displayed as mean ± (SEM).

| | Control | | Chromanol 293b | | 100 nM Iso | | Chromanol 293b + 100 nM Iso | |
|---|---|---|---|---|---|---|---|---|
| AP Amplitude (mV) | | | | | | | | |
| Adult | 123 | (3.4) | 117 | (3.1) | 119 | (2.9) | 118 | (2.6) |
| Old | 113 | (3.3) | 113 | (3.9) | 109 | (3.3) | 110 | (3.3) |
| Diastolic Membrane Potential (mV) | | | | | | | | |
| Adult | -70 | (1.1) | -68 | (1.5) | -71 | (1.8) | -71 | (1.6) |
| Old | -71 | (1.6) | -71 | (1.6) | -72 | (1.6) | -72 | (2.4) |

### 5.3.3 Relative Influence of Chromanol 293b-Sensitive Current on AP Variables during Control Conditions and Adrenergic Stimulation

A mixed ANOVA revealed, chromanol 293b-sensitive current had greater influence on AP amplitude in adult rats compared with old rats ($p = 0.028$). No further significant main ageing effects were identified. However, analyses showed chromanol 293b-sensitive current influence on $APD_{90}$ significantly increased during isoproterenol stimulation compared with control conditions in adult rats only ($p = 0.02$), whilst chromanol 293b-sensitive current influence on $APD_{90}$ remained the same during isoproterenol stimulation and control conditions in old rats (figure 24). No significant effects were yielded in $APD_{25\text{-}50}$ or diastolic membrane potential, though a trend toward greater chromanol 293b-sensitive current influence on $APD_{50}$ in old rats compared with adult rats was observed ($p = 0.127$; partial $eta^2 = 0.125$). Furthermore, chromanol 293b-sensitive current influence on $APD_{75}$ and $APD_{100}$ was increased during isoproterenol stimulation compared with control conditions ($p < 0.02$) (figure 24). Conversely the influence of chromanol 293b-sensitive current on AP amplitude

was greater during control conditions compared with isoproterenol stimulation (p = 0.04) (table 8).

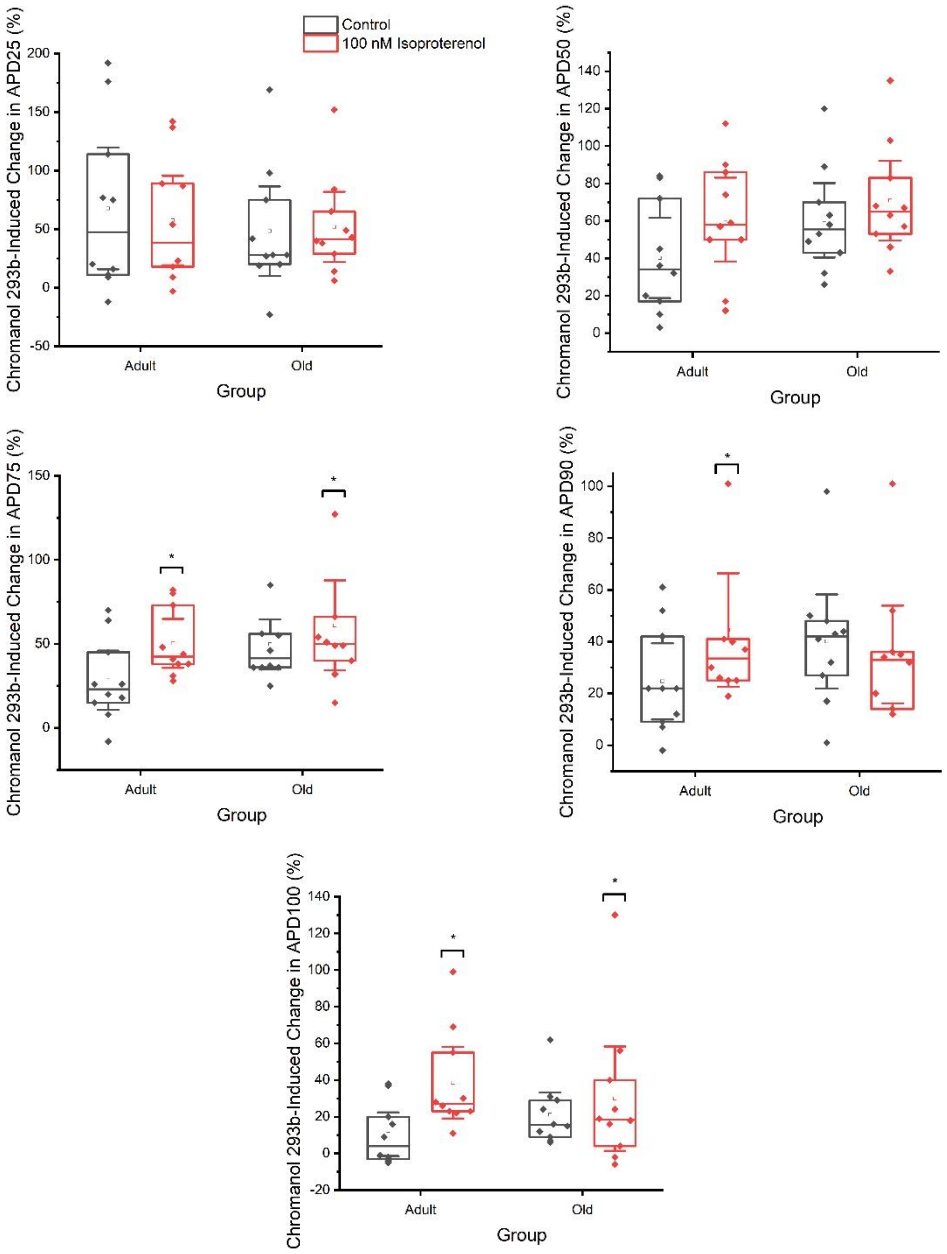


Figure 24. Influence of chromanol 293b-sensitive current on APD in adult and old rat ventricular myocytes during control conditions and adrenergic stimulation. * Indicates a significant difference compared with control conditions. Box plots display mean (open square), median (solid middle line), upper, and lower quartiles (solid upper and lower lines) and confidence intervals (error bars).

Table 8. Influence of chromanol 293b-sensitive current on AP amplitude and diastolic membrane potential in adult and old rats during control conditions and adrenergic stimulation. Data displayed as mean ± (SEM). Ψ Indicates a significant difference between adult and old rats. * Indicates a significant difference compared with control.

| | Control | | 100 nM Iso | |
|---|---|---|---|---|
| AP Amplitude (mV) | Ψ | | | |
| Adult | -5 % | (1.0) | -1 % | (1.0)* |
| Old | 0 % | (2.0) | 1 % | (1.0)* |
| Diastolic Membrane Potential (mV) | | | | |
| Adult | -3 % | (1.0) | -1 % | (1.0) |
| Old | 1 % | (1.0) | 0 % | (1.0) |

## 5.4 Discussion

The aim of this study was to assess the effect of ageing on $I_{Ks}$ tail current response to adrenergic stimulus and to assess the impact of ageing on the influence of $I_{Ks}$ on APD during control and during adrenergic stimulation conditions in rat ventricular myocytes.

As a result of significant variations in voltage-clamp recordings obtained in rat ventricular myocytes during this work, peak $I_{Ks}$ tail currents as well as absolute peak $I_{Ks}$ currents could not be accurately and reliably analysed and quantified with any confidence and consequently such data could not be presented in the results section of this chapter. Furthermore, the lack of additional experiments helping to confirm the selective block of $I_{Ks}$ by chromanol 293b at the dose used in this study, coupled with the concerns highlighted by previous literature (Du et al., 2003; Sun et al., 2001; Árpádffy-Lovas et al., 2022) that chromanol 293b-induced changes may be

attributable to other $K^+$ channel currents; mean the findings from the current-clamp investigations in this work must be referred to and interpreted as chromanol 293b-sensitive current influences on APD. Although research indeed confirms $I_{Ks}$ is blocked by chromanol 293b (Bosch et al., 1998) and similar work has utilised the same dose used in this work (Wang and Fitts, 2020), findings from other studies are indicative of $I_{to}$ and even $I_{Kur}$ current block at relatively similar doses (Du et al., 2003; Sun et al., 2001; Árpádffy-Lovas et al., 2022; Bosch et al., 1998) therefore the APD changes induced by chromanol 293b in this work cannot be reliably determined to be a result of $I_{Ks}$ current influences alone with confidence without the performance of further experiments.

The main current-clamp findings of this study were: early AP repolarisation ($APD_{25}$) and AP plateau ($APD_{50}$) were shortened in old rats (44 - 45 %) compared with adult rats, whilst no significant ageing main effects in raw findings for AP amplitude, $APD_{75}$, $APD_{90}$, $APD_{100}$ or diastolic membrane potential were observed. However, significant ageing*condition interactions were observed in late repolarisation ($APD_{75-90}$), where greater changes were observed in adult rats compared with old rats in response to chromanol 293b superfusion, evident from the increased chromanol 293b-induced $APD_{75-90}$ prolongation during isoproterenol compared with control conditions in adult rats compared with old rats.

Furthermore, regarding the percentage change in AP variables as a result of chromanol 293b superfusion during control conditions compared with isoproterenol stimulation: no significant main effects for ageing were observed in early repolarisation and AP plateau, though a trend toward greater chromanol 293b-sensitive current influence on $APD_{50}$ in old rats compared with adult rats existed. Late AP repolarisation ($APD_{75\ \&\ 100}$) was typically influenced more greatly by chromanol 293b-sensitive current during isoproterenol stimulation compared with control conditions, and also exhibited greater chromanol 293b-sensitive current influence on $APD_{90}$ during isoproterenol stimulation compared with control conditions in adult rats ($APD_{90}$), whilst old rats displayed almost no change in chromanol 293b-sensitive current influence on $APD_{90}$ between control and isoproterenol stimulation.

### 5.4.1 The Impact of Ageing on the Influence of Chromanol 293b-Sensitive Current on AP Repolarisation

Concerning the basal changes in raw APD with chromanol 293b superfusion, a particularly interesting finding was the significant reduction in APD during early AP repolarisation and AP plateau overall in old rats compared with adult rats. Such findings (though not statistically significant) have been consistently observed throughout this project (chapter 3) and have been previously observed in literature (Liu et al., 2000). Perhaps equally interesting was the trend toward greater chromanol 293b-sensitive current influence on $APD_{50}$ in old rats compared with adult rats when percentage APD change during chromanol 293b superfusion in control conditions were considered, coupled with the lack of overall ageing effects during control conditions elsewhere in the analysis. Such findings may point toward a relative age-related maintenance of chromanol 293b-sensitive current influence on APD during control / basal conditions, which could indicate that $I_{Ks}$ function may not undergo significant intrinsic degradation in old rat ventricles. Indeed, some recent research has found KCNQ1 and KCNE1 protein levels are maintained in adult (8 months of age) and old (24 months of age) rat hearts (Olgar et al., 2022). Though the same study revealed an age-related decrease in $I_{Ks}$ current (Olgar et al., 2022). Meanwhile, a recent study in guinea pigs (1 – 3 vs ≥ 24 months of age) reported no significant age-related changes in $I_{Ks}$ current during basal / control conditions, as well as no age-related changes in KCNQ1 and KCNE1 mRNA expression (Zou et al., 2021). However, the above notion that $I_{Ks}$ function may not undergo significant age-related intrinsic remodelling is purely speculation without further confirmatory experiments to reliably quantify how much the influence of chromanol 293b-sensitive current on rat ventricular APD in adult and old hearts can be attributed to $I_{Ks}$ current alone in this work as opposed to a potentially combined $I_{Ks}$, $I_{to}$ and $I_{Kur}$ current contribution (Du et al., 2003; Sun et al., 2001; Árpádffy-Lovas et al., 2022; Bosch et al., 1998).

### 5.4.2 The Impact of Ageing on the Influence of Chromanol 293b-Sensitive Current on AP Repolarisation in Response to Adrenergic Stimulation

The data yielded from current-clamp experiments performed in this work indicate the impact of chromanol 293b-sensitive current on AP repolarisation and APD is indeed altered with ageing in the rat with figure 23 demonstrating greater prolongation in elements of late AP repolarisation ($APD_{75-90}$) during chromanol 293b superfusion in

response to adrenergic stimulation in adult compared with old rats. Such changes are further made clear in figure 24 where the percentage change in $APD_{90}$ induced by chromanol 293b superfusion was significantly greater during isoproterenol compared with control conditions in adult rats only. Meanwhile during late AP repolarisation, the percentage change induced by chromanol 293b superfusion was similar between control and adrenergic stimulation conditions in old rat ventricular myocytes. As such this may highlight a breakdown in adrenergic signalling of $I_{Ks}$ in old age, though, as mentioned previously, further experiments are required to confirm the absence of any potential interference from $I_{to}$ and $I_{Kur}$ currents during chromanol 293b superfusion in this study (Du et al., 2003; Sun et al., 2001; Árpádffy-Lovas et al., 2022; Bosch et al., 1998).

This is the first study to our knowledge to investigate the impact of ageing on the influence of chromanol 293b-sensitive current and its response to adrenergic stimulation on rat ventricular myocyte APs. A recent study investigating age-related changes in $I_{Ks}$, similar, in part, to the investigations performed in this work and more closely the original aims of this chapter, found isoproterenol significantly increased $I_{Ks}$ tail current in adult guinea pig hearts (1 – 3 months of age) but decreased $I_{Ks}$ tail current in old guinea pig hearts (≥ 24 months of age) (Zou et al., 2021). Interestingly, this isoproterenol-induced reduction in $I_{Ks}$ tail current in old hearts was displayed to reverse with superfusion of a $\beta_2$AR antagonist, suggesting $\beta_2$AR may inhibit $I_{Ks}$ current response to adrenergic stimulation in old age (Zou et al., 2021). However, the study by Zou et al. utilised very large doses of isoproterenol (1 and 3 μM) (Zou et al., 2021) which may have influenced findings, particularly as our work in chapter 3 demonstrates - predominantly in old hearts - less predictable data (APD prolongation) during 1 μM doses of isoproterenol. Such findings may also indicate increasing involvement of $\beta_2$AR with increasing isoproterenol doses that provide a saturating adrenergic response which when coupled with the potential re-configuration of $\beta_1$AR and $\beta_2$AR suggested to occur with ageing (Wachter and Gilbert, 2012) may explain such outcomes with advanced age. For example it may be that in old age, such high doses of isoproterenol as those utilised in the study by Zou et al. saturate $\beta_1$AR which may be lower in expression (Ungerer et al., 1993; White et al., 1994) and / or activity (Narayanan and Derby, 1982) and are subsequently more susceptible to the influence of $\beta_2$AR thought to maintain expression (Wachter and Gilbert, 2012) but increase

$\beta_2$AR – $G_i$ signalling (Zou et al., 2021; Wachter and Gilbert, 2012). A loss of $I_{Ks}$ current or - in the case of this study – a loss of chromanol 293b-sensitive current influence on AP repolarisation in response to adrenergic stimulation is capable of potentially impairing the response to exercise through slowing the shortening of AP repolarisation, limiting the capacity for shortening under increasing intensities (Chen and Kass, 2011; Terrenoire et al., 2005) and coping with the increasingly brief diastolic interval, or may limit the ability to have an increasingly brief diastolic interval at all.

It should be considered that humans rely heavily on $I_{Ks}$ for the modulation of AP repolarisation, particularly during adrenergic stimulation through physical activity. It could be speculated that mild to moderate changes in chromanol 293b-sensitive current influence on APD with ageing in rat ventricular myocytes as found in this study, if found in humans in similar or perhaps lesser magnitudes, may yield much wider ranging influence and consequences for overall cardiac function and response to exercise in old age (Joukar, 2021). However, once more, the potential influence of other repolarising $K^+$ channel currents on the age-related differences in chromanol 293b-sensitive current in rats highlighted in this study coupled with the likely impact of species differences may provide contrast to such speculation. For example, the other repolarising $K^+$ currents potentially contributing to the findings of the chromanol 293b investigations in this study alongside $I_{Ks}$ ($I_{to}$ and $I_{Kur}$) exist in vastly different quantities in rats compared with humans (Varró et al., 1993; Árpádffy-Lovas et al., 2022). It is understood that $I_{to}$ and $I_{Kur}$ currents are more prominent in the rat heart and have greater influence on ventricular AP repolarisation (Varró et al., 1993; Árpádffy-Lovas et al., 2022). Therefore it may also be speculated that the magnitude of age-related chromanol 293b-sensitive current findings in rat ventricular myocytes on the loss of cardiac response to exercise in old age may translate to a lesser impact in humans.

The findings from these current-clamp trials investigating chromanol 293b-sensitive current influence on APD may help to understand the overall APD response to exercise and may explain, in part, the noted trends toward a reduced APD response to isoproterenol in old rats as well as the reduced ability to follow higher cardiac pacing rates demonstrated in chapter 3. Meanwhile, the trend toward greater chromanol 293b-sensitive current influence on AP plateau in old rats compared with adult rats provided a very peculiar finding. The underlying mechanism of this is unknown. Though it is

in line with the documented briefer early AP repolarisation and plateau findings frequently yielded in this project in old rats. It could be that the trend toward greater chromanol 293b-sensitive current influence in old rats compared with adult rats is largely influenced by the trend toward a negative isoproterenol-induced LTCC current response shown in chapter 4. A reduction in LTCC current during isoproterenol may help facilitate a greater / exaggerated effect on APD when chromanol 293b superfusion occurs in old compared with adult rats where the LTCC current was found to maintain peak current during adrenergic stimulation. However, this is speculative and requires information on the interaction with intracellular $Ca^{2+}$. Lastly, the overall greater influence of chromanol 293b-sensitive current on APD, particularly late AP repolarisation during isoproterenol compared with control conditions was an expected finding, in line with literature (Kang et al., 2017; Wang and Fitts, 2020), though this is the first study to be conducted in this particular area involving old rat ventricular myocytes. This further highlights the control of repolarising $K^+$ channels in dictating / modulating a response to exercise, at least in terms of excitation.

## 5.5 Conclusion

In summary, this study demonstrates the influence of chromanol 293b-sensitive current on APD under basal conditions and in response to adrenergic stimulation in adult and old rat ventricular myocytes. The findings indicate the influence of chromanol 293b-sensitive current on late AP repolarisation response to isoproterenol is reduced in old rats compared with adult rats. Overall, these results may help to understand the outcomes in chapter 3, where an age-related prolongation of late AP repolarisation was identified, without incriminating significant specific intrinsic rate-dependent changes or changes in adrenergic response with ageing, yet an inability to follow higher cardiac pacing rates was observed. Though further study is required, these results provide confirmation of the role of repolarising $K^+$ channel currents in formulating the adrenergic response in excitation and indicate the potential role of impaired $\beta_1$AR – repolarising $K^+$ channel signalling in the age-related loss of exercise tolerance. The results of this work and work of the previous chapters are seemingly suggestive of the potential existence of a range of components contributing to mild-moderate decrements which accumulate to facilitate the cardiac ageing phenomenon. Further study, using more selective $I_{Ks}$ blockers (HMR-1556, Árpádffy-Lovas et al.,

2022) alongside the use of additional ion channel blockers or other agents that enhance $I_{Ks}$ to confirm the extent to which the age-related changes yielded in this study are attributable to $I_{Ks}$ alone combined with additional studies of other ion channels, particularly during increased pacing frequencies may help elucidate physiologically relevant remodelling and thus lead to the better overall understanding of the aged heart.

# Chapter 6: Effects of Ageing on the Modulation of Repolarising $K^+$ Currents during AP Repolarisation and Response to Isoproterenol in Rat Ventricular Myocytes

## 6.1 Introduction

Action potential repolarisation in ventricular myocytes is controlled through the delicate balance of repolarising and depolarising currents (Grunnet, 2010; Jeevaratnam et al., 2018; Sampson and Kass, 2010). Maintaining the balance of repolarisation is equally important for the protection from potential arrhythmias and the efficient utilisation of the repolarisation reserve and in achieving full dynamic range of CO (Jeevaratnam et al., 2018; Sampson and Kass, 2010; Feridooni et al., 2015; Varshneya et al., 2018). It is likely, changes in components helping to control repolarisation are a contributing mechanism/ factor to the loss of the tolerable range of response to adrenergic stimulation in the heart with advanced age. A major component of control of this is the $I_{Ks}$ current, with additional contributions from other key, largely $K^+$ currents, such as $I_{Kr}$ and $I_{K1}$. (Grunnet, 2010; Jeevaratnam et al., 2018; Sampson and Kass, 2010).

The three repolarising $K^+$ currents each have their own role in shaping myocyte repolarisation and the stability of the cardiac AP. Slowly activating delayed rectifying $K^+$ channels are responsible mainly for modulating AP repolarisation in ventricular myocytes under increases in rate due to increased current activation and current accumulation caused by slow channel inactivation coupled with diminishing diastolic intervals (Feridooni et al., 2015; Banyasz et al., 2014; Kang et al., 2017; Jeevaratnam et al., 2018). In response to adrenergic stimulation $I_{Ks}$ current has been found to increase ~ 22 % to in excess of ~ 10-fold (Banyasz et al., 2014; Wang and Fitts, 2020). Rapid delayed rectifying $K^+$ channels are responsible predominantly for modulating

AP repolarisation during basal conditions in most mammals (Feridooni et al., 2015). However the evidence in rats is contentious, with recent research suggesting $I_{Ks}$ is more prominent in expression and current at resting HR and during adrenergic stimulation than $I_{Kr}$ (Wang and Fitts, 2020). In fact, in rats, difficulty in the detection of $I_{Kr}$ has been reported, contrary to other species (Wang and Fitts, 2020). Furthermore, due to its rapid inactivation, current accumulation is less likely during increased stress and thus is less dominant during adrenergic stimulation (Jeevaratnam et al., 2018; Banyasz et al., 2014; Kang et al., 2017). Previous research has reported both reduced $I_{Kr}$ current in guinea pigs (~ 30 %) and increased current in guinea pigs and canines (35 – 50 %) in response to adrenergic stimulation (Heath and Terrar, 2000; Harmati et al., 2011; Banyasz et al., 2014). Little evidence currently exists in rat models. Inward rectifying $K^+$ channels are responsible for returning to and ensuring stabilisation of the resting membrane potential in ventricular myocytes (Jeevaratnam et al., 2018). Similarly mixed findings have been demonstrated in $I_{K1}$ in response to adrenergic stimulation, with increases of ~ 20 – 100 % as well as current inhibition reportedly induced by isoproterenol (Banyasz et al., 2014; Koumi et al., 1995).

Age-related studies investigating $I_{Ks}$, $I_{Kr}$ and $I_{K1}$ separately has found reductions in $I_{Ks}$ expression in non-mammalian models (67 %), whilst channel knock-out has demonstrated key characteristics of the ageing phenomenon (propensity for arrhythmia, prolonged APD and impaired response to stress) (Nishimura et al., 2011; Ocorr et al., 2007; Wessells and Bodmer, 2007). Meanwhile, little information on $I_{Kr}$ exists in the context of ageing. Lastly, $I_{K1}$ has been found to increase in peak current (24 – 46 %) in old rats, with upregulations in current linked to enhanced AP shortening (25 – 60 %) in gain-of-function mice studies (Walker et al., 1993; Liu et al., 2000; Li et al., 2004).

Potentially valuable insight exists in the exploration of how these currents function together to determine whole-cell electrical response to vital stressors like adrenergic stimulation in comparison to basal conditions. Research performed in this particular vein is relatively new as a result of the required technique involved in the collective investigation of multiple currents at the same time (Banyasz et al., 2011; Banyasz et al., 2014). This type of investigation involves the use of AP-clamp techniques, which have been adapted in recent years to perform multi-channel investigations often

termed “onion peeling” and has been described in full in chapter 2 (Chen-Izu et al., 2012; Banyasz et al., 2011; Banyasz et al., 2014).

Understanding the underlying mechanisms involved in the age-related loss of cardiac reserve is paramount moving forward in the study of cardiac ageing. The employment of the AP-clamp technique provides currently one of the best tools to achieve significant findings related to the modulation of AP repolarisation and how the specific behaviour of responsible ion channels during adrenergic stimulation function to provide coordinated functional responses. To our knowledge, the multi-channel approach described above has not yet been used in respect to the ageing phenomenon. Therefore, the aim of this study was to utilise multi-channel AP-clamp techniques (“onion peeling”) to evaluate age-related changes at rest and during adrenergic stimulation in $I_{Ks}$, $I_{Kr}$ and $I_{K1}$ current and explore how they collectively influence AP repolarisation in old age. However, as a result of the findings in chapter 5 and the subsequent discussion regarding the selectivity of chromanol 293b as a blocker of $I_{Ks}$ at the dose used in this project (see section 5.3.1 – section 5.5) (Du et al., 2003; Sun et al., 2001; Árpádffy-Lovas et al., 2022), in the absence of further confirmatory experiments, the aim of this study therefore was to evaluate age-related changes at rest and during adrenergic stimulation in chromanol 293b-sensitive, $I_{Kr}$ and $I_{K1}$ currents and explore how they collectively influence AP repolarisation in old age.

## 6.2 Methods

### 6.2.1 Specific Experimental Procedures

Compensatory currents were measured in adult (3 months of age) and old (22 - 23 months of age) male Wistar rat ventricular myocytes (adult, n = 16; old, n = 14) using AP-clamp methods described above (section 2.2.5). After the achievement of whole-cell configuration, myocytes were paced at 1 Hz in current-clamp mode until steady-state APs were recorded. Steady-state APs were input as the stimulus file and baseline recordings were made in voltage-clamp mode. Chromanol 293b (30 µM), E4031 (1 µM) and Barium chloride ($BaCl_2$; 50 µM) were then sequentially added to the bath, each time recording the compensatory current elicited after 2 – 3 minute wash-on intervals (Banyasz et al., 2014; Banyasz et al., 2011). A period of 3 - 5 minutes normal Tyrode superfusion was allowed for washout. Isoproterenol (100 nM) was then superfused for 3 - 5 minutes before a new steady-state AP was recorded in current-

clamp mode and used as the voltage command during voltage-clamp recordings. Baseline recordings were achieved once more and then combined doses of the blockers and isoproterenol were sequentially superfused. Compensatory current data was recorded once more after each blocker, completing the myocyte recording. Recordings for each stage of the experiment were averaged and baseline recordings during control and isoproterenol superfusion were subtracted from the respective currents induced by each blocker using Clampfit software. The difference between baseline and compensatory current recordings induced by chromanol 293b were defined as chromanol 293b-sensitive current. The difference induced by further E4031 superfusion and lastly $BaCl_2$ superfusion were defined as $I_{Kr}$ and $I_{K1}$ currents, respectively. All cell data was then averaged per heart and all variables (peak current; integral current; current at 20 mV; current at 0 mV; current at -20 mV; current at $APD_{90}$; current at $APD_{95}$) were compared between adult (N = 8) and old (N = 8) male Wistar rats.

### 6.2.2 Specific Statistical Analyses

A Mixed ANOVA was performed on all AP-clamp data to provide comparison between chromanol 293b-sensitive, $I_{Kr}$ and $I_{K1}$ currents in adult and old hearts during control conditions and isoproterenol stimulation at 1 Hz pacing. In cases where variables violated the assumption of approximate normal distribution, data transformations (log 10) were used. Data transformation (log 10) was performed on $APD_{25}$, $APD_{50}$, $APD_{75}$, $APD_{90}$, $APD_{100}$, chromanol 293b-sensitive current at $APD_{90}$, peak $I_{Kr}$ current and peak $I_{K1}$ current and in all cases satisfied the assumption of approximate normal distribution. Where assumptions of sphericity were violated, the Huynh Feldt correction was used. Where assumptions of homogeneity were violated (peak $I_{Kr}$ current; $I_{Kr}$ integral current; $I_{Kr}$ current at 20 mV; $I_{Kr}$ current at 0 mV; $I_{Kr}$ current at -20 mV; $I_{K1}$ current at $AP_{90}$; $I_{K1}$ current at $AP_{95}$), Tamhane's T2 was used. In variables where the assumption of no significant outliers was violated (peak $I_{Kr}$ current; $I_{Kr}$ current at 20 mV; $I_{Kr}$ current at $AP_{95}$), data Winsorization was performed (Kwak and Kim, 2017; Liao et al., 2016). In all cases except $I_{Kr}$ current at 20 mV, data Winsorization did not significantly alter the outcome of the mixed ANOVA compared with non-Winsorized data. In the case of $I_{Kr}$ current at 20 mV data Winsorization revealed a significant ageing*isoproterenol interaction ($p = 0.038$; partial $eta^2 = 0.272$)

that was not highlighted in the original non-Winsorized data ($p = 0.227$; partial $eta^2 = 0.103$). All other mixed ANOVA assumptions were met.

## 6.3 Results

### 6.3.1 Brief Summary of Recordings

AP-clamp recordings measuring chromanol 293b-sensitive, $I_{Kr}$ and $I_{K1}$ currents during control conditions and adrenergic stimulation (100 nM isoproterenol) at 1 Hz pacing were successfully collected in adult (N = 8; n = 16) and old rats (N = 8; n = 14). Average access resistance was 27 ± 1.3 MΩ. Average cell capacitance was 142 ± 11.4 pF in adult rats and 145 ± 7.1 pF in old rats. An unpaired t-test found no significant difference in cell capacitance between adult and old rats ($p = 0.838$). Examples of raw recordings are shown in figure 25. Visually, figure 25 A – B shows the ventricular myocyte AP is prolonged in old rats, with AP plateau and late repolarisation particularly impacted. In addition, figure 25 - 26 illustrates the modulation of each current during the AP and their subsequent responses to adrenergic stimulation. In these examples, chromanol 293b-sensitive current appears prominent predominantly during the plateau of the AP and visibly increases in response to isoproterenol, albeit less so with ageing. Meanwhile, $I_{Kr}$ and $I_{K1}$ become apparently more prominent predominantly during late repolarisation and display age-dependent mixed responses to adrenergic stimulation with primarily negative responses observed in adult rats, whilst little adrenergic response is observed in both currents in old rats.

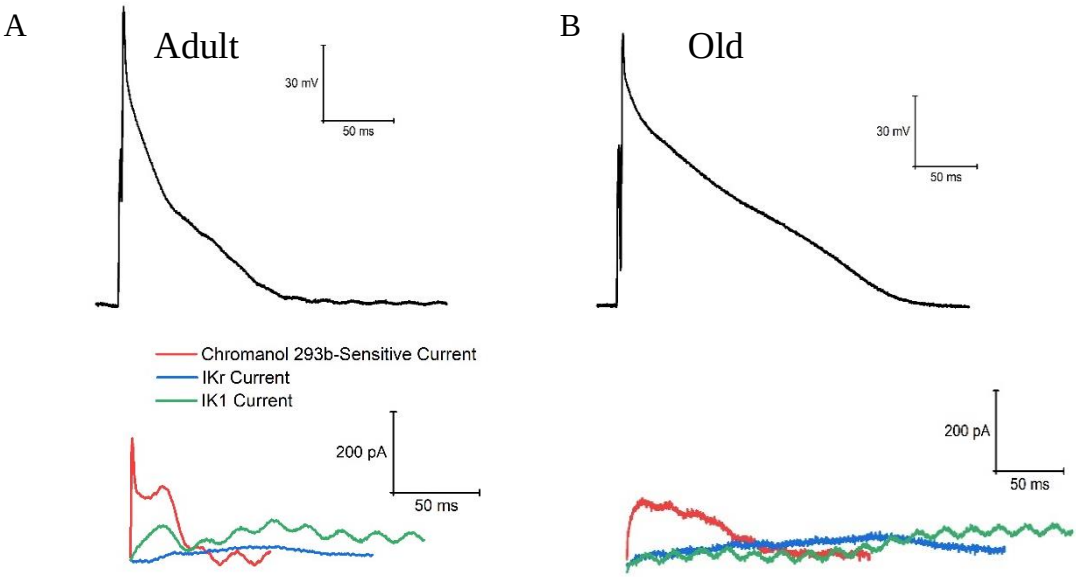


Figure 25. Examples of steady-state APs used during AP-clamp and the subsequent chromanol 293b-sensitive, $I_{Kr}$ and $I_{K1}$ currents recorded during control conditions at 1 Hz in adult (A) and old (B) rat ventricular myocytes.

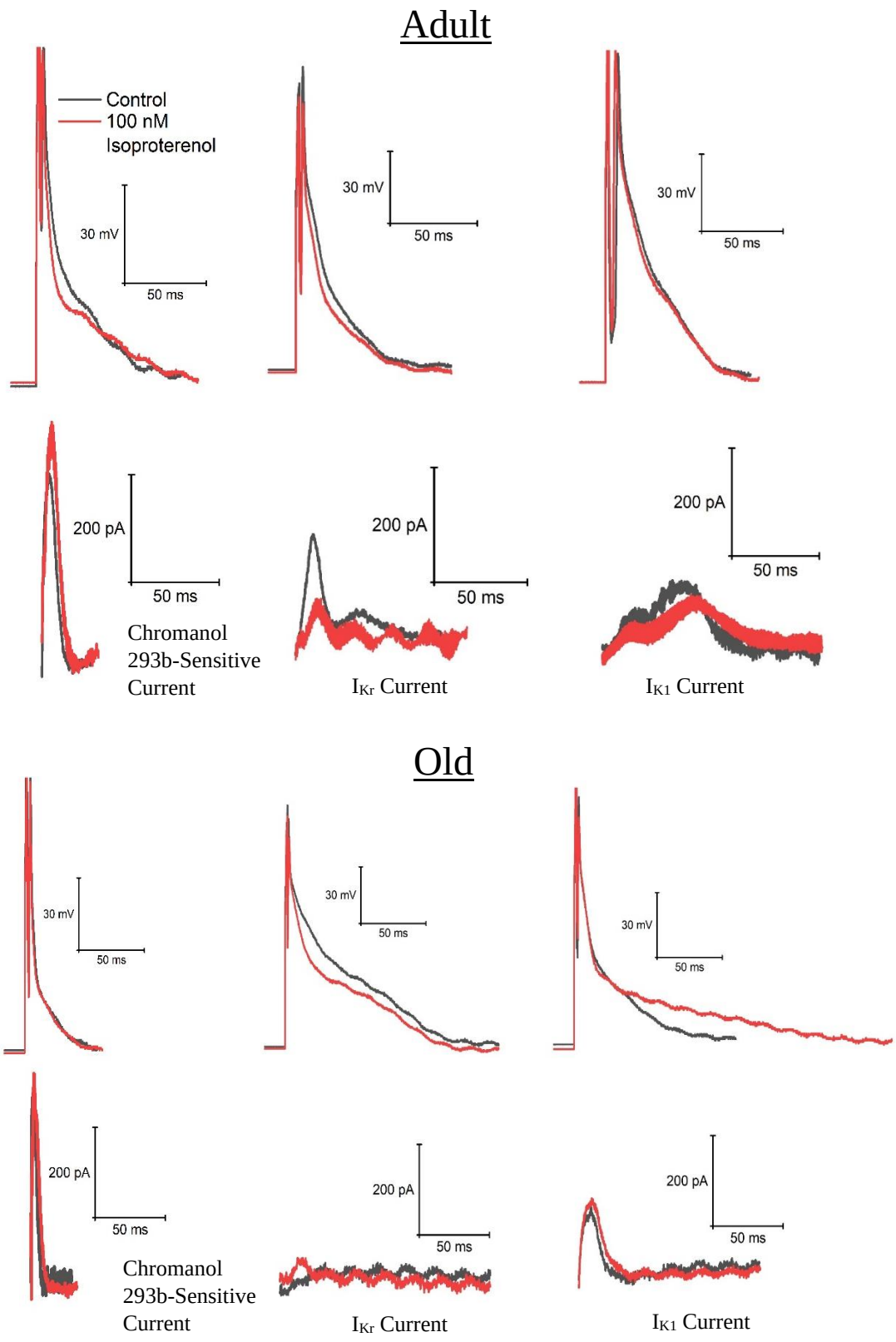


Figure 26. Individual examples of steady-state APs used during AP-clamp and the corresponding chromanol 293b-sensitive, $I_{Kr}$ and $I_{K1}$ currents recorded during control and adrenergic stimulation conditions at 1 Hz in rat ventricular myocytes.

### 6.3.2 Effects of Ageing and Adrenergic Stimulation on APD / the AP-Clamp Stimulus

A mixed ANOVA found late AP repolarisation ($APD_{75\text{-}100}$) was prolonged in old rats compared with adult rats ($p < 0.01$). In adult rats, AP plateau ($APD_{50}$) was prolonged during isoproterenol compared with control conditions ($p = 0.041$). Similarly, overall early AP repolarisation ($APD_{25}$) was prolonged during isoproterenol compared with control conditions ($p = 0.035$) (figure 27 A – F). In addition, during isoproterenol, diastolic membrane potential became more negative in adult compared with old rats ($p = 0.023$) (table 9). Analyses also found AP amplitude was reduced and diastolic membrane potential was more negative during isoproterenol compared with control conditions ($p < 0.03$) (table 9).

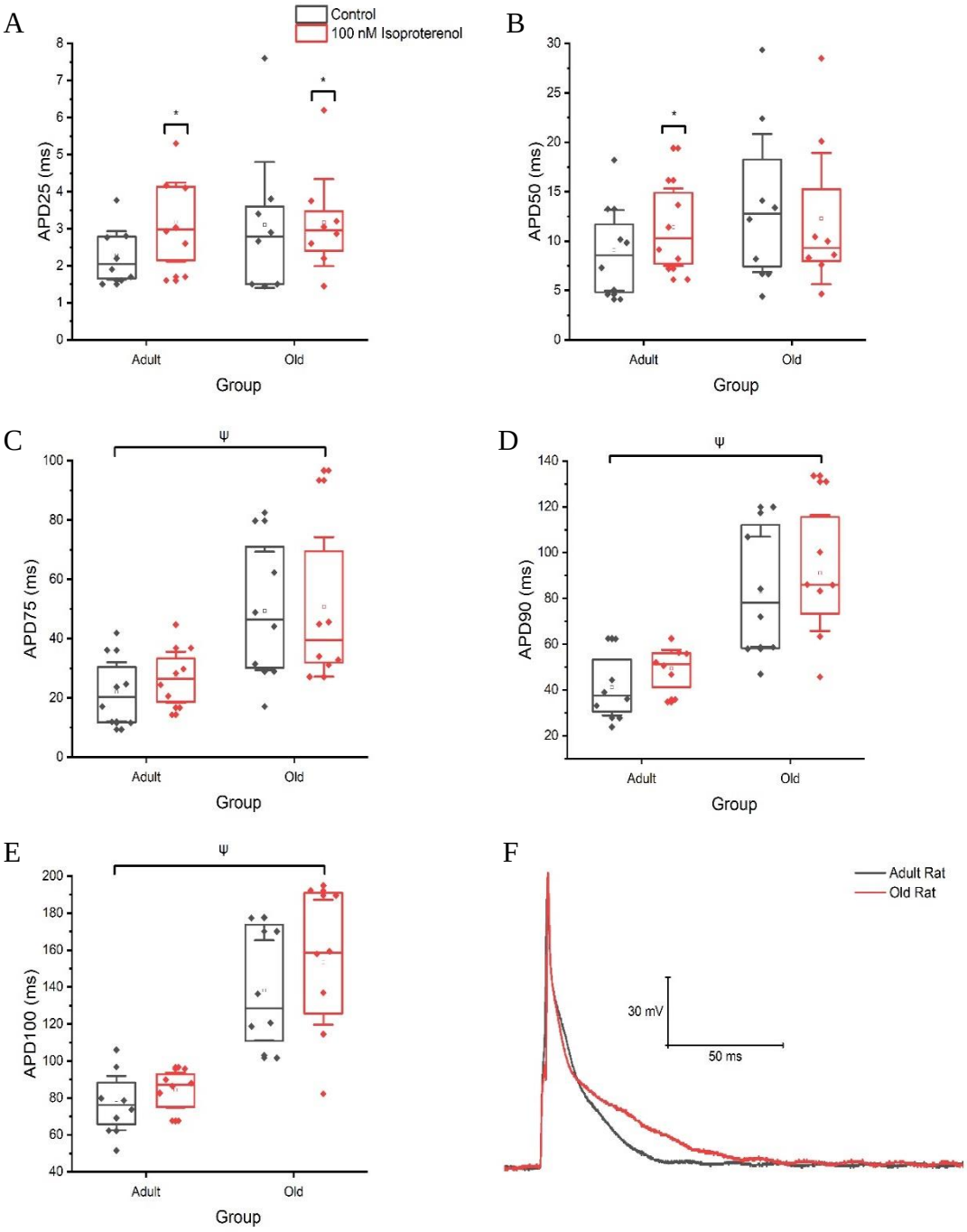


Figure 27. Influence of ageing on $APD_{25}$ (A), $APD_{50}$ (B), $APD_{75}$ (C), $APD_{90}$ (D) and $APD_{100}$ (E) and response to adrenergic stimulation in the steady-state rat ventricular myocyte AP recorded at 1 Hz pacing subsequently used as stimuli during AP-clamp. (F) A typical current-clamp recording during control conditions reflecting the impact of ageing on the rat ventricular AP. Ψ Indicates a significant difference between adult and old rats. * Indicates a significant difference compared with control. Box plots display mean (open square), median (solid middle line), upper, and lower quartiles (solid upper and lower lines) and confidence intervals (error bars).

Table 9. Influence of ageing on AP amplitude and diastolic membrane potential in adult and old rats during control conditions and adrenergic stimulation. Data displayed as mean ± (SEM). Ψ Indicates a significant difference between adult and old rats. * Indicates a significant difference compared with control.

| | Control | | 100 nM Iso | |
|---|---|---|---|---|
| AP Amplitude (mV) | | | | |
| Adult | 119 | (1.7) | 115* | (1.7) |
| Old | 117 | (1.8) | 115* | (2.0) |
| Diastolic Membrane Potential (mV) | | | | |
| Adult ψ | -73 | (3.0) | -81* | (3.0) |
| Old ψ | -67 | (1.7) | -71* | (1.7) |

### 6.3.3 Influence of Ageing and Adrenergic Stimulation on the Chromanol 293b-Sensitive current

There were no significant main effects on peak chromanol 293b-sensitive current, however there was a trend toward greater peak current in myocytes from adult rats compared with myocytes from old rats ($p = 0.120$; partial $eta^2 = 0.164$), particularly during isoproterenol superfusion ($p = 0.174$; partial $eta^2 = 0.128$) (figure 28). Chromanol 293b-sensitive integral current and chromanol 293b-sensitive current at $APD_{95}$ were greater in adult rats compared with old rats ($p < 0.02$) particularly during isoproterenol ($p < 0.002$). Furthermore, chromanol 293b-sensitive current at -20 mV and $APD_{90}$ was greater in adult rats compared with old rats ($p < 0.05$) (figure 28). Moreover, chromanol 293b-sensitive integral current, chromanol 293b-sensitive current at $APD_{90}$ and chromanol 293b-sensitive current at $APD_{95}$ were greater during isoproterenol compared with control conditions in adult rats only ($p < 0.02$). No significant main effects were found in chromanol 293b-sensitive current at 20 mV and 0 mV.

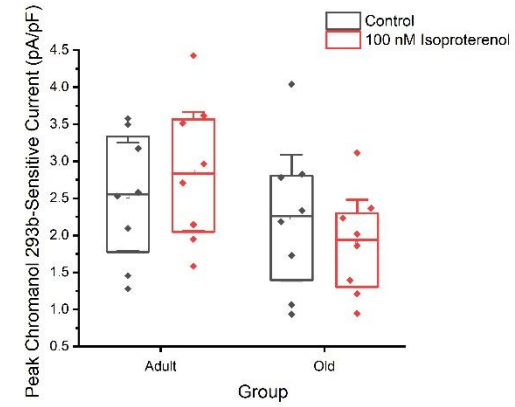
Control
100 nM Isoproterenol
Peak Chromanol 293b-Sensitive Current (pA/pF)
Adult
Old
Group

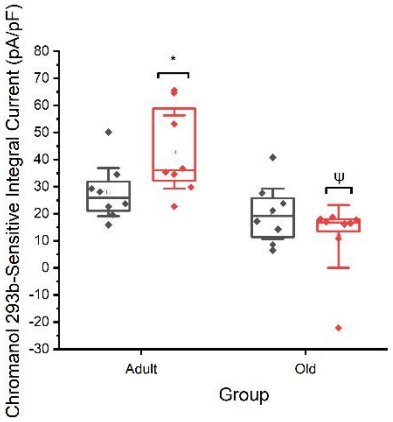
Chromanol 293b-Sensitive Integral Current (pA/pF)
*
Ψ
Adult
Old
Group

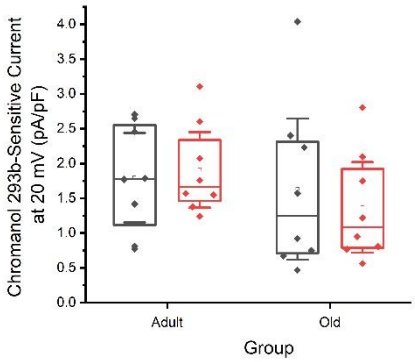
Chromanol 293b-Sensitive Current at 20 mV (pA/pF)
Adult
Old
Group

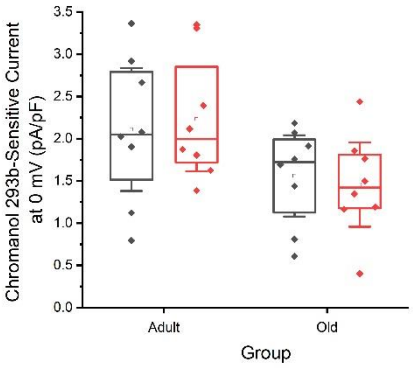
Chromanol 293b-Sensitive Current at 0 mV (pA/pF)
Adult
Old
Group

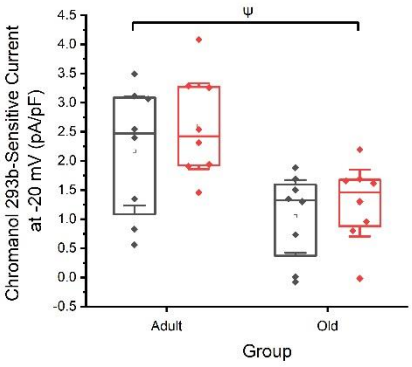
Ψ
Chromanol 293b-Sensitive Current at -20 mV (pA/pF)
Adult
Old
Group

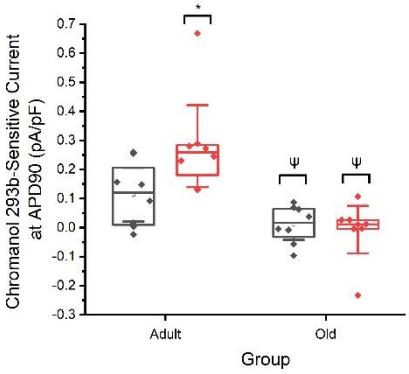
*
Ψ
Ψ
Chromanol 293b-Sensitive Current at APD90 (pA/pF)
Adult
Old
Group

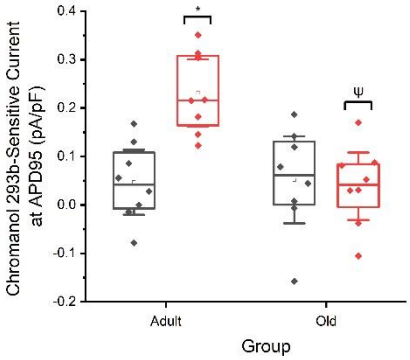
*
Ψ
Chromanol 293b-Sensitive Current at APD95 (pA/pF)
Adult
Old
Group

Figure 28. Impact of ageing on peak chromanol 293b-sensitive current, chromanol 293b-sensitive integral current and chromanol 293b-sensitive current at 20 mV, 0 mV, -20 mV, $APD_{90}$ and $APD_{95}$. Ψ Indicates a significant difference between adult and old rats. * Indicates a significant difference compared with control. Box plots display mean (open square), median (solid middle line), upper, and lower quartiles (solid upper and lower lines) and confidence intervals (error bars).

### 6.3.4 Influence of Ageing and Adrenergic Stimulation on $I_{Kr}$

A mixed ANOVA yielded no significant main effects in peak $I_{Kr}$ current, $I_{Kr}$ current at $APD_{90}$ and $I_{Kr}$ current at $APD_{95}$. However, $I_{Kr}$ integral current, alongside $I_{Kr}$ current at 20 mV, 0 mV and -20 mV were greater in old rats compared with adult rats during isoproterenol ($p < 0.02$) (figure 29). In addition, $I_{Kr}$ integral current, along with $I_{Kr}$ current at 20 mV, 0 mV and -20 mV were greater during control compared with isoproterenol conditions in adult rats only ($p < 0.03$) (figure 29).

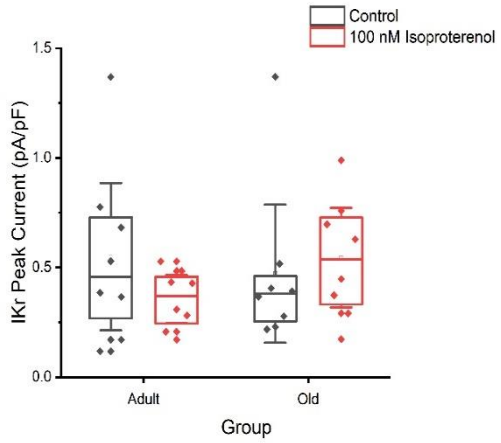
Control
100 nM Isoproterenol
IKr Peak Current (pA/pF)
1.5
1.0
0.5
0.0
Adult
Old
Group

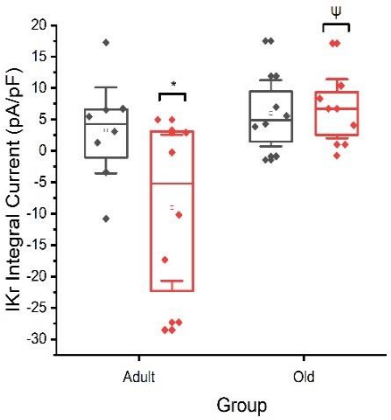
IKr Integral Current (pA/pF)
20
15
10
5
0
-5
-10
-15
-20
-25
-30
*
Ψ
Adult
Old
Group

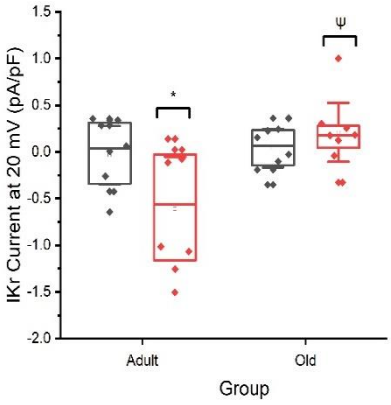
IKr Current at 20 mV (pA/pF)
1.5
1.0
0.5
0.0
-0.5
-1.0
-1.5
-2.0
*
Ψ
Adult
Old
Group

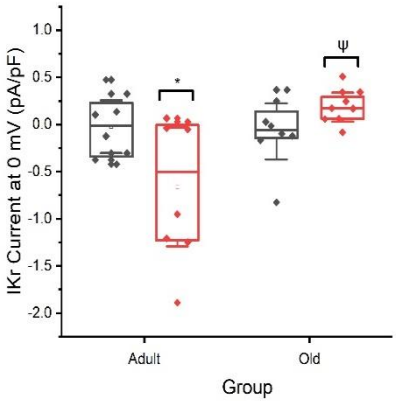
IKr Current at 0 mV (pA/pF)
1.0
0.5
0.0
-0.5
-1.0
-1.5
-2.0
*
Ψ
Adult
Old
Group

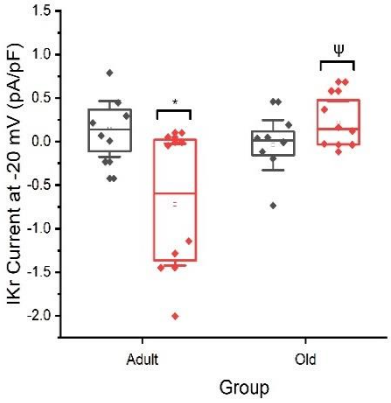
IKr Current at -20 mV (pA/pF)
1.5
1.0
0.5
0.0
-0.5
-1.0
-1.5
-2.0
*
Ψ
Adult
Old
Group

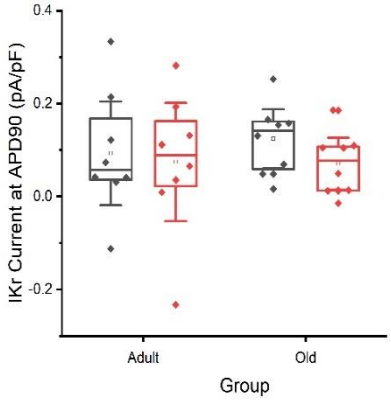
IKr Current at APD90 (pA/pF)
0.4
0.2
0.0
-0.2
Adult
Old
Group

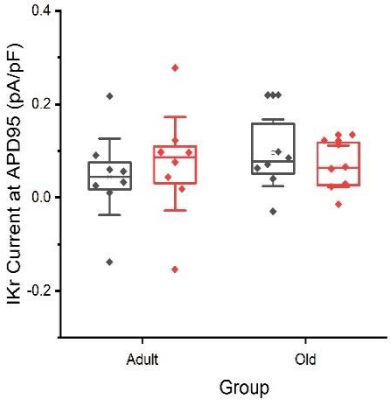
IKr Current at APD95 (pA/pF)
0.4
0.2
0.0
-0.2
Adult
Old
Group

Figure 29. Impact of ageing on $I_{Kr}$ peak current, $I_{Kr}$ integral current and $I_{Kr}$ current at 20 mV, 0 mV, -20 mV, $APD_{90}$ and $APD_{95}$. Ψ Indicates a significant difference between adult and old rats. * Indicates a significant difference compared with control. Box plots display mean (open square), median (solid middle line), upper, and lower quartiles (solid upper and lower lines) and confidence intervals (error bars).

### 6.3.5 Influence of Ageing and Adrenergic Stimulation on $I_{K1}$

Analyses yielded no significant main effects in peak $I_{K1}$ current. However, $I_{K1}$ integral current was more negative in old compared with adult rats ($p = 0.007$) (figure 30). $I_{K1}$ integral current was also more negative during isoproterenol compared with control conditions ($p = 0.006$). Lastly, $I_{K1}$ current at $AP_{90}$ and $AP_{95}$ was greater in adult rats compared with old rats ($p < 0.02$) (figure 30).

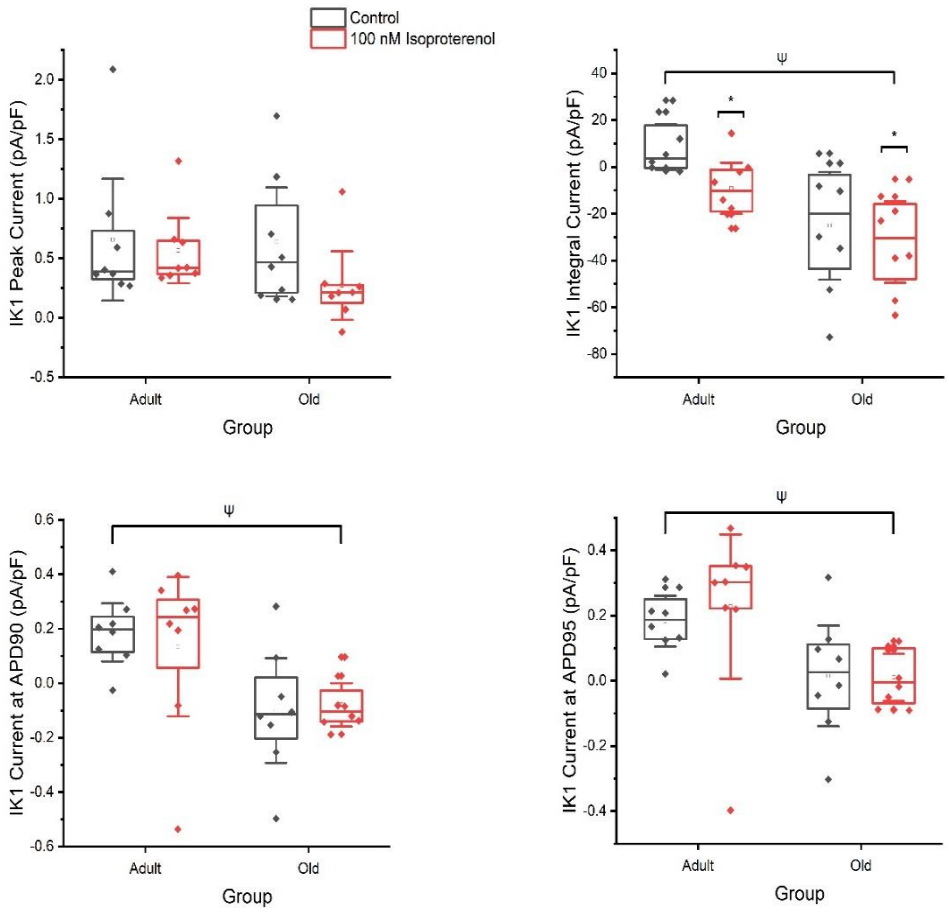


Figure 30. Impact of ageing on $I_{K1}$ peak current, $I_{K1}$ integral current and $I_{K1}$ current at $APD_{90}$ and $APD_{95}$. Ψ Indicates a significant difference between adult and old rats. * Indicates a significant difference compared with control. Box plots display mean (open square), median (solid middle line), upper, and lower quartiles (solid upper and lower lines) and confidence intervals (error bars).

## 6.4 Discussion

The aim of this study was to measure age-related changes during control conditions and during adrenergic stimulation in chromanol 293b-sensitive, $I_{Kr}$ and $I_{K1}$ currents. The main AP findings of this study were: Late AP repolarisation ($APD_{75-100}$) prolonged in old rats (81 - 105 %), whilst isoproterenol stimulation: reduced AP amplitude (3 %) and prolonged early AP repolarisation (18 %) and AP plateau (26 %) (in adult rats). The main ion channel findings of this study were: peak chromanol 293b-

sensitive, $I_{Kr}$ and $I_{K1}$ currents were not significantly different between adult and old rats, however there was a trend toward reduced peak chromanol 293b-sensitive current in old rats (23 %), particularly during isoproterenol superfusion (34 %). Chromanol 293b-sensitive integral current was reduced in old rats (55 %) particularly during isoproterenol relative to adult rats (73 %). Similarly, chromanol 293b-sensitive current at -20 mV and $APD_{90}$ was reduced in old rats (51 - 99 %) and chromanol 293b-sensitive current at $APD_{95}$ was reduced in old rats during isoproterenol stimulation (84 %). Conversely, during Isoproterenol stimulation, $I_{Kr}$ integral current (235 %) and $I_{Kr}$ current at 20 mV (390 %), 0 mV (467 %) and -20 mV (427 %) were greater in old rats whereas $I_{K1}$ integral current (110-fold), $I_{K1}$ current at $APD_{90}$ (156 %) and $I_{K1}$ current at $APD_{95}$ (95 %) were reduced in old rats. In addition, isoproterenol stimulation increased chromanol 293b-sensitive integral current (53 %) and chromanol 293b-sensitive current at $APD_{90}$ (155 %) and $APD_{95}$ (360 %) in adult rats only. In contrast, $I_{Kr}$ integral current (376 %) and $I_{Kr}$ current at 20 mV (1425 %), 0 mV (175 %) and -20 mV (580 %) reduced during isoproterenol superfusion in adult rats only. Lastly, $I_{K1}$ integral current also reduced (150 %) with the introduction of isoproterenol.

### 6.4.1 Impact of Ageing on APD and the Response to Adrenergic Stimulation

The findings displayed in figure 27 demonstrating the age-related prolongation in late AP repolarisation were unsurprising and are supported by previous literature (Liu et al., 2000; Liu et al., 2014; Gan et al., 2013; Feridooni et al., 2015; Huang et al., 2006; Waldeyer et al., 2009; Feridooni et al., 2017), as well as findings from experiments performed in chapter 3.

However, once more, similar to the findings of chapter 3, the lack of significant interaction between ageing and adrenergic stimulation particularly in late AP repolarisation were more surprising. Equally unexpected, were the findings which yielded an overall prolongation in early AP repolarisation and AP plateau in adult rat ventricular myocytes in response to adrenergic stimulation coupled with the reduction in AP amplitude. Such findings, in part, support previous work indicating a prolongation of APD in response to isoproterenol (Farrell and Howlett, 2007), though are contrary to our previous findings in chapter 3. However the isoproterenol-induced AP amplitude increase reported in chapter 3 occurred at 6 Hz pacing whilst this

particular study utilised 1 Hz pacing which may help to explain the differences in findings between the work in chapter 3 and the work in this chapter. Even though, in terms of statistical significance, the isoproterenol-induced prolongation of $APD_{25-50}$ does not align with our previous findings, and appears to contradict the logical progression that, particularly in adult rats, adrenergic stimulation triggers AP shortening, such findings indeed appear to continue a pattern of peculiar behaviour observed during early AP repolarisation and the AP plateau in rat ventricular myocytes. Once more, the underlying mechanism is unclear, but it is likely related to the aforementioned balance of LTCC and outward $K^+$ channel currents particularly during adrenergic stimulation, or intracellular $Ca^{2+}$ flux and NCX (Jeevaratnam et al., 2018; Sampson and Kass, 2010).

Taken together, at 1Hz pacing, ageing prolonged APD but did not significantly change the adrenergic response, though this was likely influenced by the lack of significant overall response to isoproterenol that has been previously demonstrated in this project and others (Wang and Fitts, 2017; Kamada et al., 2019). It may be that the application and washout of numerous $K^+$ channel blockers on the rat ventricular myocyte under basal conditions initially prior to recording the isoproterenol response influenced the results and facilitated a more blunted and less visible response to adrenergic stimulation. However, this study utilised previously documented activation and washout periods of the $K^+$ blockers and adrenergic stimulant used and also followed a similar methodology established in existing literature (Ding et al., 2002; Harding et al., 1988; Lim et al., 1999; Johnson et al., 2012; Banyasz et al., 2014; Banyasz et al., 2011) therefore, the potential influence of incomplete drug washout on the results should be minimal. However, the lack of APD response overall to adrenergic stimulation should be considered when interpreting the following ion channel modulation and applying to a wider context of the cardiac ageing phenomenon, given these APs provided the steady-state stimulus for these ion channel investigations.

### 6.4.2 Impact of Ageing on Chromanol 293b-Sensitive, $I_{Kr}$ and $I_{K1}$ Current and the Response to Adrenergic Stimulation

The lack of age-related changes in peak chromanol 293b-sensitive, $I_{Kr}$ and $I_{K1}$ current, despite the existence of a trend toward an age-related reduction in chromanol 293b-sensitive current, particularly during adrenergic stimulation was somewhat expected

given our findings elsewhere in this work as well as findings from limited available existing research (Walker et al., 1993; Cerbai et al., 1994; Liu et al., 2000).

Though few changes occurred in the peak current of the repolarising $K^+$ channels measured in this study, chromanol 293b-sensitive integral current, chromanol 293b-sensitive current at -20 mV, chromanol 293b-sensitive current at $APD_{90}$ and chromanol 293b-sensitive current at $APD_{95}$ were significantly reduced in old rat ventricular myocytes compared with adult rat ventricular myocytes. This may indicate significant $K^+$ channel current remodelling with ageing, which may contribute to the prolongation of APD in old age and similarly help to explain the prolongation of late AP repolarisation in this study alongside chapter 3 also. The chromanol 293b-sensitive current findings of this study described above, may also underlie the findings in chapter 5.

The clear reduction in chromanol 293b-sensitive integral current alongside chromanol 293b-sensitive current at -20 mV, $APD_{90}$ and $APD_{95}$ are certainly indicative of the wide influence $I_{Ks}$, or other repolarising $K^+$ channel currents, wield in the modulation of APD and may indicate that channel open time declines in old age. Such findings may also be an indicator of constrained / limited recruitment, potentially via a reduction in available channel pores or overall channel expression, leading to a preserved peak but limited overall function throughout the duration of the AP. Research has found protein and mRNA expression of KCNQ1 and KCNE, which form the complex responsible for $I_{Ks}$ current, remain unchanged in old age (Olgar et al., 2022; Zou et al., 2021), whilst $I_{Ks}$ current under basal / control conditions has been reported to similarly remain unchanged in guinea pigs, but has been shown to decrease in rats with ageing (Zou et al., 2021; Olgar et al., 2022).

The increase in chromanol 293b-sensitive integral current and chromanol 293b-sensitive current at $APD_{90}$ and $APD_{95}$ in response to adrenergic stimulation in adult but not old rat ventricular myocytes may reaffirm previous findings displaying the important role of $I_{Ks}$ on AP repolarisation during stress in normal healthy hearts (Wang and Fitts, 2020) and supports our previous current-clamp findings in chapter 5. Most importantly, it could highlight a potential breakdown in adrenergic signalling of $I_{Ks}$ in old age and potentially highlight $I_{Ks}$ as a possible therapeutic target in the cardiac ageing phenomenon in order to combat the age-related loss of repolarisation reserve.

It is important to note that such age-related differences in chromanol 293b-sensitive current response to isoproterenol were observed during stimulation by an AP recorded from the same myocyte at 1 Hz that did not display a significant shortening in response to isoproterenol as we have previously shown (chapter 3). Whether a similar response would occur when stimulated by an AP which demonstrates clear isoproterenol-induced AP shortening is unknown. Though it might be speculated that a more exaggerated difference in $I_{Ks}$ response to adrenergic stimulation between adult and old rat ventricular myocytes may be observed when stimulated by a more brief AP typical of the impact of isoproterenol on APD (Wang and Fitts, 2017; Kamada et al., 2019). The same may be speculated too regarding the use of more physiologically relevant pacing rates.

To date, the only study to our knowledge to undertake a similar investigation intending to explore age-related remodelling of $I_{Ks}$ current and its response to adrenergic stimulation reported a significant difference in the adrenergic response of the $I_{Ks}$ current between adult (1 – 3 months of age) and old (≥ 24 months of age) guinea pig ventricular myocytes, with adult myocytes displaying a moderate increase and old myocytes demonstrating a reduction in $I_{Ks}$ current (Zou et al., 2021).

However, as previously discussed in section 5.3 – 5.5, without further confirmatory experiments, the findings regarding chromanol 293b-sensitive current in this study cannot be reliably confirmed to result solely from changes in $I_{Ks}$ current (Du et al., 2003; Sun et al., 2001; Árpádffy-Lovas et al., 2022). According to existing literature, at the chromanol dose used in this study, such findings may also be a result of changes in $I_{to}$ and $I_{Kur}$ current (Du et al., 2003; Sun et al., 2001; Árpádffy-Lovas et al., 2022; Bosch et al., 1998). Therefore, although the reduction in chromanol 293b-sensitive current and its response to adrenergic stimulation in old rats compared with adult rats is certainly indicative of age-related remodelling of repolarising $K^+$ channels and their response to $\beta_1$AR signalling, the above inferences to age-related changes in $I_{Ks}$ function are speculation without further supporting evidence. Though chromanol 293b indeed blocks $I_{Ks}$ successfully (Bosch et al., 1998), the dose used could have also blocked, albeit not to the same extent as $I_{Ks}$, other repolarising $K^+$ currents (Du et al., 2003; Sun et al., 2001; Árpádffy-Lovas et al., 2022; Bosch et al., 1998). This means that, although the findings of this study likely implicate $I_{Ks}$ to a higher degree due to its lower chromanol 293b-induced IC50 compared with other currents potentially

attributable to the chromanol 293b-sensitive current findings (Du et al., 2003; Sun et al., 2001; Árpádffy-Lovas et al., 2022; Bosch et al., 1998), the previously suggested age-related remodelling of $K^+$ channels may be a result of: changes in the kinetics of separate or combined $I_{Ks}$, $I_{to}$ or $I_{Kur}$ current, changes in the relative contribution to the modulation of repolarisation, or changes in the separate or combined coupling of such currents to $\beta_1$AR signalling in the ventricle with old age. Without further study, interpretation is difficult. The use of more selective $I_{Ks}$ block (HMR-1556, Árpádffy-Lovas et al., 2022) or the use of chromanol 293b alongside $I_{to}$ and $I_{Kur}$ block as well as the successful performance of voltage-clamp studies to confirm understood channel current characteristics would help with the translation of the findings of this study and improve the overall understanding of the impact of ageing on repolarising $K^+$ channels and how their remodelling may underlie the loss of cardiac response to exercise in old age.

The greater $I_{Kr}$ integral current and $I_{Kr}$ current at 20 mV, 0 mV and -20 mV recorded in old compared with adult rat ventricular myocytes during adrenergic stimulation provides considerable contrast to the findings related to chromanol 293b-sensitive current in this study explained above and could indicate the potential existence of mixed remodelling of repolarising $K^+$ channel response to adrenergic stimulation in old age. The greater $I_{Kr}$ integral current and $I_{Kr}$ current at 20 mV, 0 mV and -20 mV yielded in old rats compared with adult rats during adrenergic stimulation in this study was likely influenced by the significant isoproterenol-induced reduction in $I_{Kr}$ integral current and $I_{Kr}$ current at 20 mV, 0 mV and -20 mV in adult rats but not old rats.

The reduction in $I_{Kr}$ current in adult rat ventricular myocytes may help explain the isoproterenol-induced prolongation of early AP repolarisation and AP plateau also reported in this study in adult rats, particularly as the observed current changes were primarily between 20 mV and -20 mV, reflecting such phases of the AP waveform. However, the contribution of other currents may have also been a factor in early AP and AP plateau prolongation. For example, $I_{to}$ is heavily relied on in rats for AP repolarisation of ventricular myocytes (Joukar, 2021) and should be considered in the future study of age-related changes in ventricular AP repolarisation response to changes in pacing rate and adrenergic stimulation.

The underlying mechanism of the described isoproterenol-induced reduction in $I_{Kr}$ current in adult rats is unclear. A reduction in $I_{Kr}$ current in response to isoproterenol may reflect the overwhelming dominance of $I_{Ks}$ current during adrenergic stimulation in particular and highlight a lesser role for $I_{Kr}$ in modulating AP repolarisation in this state as has been indicated in previous research (Wang and Fitts, 2020; Banyasz et al., 2014; Jost et al., 2007). It may therefore be speculated that in old age, the apparent loss of chromanol 293b-sensitive current response to adrenergic stimulation as described above, may lead to the greater reliance on $I_{Kr}$ to regulate APD and explain the measured differences in $I_{Kr}$ response to adrenergic stimulation between adult and old rats recorded in this study. Alternatively, as mentioned previously, such results may indicate mixed $K^+$ channel remodelling with ageing whereby the negative $I_{Kr}$ current response to isoproterenol in adult rats is normal and required to help balance the APD shortening typically stimulated by adrenergic stimulation which is lost in old age, leading to prolonged APD and poorer response to exercise (Liu et al., 2000; Liu et al., 2014; Gan et al., 2013; Feridooni et al., 2015; Huang et al., 2006; Waldeyer et al., 2009; Feridooni et al., 2017).

However, as figure 29 displays, the $I_{Kr}$ current variables in adult rat ventricular myocytes during adrenergic stimulation are negative, meaning an altogether different mechanism may be responsible for such changes. Given that anecdotally in this study, $I_{Kr}$ currents were very difficult to detect in rat ventricular myocytes, a finding that has been previously demonstrated in existing literature (Wang and Fitts, 2020), and the fact that the current magnitudes of $I_{Kr}$ were often very small, it is plausible that due to the nature of current subtraction in this particular methodology that any changes accumulated in $I_{Ks}$ / chromanol 293b-sensitive current from the continued use of chromanol 293b may have contaminated the calculated $I_{Kr}$ current. Although, as previously explained, adequate activation times and washout periods were accounted for and were in line with previous studies (Ding et al., 2002; Harding et al., 1988; Lim et al., 1999; Johnson et al., 2012; Banyasz et al., 2014; Banyasz et al., 2011) which should have minimised such a potential impact, some existing research has indicated a significant elevation of $I_{Ks}$ current when other $K^+$ channels are suppressed which has been associated with exaggerated AP prolongation (Geelen et al., 1999; Guerard et al., 2008; Jost et al., 2005; Volders et al., 2003). This could mean that the sequential block of $I_{Kr}$ and $I_{K1}$ after initial chromanol 293b superfusion facilitated an increase in $I_{Ks}$ /

chromanol 293b-sensitive current, therefore helping to explain the observed negative findings in $I_{Kr}$ current, as any transient or continued increase in chromanol 293b-sensitive compensatory current during the sequential application of blockers may have led to an underestimation of $I_{Kr}$ currents.

The apparent maintenance of $I_{Kr}$ current during basal conditions in old age coupled with the demonstrated reductions in chromanol 293b-sensitive current (figure 28 - 29) and the notable difference in magnitude between the two repolarising $K^+$ currents potentially furthers the pattern of findings identifying $I_{Ks}$ as the main contributor to AP repolarisation. Though it is understood other currents may have contributed to the chromanol 293b-sensitive current findings in this study as explained previously (Du et al., 2003; Sun et al., 2001; Árpádffy-Lovas et al., 2022; Bosch et al., 1998). Nonetheless, such findings could suggest that $I_{Kr}$ may escape age-related intrinsic remodelling and potentially indicates a significantly reduced or complete lack of involvement in the age-related prolongation of APD found in this study and others. Previous research in this area is very limited, however a study in guinea pigs reported no age-related changes in $I_{Kr}$ current of ventricular myocytes (Zou et al., 2021), providing some support to the $I_{Kr}$ findings in this study. However, in contrast to the findings of this study, previous research investigating the response of $I_{Kr}$ to adrenergic stimulation suggest $I_{Kr}$ current increases during isoproterenol superfusion (Sakatani et al., 2006; Şengül Ayan et al., 2020).

The reduction in $I_{K1}$ integral current alongside $I_{K1}$ current at $APD_{90}$ and $APD_{95}$ in old rats compared with adult rats may once again be indicative of age-related remodelling of the repolarising $K^+$ currents and may underlie, in part, the prolongation of APD reported in this study and potentially the age-associated APD prolongation during basal conditions commonly reported in research (Liu et al., 2000; Liu et al., 2014; Gan et al., 2013; Feridooni et al., 2015; Huang et al., 2006; Waldeyer et al., 2009; Feridooni et al., 2017). Meanwhile, the reduction in $I_{K1}$ integral current with the introduction of adrenergic stimulation appears to contradict the isoproterenol-induced shift toward more negative diastolic membrane potentials reported in this study as well as chapter 3 and previous research (Crumbie, 2016; Farrell and Howlett, 2007). However such $I_{K1}$ changes are consistent with previous literature where $I_{K1}$ has been reported to show mixed responses to adrenergic stimulation (Chiamvimonvat et al., 2017). It might be that other currents contributing to the diastolic membrane potential are responsible for

the diastolic membrane potential response to adrenergic stimulation, though this is unclear. Moreover, the absence of age-related changes in $I_{K1}$ current in response to adrenergic stimulation compared with those reported in basal function may suggest that $I_{K1}$ has little to no role in the age-associated loss in sensitivity of AP repolarisation to adrenergic signalling, unless of course the changes in basal function facilitate a constriction of the maximal response. Research so far has found $I_{K1}$ current predominantly remains unchanged in old rat hearts, with some suggestion of an age-related increase in $I_{K1}$ current, though this may depend on the strain used (Long-Evans) (Walker et al., 1993; Cerbai et al., 1994; Liu et al., 2000).

However, much like the previously explained variables of $I_{Kr}$ current, figure 30 also demonstrates that negative $I_{K1}$ integral current values were observed, and therefore should be considered in its subsequent interpretation. Unlike $I_{Kr}$ current, $I_{K1}$ current and its contribution during the AP was more visible during experimental observations. However such findings may have similarly been influenced by contamination or underestimation in the same manner as described for $I_{Kr}$ previously. Alternatively, any slight potential changes in the diastolic membrane potential during $I_{K1}$ block may have masked the involvement of $I_{K1}$ current somewhat. For example, any changes in diastolic membrane potential may result in changes to the compensatory currents measured, which when subtracted later from the effects of chromanol 293b-sensitive current and $I_{Kr}$ current may cause $I_{K1}$ current to be underestimated or influenced in terms of direction.

Although previous research regarding $I_{Kr}$ and $I_{K1}$ block through E4031 and $BaCl_2$ superfusion respectively at the doses used in this study does not implicate potential current contamination in the same way suggested for chromanol 293b superfusion, the potential usefulness of further confirmatory experiments to reliably and accurately determine $I_{Kr}$ and $I_{K1}$ current in the same manner suggested for $I_{Ks}$ current should not be disregarded. It could be argued that given the difficulties in $I_{Kr}$ current measurement stated in this study and previous work (Wang and Fitts, 2020), coupled with the lack of conventional voltage-clamp experiments examining E4031-sensitive current and $BaCl_2$-sensitive current or experiments examining E4031-sensitive current and $BaCl_2$-sensitive current on AP repolarisation, it is difficult to interpret the role of both $I_{Kr}$ and $I_{K1}$ on AP repolarisation in the rat ventricle with ageing. It could also be argued that the AP-clamp data laid out in this chapter is insufficient by itself to provide compelling

evidence that $I_{Kr}$ plays a functionally significant role in rat ventricular myocyte repolarization. Further, such confirmatory experiments would help to clarify and better understand some findings in the repolarising $K^+$ channels measured in this study that do not completely align with the classic characteristics of these currents. For example, figure 25 A provides an example where chromanol 293b-sensitive current appears to demonstrate an almost instantaneous activation which then declines early in AP repolarisation before exhibiting a second peak later in the AP, which is in part, uncharacteristic of the understood traditional $I_{Ks}$ current and may indicate contamination by $I_{to}$ current - as previously discussed - on this occasion. Similarly, in figure 25 B the example $I_{K1}$ trace appears to show $I_{K1}$ current increasing as the AP repolarises on this occasion, which is not entirely consistent with the known voltage-dependence of $I_{K1}$.

## 6.5 Conclusion

This study provides novel information regarding the function of ion channels contributing to repolarisation under basal and adrenergic stimulation conditions in adult and old rat ventricular myocytes during self-AP stimulation at 1 Hz. The findings in this study further demonstrate the age-related prolongation of late AP repolarisation that has been reported throughout this project. In addition, the findings of this study show a mixed picture of age-related remodelling of repolarising $K^+$ channels as chromanol 293b-sensitive current and $I_{K1}$ current appear most important to the changes in basal function in old age, whilst chromanol 293b-sensitive current and $I_{Kr}$ current appear most important to the changes in adrenergic response in old age. Whilst this work provides insight into the effects of ageing and adrenergic stimulation on some of the components contributing to AP repolarisation, further research is required involving voltage-clamp recordings alongside research using conditions enhancing the reliability and selectivity of $I_{Ks}$ recordings in particular, as well as research involving simultaneous measurement of other components contributing to repolarisation such as $I_{to}$, $I_{Kur}$, LTCC, NCX and SR $Ca^{2+}$ release. Equally, future similar studies should consider the use of more physiological pacing frequencies to help better understand the effects of ageing on electrophysiological exercise response as in vivo.

# Chapter 7: Modelling the Effect of Rate and Adrenergic Stimulation on APD in Adult Rat Ventricular Myocytes

## 7.1 Introduction

Cardiac excitation is integral to coordinated global cardiac contraction through the cohesive and efficient coupling of excitatory and contractile processes at the cell level (Bers, 2002). Cardiac excitation and contraction at the cell level can be investigated through a range of experimental techniques though such techniques are often relatively low yield in terms of data production, such as electrophysiology. Recent years have seen an increase in the use of computational models alongside experimental work. These provide a valuable tool for performing high yield simulation experiments that integrate and explain disparate experimental data and facilitate the streamlining of the experimental approach (Yang and Saucerman, 2011; Pandit et al., 2001; Gattoni et al., 2016). A tremendous amount of effort since the work of Hodgkin and Huxley has been applied to develop various mathematical and computational models of the heart (Hodgkin and Huxley, 1952; Hodgkin and Huxley, 1952b; Hodgkin and Huxley, 1952a; Hodgkin and Huxley, 1952c; Hodgkin and Huxley, 1952; Noble, 1962). Two of the most prominent and recent models focusing on cardiomyocyte excitation in the rat are the 2001 model by Pandit et al. (Pandit et al., 2001) and the 2016 model by Gattoni et al. (Gattoni et al., 2016). However, these models are unable to pace myocytes at frequencies greater than 6 Hz and therefore do not provide insight to rat ventricular myocyte excitatory behaviour through the full range of physiological rates, as the rat heart typically functions up to approximately 10 Hz which reflects strenuous exercising HR. In addition, despite the considerable work by a number of research groups, the adrenergic response at physiological temperatures and pacing rates is yet to be reliably modelled (Yang and Saucerman, 2011; Roberts et al., 2012; Saucerman et al., 2003). This is largely a result of the lack of experimental studies investigating electrical activity and excitation in myocytes under physiological conditions and rates.

Further research is required to reliably model myocyte excitation under a variety of physiological conditions in the adult rat. A robust rat model that is able to accurately simulate in vivo ventricular function is vital to integrate and explain disparate experimental data, isolate key components of interest and streamline experimental volume, and therefore reduce animal use in research, and ultimately feed into a continuous cycle of model development and validation through incorporation of laboratory data and then prediction.

Recently, a novel computational rat ventricular myocyte model of electrophysiology and $Ca^{2+}$ handling has been developed in our laboratory by Stevenson-Cocks et al. (the Leeds rat (LR) model) (Stevenson-Cocks, 2019). The LR model allows pacing up to and above 10 Hz frequencies, enabling simulation of high exercising rat HR (Stevenson-Cocks, 2019). However, very little AP data at pacing frequencies physiological to a rat is currently available to provide comparison and validation in this model particularly up to 10 Hz pacing. Equally, whether the LR model is able to accurately model the AP response to the adrenergic stimulation that would be associated with such high HR through increased pacing frequency is not known, again due to the lack of current experimental data to compare against. Findings from our laboratory experiments, (Howlett et al., 2022) facilitate the full mapping of the adrenergic response in the rat ventricular AP, dependent and independent of rate changes, under physiological temperatures in adult hearts. Furthermore, our previous laboratory experiments investigating LTCC, chromanol 293b-sensitive, $I_{Kr}$ and $I_{K1}$ channels demonstrate a role for repolarising $K^+$ channels in ageing and the response to adrenergic stimulation in old age (chapters 4 – 6). This laboratory work and the foundations laid by the LR model together will help facilitate the development of a reliable physiologically relevant adult rat ventricular myocyte model which will be vital in aiding the future study of currently unanswered questions in the field of cardiac electrophysiology, cardiac ageing and arrhythmogenesis.

Therefore, the initial aim of this study was to further develop an existing computational rat AP model created previously in our lab (Stevenson-Cocks, 2019), using experimental data (Howlett et al., 2022) to reliably model adult rat AP data at physiologically relevant rates. The next aim of the study was to use existing literature and experimental data to reliably model the adrenergic response in the adult rat at physiologically relevant pacing frequencies.

## 7.2 Methods

### 7.2.1 Computational Model Structure

This study used a computational model recently developed within our laboratory (Stevenson-Cocks, 2019). This Model (the LR model) is based on previous works by Gattoni et al. and Colman et al. (Stevenson-Cocks, 2019; Colman et al., 2017; Colman, 2019; Gattoni et al., 2016) utilising electrophysiological components of Gattoni et al. (Gattoni et al., 2016) and the $Ca^{2+}$ handling components of Colman et al. (Colman et al., 2017).

However, several modifications were made to the LR model prior to undertaking the work in this study and is described as the modified LR (mLR) model throughout this work. This work also required the generation of model variants for the adult ventricular myocyte under control and adrenergic stimulation conditions. These model variants were developed to enable investigation of AP repolarisation in response to increased rate and adrenergic stimulation.

### 7.2.2 Model Modifications

External ion concentration constants were changed to match experimental data collection protocols (table 10). Initial conditions of model variables (voltage, intracellular ion concentrations, ion channel gating variables etc.) were taken at quiescent steady-state, i.e. when the stated variables no longer changed when the model was run with no stimulation, to better resemble experimental set up (table 11). The LR model was further modified through a manual iteration process whereby model components were adjusted to adequately mimic experimental set-up of the laboratory trials and provide a relatively good fit to available experimental data. The steady-state $K^+$ current ($I_{ss}$) from the original LR model was replaced with $I_{Kr}$ and $I_{Ks}$ currents using formulae from the Korhonen et al. model of neonatal rat ventricular myocytes (Korhonen et al., 2009). Current maximal conductance were modified in order to maintain the relative balance in $K^+$ currents, during the final AP of 1 Hz pacing for 60 s, $I_{to}$ : $I_{K1}$ : $I_{ss}$ = 88.7 % : 6.4 % : 4.9 % (where $I_{ss} = I_{kr} + I_{Ks}$) as in the original LR model, in order to maintain the model's repolarisation dynamics. The relative balance of $I_{ss}$ was simply replaced by $I_{Kr}$ and $I_{Ks}$ and the conductance adjusted to give a relative peak current balance of, $I_{to}$ : $I_{K1}$ : $I_{Kr}$ : $I_{Ks}$ = 88.7 % : 6.4 % : 0.9 % : 4.0 %.

Maximal conductance of ion channels were also modified to concomitantly provide a relative match in APD variables between the model data and the experimental data. Finally, the time constant of activation of $I_{Ks}$ was changed to 100 ms so that model APD restitution matched experimental values as closely as possible.

Table 10. External ion concentration constant modifications to the LR model (Stevenson-Cocks, 2019).

| | **Modified LR Model** | **Original LR Model** |
|---|---|---|
| Extracellular $Na^+$ concentration ($[Na^+]_o$) | 136.0 mM | 140.0 mM |
| Extracellular $Ca^{2+}$ concentration ($[Ca^{2+}]_o$) | 1.0 mM | 1.8 mM |
| Extracellular $K^+$ concentration ($[K^+]_o$) | 4.0 mM | 5.4 mM |

Table 11. Initial state conditions of the mLR model.

| **Symbol** | **Name** | **Initial State** |
|---|---|---|
| V | Membrane potential (mV) | -67.843053 |
| Ina_m | $I_{Na}$ activation gate m | 0.028908 |
| Ina_h | $I_{Na}$ inactivation gate h | 0.204194 |
| Ina_j | $I_{Na}$ inactivation gate j | 0.204194 |
| Ito_r | $I_{to}$ activation gate r | 0.006610 |
| Ito_s | $I_{to}$ inactivation gate s | 0.963549 |
| Ito_slow | $I_{to}$ inactivation gate slow | 0.963549 |
| If_y | $I_f$ inactivation gate y | 0.001168 |
| Ca_cyto | $Ca^{2+}$ concentration in cytoplasm (μM) | 0.074005 |

| | | |
|---|---|---|
| Ca_ss | $Ca^{2+}$ concentration in subspace (µM) | 0.074134 |
| Ca_ds | $Ca^{2+}$ concentration in dyadic cleft (µM) | 0.074844 |
| Ca_jsr | $Ca^{2+}$ concentration in junctional SR (µM) | 773.296210 |
| Ca_nsr | $Ca^{2+}$ concentration in network SR (µM) | 773.296210 |
| LTCC_d1 | $I_{Ca}$ activation state d1 | 0.999972 |
| LTCC_d2 | $I_{Ca}$ activation state d2 | 0.000027 |
| LTCC_d3 | $I_{Ca}$ activation state d3 | 0.000001 |
| LTCC_f | $I_{Ca}$ voltage-induced inactivation state f | 0.999509 |
| LTCC_fca | $I_{Ca}$ $Ca^{2+}$-induced inactivation state fca | 0.984678 |
| RyR_CA | RyR “closed” activated state | 1.0 |
| RyR_OA | RyR “open” activated state | 0.000004 |
| RyR_OI | RyR “open” inactivated state | 0.0 |
| RyR_CI | RyR “closed” inactivated state | 0.0 |
| RyR_M | Monomer binding (mM) | 0.000047 |
| RyR_Mi | Monomer binding inactivation (mM) | 0.000496 |
| P0 | Permissive tropomyosin with 0 cross bridges | 0.001667 |
| P1 | Permissive tropomyosin with 1 cross bridge | 0.001442 |
| P2 | Permissive tropomyosin with 2 cross bridges | 0.002692 |
| P3 | Permissive tropomyosin with 3 cross bridges | 0.002345 |
| N0 | Nonpermissive tropomyosin with 0 cross bridges | 0.990418 |
| N1 | Nonpermissive tropomyosin with 1 cross bridge | 0.001436 |
| Htrpn_ca | Concentration of $Ca^{2+}$ bound to high affinity troponin sites (mM) | 0.130557 |
| Ltrpn_ca | Concentration of $Ca^{2+}$ bound to low affinity troponin sites (µM) | 0.018066 |
| Nai | Intracellular $Na^{+}$ concentration (mM) | 5.853891 |
| Ki | Intracellular $K^{+}$ concentration (mM) | 68.3 |

| | | |
|---|---|---|
| CKO | Channel closed state | 0.992975 |
| CK1 | Channel closed state | 0.002940 |
| CK2 | Channel closed state | 0.0019 |
| OK | Channel open state | 0.001666 |
| IK | Channel inactivated state | 0.000519 |
| Iks_n | $I_{Ks}$ gate n | 0.002189 |

Table 12. Maximal ion channel conductance ($\bar{g}$) modifications to the LR model (Stevenson-Cocks, 2019).

| **Ion Channel** | **Modified LR Model** | **Original LR Model** |
|---|---|---|
| $\bar{g}_{Na}$ | 7.0 mS/µF | 7.0 mS/µF |
| $\bar{g}_{to}$ | 0.116 mS/µF | 0.196 mS/µF |
| $\bar{g}_{ss}$ | N/A | 0.12 mS/µF |
| $\bar{g}_{Kr}$ | 0.13 mS/µF | N/A |
| $\bar{g}_{Ks}$ | 0.295 mS/µF | N/A |
| $\bar{g}_{K1}$ | 0.000017 S | 0.00004 S |
| $\bar{g}Na^+ : K^+$ ATPase | 13.8 mS/µF | 13.8 mS/µF |

### 7.2.3 Generation of Model Variants

For this project, some model variants were developed from the main mLR model discussed above (Stevenson-Cocks, 2019). These model variants were developed to enable investigation of AP repolarisation in response to increased rate and adrenergic stimulation. Essentially, two model variants were required: adult rat and adult rat during adrenergic stimulation.

The default LR model after the incorporation of the modifications described above was defined as the adult rat variant model (table 10 - 12). The adult rat during adrenergic stimulation variant included the exact same modifications used in the adult rat variant, but with some changes to ion channel fluxes in order to mimic adrenergic

stimulation (table 13). The ion channel changes described in table 13 are based on those used in other studies and are centred on changes observed in experimental investigations and have been suggested to provide a simulation of the adrenergic response as in vivo (Stevenson-Cocks, 2019; Dibb et al., 2007; Sankaranarayanan et al., 2017; Sankaranarayanan et al., 2016; Colman, 2019).

Table 13. Ion channel modifications used in the adult rat during adrenergic stimulation model variant.

| **Ion Channel** | **Scaling Factor** |
|---|---|
| LTCC Current | 1.5 |
| $I_{to}$ Current | 1.5 |
| $I_{Kr}$ Current | 2.0 |
| $I_{Ks}$ Current | 2.0 |
| SERCA2a | 2.0 |

### 7.2.4 Simulation Protocols

**Action Potential Duration Response to Changes in Activation Frequency and Isoproterenol.** To study the effect of activation frequency on rat ventricular myocytes, a restitution protocol was used to closely mimic the data collection protocol of the experimental trials. The model restitution protocol uses an initial period of quiescence before pacing at 1 Hz for 60 s and then recording the APD of the final AP produced. Next, the model immediately increases pacing frequency to 2 Hz for a period of 60 s before recording the APD of the final AP produced once more. This process was continued for 4, 6, 8 and 10 Hz pacing frequencies. To study the effect of isoproterenol on rat ventricular myocytes, the protocol was repeated using the adult rat during

adrenergic stimulation model variant. All model simulation results were then compared with experimental results.

**Ion Channel Responses to Changes in Activation Frequency and Isoproterenol.** To study the effect of activation frequency and isoproterenol on ion channel function in rat ventricular myocytes, the model was paced initially at 1 Hz for 60 s followed by 2, 4, 6, 8 and 10 Hz. Peak current results for LTCC, $I_{K1}$, $I_{Kr}$ and $I_{Ks}$ were compared between the model and the available experimental data at 1 Hz carried out as per chapters 4 and 6. For the purpose of comparison, chromanol 293b-sensitive, E4031-sensitive and $BaCl_2$-sensitive currents measured in chapter 6 were assumed to reflect $I_{Ks}$, $I_{Kr}$ and $I_{K1}$ current findings respectively. Though, as mentioned previously, it is understood further supporting experiments are required to reliably and accurately confirm such findings are indeed a result of pure $I_{Ks}$, $I_{Kr}$ and $I_{K1}$ currents respectively. Simulations performed at 2, 4, 6, 8 and 10 Hz and the subsequent peak values for the LTCC, $I_{K1}$, $I_{Kr}$ and $I_{Ks}$ currents were plotted to demonstrate projected rate-dependent changes as predicted by the mLR model. This protocol was performed in all model variants.

## 7.3 Results

### 7.3.1 Comparing the Influence of Pacing Frequency and Adrenergic Stimulation on Adult Rat Ventricular Myocyte AP Variables Between Experimental and Model Data

#### *7.3.1$_i$ $APD_{50}$*

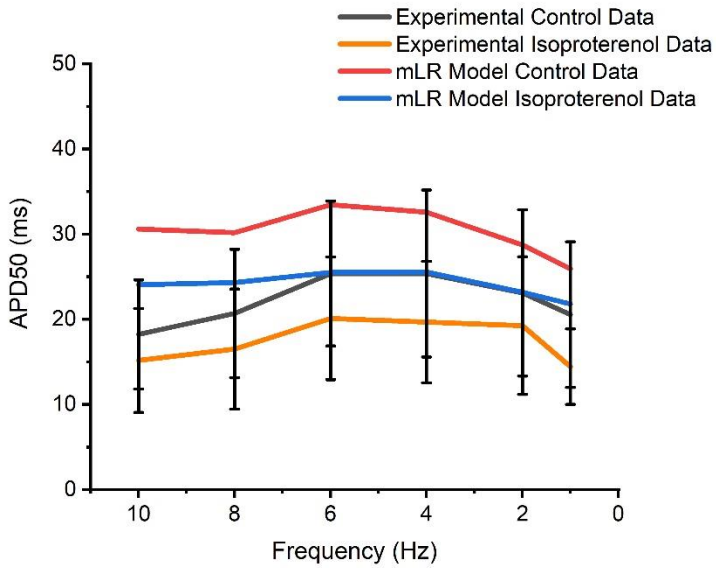


Figure 31. Comparison of $APD_{50}$ during control conditions and during adrenergic stimulation between experimental data (Howlett et al., 2022) and data from the mLR model used in this work. Experimental data presented as mean with 95 % confidence interval (1.96 x SEM) error bars. Experimental data based on N = 8. Experimental isoproterenol data based on findings from 5 nM isoproterenol dose.

Figure 31 provides comparison of $APD_{50}$ between experimental data and data from the mLR model. Both experimental and mLR model control data display a steady prolongation in $APD_{50}$ between 1 to 6 Hz pacing and the mLR model control data falls within the 95 % confidence interval of experimental data at 1 - 6 Hz pacing. Figure 31 also shows $APD_{50}$ from the experimental and mLR model demonstrate similar rate-dependent changes during adrenergic stimulation, evidenced by a steady prolongation in $APD_{50}$ between approximately 1 and 6 Hz pacing, before shortening at the highest pacing frequencies. However, experimental $APD_{50}$ values are more brief and the mLR

model only produces $APD_{50}$ data within the 95 % confidence interval of the experimental data at 2 – 6 Hz pacing during adrenergic stimulation. Although, the relative response in $APD_{50}$ to isoproterenol produced by the mLR model remained within the 95% confidence interval of the experimental data at all pacing frequencies except 1 Hz (1 Hz: -16 vs -30 %, 2 Hz: -19 vs -17 %, 4 Hz: -22 vs -22 %, 6 Hz: -24 vs -21 %, 8 Hz: -19 vs -20 %, 10 Hz: -21 vs -17 %).

### *7.3.1$_{ii}$ $APD_{90}$*

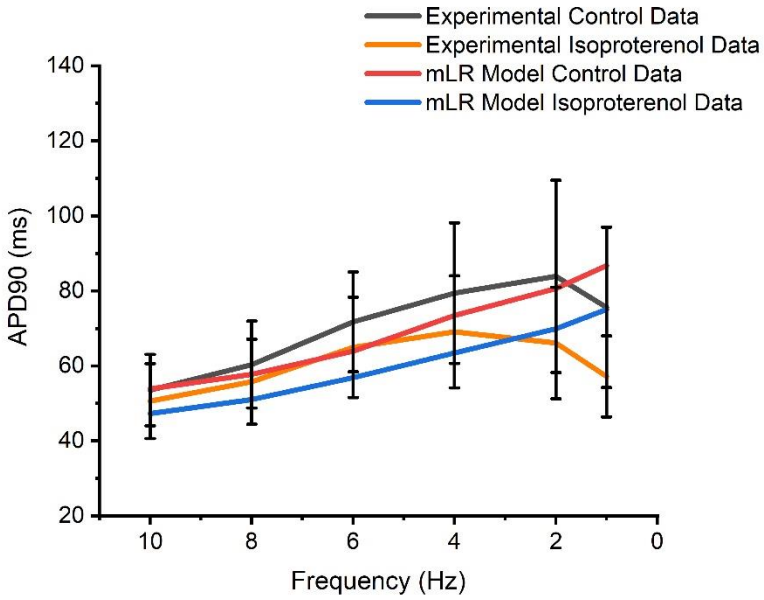


Figure 32. Comparison of $APD_{90}$ during control conditions and during adrenergic stimulation between experimental data (Howlett et al., 2022) and data from the mLR model used in this work. Experimental data presented as mean with 95 % confidence interval (1.96 x SEM) error bars. Experimental data based on N = 8. Experimental isoproterenol data based on findings from 5 nM isoproterenol dose.

Action potential data ($APD_{90}$) from mLR model control simulations were compared with experimental control data at a range of pacing frequencies (1 – 10 Hz) (figure 32 – 33). Experimental $APD_{90}$ control data demonstrates a prolongation of $APD_{90}$ at pacing frequencies similar to basal rat HR compared with 1 Hz pacing, whilst pacing frequencies similar to strenuous exercising rat HR trigger much more rapid $APD_{90}$

control values. Meanwhile, the mLR model suggests $APD_{90}$, unlike the experimental data, progressively shortens across 2 and 4 Hz before equally becoming much more rapid at the highest pacing frequencies during control conditions. When comparing the two data sets, figure 32 shows the mLR model produces $APD_{90}$ data within the 95 % confidence interval of the experimental values at all pacing frequencies and produces $APD_{90}$ values between 1 – 15 % of the experimental data during control conditions. The mLR model is best able to predict similar $APD_{90}$ values to experimental findings at 10 Hz, displaying just a 1 % difference. Differences of only 4% between groups can be observed at 8 Hz and 2 Hz pacing, suggesting the adult rat variant model is able to reliably model adult rat ventricular myocyte $APD_{90}$ at a wide range of physiological frequencies during control conditions.

Moreover, figure 32 shows $APD_{90}$ from the mLR model remains within the 95 % confidence interval of the experimental data at all pacing frequencies except 1 Hz during adrenergic stimulation. The magnitude of $APD_{90}$ shortening in response to isoproterenol produced by the mLR model was found to be similar (1 Hz: -13 vs -24 %, 2 Hz: -13 vs -21 %, 4 Hz: -14 vs -13 %, 6 Hz: -11 vs -9 %, 8 Hz: -12 vs -8 %, 10 Hz: -12 vs -5 %) remaining within the 95 % confidence interval of the experimental data at the majority of pacing frequencies (2 - 8 Hz) and deviating at only the lowest and highest pacing frequency due to the greater rate-dependency observed in experimental compared with modelled data, evidenced by greater isoproterenol-induced shortening at lower pacing frequencies (1 Hz: 24 % vs 10 Hz: 5 %).

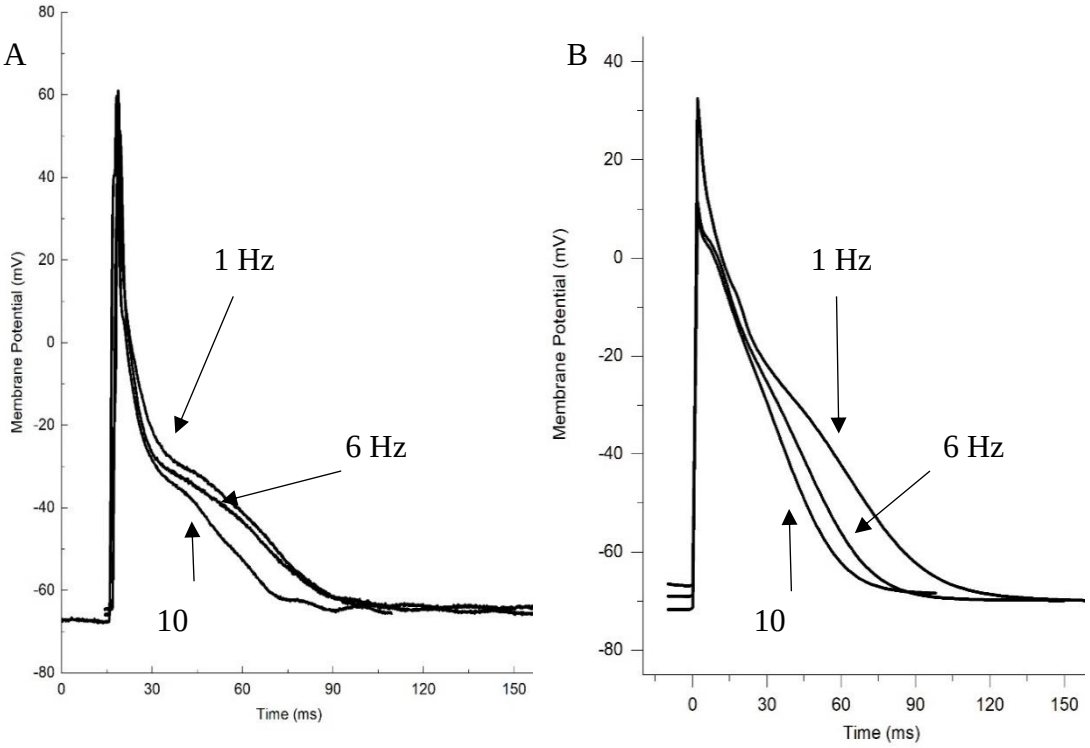


Figure 33. Example action potential traces from experimental data (A) (Howlett et al., 2022) and simulated AP traces from the mLR model (B). Traces recorded at 1, 6 and 10 Hz pacing as displayed.

### *7.3.1$_{iii}$ Diastolic Membrane Potential*

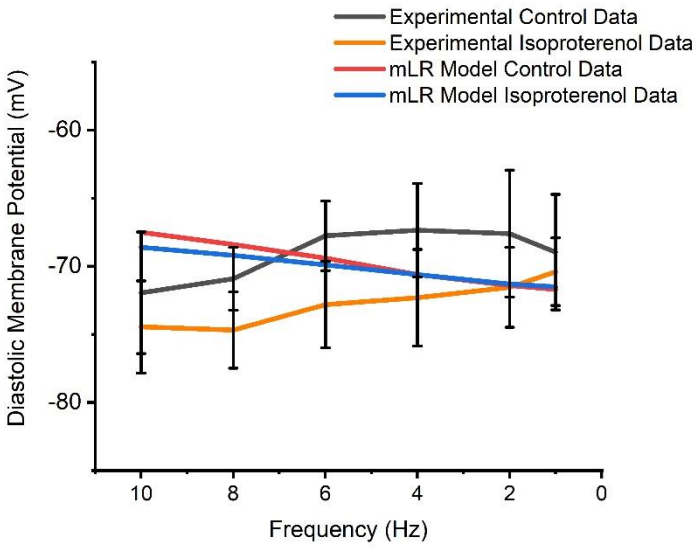


Figure 34. Comparison of diastolic membrane potential during control conditions and during adrenergic stimulation between experimental data (Howlett et al., 2022) and data from the mLR model used in this work. Experimental data presented as mean with 95 % confidence interval (1.96 x SEM) error bars. Experimental data based on N = 8. Experimental isoproterenol data based on findings from 5 nM isoproterenol dose.

As figure 34 shows, the mLR model simulates diastolic membrane potential within the 95 % confidence interval of the experimental data at all pacing frequencies except 8 Hz during control conditions. Both datasets demonstrate similar kinetics as pacing frequency is increased, with deviations in diastolic membrane potential limited to 1 – 6 %, where the greatest change occurs at 10 Hz (+ 6 %, experimental data vs -5 %, mLR model data). Between-group differences were also limited to a maximum magnitude of 5 % throughout. Figure 34 shows diastolic membrane potential from the mLR model remains relatively unchanged during conditions of simulated adrenergic stimulation irrespective of pacing frequency in contrast to experimental data. Simulated relative responses of diastolic membrane potential to isoproterenol also remained within the 95 % confidence interval of the experimental data at lower pacing frequencies (1 - 4 Hz; 1 - 2 Hz).

### *7.3.1$_{iv}$ AP Amplitude*

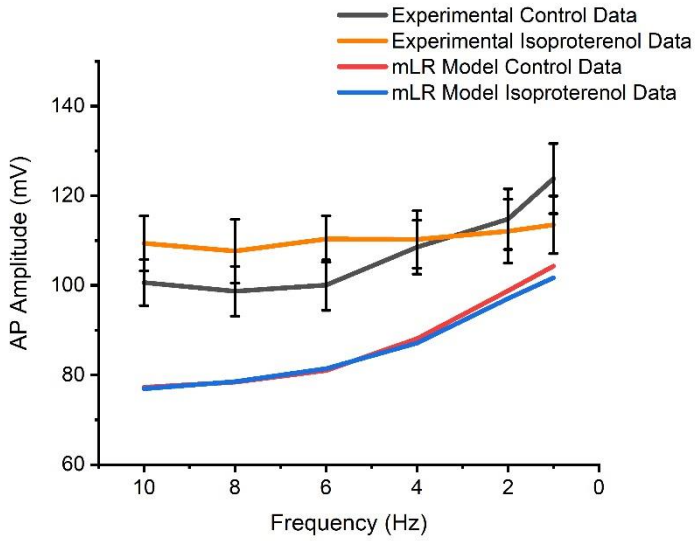


Figure 35. Comparison of AP amplitude during control conditions and during adrenergic stimulation between experimental data (Howlett et al., 2022) and data from the mLR model used in this work. Experimental data presented as mean with 95 % confidence interval (1.96 x SEM) error bars. Experimental data based on N = 8. Experimental isoproterenol data based on findings from 5 nM isoproterenol dose.

Comparisons between experimental and mLR model control data (figure 35) show AP amplitude was reduced in mLR model simulations (14 – 23 %). The greatest differences in AP amplitude between the two datasets were observed at 8 – 10 Hz pacing. However, within-groups differences remained similar. Figure 35 shows AP amplitude from the mLR model remained relatively unchanged during conditions of simulated adrenergic stimulation irrespective of pacing frequency, whilst experimental data displayed AP amplitude became more negative during isoproterenol stimulation at low frequencies (1 – 2 Hz) and more positive at pacing beyond 6 Hz (9 – 10 %). However, relative responses of AP amplitude to simulated isoproterenol remained within the 95 % confidence interval of the experimental data at half of the pacing frequencies (2, 4, 8 Hz).

### 7.3.2 Comparing Ion Channel Current and Responses to Adrenergic Stimulation Between Experimental and Model Data of the Adult Rat

#### *7.3.2$_i$ LTCC*

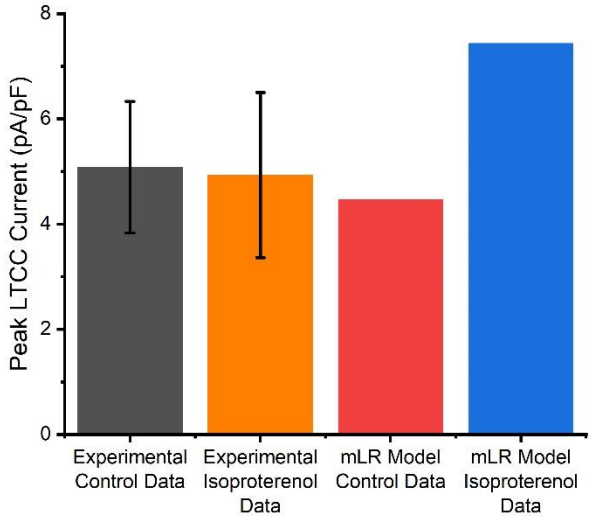


Figure 36. Comparison of peak LTCC current during control conditions and during adrenergic stimulation between experimental data (chapter 4) and data from the mLR model used in this work. All data recorded at 1 Hz or 1000 ms BCL and experimental data presented as mean with 95 % confidence interval (1.96 x SEM) error bars. Experimental data based on N = 8. Experimental isoproterenol data based on findings from 100 nM isoproterenol dose.

Peak LTCC current data simulated by the mLR model was compared with available experimental data (chapter 4) recorded at 1 Hz pacing (figure 36). At 1 Hz pacing, the mLR model produced a peak LTCC current of 4.46 pA/pF, providing close comparison to experimental data (5.08 ± 1.20 pA/pF; mean ± SD) with a difference of just 12 %. Figure 36 demonstrates the peak current simulated by the mLR model remains within the 95 % confidence interval of the experimental data during control conditions. However, peak LTCC current data during adrenergic stimulation simulated by the mLR model was considerably greater than experimental peak LTCC current (1.5-fold) (figure 36). The relative isoproterenol-induced peak current response was also markedly different between the two groups (mLR model: + 67 % vs experimental data: -3 ± 22 %; mean ± SD).

Figure 37 depicts the changes predicted by the mLR model in LTCC current if pacing frequency is increased during control conditions and during adrenergic stimulation. The mLR model suggests peak LTCC current increases by magnitudes between 6 – 15 % with increases in pacing frequency in the absence of isoproterenol. The greatest increase in peak current (15 %) is shown to occur at frequencies similar to basal rat HR (4 - 6 Hz) before a slight reduction at frequencies similar to strenuous exercising rat HR (8 - 10 Hz). Furthermore, the mLR model suggests peak LTCC current increases by lesser magnitudes with increases in pacing frequency during isoproterenol than during control conditions (0.5 – 4 % vs 6 – 15 %), though a similar rate-dependent trajectory is observed. Peak LTCC current is displayed (figure 37) to increase by a magnitude of 48 – 67 %, with the greatest isoproterenol-induced increase in peak current occurring at the slowest pacing frequency (1 Hz: 67 %) and the smallest occurring at the highest pacing frequencies (8 - 10 Hz: 48 – 51 %).

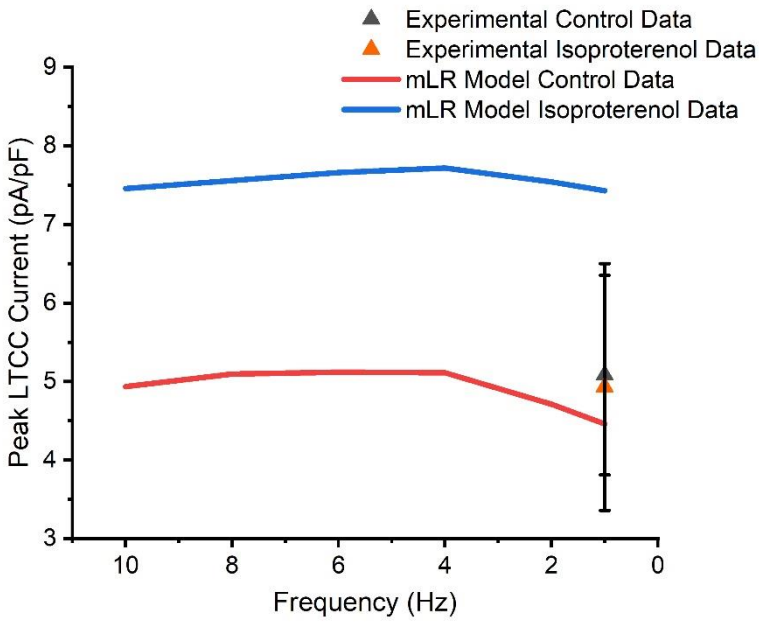


Figure 37. Projected peak LTCC current from the mLR model during control conditions and during adrenergic stimulation.

### *7.3.2$_{ii}$ $I_{K1}$*

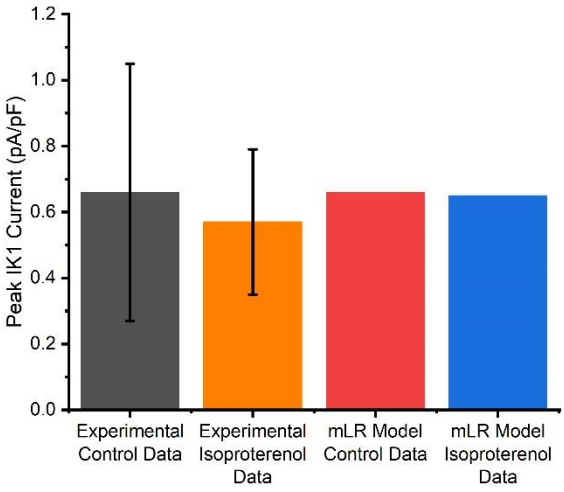


Figure 38. Comparison of peak $I_{K1}$ current during control conditions and during adrenergic stimulation between experimental data (chapter 6) and data from the mLR model used in this work. All data recorded at 1 Hz or 1000 ms BCL and experimental data presented as mean with 95 % confidence interval (1.96 x SEM) error bars. Experimental data based on $BaCl_2$-sensitive current findings from chapter 6, assumed to reflect $I_{K1}$ current. Experimental data based on N = 8. Experimental isoproterenol data based on findings from 100 nM isoproterenol dose.

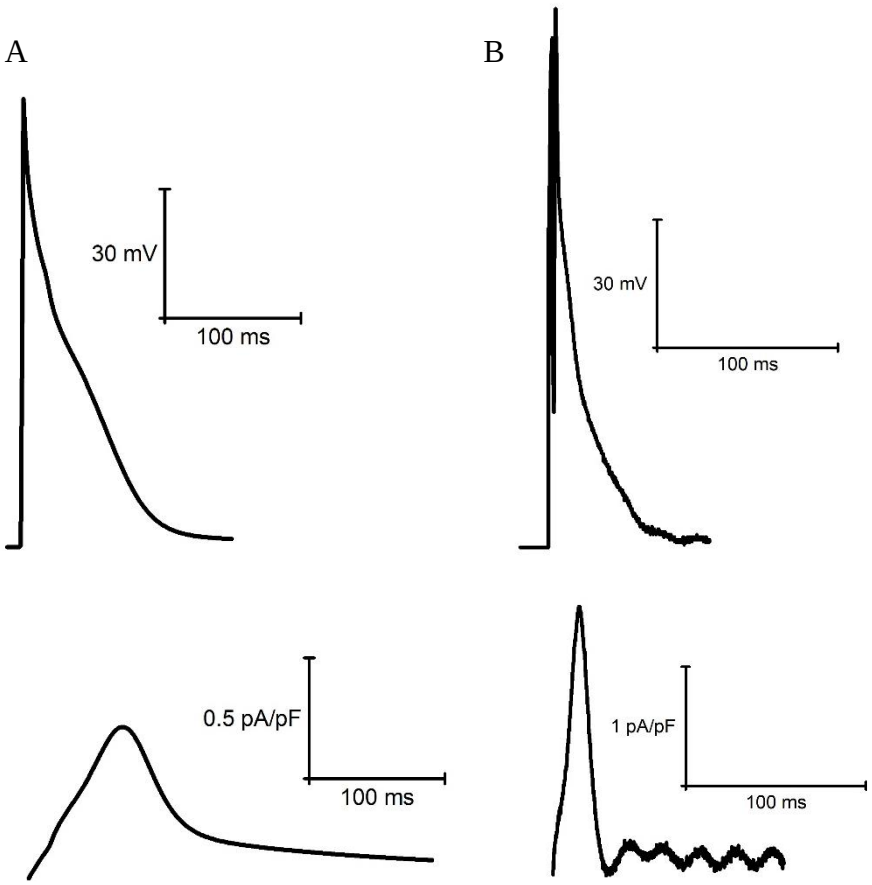


Figure 39. Example steady-state AP and $I_{K1}$ current traces from the mLR model (A) and laboratory investigations (B) (chapter 6). All data recorded at 1 Hz or 1000 ms BCL. Experimental data based on $BaCl_2$-sensitive current findings from chapter 6, assumed to reflect $I_{K1}$ current.

Peak $I_{K1}$ current data simulated at 1 Hz (figure 38 - 39) by the mLR model remained within the 95 % confidence interval of the experimental data (chapter 6) during control conditions (figure 38). At 1 Hz pacing, the model simulated a peak $I_{K1}$ current of 0.66 pA/pF, measuring the same as the experimental data (0.66 ± 0.57 pA/pF; mean ± SD). Peak $I_{K1}$ current data during adrenergic stimulation simulated by the mLR model also remained within the 95 % confidence interval of the experimental data (figure 38). In addition, the relative response to adrenergic stimulation was negative in both groups, with this negative adrenergic response more exaggerated in experimental compared with mLR model data (-14 ± 96 % vs -1 %; mean ± SD). The relative isoproterenol-

induced changes in $I_{K1}$ current produced by the mLR model similarly remained within the 95 % confidence interval of the experimental data.

Figure 38 depicts the predicted peak $I_{K1}$ current by the mLR model as pacing frequency is increased during control conditions and adrenergic stimulation. During control conditions the mLR model demonstrates very little change in $I_{K1}$ current at greater pacing frequencies, with peak current steadily reducing by magnitudes of 1 %, 5 %, 8 %, 9 % and 9 % at 2, 4, 6, 8 and 10 Hz frequencies respectively compared with 1 Hz pacing. Moreover, the mLR model suggests isoproterenol has very little to no impact on the rate-dependent changes in peak $I_{K1}$ current (-1 %) and changes in peak current independent of rate.

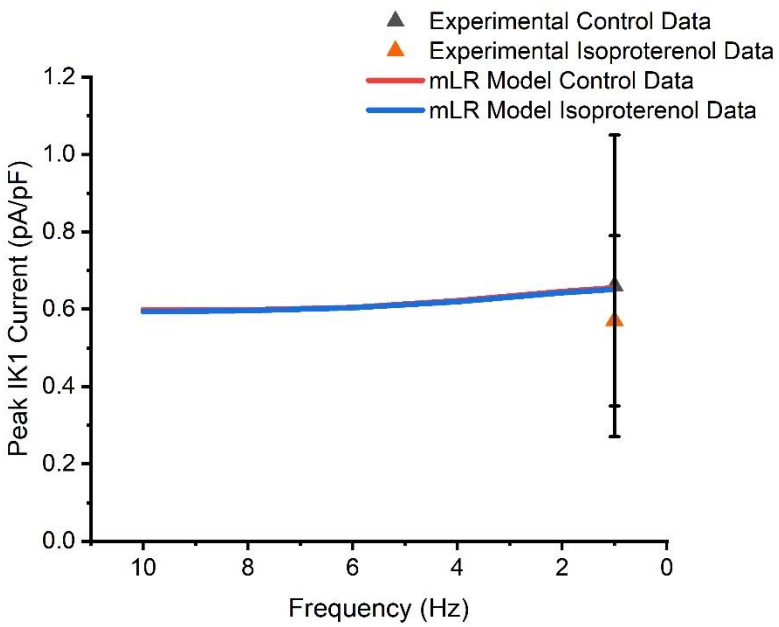


Figure 40. Projected peak $I_{K1}$ current from the mLR model during control conditions and during adrenergic stimulation. Experimental data based on $BaCl_2$-sensitive current findings from chapter 6, assumed to reflect $I_{K1}$ current.

### 7.3.2$_{iii}$ $I_{Kr}$

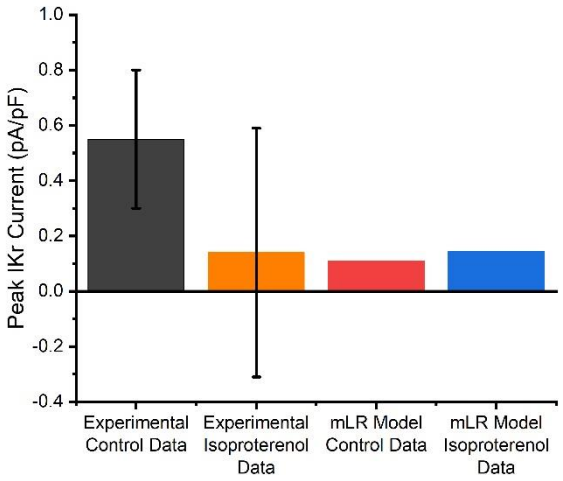


Figure 41. Comparison of peak $I_{Kr}$ current during control conditions and during adrenergic stimulation between experimental data (chapter 6) and data from the mLR model used in this work. All data recorded at 1 Hz or 1000 ms BCL and experimental data presented as mean with 95 % confidence interval (1.96 x SEM) error bars. Experimental data based on E4031-sensitive current findings from chapter 6, assumed to reflect $I_{Kr}$ current. Experimental data based on N = 8. Experimental isoproterenol data based on findings from 100 nM isoproterenol dose.

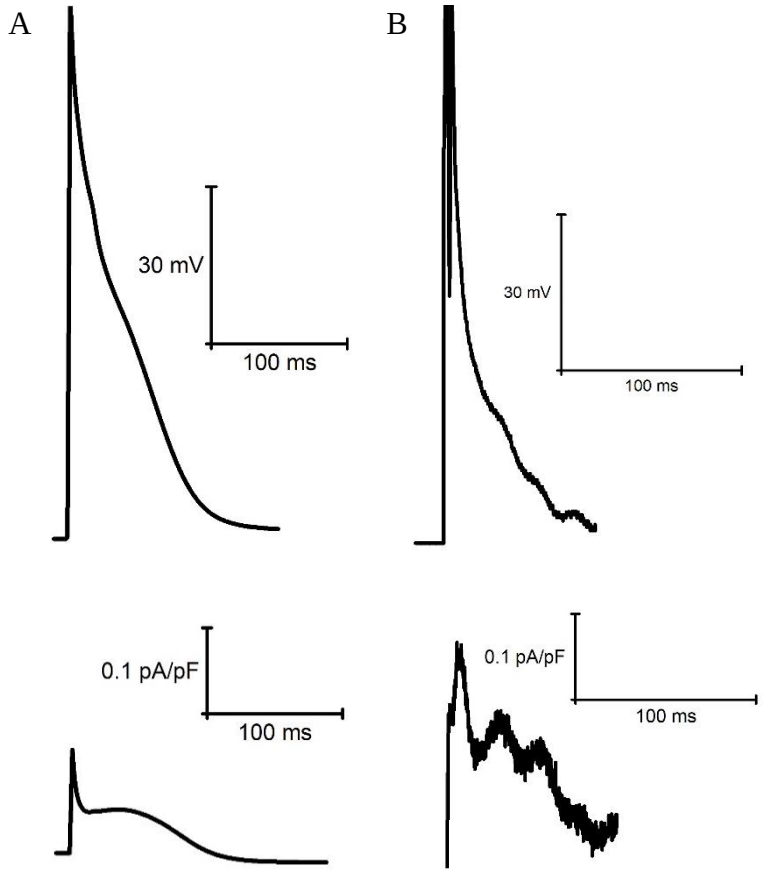


Figure 42. Example steady-state AP and $I_{Kr}$ current traces from the mLR model (A) and laboratory investigations (B) (chapter 6). All data recorded at 1 Hz or 1000 ms BCL. Experimental data based on E4031-sensitive current findings from chapter 6, assumed to reflect $I_{Kr}$ current.

Peak $I_{Kr}$ current data simulated by the mLR model was compared with available experimental data (chapter 6) at 1 Hz pacing during control conditions (figure 41 - 42). Peak modelled $I_{Kr}$ current was approximately 5-fold less than experimental data (0.11 pA/pF vs 0.55 ± 0.38 pA/pF; mean ± SD). Peak $I_{Kr}$ current data during adrenergic stimulation simulated by the mLR model remained within the 95 % confidence interval of the experimental data (figure 41). In addition, the relative isoproterenol-induced changes in $I_{Kr}$ current produced by the mLR model also remained within the 95 % confidence interval of the experimental data. However, there were clear directional differences between the two groups in response to adrenergic stimulation. Peak current data from the mLR model displayed a 35 % increase in response to

isoproterenol compared with control conditions, conversely experimental data displayed a 74 ± 463 % reduction in peak $I_{Kr}$.

Figure 43 displays rate-dependent $I_{Kr}$ current changes predicted by the mLR model during control conditions and during adrenergic stimulation. During control conditions, the projected peak $I_{Kr}$ current increases exponentially as pacing frequency is increased, particularly from basal rat HR (4 - 6 Hz) to strenuous exercising rat HR (8 - 10 Hz). Compared with 1 Hz pacing, model simulations suggest peak current increases in excess of 6-fold and 13-fold at 6 Hz and 10 Hz during control conditions respectively. Similar to the predictions in $I_{K1}$ current, the mLR model suggests isoproterenol has very little to no impact on the rate-dependent changes in peak $I_{Kr}$ current. However, peak $I_{Kr}$ current demonstrated slightly blunted isoproterenol-induced increases at the highest pacing frequencies (8 – 10 Hz: 23 – 24 %) compared with the lowest pacing frequencies (1 - 2 Hz: 35 – 33 %).

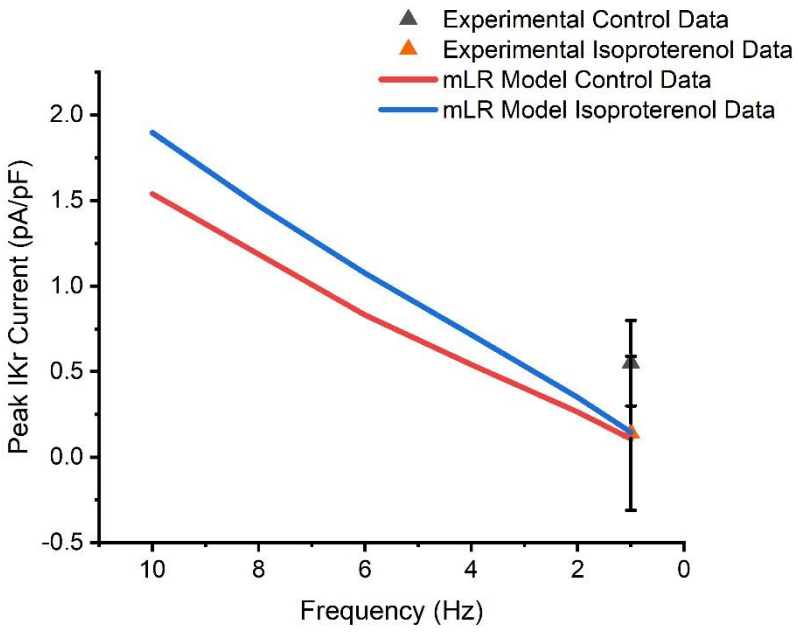


Figure 43. Projected peak $I_{Kr}$ current from the mLR model during control conditions and during adrenergic stimulation. Experimental data based on E4031-sensitive current findings from chapter 6, assumed to reflect $I_{Kr}$ current.

### *7.3.2$_{iv}$ $I_{Ks}$*

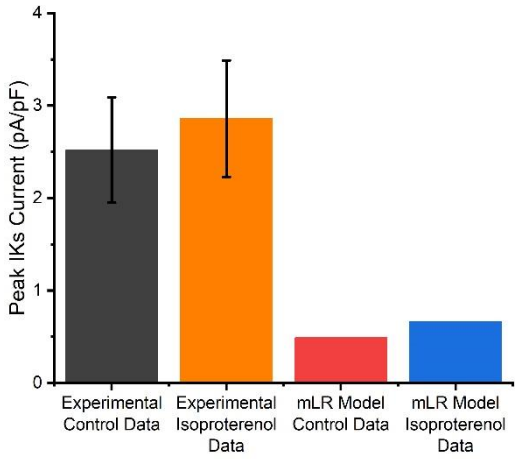


Figure 44. Comparison of peak $I_{Ks}$ current during control conditions and during adrenergic stimulation between experimental data (chapter 6) and data from the mLR model used in this work. All data recorded at 1 Hz or 1000 ms BCL and experimental data presented as mean with 95 % confidence interval (1.96 x SEM) error bars. Experimental data based on chromanol 293b-sensitive current findings from chapter 6, assumed to reflect $I_{Ks}$ current. Experimental data based on N = 8. Experimental isoproterenol data based on findings from 100 nM isoproterenol dose.

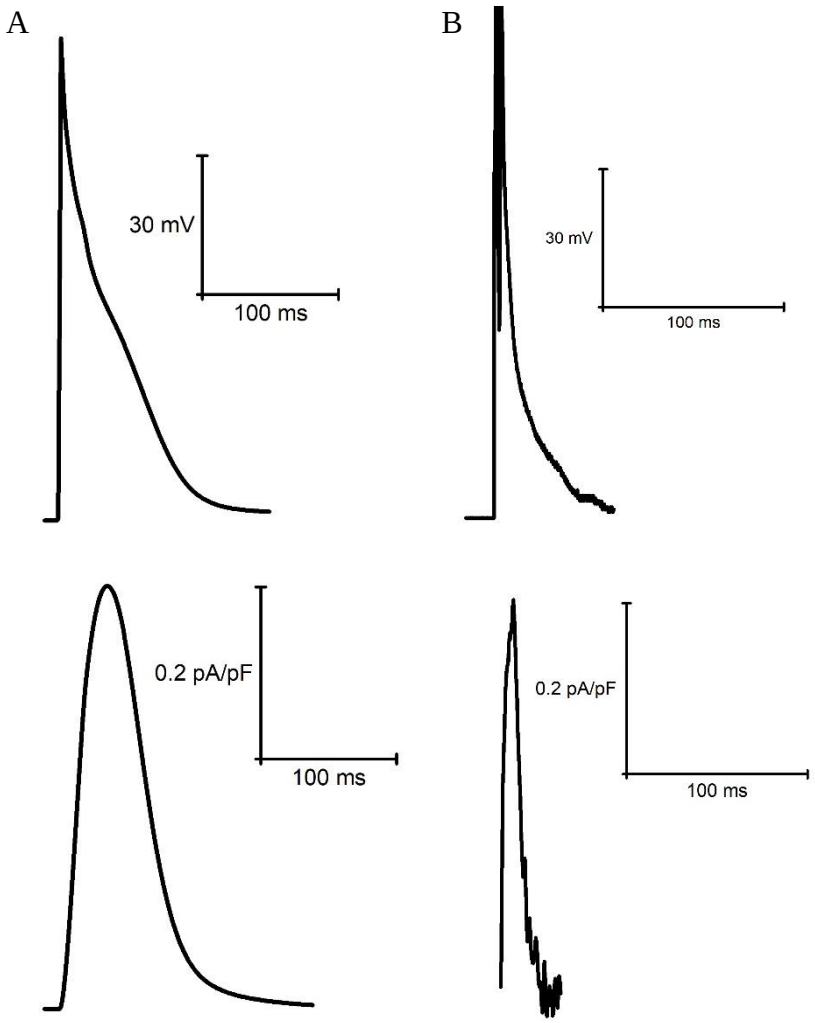


Figure 45. Example steady-state AP and $I_{Ks}$ current traces from the mLR model (A) and laboratory investigations (B) (chapter 6). All data recorded at 1 Hz or 1000 ms BCL. Experimental data based on chromanol 293b-sensitive current findings from chapter 6, assumed to reflect $I_{Ks}$ current.

Peak $I_{Ks}$ current data simulated by the mLR model was also compared with the available chromanol 293b-sensitive current experimental data (chapter 6) at 1 Hz pacing (figure 44 – 46). Similar to $I_{Kr}$, peak $I_{Ks}$ current simulated by the mLR model was approximately 5-fold less than that of the chromanol 293b-sensitive current experimental data during control conditions (0.49 pA/pF vs 2.52 ± 0.82 pA/pF; mean ± SD). Similarly, figure 44 shows peak $I_{Ks}$ current data during adrenergic stimulation simulated by the mLR model remained much lower than chromanol 293b-sensitive current experimental data (0.67 pA/pF vs 2.86 ± 0.90 pA/pF; mean ± SD). The relative

isoproterenol-induced current response simulated by the mLR model remained slightly outside of the 95 % confidence interval of the chromanol 293b-sensitive current experimental data, however, these relative responses provide a much closer comparison with peak chromanol 293b-sensitive current increasing by 13 ± 27 % in experimental data and peak $I_{Ks}$ current increasing by 35 % in mLR model simulations.

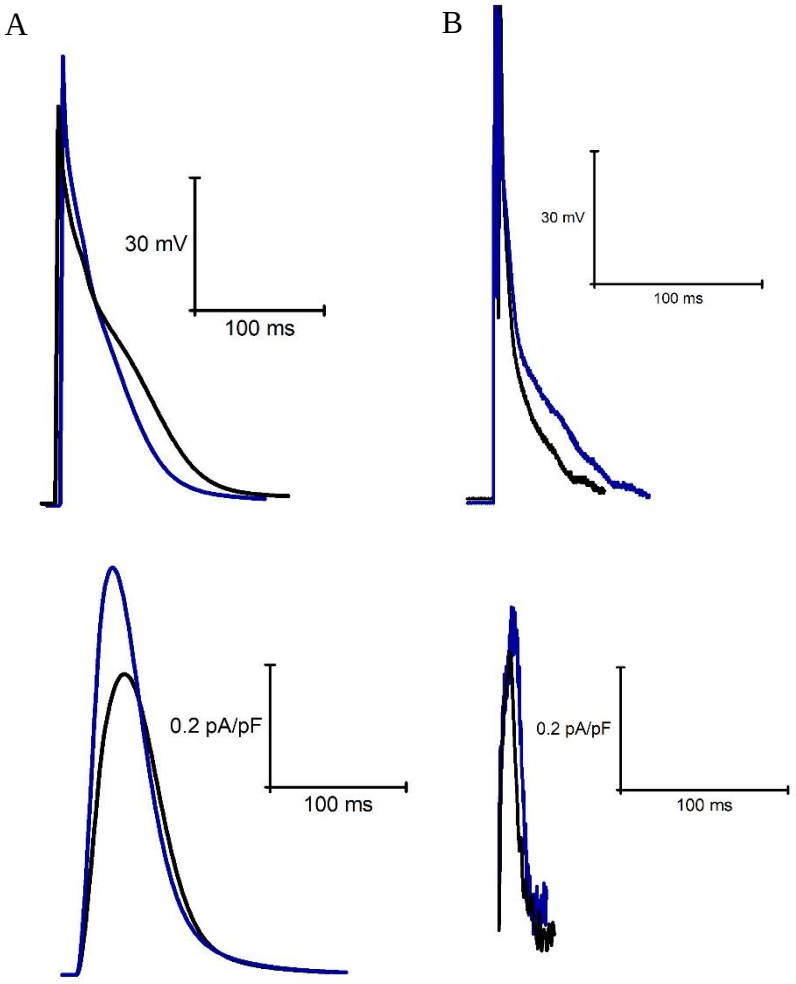


Figure 46. Example steady-state AP and $I_{Ks}$ current traces, demonstrating the upregulation in current during adrenergic stimulation (blue) compared with control conditions (black) from the mLR model (A) and laboratory investigations (B) (chapter 6). All data recorded at 1 Hz or 1000 ms BCL. Experimental data based on chromanol 293b-sensitive current findings from chapter 6, assumed to reflect $I_{Ks}$ current.

Figure 47 displays the mLR model predicted changes in peak $I_{Ks}$ current as pacing frequency is elevated during control conditions and during adrenergic stimulation. During control conditions, these simulations suggest $I_{Ks}$ peak current remains relatively constant between 1 - 4 Hz before increasing 28 %, 62 % and 95 % at 6, 8 and 10 Hz pacing respectively compared with 1 Hz. Further, the mLR model suggests isoproterenol has very little to no impact on the rate-dependent changes in peak $I_{Ks}$ current. Peak $I_{Ks}$ current also demonstrated a consistent isoproterenol-induced current increase throughout, deviating very little from a 35 – 40 % increase irrespective of pacing frequency.

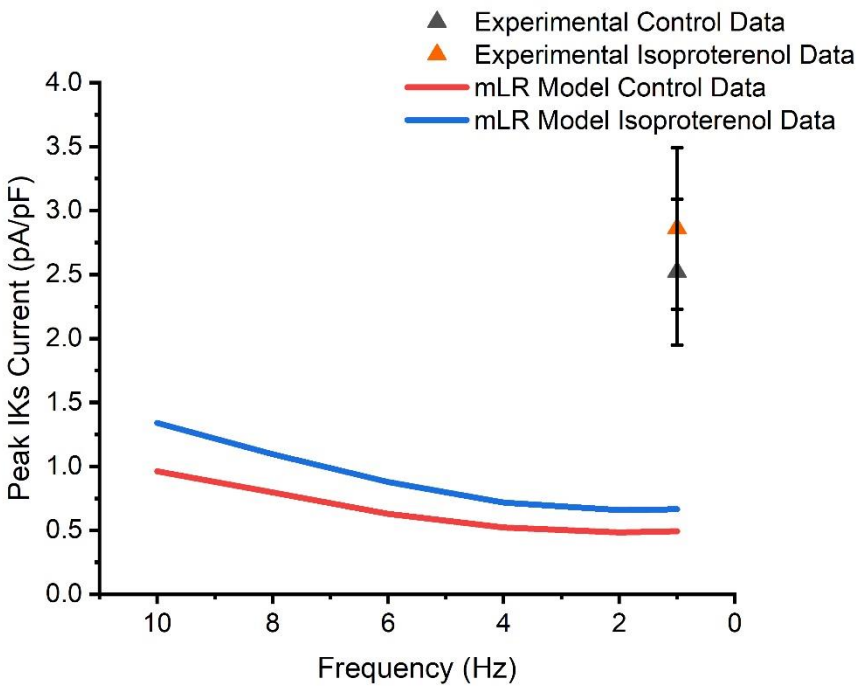


Figure 47. Projected peak $I_{Ks}$ current from the mLR model during control conditions and during adrenergic stimulation. Experimental data based on chromanol 293b-sensitive current findings from chapter 6, assumed to reflect $I_{Ks}$ current.

## 7.4 Discussion

The aim of this study was to develop a computational rat AP model (Stevenson-Cocks, 2019), using experimental data and previous literature to create two model variations

capable of reliably reproducing adult ventricular myocyte AP data at physiologically relevant rates and temperatures and their response to adrenergic stimulation.

The main findings of this work were that the adult rat variant of the mLR model was able to reproduce $APD_{50}$ and $APD_{90}$ data within the 95 % confidence interval of experimental data at a range of physiological activation frequencies. Furthermore, this variant was able to reproduce peak LTCC and $I_{K1}$ currents at 1 Hz pacing within the 95 % confidence interval of experimental data. In addition, whilst simulated peak $I_{Kr}$ and $I_{Ks}$ currents were considerably lower than peak $I_{Kr}$ and chromanol 293b-sensitive currents in the experimental data, within-groups differences between both currents were very similar, with peak $I_{Ks}$ current displayed to be ~ 5-fold greater than $I_{Kr}$ peak current at 1 Hz pacing in both simulated and laboratory settings. Though in laboratory settings, peak $I_{Ks}$ current comparative data was assumed from peak chromanol 293b-sensitive current data.

In addition, the adult rat during adrenergic stimulation variant of the mLR model was able to reproduce $APD_{50}$ response to isoproterenol within the 95 % confidence interval of experimental data at a range of physiological activation frequencies (2 - 10 Hz) and demonstrate similar rate-dependency during adrenergic stimulation to experimental data. The adult rat during adrenergic stimulation variant of the mLR model was also able to reproduce $APD_{90}$ at most pacing frequencies (2 - 10 Hz) as well as $APD_{90}$ response to isoproterenol (2 - 8 Hz) within the 95 % confidence interval of experimental data. Moreover, this variant reproduced peak $I_{Kr}$ and $I_{K1}$ currents during isoproterenol alongside relative responses to isoproterenol within the 95 % confidence interval of experimental data. Finally, relatively similar modest increases in the relative response to isoproterenol were observed between peak $I_{Ks}$ current and peak chromanol 293b-sensitive current (35 % vs 13 %) from mLR simulations and laboratory data respectively, despite an approximate 4-fold reduction in peak $I_{Ks}$ current compared with chromanol 293b-sensitive current during adrenergic stimulation.

### 7.4.1 Comparing Simulated AP Variables to Experimental Findings and Existing Literature

The results of this study's work using the adult variant of the mLR model suggest that rat ventricular myocyte $APD_{50}$ and $APD_{90}$ can be reliably simulated at a range of

pacing frequencies, including those most physiologically relevant to the rat (4 - 10 Hz respectively) (figures 31 - 32). Interestingly, the results demonstrate that $APD_{90}$ can most closely replicate experimental data at the highest pacing frequency (10 Hz). In contrast AP amplitude values simulated by the mLR model during control conditions were not within the 95 % confidence interval of the experimental data, whilst diastolic membrane potential values were simulated within the 95 % confidence interval at the majority of pacing frequencies (1 - 6, 10 Hz). The work in this study using the adult rat during adrenergic stimulation model variant also demonstrate that the mLR model is capable of reliably modelling $APD_{90}$ data during adrenergic stimulation at most pacing frequencies (2 - 10 Hz) as well as isoproterenol-induced responses in $APD_{50}$ (2 - 10 Hz) and $APD_{90}$ (2 - 8 Hz).

The mLR model simulations were also compared with existing literature in adult rat ventricular myocytes as well as the experimental findings of this work. Relatively few studies investigating APD and AP repolarisation in rat ventricular myocytes at pacing frequencies above 1 Hz, particularly at physiological rat HR exist. However, one study investigating differences in APD between base and apex regions of the rat ventricles reported $APD_{90}$ values between 55 - 76 ms (apex - base) during 1 Hz pacing, with basal $APD_{90}$ values very similar to both the experimental and mLR model findings of this study (Wang and Fitts, 2017). The study by Wang and Fitts (Wang and Fitts, 2017) also found $APD_{90}$ shortened by a magnitude of 30 – 31 % when measured at 10 Hz pacing compared with 1 Hz, mimicking $APD_{90}$ shortening of 29 % and 38 % found in the experimental and mLR model findings of this study respectively (Wang and Fitts, 2017). However, the same study found greater isoproterenol-induced $APD_{90}$ shortening at 1 Hz (40 %) compared with the experimental (24 ± 14 %) and mLR model (13 %) findings of this study, though this could be a result of the use of a greater isoproterenol dose (10 nM vs 5 nM) (Wang and Fitts, 2017).

A study by Shigematsu et al. reported similar $APD_{90}$ values (52 ms) to those yielded in the study by Wang and Fitts discussed above at 1 Hz pacing, and similarly reported prolongations in $APD_{90}$ at 2 Hz (15 %) and 5 Hz (46 %) pacing compared with 1Hz, though to a greater magnitude demonstrated in the experimental findings of this study (2 Hz: 11 %, 4 Hz: 5 %) (Shigematsu et al., 1997; Wang and Fitts, 2017). Despite the lack of $APD_{90}$ prolongation at basal rat HR simulated by the mLR model, the raw $APD_{90}$ values documented in the study by Shigematsu et al. during 5 Hz pacing

provide close comparison to those simulated at 4 Hz (75.92 ms vs 73.43 ms) (Shigematsu et al., 1997). A study by Kamada et al. reported comparatively greater $APD_{90}$ values of 100 ms at 5 Hz pacing, yet exhibited similar isoproterenol-induced (100 nM) $APD_{90}$ shortening (8 %) to both the experimental and mLR model findings in this study measured at 4 - 6 Hz during 5 nM isoproterenol stimulation (Experimental: 13 ± 16 % - 9 ± 14 %, MLR model: 14 – 11 %) (Kamada et al., 2019). However, a study by Hardy et al. reported much briefer $APD_{90}$ values (< 50 ms) at a range of pacing frequencies (1 - 8 Hz) than those found in the experimental and mLR model findings of this study, providing much closer comparison to the $APD_{90}$ values simulated by the original LR model (Stevenson-Cocks, 2019; Hardy et al., 2018). Such brief $APD_{90}$ values have also been reported in other studies at lower pacing frequencies (0.5 Hz: 32.5 ms, 1 Hz: 39.7 ms) (Liu et al., 2000; Şengül Ayan et al., 2020). However, the study by Hardy et al. did support the rate-dependent $APD_{90}$ shortening at increased pacing frequencies (> 5 Hz) (Hardy et al., 2018). The briefer APDs reported at a range of pacing frequencies in the study by Hardy et al. compared with the experimental and mLR model findings may be a result of the use of different electrophysiological stimulation protocols as well as different patch-clamp techniques (sharp electrode vs whole-cell) (Hardy et al., 2018).

Literature measuring $APD_{90}$ at pacing frequencies lower than 1 Hz (0.1 - 0.5 Hz) provides mixed comparisons to the mLR model data and the experimental data in this work, as $APD_{90}$ data in the literature recorded at 0.5 Hz pacing was measured as 55 ms (Sakatani et al., 2006), substantially lower than the findings of this study, whilst studies recorded at 0.1 Hz and 0.2 Hz yielded $APD_{90}$ values of 76.45 ms (Jourdon and Feuvray, 1993) and 73.2 ms (Bouchard et al., 2004) respectively, providing very close comparison to the 1 Hz values shown in figure 32.

Moreover, literature focusing on AP plateau changes ($APD_{50}$) in rat ventricular myocytes has been studied even less frequently at physiological pacing frequencies relative to the rat. One study yielded $APD_{50}$ values of 21 ms, 26 ms and 41 ms at 1, 2 and 5 Hz pacing respectively (Shigematsu et al., 1997). These $APD_{50}$ values demonstrate prolongation with increases in rate toward basal rat HR, correlating well with findings from the mLR model and experimental data at 1 and 2 Hz pacing but are exaggerated when comparing $APD_{50}$ at 5 Hz pacing in literature (41 ms) to 4 - 6 Hz findings from the laboratory and simulations (laboratory data: 25.37 ± 14.15 ms –

25.37 ± 12.27 ms, mLR model data: 32.58 - 33.44 ms) (Shigematsu et al., 1997). Work by Fauconnier et al. also found rate-dependent prolongations toward basal rat HR in $APD_{50}$ (16.2 ms vs 19.4 ms), although this was reported across a lower pacing frequency range (0.1 - 3 Hz) (Fauconnier et al., 2003). At reduced frequencies in particular, $APD_{50}$ has been shown to vary considerably in research, with data at 1 Hz (19.65 ms) providing some close comparison to the $APD_{50}$ values documented in this work (figure 31) (Şengül Ayan et al., 2020), whilst measurements at lower frequencies (0.1 - 0.5 Hz) have yielded values ranging from 4.2 ms to 46.3 ms (Jourdon and Feuvray, 1993; Bouchard et al., 2004; Liu et al., 2000; Walker et al., 1993). Such differences are likely a result of the use of different animal strains, differences in pacing frequency and differences in environmental temperature (Jourdon and Feuvray, 1993; Bouchard et al., 2004; Liu et al., 2000; Walker et al., 1993).

Literature investigating AP amplitude and diastolic membrane potential in rat ventricular myocytes appear to support data simulated by the mLR model as well as experimental data by suggesting AP amplitude decreases whilst diastolic membrane potential becomes less negative with changes to pacing (Fauconnier et al., 2003; Ravens and Wettwer, 1998). In a study by Fauconnier et al. diastolic membrane potential measured -78 mV, -76 mV, -73 mV, -71 mV at 1, 2, 4 and 6 Hz pacing respectively, reflecting 3 %, 6 %, 9 % changes at 2, 4 and 6 Hz compared with 1 Hz pacing respectively (Fauconnier et al., 2003). Such values bear close resemblance to those simulated by the mLR model (figure 34). Diastolic membrane potential values recorded at lower frequencies (0.2 - 1 Hz) have often been measured to be more negative (-80 - -80.4 mV) (Bouchard et al., 2004; Xu et al., 2016; Watanabe et al., 1983). Though, in contrast, some studies have reported similar diastolic membrane potential values (-62.9 mV - -71.6 mV) at these low pacing frequencies (0.1 - 0.5 Hz) to those recorded in the model simulations of this study (figure 34) (Liu et al., 2000; Walker et al., 1993; Jourdon and Feuvray, 1993). Action potential amplitude data in the literature also appears to provide close comparison to the values documented in data from the mLR model as well as experimental findings from this study, even at pacing frequencies lower than 1 Hz (0.1 - 0.5 Hz) (91.6 mV – 117.9 mV) (figure 35) (Jourdon and Feuvray, 1993; Walker et al., 1993; Bouchard et al., 2004; Liu et al., 2000; Xu et al., 2016; Watanabe et al., 1983).

### 7.4.2 Comparing Simulated Ion Channel Fluxes to Experimental Findings and Existing Literature

The work in this study demonstrates that the mLR model is able to simulate important ion channel currents involved in modulating the AP plateau and late repolarisation such as LTCC and $I_{K1}$ currents at 1 Hz pacing and may additionally simulate the proportional kinetics / contribution to AP repolarisation of $I_{Ks}$ and $I_{Kr}$ currents (figures 36, 38, 41 and 44). Findings from the adult rat adrenergic stimulation model variant also suggest the mLR model can reliably model both peak currents during adrenergic stimulation and the relative isoproterenol-induced peak current response in some $K^+$ channels important to AP repolarisation ($I_{Kr}$; $I_{K1}$). Whilst other $K^+$ channels involved in AP repolarisation ($I_{Ks}$) that are less reliably modelled by the mLR model when compared with chromanol 293b-sensitive current experimental data, still display comparable relative isoproterenol-induced peak current responses. In addition, the amplification of LTCC current in data from the mLR model compared with experimental data, likely underlies the prolonged $APD_{50}$ yielded in modelling simulations compared with the experimental data at low pacing frequencies (1 Hz).

Much like APD investigations, studies investigating ion channel fluxes in rat ventricular myocytes at pacing frequencies above 1 Hz are very few in number and increase the difficulty of comparison and validation of the model. Studies investigating peak LTCC current in adult rat ventricular myocytes have shown a vast array of values ranging from 6 – 14.6 pA/pF at pacing frequencies of 0.1 - 2.5 Hz (Xiao et al., 1994; Liu et al., 2000; Sakatani et al., 2006; Walker et al., 1993; Jourdon and Feuvray, 1993; Scamps et al., 1990; Meszaros et al., 1997; Vizgirda et al., 2002; Zhou et al., 1998). The peak LTCC current values referred to in the literature exhibit a greater magnitude than observed in the experimental data and model simulations in this study (figure 36 - 37). Similarly, peak LTCC current response to adrenergic stimulation in the literature has been shown to range from a 28 % – 120 % increase in current, which is much more exaggerated than experimental findings in this study, but correlates well with simulations from the mLR model (67 %) (Xiao et al., 1994; Sakatani et al., 2006; Şengül Ayan et al., 2020; Scamps et al., 1990; Katsube et al., 1996; Vizgirda et al., 2002; Zhou et al., 1998).

Studies investigating peak $I_{K1}$ current in rat ventricular myocytes have reported values between -19.8 pA/pF and +6.5 pA/pF (Fauconnier et al., 2005; He et al., 2008; Kilborn and Fedida, 1990; Bébarová et al., 2014; Liu et al., 2000; Wahler, 1992; Jourdon and Feuvray, 1993), with the greatest negative peak current values recorded during voltage-clamp experiments at membrane potentials between -120 and 60 mV (Fauconnier et al., 2005; He et al., 2008; Kilborn and Fedida, 1990; Bébarová et al., 2014; Liu et al., 2000; Wahler, 1992; Jourdon and Feuvray, 1993). As the work in this study has focused on $I_{K1}$ current data during AP-clamp or simulation studies, where membrane potential is equal to or more positive than -80 mV, peak outward $I_{K1}$ currents provided the best comparison between literature and work in this study. Peak outward $I_{K1}$ current has commonly been displayed between approximately 0.5 pA/pF to 6.5 pA/pF at pacing frequencies of 0.1 - 0.5 Hz (Fauconnier et al., 2005; He et al., 2008; Kilborn and Fedida, 1990; Bébarová et al., 2014; Liu et al., 2000; Wahler, 1992; Jourdon and Feuvray, 1993). Studies by Fauconnier et al. (Fauconnier et al., 2005), He et al. (He et al., 2008), Kilborn et al. (Kilborn and Fedida, 1990) and Bebarova et al. (Bébarová et al., 2014) provide relatively similar peak outward $I_{K1}$ currents to those recorded at 1 Hz from the mLR model and experimental findings (1.17 pA/pF; ~ 0.5 pA/pF; ~ 1 pA/pF; 0.8 - 1.2 pA/pF vs 0.66 pA/pF), though peak outward $I_{K1}$ currents in the literature have been measured at lower frequencies. Meanwhile, studies by Liu et al. (Liu et al., 2000), Wahler et al. (Wahler, 1992) and Jourdon et al. (Jourdon and Feuvray, 1993) suggest peak outward $I_{K1}$ current is greater than the values found in this study (~6.5 pA/pF; 2 pA/pF; 2 pA/pF vs 0.66 pA/pF). However, the greater dose of $I_{K1}$ blocker ($BaCl_2$) used and the use of different strains of rat may, in part, explain the amplification in this current (Wahler, 1992; Liu et al., 2000).

The available studies investigating peak $I_{Kr}$ currents in rat ventricular myocytes have demonstrated values between 0.18 pA/pF – 0.48 pA/pF (Wang and Fitts, 2020; Sakatani et al., 2006). The magnitude of peak $I_{Kr}$ currents documented in the literature, correlate very closely with model simulations and laboratory findings (Wang and Fitts, 2020; Sakatani et al., 2006), in particular work by Wang and Fitts (Wang and Fitts, 2020) most closely compares to data from the mLR model (0.18 pA/pF vs 0.11 pA/pF), whilst work by Sakatani et al. (Sakatani et al., 2006) most closely compares to the experimental data recorded in this study (0.48 pA/pF vs 0.55 ± 0.38 pA/pF; mean ± SD), though $I_{Kr}$ currents recorded in the literature are measured at lower frequencies

(0.1 Hz). In contrast, the limited available research investigating the response in $I_{Kr}$ peak current to adrenergic stimulation (100 nM isoproterenol) display considerably different current modulations compared with data from experimental findings in this work (17 - 45 % vs -74 ± 463 %; mean ± SD) but closely correlate with those simulated by the mLR model (17 - 45 % vs 35 %) (Sakatani et al., 2006; Şengül Ayan et al., 2020). During experimental investigations, $I_{Kr}$ currents were incredibly difficult to measure, varied considerably and were not always identifiable, which likely contributed to differences observed between laboratory findings and findings in the literature.

Studies investigating peak $I_{Ks}$ currents in rat ventricular myocytes have described current values between 0.71 pA/pF and 1 pA/pF (Wang and Fitts, 2020; Sakatani et al., 2006) which provide closer comparison to data from the mLR model (0.49 pA/pF) than the chromanol 293b-sensitive current experimental data displayed in figure 44. Yet one study suggests $I_{Ks}$ peak current is much greater (4 pA/pF), though this is likely a result of the use of different channel blocking strategies and the measurement of peak current rather than peak tail current (Masuda et al., 2018). However, these $I_{Ks}$ values recorded in the literature are measured at 0.1 Hz pacing as opposed to 1 Hz pacing shown in figure 44 - 46, and the work by Wang and Fitts (Wang and Fitts, 2020) reflect tail currents recorded during voltage-clamp experiments (Wang and Fitts, 2020; Sakatani et al., 2006). In the study by Wang and Fitts (Wang and Fitts, 2020) 5 nM and 1 µM isoproterenol stimulated increases in peak $I_{Ks}$ tail current by magnitudes of 50 – 54 % and 62 – 66 % respectively. Relatively similar, slightly narrower, adrenergic responses in peak $I_{Ks}$ current have been reported elsewhere by Sakatani et al. (38 %) (Sakatani et al., 2006). Such isoproterenol-induced increases display similarities to simulated peak $I_{Ks}$ current responses produced by the mLR model (35 %) but are greater than the chromanol 293b-sensitive current responses observed in chapter 6 (figure 44).

The results of this study, suggest that the mLR model and associated variants are capable of reliably modelling AP variables, particularly $APD_{90}$, during control conditions and during mimicked conditions of adrenergic stimulation at a range of pacing frequencies, physiologically relevant to the adult rat and produces data that are comparable to the experimental findings of this study and many findings in the literature. The results of the work in this study also suggest that the mLR model and

associated variants can model some key contributing ion channel currents to AP repolarisation during control conditions and during adrenergic stimulation at low pacing frequencies in adult rat ventricular myocytes that provide comparative peak current or current dynamics to experimental findings from this study and findings in the literature.

However, when interpreting the findings of this chapter and contemplating the potential usage of the mLR model in the wider context, a number of important factors must be considered. Firstly, $I_{Kr}$ and $I_{Ks}$ were incorporated into the model, as previously mentioned, by splitting the $I_{ss}$ current from the original LR model and using formulae from a neonatal rat ventricular myocyte model (Korhonen et al., 2009). This was a pragmatic and time efficient approach to incorporate the two repolarising $K^+$ channel currents ($I_{Kr}$ and $I_{Ks}$), which were the intended targets of investigation throughout a large portion of this project, without disrupting the balance of outward $K^+$ currents in the original model in general and allowing, as a minimum, some insight into the changes in potential key components involved in AP repolarisation and their role in the overall electrophysiological response to adrenergic stimulation. Despite the potential utility of the mLR model described above, there are considerable physiological differences between neonatal and adult ventricular myocytes. Additionally, the $I_{ss}$ current is understood to be distinct from other known $K^+$ channel currents (Choisy et al., 2004; Sakatani et al., 2006; Himmel et al., 1999) and not simply the sum of $I_{Kr}$ and $I_{Ks}$ (Sakatani et al., 2006). Therefore the substitution of $I_{ss}$ with $I_{Kr}$ and $I_{Ks}$ does not reflect typical rat ventricular myocyte electrophysiology and may impair the reliability of findings relating to AP repolarisation from mLR model simulations. In addition, it could be argued that the results from the work in previous chapters do not provide a firm basis for the incorporation of $I_{Kr}$ especially due to its seemingly limited role in rat ventricular myocyte repolarisation (Wang and Fitts, 2020) and potentially also $I_{Ks}$ due to the issues explained earlier with chromanol 293b selectivity. Furthermore, given its understood importance alongside $I_{ss}$ in the modulation of rat ventricular AP repolarisation (Himmel et al., 1999; Árpádffy-Lovas et al., 2022), the omission of $I_{Kur}$ from the mLR model should also be considered when interpreting model simulations and similarly may impair the translational value of simulated findings in AP repolarisation.

A further related limitation is the use of experimental findings (alongside existing literature) to develop the mLR model, whereby modelled $I_{Ks}$, $I_{Kr}$ and $I_{K1}$ function are at least in part, based on chromanol 293b-sensitive, E4031-sensitive and $BaCl_2$-sensitive current findings from chapter 6 respectively. As discussed in chapters 5 and 6, without further confirmatory experiments, it is difficult to reliably assign such current findings to these individual repolarising $K^+$ currents, particularly in the case of $I_{Ks}$ or chromanol 293b-sensitive current where the chromanol 293b dose used may cause the measured current to be attributed to $I_{to}$ and $I_{Kur}$ as well as the intended $I_{Ks}$ (Du et al., 2003; Sun et al., 2001; Árpádffy-Lovas et al., 2022; Bosch et al., 1998). This means that any potential insight highlighted by the mLR model in $I_{Ks}$, $I_{Kr}$ and $I_{K1}$ current may not provide specific and reliable information about pure individual currents, though still may provide important information about $K^+$ current involvement in general in the modulation of AP repolarisation in response to $\beta_1$AR signalling.

In order for the mLR model to be of significant benefit in the wider context outside of the initial utility of having a model capable of simulating AP data under control and adrenergic stimulation conditions at a full range of pacing frequencies as may occur in-vivo in the rat during exercise, further work is required. In addition to the further experiments required to combat the issues surrounding the reliable $K^+$ current measurement and blocker selectivity as explained in previous chapters (chapter 5 and 6), further model development is necessary. Incorporating the full ensemble of ion channels shown to exist in the rat ventricle, particularly focusing on the inclusion of those involved in AP repolarisation, such as $I_{ss}$ and $I_{Kur}$ and modifying their relative influences on the modulation of APD, will go some way to improving the physiological relevance and overall validity of the mLR model in answering important questions in the field of cardiac electrophysiology as well as facilitating the improved understanding of the electrophysiological response of rat ventricular myocytes to exercise as may occur in-vivo.

## 7.5 Conclusion

The mLR model is able to reliably (qualitatively, if not quantitatively) model the adult rat ventricular myocyte AP at a range of physiological frequencies at rest and during adrenergic stimulation and the model also demonstrates, in part, comparable ion

channel dynamics to the experimental findings of this study and existing literature. The incorporation of the full range of repolarising $K^+$ channels integral to rat ventricular myocyte AP repolarisation will improve the physiological relevance of the model overall and facilitate increased validity and translational impact. Future investigation of ion channel function at increased pacing frequencies and the development of reference values for the adrenergic response in AP variables and ion channel currents will also help to both improve and validate the mLR model, and will eventually allow more efficient study of unanswered questions related to ageing and diseased hearts.

# Chapter 8: Conclusions

## 8.1 Aims

Maximum HR during exercise and stress declines with advancing age and thus leads to a reduced exercise capacity or exercise intolerance (Stratton et al., 1992; Stratton et al., 1994; Feridooni et al., 2015; Ferrara et al., 2014). An age-related loss of $\beta_1$AR signalling efficiency or $\beta_1$AR desensitisation has been frequently suggested to be heavily involved in the loss of cardiac response to exercise associated with old age (Ferrara et al., 2014; Fleg et al., 1994; Fares and Howlett, 2010; De Lucia et al., 2018; Xiao et al., 1994). Early research investigated the differences between $\beta_1$AR expression and activity which yielded less than unanimous results (Abrass and Scarpace, 1981; Davies et al., 1996; Narayanan and Derby, 1982; Narayanan and Tuckler, 1986; White et al., 1994). The lack of clear evidence indicating $\beta_1$AR expression as the primary responsible component in the suggested loss of $\beta_1$AR signalling sensitivity / efficiency has subsequently led to increased interest in downstream components of this signalling cascade. As AP repolarisation controls myocyte activation and contraction (Bers, 2002; Pinnell et al., 2007) which may contribute to the loss in contractility in old age, many studies have investigated the age-related changes in APD and a body of evidence suggests APD is prolonged in old age (Feridooni et al., 2015; Liu et al., 2000; Capasso et al., 1983a; Walker et al., 1993), though comparatively less evidence exists regarding APD changes in response to adrenergic stimulation with age. Furthermore, very few studies in this area have been performed under physiological temperatures and at physiologically relevant HR and adrenergic stimulation. Similarly, studies in ion channels have predominantly reported on age-related remodelling of basal function and have been equally limited to non-physiologically relevant conditions and have rarely / never focused on their influence exerted on the myocyte AP and the response to conditions of emulated exercise. Bridging the above gaps in the potential remodelling of the AP and responsible ion channels in old age would go some way in improving our understanding of the underlying mechanisms contributing to the age-related loss in cardiovascular reserve and exercise capacity. However, such experiments, particularly those involving ion channels are technically very difficult to perform and thus highlight the potential need

/ use for computational modelling. However the most relevant rat electrophysiological cardiac computational model (Gattoni et al., 2016) is limited to pacing frequencies ≤ 6 Hz, which in the rat, represents a HR approximately equivalent to – or moderately above – resting basal function (~ 240 bpm) (Carnevali and Sgoifo, 2014; Farmer and Levy, 1968). A computational rat model enabling pacing at frequencies above 6 Hz, towards rates that more closely align with those attained during exercise (~ 480 – 600 bpm) (Brooks and White, 1978; Bolter and Atkinson, 1988; Barnard et al., 1974; Wisløff et al., 2001) would help to better understand electrophysiological changes occurring across the full range of physiologically relevant rates and lay the foundation for the more effective study of cardiac ageing.

Therefore the aims of this work were: 1) to assess the influence of age on AP form and response of ventricular myocytes to adrenergic stimulation. 2) To investigate key components of the AP that may be responsible for the duration of the AP and thus set minimal stable cycle length of the heart during exercise. 3) To further develop and use a computational electrophysiological rat heart model recently developed in our lab to test the relative influence of observed changes in ionic currents along with those documented by others with the view to facilitate the future generation of an aged heart model capable of recreating the AP and AP response to adrenergic stimulation observed in this work and others.

## 8.2 Summary of Results

The work in chapter 3 revealed $APD_{90}$ was significantly prolonged in old compared with adult rat ventricular myocytes. Despite the existence of a trend towards an age-related prolongation in other components related to late AP repolarisation ($APD_{75}$ and $APD_{100}$) alongside a trend toward an age-related blunting of isoproterenol-induced $APD_{50\text{-}75}$ shortening in old rat ventricular myocytes, the prolongation in $APD_{90}$ in old rat hearts remained the only statistically significant difference between adult and old rats. Elsewhere, independent of age and pacing frequency, adrenergic stimulation was displayed to significantly shorten AP plateau and late AP repolarisation, whilst diastolic membrane potential became more negative in rat ventricular myocytes. With increased pacing frequency, APD was observed to prolong until 6 Hz, where AP plateau and late AP repolarisation shortened. However, this effect was observed in $APD_{50\text{-}75}$ only during adrenergic stimulation, whilst later in the AP ($APD_{90\text{-}100}$) the

effect was observed independent of adrenergic stimulation. Furthermore, AP amplitude and upstroke velocity were found to decline during increased pacing, though the addition of adrenergic stimulation appeared to offset, to some extent, the decline in AP amplitude at 6 Hz.

In chapters 4 – 6, ion channels responsible for modulating AP repolarisation and potentially also responsible, in part, for the age-related prolongation in APD and the inability to maintain rates > 6 Hz found in chapter 3 alongside the loss of exercise capacity in old age through a reported loss in adrenergic signalling sensitivity in literature (Feridooni et al., 2015; Ferrara et al., 2014), were investigated in adult and old rat ventricular myocytes during basal conditions as well as conditions of adrenergic stimulation.

The work in chapter 4 revealed no statistically significant changes in LTCC current during basal and adrenergic stimulation conditions between adult and old rat ventricular myocytes. However ventricular myocytes from old rat hearts showed a trend toward reduced LTCC current during basal and adrenergic stimulation conditions compared with ventricular myocytes from adult rat hearts.

In chapter 5, the influence of chromanol 293b-sensitive current on AP repolarisation in adult and old rat ventricular myocytes was investigated using current-clamp. The results of these current-clamp investigations found, independent of age, the influence of chromanol 293b-sensitive current on late AP repolarisation ($APD_{75}$ and $APD_{100}$) was greater during adrenergic stimulation than basal conditions. In adult rat ventricular myocytes, the influence of chromanol 293b-sensitive current on $APD_{90}$ was significantly greater during adrenergic stimulation compared with control conditions, whilst the influence of chromanol 293b-sensitive current on $APD_{90}$ in old rat ventricular myocytes yielded no difference between control and adrenergic stimulation conditions. Conversely, no significant ageing effects were identified between the influences of chromanol 293b-sensitive current on APD in adult and old rat ventricular myocytes during control conditions, though a trend toward greater chromanol 293b-sensitive current influence on $APD_{50}$ in old rats existed.

In chapter 6, building on the work in chapter 5, onion peeling – an AP-clamp technique developed relatively recently (Banyasz et al., 2011; Banyasz et al., 2014) – was used to identify chromanol 293b-sensitive current during stimulation by a self-AP during

control and adrenergic stimulation conditions, this time alongside other currents contributing to AP repolarisation ($I_{Kr}$ and $I_{K1}$) in adult and old rat ventricular myocytes. The results of this work displayed peak chromanol 293b-sensitive, $I_{Kr}$ and $I_{K1}$ currents were similar between adult and old rats, though old rats displayed a trend towards reduced peak chromanol 293b-sensitive current, particularly during adrenergic stimulation. However, significant reductions were yielded in chromanol 293b-sensitive integral current and chromanol 293b-sensitive current at -20 mV and $APD_{90}$ in old rats compared with adult rats during control conditions. Similarly $I_{K1}$ integral current and $I_{K1}$ current at $APD_{90}$ and $APD_{95}$ were also reduced in old rats. Independent of ageing, $I_{K1}$ integral current reduced during adrenergic stimulation. Meanwhile, chromanol 293b-sensitive integral current and chromanol 293b-sensitive current at $APD_{90}$ and $APD_{95}$ increased during adrenergic stimulation in adult rats only, which contributed to the observed reduction in chromanol 293b-sensitive integral current and chromanol 293b-sensitive current at $APD_{95}$ in old compared with adult rat ventricular myocytes during adrenergic stimulation. In contrast, $I_{Kr}$ integral current and $I_{Kr}$ current at 20 mV, 0 mV and -20 mV reduced in response to adrenergic stimulation in adult rat ventricular myocytes only, which contributed to the increased $I_{Kr}$ integral current and $I_{Kr}$ current at 20 mV, 0 mV and -20 mV recorded in old compared with adult rat ventricular myocytes during adrenergic stimulation.

Finally in chapter 7, the results obtained from chapters 3 – 6 and from previous work (Howlett et al., 2022) were used to further develop a computational rat AP model recently developed within our laboratory (Stevenson-Cocks, 2019) and provide data for comparison to model simulations, of which the outcomes were compared with existing literature. In this work, the mLR model appeared to model $APD_{50}$ and $APD_{90}$ data within the 95 % confidence interval of experimental data at a range of physiological pacing rates and also appeared to model the $APD_{50}$ and $APD_{90}$ response to adrenergic stimulation within the 95 % confidence interval of experimental data at almost all pacing frequencies investigated. Moreover, the mLR model reproduced peak LTCC current and peak $I_{K1}$ current within the 95 % confidence interval of experimental data and also modelled a similar balance between $I_{Ks}$ and $I_{Kr}$ currents to the chromanol 293b-sensitive and $I_{Kr}$ current findings from our experimental data. Furthermore, the mLR model produced peak $I_{Kr}$ and $I_{K1}$ current responses to adrenergic stimulation within the 95 % interval of experimental data.

## 8.3 Limitations

Every effort was made throughout this project to reduce limitations and curtail any potential effects on the outcomes of this study, however, some inevitably remained.

The overall age-related changes observed throughout this study apply to rat ventricular myocytes aged 3 months of age compared with 22 - 23 months of age only and subsequently provide limited insight toward the trajectory of ageing and subsequent remodelling that may occur along the way. Equally, the age-related inferences made in this study do not consider the extent of ageing and no age-related biomarkers were monitored to make inferences regarding instances of accelerated biological ageing. Furthermore, all electrophysiological data was obtained from a randomised sample from a homogeneous pool of ventricular myocytes and therefore may be influenced by the widely known heterogeneity of cardiac myocytes.

In chapters 3 – 6, as a result of COVID-19 laws and guidelines, the duration between rat sacrifice and the installation of the heart to the Langendorff rig was prolonged in old rats compared with adult rats. However, such delays were typically limited to 2 – 3 minutes whereby the heart was maintained on ice and in cardioplegic solution.

In addition, in chapters 3 – 7, the experimental solutions contained EGTA, a $Ca^{2+}$ buffer. Although the use of EGTA is prevalent in many similar studies like ours, to help facilitate stability during patch-clamping, EGTA affects normal physiological $Ca^{2+}$ buffering and in turn is potentially capable of impacting (through $Ca^{2+}$-related processes) AP repolarisation.

Notably, as discussed in chapter 3, one study which reported similar rate-dependent changes in rat ventricular myocyte APD during whole-cell patch-clamp experiments later found in the same study such rate-dependent APD prolongations with increases in pacing frequency from 0.2 – 5 Hz, were not exhibited during similar investigations performed using sharp electrophysiological techniques (Shigematsu et al., 1997). This may infer that different results from the overall work in these chapters may be yielded without intracellular $Ca^{2+}$ chelation and therefore should be considered when interpreting the experimental findings laid out in chapter 3 – 6 as well as chapter 7 since these experimental findings, in part, contributed to the development of the mLR model. However, in mitigation, it is unlikely that rat ventricular myocytes could have

sustained such high pacing frequencies during the patch-clamp recordings throughout this work without intracellular $Ca^{2+}$ chelation, a vital component of this project which helps map the age-related changes in electrophysiological response to $\beta_1$AR signalling.

In Chapter 4 the aim of the study was to investigate age-related changes in peak LTCC current in rat ventricular myocytes and their response to adrenergic stimulation and therefore the results cannot make direct inferences regarding LTCC kinetics and overall coupling to contractility. This was outside of the scope of this particular experiment and relies on existing literature to provide wider context relating to these components. Unfortunately, planned experiments pertaining to such components were impaired as a result of the COVID-19 pandemic. In addition, the LTCC current fluxes recorded in chapter 4 were derived from a voltage protocol alone without the use of pharmacology to block the LTCC current and therefore may have been influenced by the flow of other currents along the way.

In chapters 4 – 6, the ion current fluxes measured in adult and old rat ventricular myocytes during basal and adrenergic stimulation conditions provide insight to age-related changes at 1 Hz pacing and thus do not reveal direct information relating to the age-related changes during physiological pacing frequencies.

As previously mentioned throughout this work, the potential off-target blocking of other ion channels with the use of chromanol 293b, E4031 and $BaCl_2$ are important considerations for the interpretation and potential translation of findings laid out in chapters 5 – 7. At the chromanol 293b dose used throughout this work, research indicates chromanol 293b-sensitive current and its influence on AP repolarisation may be attributed to $I_{Ks}$, $I_{to}$ and $I_{Kur}$ currents as opposed to $I_{Ks}$ current alone (Du et al., 2003; Sun et al., 2001; Árpádffy-Lovas et al., 2022; Bosch et al., 1998). In addition, the noted $I_{Kr}$ current recording difficulty in this work and existing research (Wang and Fitts, 2020), as well as the documented potential deviations in understood $I_{K1}$ current characteristics displayed in example recordings in chapter 6 (figure 25 B), the lack of supplementary experiments to confirm with absolute certainty the recording of individual $I_{Kr}$ and $I_{K1}$ as well as $I_{Ks}$ currents should be taken into account when interpreting the findings in chapter 6. Therefore the patch-clamp recordings from this work alone are likely insufficient to reliably and accurately determine the individual

influences of $I_{Ks}$ current and also highlights the increased difficulty in the interpretation of $I_{Kr}$ and $I_{K1}$ current findings and the overall need for the performance of further experiments using additional $K^+$ blockers or a more selective $I_{Ks}$ blocker. Though the chromanol 293b-sensitive current recordings in particular – alongside $I_{Kr}$ and $I_{K1}$ current recordings - demonstrated in this work indeed potentially highlight the remodelling of repolarising $K^+$ channels in the rat ventricular myocyte, their influence on AP repolarisation and their coupling to $\beta_1$AR signalling.

Regarding chapter 7, the gold standard method of model validation consists of comparison to datasets not involved in model development. However, the experimental findings in this study provide novel findings in adult rat ventricular myocytes at a range of physiologically relevant pacing frequencies with and without adrenergic stimulation, which has been lacking previously in the literature. Therefore, the gold standard method could not be adopted. Moreover, although simulated ion channel fluxes at higher frequencies appear plausible, very little reference data currently exists to provide comparison or aid model validation. Similarly, the lack of APD data in the literature at pacing frequencies greater than 1 Hz increases the difficulty of comparison and model validation. In addition, ion channel fluxes simulated by the mLR model were predominantly compared with data recorded at lower frequencies during voltage-clamp trials and therefore are unable to provide accurate direct comparison to currents simulated at 1 Hz pacing or greater. Furthermore, whilst every effort was made to replicate the experimental set up in the mLR model, certain components could not be matched, such as the intracellular pipette contents, which may have influenced the simulated APD through alterations in $K^+$ content and $Ca^{2+}$ buffering.

Further limitations regarding the work in chapter 7 are related to the omission of key repolarising $K^+$ currents and the impact of $K^+$ blocker selectivity on the experimental findings used, in part, in the development of the mLR model. Essentially, the substitution of $I_{ss}$ for $I_{Ks}$ and $I_{Kr}$ and the lack of $I_{Kur}$ in the mLR model may impair the physiological relevance of findings regarding AP repolarisation and ion channel currents from mLR simulations given the that $I_{ss}$ is understood to be distinct from other recognised $K^+$ currents alongside the significant role of $I_{ss}$ and $I_{Kur}$ currents in rat ventricular myocyte AP repolarisation (Choisy et al., 2004; Sakatani et al., 2006; Himmel et al., 1999; Árpádffy-Lovas et al., 2022). This, coupled with the explained

potential for off-target blocking of E4031 and $BaCl_2$ and particularly chromanol 293b during experiments in chapter 6, later used for mLR model development may influence the translational value of model ion flux findings due to the increased difficulty of identifying changes in individual repolarising currents and their influence on the AP without further work / model development (Du et al., 2003; Sun et al., 2001; Árpádffy-Lovas et al., 2022; Bosch et al., 1998). Though, these limitations reflect important considerations and highlight the need for further experimental studies (to provide necessary data) as well as the need for model development based on existing data where all currents should be incorporated, the model as it stands is novel and does at least qualitatively simulate AP data comparable to our studies and available existing literature at high rates under control and adrenergic stimulation conditions. Similarly the model is able to provide some potential insight to the overall $K^+$ current changes that may underly rat AP responses to $\beta_1$AR signalling in adult rat ventricular myocytes. Though to be a truly valid adult rat electrophysiological model, it must resemble to a high degree the physiological environment of the rat heart for the outcomes to be both meaningful and easily transferable in the wider context of the field.

Finally, the translational value of the findings of this work in its entirety to the ageing phenomenon in humans should be considered. Rat models have been commonly used in studies focusing on cardiac remodelling with advancing age as the age-related prolongation of AP repolarisation in general is a conserved phenomenon observed across species and also due to their relative low cost, greater availability and similar propensity for cardiac disorders as humans coupled with their relatively similar ion channel presence – though different in expression and influence – to humans, faster ageing and the ability for effective and easy comparison to existing evidence as a result of their extensive historical use (Josephson et al., 2002; Liu et al., 2000; Walker et al., 1993; Farrell and Howlett, 2008; Scarpace et al., 1991; Tobise et al., 1994; Narayanan and Derby, 1982; Olgar et al., 2022; Wang and Fitts, 2020; Joukar, 2021; Tellez et al., 2011; Huang et al., 2006; Feridooni et al., 2015; Gan et al., 2013; Liu et al., 2014; Waldeyer et al., 2009; Feridooni et al., 2017; Reardon and Malik, 1996; Rabkin et al., 2016). Though, due to the considerable differences in ventricular myocyte AP configuration between rats and humans explained in section 1.8, such as the differences in APD, repolarisation and cardiac reserve as well as the differences in ion channel existence, particularly those involved in repolarisation and the rate-dependent

changes in APD, the relevance of the outcomes of this study overall to humans is open to question currently and requires further study in larger species that more closely resemble the electrophysiological make-up and AP morphology in humans (Varró et al., 1993; Árpádffy-Lovas et al., 2022; Joukar, 2021; Regan et al., 2005; Pond et al., 2000; Tande et al., 1990).

## 8.4 Potential Applications and Future Study

The findings of this project provide novel reference APD data for adult and old rat ventricular myocytes at a range of pacing frequencies and doses of adrenergic stimulation, helping, in part, to map the rat heart response to (emulated) exercise as would occur in-vivo. The findings highlight the importance of late AP repolarisation in the age-related electrical remodelling of the heart but may create more questions regarding the age-related remodelling of $\beta_1$AR signalling in the heart and the response to exercise. In chapter 3, the APD response to adrenergic stimulation was maintained in old rat ventricular myocytes, but showed a trend toward a blunted isoproterenol-induced APD shortening. Whether the adrenergic response is maintained or significantly different between adult and old rat ventricular myocytes at pacing frequencies beyond 6 Hz, toward the peak of physiological rat HR range is unknown, though work in our lab indeed indicated a potential age-related limitation in that pacing old rat ventricular myocytes at the highest physiologically relevant pacing frequencies was extremely difficult / not possible (on this occasion with our methods).

Furthermore, briefly, the ion channel investigations of this work suggest that peak LTCC, chromanol 293b-sensitive, $I_{Kr}$ and $I_{K1}$ current are maintained in old rat ventricular myocytes. However, it is clear that other measures of ion current flux and the influence they have on APD are significantly altered with ageing, especially during adrenergic stimulation. Overall the ion channel results of this study may help to understand the changes observed in chapter 3, however differences in activation frequency may limit direct understanding to APD findings at lower pacing frequencies, though still provide insight to the complex electrophysiological remodelling that occurs with ageing in the heart.

The inability, at the myocyte level, of the old rat heart to follow high pacing rates may indicate that the inability to achieve a high HR in old age is not simply due to conduction issues or limitations within pacemaker and nodal tissues (Larson et al.,

2013; Christou and Seals, 2008) and is indeed significantly contributed to by electrophysiological changes in ventricular myocytes and their responses to adrenergic signalling. Furthermore, though statistically significant reductions in APD response to adrenergic signalling were not found in chapter 3, the noted trends toward an age-related blunting of APD response to adrenergic stimulation coupled with the significant main ageing effect on overall $APD_{90}$ between adult and old rats may suggest a loss of efficacy of $\beta_1$AR signalling at least partially contributes to the prolongation of late AP repolarisation and the limitation in myocyte repolarisation reserve and in turn cardiac reserve as previously postulated in the literature (Ferrara et al., 2014; Fleg et al., 1994; Fares and Howlett, 2010; De Lucia et al., 2018; Xiao et al., 1994). The changes in APD observed throughout this study with ageing appear to be heavily contributed to by repolarising $K^+$ current flux, particularly chromanol 293b-sensitive current flux, its balance with LTCC current, and its activation through adrenergic stimulation. Though, without further study, it is unclear how important these $K^+$ channels are to the prolongation of APD throughout the entire range of physiological pacing frequencies. Equally, without further confirmatory experiments to reliably identify the impact of individual $I_{Ks}$, alongside $I_{Kr}$ and $I_{K1}$ current and without the study of other ion channels contributing to AP repolarisation such as $I_{to}$, $I_{Kur}$, NCX and intracellular $Ca^{2+}$, the exact intricacies of how myocytes modulate AP repolarisation differently in old compared with adult hearts is not completely clear.

It may be that the prolongation of APD is a result of the combination of maintained LTCC current and reduced chromanol 293b-sensitive and $I_{K1}$ flux found in this study and slowed LTCC inactivation reported in previous studies (Herraiz et al., 2013; Josephson et al., 2002; Liu et al., 2000; Walker et al., 1993), whereby increased net $Ca^{2+}$ entry and reduced net outward $K^+$ current extend AP plateau somewhat and extend late repolarisation to a greater extent respectively. However this remodelling does not typically impact global cardiac function under basal / control conditions. Meanwhile, the presence of stress or the participation in exercise (particularly at more vigorous intensities) may potentiate the effects of these age-related electrophysiological decrements and facilitates, in part, the limitation of repolarisation reserve. Moreover, the age-related loss in chromanol 293b-sensitive current response to $\beta_1$AR signalling may considerably exacerbate the impairment of repolarisation reserve during exercise / stress through its reduced ability to tip the balance of inward

and outward current flux in the favour of faster repolarisation as would normally occur in young healthy individuals via current accumulation resulting from its slow inactivation and efficient activation via adrenergic signalling (Ravens and Wettwer, 1998; Jost et al., 2007). This means at higher intensities, the ability of myocytes to abbreviate APD in line with briefer diastolic intervals is considerably diminished and may indeed translate to global contractile limitations and the subsequent loss of exercise tolerance and potentially increased arrhythmia risk / vulnerability to cardiac events in old age (Jost et al., 2007).

The electrophysiological remodelling observed in this work may have some clinical implications for the elderly general population undertaking exercise training, due to the increased vulnerability to cardiac events and arrhythmogenesis as a result of the age-related limitations on AP repolarisation at higher HR and the deterioration of the cardioprotective impact normally provided by $I_{Ks}$ during stress / exercise coupled with the likely impact of reduced QT interval stability (Jost et al., 2007). Though further experiments are required to confirm the extent to which changes in $I_{Ks}$ might be responsible for the age-related decrease in chromanol 293b-sensitive current and its response to $\beta_1$AR signalling in old age reported in this study. Equally, perhaps more seriously, this work may have clinical implications for elderly patients taking anti-arrhythmic drugs, such as dofetilide and quinidine, as the age-related remodelling of $K^+$ channels and $\beta_1$AR signalling may influence the effectiveness of the drug action particularly during exercise or stress (Yang et al., 2003) and trigger worsening symptoms, drug-related side effects and increase risk of cardiac events especially as the impairment / block of more than one $K^+$ channel has been suggested to cause excessive changes in myocyte repolarisation (Biliczki et al., 2002).

Focusing on therapeutic strategies that involve the potential rejuvenation of components key to $\beta_1$AR signalling and general cellular electrophysiological function may help tackle the cardiac ageing phenomenon. Studies have shown adrenergic sensitivity can be restored to some level through exercise training and / or pharmacology (Roh et al., 2016; Spina et al., 1998; Leosco et al., 2008). Restoring adrenergic sensitivity has been shown to blunt age-related cardiac decrements and even restore (to some extent) previous losses (Roh et al., 2016; Spina et al., 1998), though further study is required. Interestingly, recent research has found antagonism of the $\beta_2$AR is capable of reversing the age-related reduction in $I_{Ks}$ current during

adrenergic stimulation in guinea pigs (Zou et al., 2021), though it is currently unclear if the same effect occurs in other animals.

Taken together, this work will provide a reference point for future electrophysiological studies similarly investigating age-related remodelling or alternatively, studies focusing on translation to humans or studies focusing on the impact of gender or disease. Equally, as per chapter 7, the findings of this work will help the development and potential validation of computational electrophysiological rat heart models and will be specifically used to once more modify the mLR model (Stevenson-Cocks, 2019) with the ambition to develop a comparative old rat computational model to the adult model involved in chapter 7, capable of reliably simulating APD and its response to emulated exercise.

As mentioned previously, further experiments utilising a more specific $I_{Ks}$ blocker or simply additional $K^+$ blockers to exclude any interference by $I_{to}$ and $I_{Kur}$ are necessary to supplement the outcomes of this study and help to determine the level of $I_{Ks}$ influence in the chromanol 293b-sensitive current findings demonstrated in this work and in turn determine the magnitude of its potential role in the age-related loss in cardiac response to exercise. Similarly, once more, additional experiments using voltage-clamp modalities to reliably and accurately determine $I_{Kr}$ and $I_{K1}$ measurement in the E4031-sensitive and $BaCl_2$-sensitive current recordings shown in this work and also determine $I_{Kr}$ and $I_{K1}$ involvement in rat ventricular myocyte AP repolarisation and in turn, the ageing phenomenon. Future investigation of age-related changes in LTCC and its response to $\beta_1$AR signalling utilising conditions that are more favourable for triggering a significant adrenergic response as shown in the literature, as well as utilising more selective recording conditions which also incorporate the analysis of channel kinetics are warranted to better understand the age-related remodelling underlying the loss of cardiac response to exercise in old age.

Future similar studies incorporating the investigation of a number of ion channels, particularly those understood to be key to rat AP repolarisation such as $I_{to}$, $I_{ss}$ and $IK_{ur}$, as well as $Ca^{2+}$ cycling, using physiologically relevant pacing frequencies would go some way toward improving the overall understanding of the cardiac electrophysiological adaptations and their translation to contractile limitations in old hearts particularly in response to exercise and will further facilitate the availability of

more robust computational models. Such experiments can be more effectively performed through the use of onion peeling (Banyasz et al., 2011; Banyasz et al., 2014) and have the additional benefit of a more physiologically relevant myocyte impulse stimulus.

Future studies utilising such AP-clamp techniques may also benefit from incorporation of a model / simulated steady-state human ventricular AP stimuli during recordings on rat ventricular myocytes. This set-up, referred to as "electrical transgenesis" may help improve the translational value of experimental outcomes through the analysis of ion channels activated over a time-course more aligned with human hearts and in turn provide greater insight into the electrophysiological remodelling that occurs in human ageing without the elevated difficulty of acquiring human ventricular tissue (Cooper et al., 2010).

Supplementing such future studies with structural investigations of key components involved in excitation-contraction coupling and $\beta_1$AR signalling will further help to improve the understanding of the cardiac ageing phenomenon and help toward identifying whether key age-related remodelling that leads to the limitation of the cardiac response to exercise in old age is influenced more greatly by alterations in: receptor / ion channel number, intrinsic / basal ion channel flux or the coupling of adrenergic signalling to ion channel flux.

Given the known heterogeneity of the cardiac AP, it may be that age-related remodelling is not uniform across the entire heart and even across ventricular regions, thus similar investigations to those in this work are required on different regions and layers of the heart. Improving understanding of the impact of ageing on the electrophysiological heterogeneity of the heart may help to identify specific therapeutic targets to combat the decrements associated with cardiac ageing and reduce arrythmia risk in old age.

Naturally, similar investigations to those in this study are required using whole-heart set-ups to understand the impact of myocyte changes with ageing on the wider electrical function of the heart, contextualising APD changes to changes in the ECG. More readily, the performance of similar experiments to those conducted in this study using ventricular tissue and sharp electrophysiological recording techniques as opposed to ventricular myocytes and whole-cell patch-clamp techniques may benefit

future investigation of the ageing phenomenon. For example, recording adult and old rat AP from intact ventricular muscle using sharp electrophysiological techniques may still allow observations across a reasonable range of pacing frequencies with and without adrenergic stimulation, though attenuating potential influences on AP repolarisation findings from cell dialysis with pipette contents – which allows for deviation from a physiological intracellular environment – and intracellular $Ca^{2+}$ chelation by EGTA. Equally, where possible, the utilisation of human tissue, or at least tissues that more closely resemble human electrophysiology, such as rabbit, pig or dog are required to help translate the findings laid out in this work and provide greater insight into cardiac ageing as typically demonstrated in humans.

Finally, further studies investigating the effect of non-pharmacological strategies such as exercise on the ageing heart are required to understand whether the cardiac response to exercise can be preserved or the age-related decline blunted with prior exercise or even restored with exercise training in old age and in turn the optimal method of exercise training required to achieve this. Similar studies using a combination of pharmacological intervention and non-pharmacological intervention are also required to determine the additive benefit or consequence of their combination on combatting / treating age-related cardiac deterioration.

# Chapter 9: References


Abete, P., Ferrara, N., Cioppa, A., Ferrara, P., Bianco, S., Calabrese, C., Napoli, C. and Rengo, F. 1996. The Role of Aging on the Control of Contractile Force by Na-Ca 2 Exchange in Rat Papillary Muscle. *Journal of Gerontology*. **51**(5), pp.M25I-M259.

Abrass, I.B., Davis, J.L. and Scarpace, P.J. 1982. Isoproterenol responsiveness and myocardial β-adrenergic receptors in young and old rats. *Journal of Gerontology*. **37**(2), pp.156-160.

Abrass, I.B. and Scarpace, P.J. 1981. Human lymphocyte beta-adrenergic receptors are unaltered with age. *Journal of gerontology*. **36**(3), pp.298-301.

Agostoni, P., Vignati, C., Gentile, P., Boiti, C., Stefania, M., Farina, M., Salvioni, E., Mapelli, M., Magrì, D. and Paolillo, S. 2017. Reference values for peak exercise cardiac output in healthy individuals.

Ahlquist, R.P. 1948. A study of the adrenotropic receptors. *American Journal of Physiology-Legacy Content*. **153**(3), pp.586-600.

Ai, X. 2015. SR calcium handling dysfunction, stress-response signaling pathways, and atrial fibrillation. *Frontiers in physiology*. **6**, p46.

Akashi, Y.J., Nef, H.M. and Lyon, A.R. 2015. Epidemiology and pathophysiology of Takotsubo syndrome. *Nature Reviews Cardiology*. **12**(7), p387.

Andersson, C. and Vasan, R.S. 2018. Epidemiology of cardiovascular disease in young individuals. *Nature Reviews Cardiology*. **15**(4), p230.

Armstrong, C.M. and Gilly, W.F. 1992. [5] Access resistance and space clamp problems associated with whole-cell patch clamping. *Methods in enzymology*. Elsevier, pp.100-122.

Árpádffy-Lovas, T., Mohammed, A.S.A., Naveed, M., Koncz, I., Baláti, B., Bitay, M., Jost, N., Nagy, N., Baczkó, I. and Virág, L. 2022. Species-dependent differences in the inhibition of various potassium currents and in their effects on repolarization in cardiac ventricular muscle. *Canadian Journal of Physiology and Pharmacology*. **100**(9), pp.880-889.

Attwell, D., Cohen, I. and Eisner, D. 1981. The effects of heart rate on the action potential of guinea-pig and human ventricular muscle. *The journal of physiology*. **313**(1), pp.439-461.

Banyasz, T., Horvath, B., Jian, Z., Izu, L.T. and Chen-Izu, Y. 2011. Sequential dissection of multiple ionic currents in single cardiac myocytes under action potential-clamp. *Journal of molecular and cellular cardiology.* **50**(3), pp.578-581.

Banyasz, T., Jian, Z., Horvath, B., Khabbaz, S., Izu, L.T. and Chen-Izu, Y. 2014. Beta-adrenergic stimulation reverses the I Kr–I Ks dominant pattern during cardiac action potential. *Pflügers Archiv-European Journal of Physiology.* **466**(11), pp.2067-2076.

Bao, L., Taskin, E., Foster, M., Ray, B., Rosario, R., Ananthakrishnan, R., Howlett, S.E., Schmidt, A.M., Ramasamy, R. and Coetzee, W.A. 2013. Alterations in ventricular KATP channel properties during aging. *Aging cell.* **12**(1), pp.167-176.

Barbieri, M., Varani, K., Cerbai, E., Guerra, L., Li, Q., Borea, P.A. and Mugelli, A. 1994. Electrophysiological basis for the enhanced cardiac arrhythmogenic effect of isoprenaline in aged spontaneously hypertensive rats. *Journal of molecular and cellular cardiology.* **26**(7), pp.849-860.

Barnard, R.J., Duncan, H.W. and Thorstensson, A.T. 1974. Heart rate responses of young and old rats to various levels of exercise. *Journal of applied physiology.* **36**(4), pp.472-474.

Barnes, R.F., Raskind, M., Gumbrecht, G. and Halter, J.B. 1982. The effects of age on the plasma catecholamine response to mental stress in man. *The Journal of Clinical Endocrinology & Metabolism.* **54**(1), pp.64-69.

Bébarová, M., Matejovic, P., Pásek, M., Simurdova, M. and Simurda, J. 2014. Dual effect of ethanol on inward rectifier potassium current IK1 in rat ventricular myocytes. *J Physiol Pharmacol.* **65**(4), pp.497-509.

Behar, J., Ganesan, A., Zhang, J. and Yaniv, Y. 2016. The autonomic nervous system regulates the heart rate through cAMP-PKA dependent and independent coupled-clock pacemaker cell mechanisms. *Frontiers in physiology.* **7**, p419.

Behar, J. and Yaniv, Y. 2017. Age-related pacemaker deterioration is due to impaired intracellular and membrane mechanisms: Insights from numerical modeling. *The Journal of general physiology.* **149**(10), pp.935-949.

Bers, D.M. 2002. Cardiac excitation–contraction coupling. *Nature.* **415**(6868), p198.

Biliczki, P., Virág, L., Iost, N., Papp, J.G. and Varró, A. 2002. Interaction of different potassium channels in cardiac repolarization in dog ventricular preparations: role of repolarization reserve. *British journal of pharmacology.* **137**(3), pp.361-368.

Bolter, C.P. and Atkinson, K.J. 1988. Maximum heart rate responses to exercise and isoproterenol in the trained rat. *American Journal of Physiology-Regulatory, Integrative and Comparative Physiology.* **254**(5), pp.R834-R839.

Bosch, R.F., Gaspo, R., Busch, A.E., Lang, H.J., Li, G.-R. and Nattel, S. 1998. Effects of the chromanol 293B, a selective blocker of the slow, component of the delayed rectifier K+ current, on repolarization in human and guinea pig ventricular myocytes. *Cardiovascular research.* **38**(2), pp.441-450.

Bouchard, R., Clark, R.B., Juhasz, A.E. and Giles, W.R. 2004. Changes in extracellular K+ concentration modulate contractility of rat and rabbit cardiac myocytes via the inward rectifier K+ current IK1. *The Journal of physiology.* **556**(3), pp.773-790.

Boyden, P.A., Hirose, M. and Dun, W. 2010. Cardiac Purkinje cells. *Heart Rhythm.* **7**(1), pp.127-135.

Boyett, M.R., Honjo, H. and Kodama, I. 2000. The sinoatrial node, a heterogeneous pacemaker structure. *Cardiovascular research.* **47**(4), pp.658-687.

Brodland, G.W. 2015. How computational models can help unlock biological systems. In: *Seminars in cell & developmental biology*: Elsevier, pp.62-73.

Brooks, G.A. and White, T.P. 1978. Determination of metabolic and heart rate responses of rats to treadmill exercise. *Journal of applied physiology.* **45**(6), pp.1009-1015.

Canepari, M., Polla, B., Gualea, M., Zanardi, C. and Reggiani, C. 1994. Age-dependent reduction of the response of rat cardiac muscle to the phosphodiesterase inhibitor milrinone. *Archives internationales de physiologie, de biochimie et de biophysique.* **102**(5), pp.265-269.

Capasso, J., Malhotra, A., Remily, R., Scheuer, J. and Sonnenblick, E. 1983a. Effects of age on mechanical and electrical performance of rat myocardium. *American Journal of Physiology-Heart and Circulatory Physiology.* **245**(1), pp.H72-H81.

Capasso, J., Remily, R. and Sonnenblick, E. 1983b. Age-related differences in excitation-contraction coupling in rat papillary muscle. *Basic research in cardiology.* **78**(5), pp.492-504.

Carmeliet, E. 2006. Action potential duration, rate of stimulation, and intracellular sodium. *Journal of cardiovascular electrophysiology.* **17**, pp.S2-S7.

Carnevali, L. and Sgoifo, A. 2014. Vagal modulation of resting heart rate in rats: the role of stress, psychosocial factors, and physical exercise. *Frontiers in physiology.* **5**, p118.

Carter, J.B., Banister, E.W. and Blaber, A.P. 2003. The effect of age and gender on heart rate variability after endurance training. *Medicine & Science in Sports & Exercise.* **35**(8), pp.1333-1340.

Cerbai, E., Barbieri, M., Li, Q. and Mugelli, A. 1994. Ionic basis of action potential prolongation of hypertrophied cardiac myocytes isolated from hypertensive rats of different ages. *Cardiovascular research.* **28**(8), pp.1180-1187.

Cheah, L.-T. and Lancaster, M.K. 2015a. Age-associated Reductions in Junctophilin-2 and Amphiphysin-2 Associate With Disruption of T-tubules and Intracellular Calcium Regulation in Myocytes From the Mouse Left Ventricle. *Circulation.* **132**(suppl_3), pp.A13130-A13130.

Cheah, L.-t. and Lancaster, M.K. 2015b. Age-associated Reductions in Junctophilin-2 and Amphiphysin-2 Associate With Disruption of T-tubules and Intracellular Calcium Regulation in Myocytes From the Mouse Left Ventricle. *Circulation.* **132**(Suppl_3), pA13130.

Cheitlin, M. 2003. Cardiovascular physiology-changes with aging. *The American journal of geriatric cardiology.* **12**(1), p9.

Chen-Izu, Y., Izu, L.T., Nanasi, P.P. and Banyasz, T. 2012. From action potential-clamp to 'onion-peeling'technique–recording of ionic currents under physiological conditions. *Patch Clamp Technique.* pp.143-162.

Chen-Izu, Y., Xiao, R.-P., Izu, L.T., Cheng, H., Kuschel, M., Spurgeon, H. and Lakatta, E.G. 2000. Gi-dependent localization of β2-adrenergic receptor signaling to L-type Ca2+ channels. *Biophysical Journal.* **79**(5), pp.2547-2556.

Chen, B., Li, Y., Jiang, S., Xie, Y.-P., Guo, A., Kutschke, W., Zimmerman, K., Weiss, R.M., Miller, F.J. and Anderson, M.E. 2012. β-Adrenergic receptor antagonists ameliorate myocyte T-tubule remodeling following myocardial infarction. *The FASEB Journal.* **26**(6), pp.2531-2537.

Chen, L. and Kass, R.S. 2011. A-kinase anchoring protein 9 and IKs channel regulation. *Journal of cardiovascular pharmacology.* **58**(5), p459.

Chiamvimonvat, N., Chen-Izu, Y., Clancy, C.E., Deschenes, I., Dobrev, D., Heijman, J., Izu, L., Qu, Z., Ripplinger, C.M. and Vandenberg, J.I. 2017. Potassium currents in

the heart: functional roles in repolarization, arrhythmia and therapeutics. *The Journal of physiology.* **595**(7), pp.2229-2252.

Choisy, S.C., Hancox, J.C., Arberry, L.A., Reynolds, A.M., Shattock, M.J. and James, A.F. 2004. Evidence for a novel K+ channel modulated by α1A-adrenoceptors in cardiac myocytes. *Molecular pharmacology.* **66**(3), pp.735-748.

Chouabe, C., Ricci, E., Amsellem, J., Blaineau, S., Dalmaz, Y., Favier, R., Pequignot, J.-M. and Bonvallet, R. 2004. Effects of aging on the cardiac remodeling induced by chronic high-altitude hypoxia in rat. *American Journal of Physiology-Heart and Circulatory Physiology.* **287**(3), pp.H1246-H1253.

Choudhury, M., Boyett, M.R. and Morris, G.M. 2015. Biology of the sinus node and its disease. *Arrhythmia & electrophysiology review.* **4**(1), p28.

Christou, D.D. and Seals, D.R. 2008. Decreased maximal heart rate with aging is related to reduced β-adrenergic responsiveness but is largely explained by a reduction in intrinsic heart rate. *Journal of applied physiology.* **105**(1), pp.24-29.

Clark, R., Bouchard, R., Salinas-Stefanon, E., Sanchez-Chapula, J. and Giles, W. 1993. Heterogeneity of action potential waveforms and potassium currents in rat ventricle. *Cardiovascular research.* **27**(10), pp.1795-1799.

Colman, M.A. 2019. Arrhythmia mechanisms and spontaneous calcium release: Bi-directional coupling between re-entrant and focal excitation. *PLoS computational biology.* **15**(8), pe1007260.

Colman, M.A., Pinali, C., Trafford, A.W., Zhang, H. and Kitmitto, A. 2017. A computational model of spatio-temporal cardiac intracellular calcium handling with realistic structure and spatial flux distribution from sarcoplasmic reticulum and t-tubule reconstructions. *PLoS computational biology.* **13**(8), pe1005714.

Cooper, P.J., Soeller, C. and Cannell, M.B. 2010. Excitation–contraction coupling in human heart failure examined by action potential clamp in rat cardiac myocytes. *Journal of molecular and cellular cardiology.* **49**(6), pp.911-917.

Crumbie, H.E. 2016. *Beta-adrenergic receptor signalling and excitation-contraction coupling in the heart: impact of circadian rhythms and beta-3 receptors*. thesis, University of Leicester.

Davies, C., Ferrara, N. and Harding, S. 1996. β-Adrenoceptor function changes with age of subject in myocytes from non-failing human ventricle. *Cardiovascular research.* **31**(1), pp.152-156.

De Lucia, C., Eguchi, A. and Koch, W.J. 2018. New insights in cardiac β-adrenergic signaling during heart failure and aging. *Frontiers in pharmacology*. **9**, p904.

Dibb, K., Eisner, D. and Trafford, A. 2007. Regulation of systolic [Ca2+] i and cellular Ca2+ flux balance in rat ventricular myocytes by SR Ca2+, L-type Ca2+ current and diastolic [Ca2+] i. *The Journal of physiology*. **585**(2), pp.579-592.

Ding, W.G., Toyoda, F. and Matsuura, H. 2002. Blocking action of chromanol 293B on the slow component of delayed rectifier K+ current in guinea-pig sino-atrial node cells. *British journal of pharmacology*. **137**(2), pp.253-262.

Du, X.-L., Lau, C.-P., Chiu, S.-W., Tse, H.-F., Gerlach, U. and Li, G.-R. 2003. Effects of chromanol 293B on transient outward and ultra-rapid delayed rectifier potassium currents in human atrial myocytes. *Journal of molecular and cellular cardiology*. **35**(3), pp.293-300.

Dun, W. and Boyden, P.A. 2008. The Purkinje cell; 2008 style. *Journal of molecular and cellular cardiology*. **45**(5), pp.617-624.

Endoh, M. 2004. Force–frequency relationship in intact mammalian ventricular myocardium: physiological and pathophysiological relevance. *European journal of pharmacology*. **500**(1-3), pp.73-86.

Fares, E. and Howlett, S.E. 2010. Effect of age on cardiac excitation–contraction coupling. *Clinical and Experimental Pharmacology and Physiology*. **37**(1), pp.1-7.

Farmer, J. and Levy, G. 1968. A simple method for recording the electrocardiogram and heart rate from conscious animals. *British Journal of Pharmacology and Chemotherapy*. **32**(1), pp.193-200.

Farrell, S.R. and Howlett, S.E. 2007. The effects of isoproterenol on abnormal electrical and contractile activity and diastolic calcium are attenuated in myocytes from aged Fischer 344 rats. *Mechanisms of ageing and development*. **128**(10), pp.566-573.

Farrell, S.R. and Howlett, S.E. 2008. The age-related decrease in catecholamine sensitivity is mediated by ß1-adrenergic receptors linked to a decrease in adenylate cyclase activity in ventricular myocytes from male Fischer 344 rats. *Mechanisms of ageing and development*. **129**(12), pp.735-744.

Fauconnier, J., Bedut, S., Le Guennec, J.-Y., Babuty, D. and Richard, S. 2003. Ca2+ current-mediated regulation of action potential by pacing rate in rat ventricular myocytes. *Cardiovascular research*. **57**(3), pp.670-680.

Fauconnier, J., Lacampagne, A., Rauzier, J.-M., Vassort, G. and Richard, S. 2005. Ca2+-dependent reduction of IK1 in rat ventricular cells: a novel paradigm for arrhythmia in heart failure? *Cardiovascular research.* **68**(2), pp.204-212.

Feridooni, H., Kane, A., Ayaz, O., Boroumandi, A., Polidovitch, N., Tsushima, R., Rose, R. and Howlett, S. 2017. The impact of age and frailty on ventricular structure and function in C57BL/6J mice. *The Journal of physiology.* **595**(12), pp.3721-3742.

Feridooni, H.A., Dibb, K.M. and Howlett, S.E. 2015. How cardiomyocyte excitation, calcium release and contraction become altered with age. *Journal of molecular and cellular cardiology.* **83**, pp.62-72.

Ferrara, N., Komici, K., Corbi, G., Pagano, G., Furgi, G., Rengo, C., Femminella, G.D., Leosco, D. and Bonaduce, D. 2014. β-adrenergic receptor responsiveness in aging heart and clinical implications. *Frontiers in physiology.* **4**, p396.

Ferrucci, L., Cooper, R., Shardell, M., Simonsick, E.M., Schrack, J.A. and Kuh, D. 2016. Age-related change in mobility: perspectives from life course epidemiology and geroscience. *Journals of Gerontology Series A: Biomedical Sciences and Medical Sciences.* **71**(9), pp.1184-1194.

Fields, L.A., Koschinski, A. and Zaccolo, M. 2016. Sustained exposure to catecholamines affects cAMP/PKA compartmentalised signalling in adult rat ventricular myocytes. *Cellular signalling.* **28**(7), pp.725-732.

Fink, M., Niederer, S.A., Cherry, E.M., Fenton, F.H., Koivumäki, J.T., Seemann, G., Thul, R., Zhang, H., Sachse, F.B. and Beard, D. 2011. Cardiac cell modelling: observations from the heart of the cardiac physiome project. *Progress in biophysics and molecular biology.* **104**(1-3), pp.2-21.

Fink, M.A., Zakhary, D.R., Mackey, J.A., Desnoyer, R.W., Apperson-Hansen, C., Damron, D.S. and Bond, M. 2001. AKAP-mediated targeting of protein kinase a regulates contractility in cardiac myocytes. *Circulation research.* **88**(3), pp.291-297.

Flaatten, H., Skaar, E. and Joynt, G.M. 2018. Understanding cardiovascular physiology of ageing. *Intensive care medicine.* **44**(6), pp.932-935.

Fleg, J.L., O'connor, F., Gerstenblith, G., Becker, L., Clulow, J., Schulman, S.P. and Lakatta, E. 1995. Impact of age on the cardiovascular response to dynamic upright exercise in healthy men and women. *Journal of Applied Physiology.* **78**(3), pp.890-900.

Fleg, J.L., Schulman, S., O'Connor, F., Becker, L.C., Gerstenblith, G., Clulow, J.F., Renlund, D.G. and Lakatta, E.G. 1994. Effects of acute β-adrenergic receptor blockade

on age-associated changes in cardiovascular performance during dynamic exercise. *Circulation.* **90**(5), pp.2333-2341.

Fleg, J.L., Tzankoff, S.P. and Lakatta, E.G. 1985. Age-related augmentation of plasma catecholamines during dynamic exercise in healthy males. *Journal of Applied Physiology.* **59**(4), pp.1033-1039.

Fontes, M.S., van Veen, T.A., de Bakker, J.M. and van Rijen, H.V. 2012. Functional consequences of abnormal Cx43 expression in the heart. *Biochimica et Biophysica Acta (BBA)-Biomembranes.* **1818**(8), pp.2020-2029.

Francis Stuart, S.D., Wang, L., Woodard, W.R., Ng, G.A., Habecker, B.A. and Ripplinger, C.M. 2018. Age-related changes in cardiac electrophysiology and calcium handling in response to sympathetic nerve stimulation. *The Journal of physiology.* **596**(17), pp.3977-3991.

Fu, Y.-C., Chen, R., Chen, M.-Y., Chen, Y., Wang, Y.-L., Xu, B., Yang, J., Yin, T. and Li, Y. 2013. Age-related changes in transient outward potassium current of rat ventricular myocyte. *Sheng li xue bao:[Acta Physiologica Sinica].* **65**(2), pp.185-192.

Fujimoto, N., Hastings, J.L., Bhella, P.S., Shibata, S., Gandhi, N.K., Carrick-Ranson, G., Palmer, D. and Levine, B.D. 2012. Effect of ageing on left ventricular compliance and distensibility in healthy sedentary humans. *The Journal of physiology.* **590**(8), pp.1871-1880.

Fujisawa, S., Ono, K. and Iijima, T. 2000. Time-dependent block of the slowly activating delayed rectifier K+ current by chromanol 293B in guinea-pig ventricular cells. *British journal of pharmacology.* **129**(5), pp.1007-1013.

Fujita, T., Umemura, M., Yokoyama, U., Okumura, S. and Ishikawa, Y. 2017. The role of Epac in the heart. *Cellular and molecular life sciences.* **74**(4), pp.591-606.

Gadsby, D.C. 1983. β-Adrenoceptor agonists increase membrane K+ conductance in cardiac Purkinje fibres. *Nature.* **306**(5944), pp.691-693.

Gambardella, J., Trimarco, B., Iaccarino, G. and Santulli, G. 2017. New Insights in Cardiac Calcium Handling and Excitation-Contraction Coupling.

Gan, T.-Y., Qiao, W., Xu, G.-J., Zhou, X.-H., Tang, B.-P., Song, J.G., Li, Y.-D., Zhang, J., Li, F.-P. and Mao, T. 2013. Aging-associated changes in L-type calcium channels in the left atria of dogs. *Experimental and therapeutic medicine.* **6**(4), pp.919-924.

Garcia, M.I. and Boehning, D. 2017. Cardiac inositol 1, 4, 5-trisphosphate receptors. *Biochimica et Biophysica Acta (BBA)-Molecular Cell Research.* **1864**(6), pp.907-914.

Gattoni, S., Røe, Å.T., Frisk, M., Louch, W.E., Niederer, S.A. and Smith, N.P. 2016. The calcium–frequency response in the rat ventricular myocyte: an experimental and modelling study. *The Journal of physiology.* **594**(15), pp.4193-4224.

Geelen, P., Drolet, B., Lessard, E., Gilbert, P., O'Hara, G.E. and Turgeon, J. 1999. Concomitant block of the rapid (IKr) and slow (IKs) components of the delayed rectifier potassium current is associated with additional drug effects on lengthening of cardiac repolarization. *Journal of Cardiovascular Pharmacology and Therapeutics.* **4**(3), pp.143-150.

Giovannitti Jr, J.A., Thoms, S.M. and Crawford, J.J. 2015. Alpha-2 adrenergic receptor agonists: a review of current clinical applications. *Anesthesia progress.* **62**(1), pp.31-38.

Golf, S., Løvstad, R. and Hansson, V. 1985. β-adrenoceptor density and relative number of β-adrenoceptor subtypes in biopsies from human right atrial, left ventricular, and right ventricular myocard. *Cardiovascular research.* **19**(10), pp.636-641.

Gordan, R., Gwathmey, J.K. and Xie, L.-H. 2015. Autonomic and endocrine control of cardiovascular function. *World journal of cardiology.* **7**(4), p204.

Grant, A.O. 2009. Cardiac ion channels. *Circulation: Arrhythmia and Electrophysiology.* **2**(2), pp.185-194.

Grunnet, M. 2010. Repolarization of the cardiac action potential. Does an increase in repolarization capacity constitute a new anti-arrhythmic principle? *Acta physiologica.* **198**, pp.1-48.

Guerard, N., Traebert, M., Suter, W. and Dumotier, B. 2008. Selective block of IKs plays a significant role in MAP triangulation induced by IKr block in isolated rabbit heart. *Journal of pharmacological and toxicological methods.* **58**(1), pp.32-40.

Haissaguerre, M., Vigmond, E., Stuyvers, B., Hocini, M. and Bernus, O. 2016. Ventricular arrhythmias and the His–Purkinje system. *Nature Reviews Cardiology.* **13**(3), p155.

Han, S., Bal, N.B., Sadi, G., Usanmaz, S.E., Uludag, M.O. and Demirel-Yilmaz, E. 2018. The effects of resveratrol and exercise on age and gender-dependent alterations of vascular functions and biomarkers. *Experimental gerontology.* **110**, pp.191-201.

Harding, S., Vescovo, G., Kirby, M., Jones, S., Gurden, J. and Poole-Wilson, P. 1988. Contractile responses of isolated adult rat and rabbit cardiac myocytes to isoproterenol and calcium. *Journal of molecular and cellular cardiology.* **20**(7), pp.635-647.

Hardy, M.E., Pervolaraki, E., Bernus, O. and White, E. 2018. Dynamic action potential restitution contributes to mechanical restitution in right ventricular myocytes from pulmonary hypertensive rats. *Frontiers in physiology.* **9**, p205.

Harmati, G., Banyasz, T., Barandi, L., Szentandrassy, N., Horvath, B., Szabo, G., Szentmiklosi, J., Szenasi, G., Nanasi, P. and Magyar, J. 2011. Effects of β-adrenoceptor stimulation on delayed rectifier K+ currents in canine ventricular cardiomyocytes. *British journal of pharmacology.* **162**(4), pp.890-896.

Harvey, R.D. and Belevych, A.E. 2003. Muscarinic regulation of cardiac ion channels. *British journal of pharmacology.* **139**(6), pp.1074-1084.

He, Y., Pan, Q., Li, J., Chen, H., Zhou, Q., Hong, K., Brugada, R., Perez, G.J., Brugada, P. and Chen, Y.-H. 2008. Kir2. 3 knock-down decreases IK1 current in neonatal rat cardiomyocytes. *FEBS letters.* **582**(15), pp.2338-2342.

Heath, B. and Terrar, D. 2000. Protein kinase C enhances the rapidly activating delayed rectifier potassium current, IKr, through a reduction in C-type inactivation in guinea-pig ventricular myocytes. *The Journal of Physiology.* **522**(3), pp.391-402.

Heijman, J., Volders, P.G., Westra, R.L. and Rudy, Y. 2011. Local control of β-adrenergic stimulation: effects on ventricular myocyte electrophysiology and Ca2+-transient. *Journal of molecular and cellular cardiology.* **50**(5), pp.863-871.

Herraiz, A., Alvarez, J., Molina, C., Llach, A., Fernandes, J., Ferrero, A., Padro, J., Martinez-Gonzalez, J., Cinca, J. and Hove-Madsen, L. 2013. Ageing causes a progressive loss of L-type calcium current and a depression of the SR calcium content linked to lower SERCA2 and calsequestrin-2 expression in human atrial myocytes. *European Heart Journal.* **34**(suppl_1).

Himmel, H.M., Wettwer, E., Li, Q. and Ravens, U. 1999. Four different components contribute to outward current in rat ventricular myocytes. *American Journal of Physiology-Heart and Circulatory Physiology.* **277**(1), pp.H107-H118.

Hodgkin, A.L. and Huxley, A.F. 1952a. The components of membrane conductance in the giant axon of Loligo. *The Journal of physiology.* **116**(4), pp.473-496.

Hodgkin, A.L. and Huxley, A.F. 1952b. Currents carried by sodium and potassium ions through the membrane of the giant axon of Loligo. *The Journal of physiology.* **116**(4), pp.449-472.

Hodgkin, A.L. and Huxley, A.F. 1952c. The dual effect of membrane potential on sodium conductance in the giant axon of Loligo. *The Journal of physiology.* **116**(4), pp.497-506.

Hodgkin, A.L. and Huxley, A.F. 1952. Propagation of electrical signals along giant nerve fibres. *Proceedings of the Royal Society of London. Series B-Biological Sciences.* **140**(899), pp.177-183.

Hodgkin, A.L. and Huxley, A.F. 1952. A quantitative description of membrane current and its application to conduction and excitation in nerve. *The Journal of physiology.* **117**(4), pp.500-544.

Hong, T.-T., Smyth, J.W., Gao, D., Chu, K.Y., Vogan, J.M., Fong, T.S., Jensen, B.C., Colecraft, H.M. and Shaw, R.M. 2010. BIN1 localizes the L-type calcium channel to cardiac T-tubules. *PLoS biology.* **8**(2), pe1000312.

Howlett, L.A., Kirton, H.M., Al-Owais, M.M., Steele, D. and Lancaster, M.K. 2022. Action potential responses to changes in stimulation frequency and isoproterenol in rat ventricular myocytes. *Physiological Reports.* **10**(2), pe15166.

Howlett, L.A. and Lancaster, M.K. 2021. Reduced cardiac response to the adrenergic system is a key limiting factor for physical capacity in old age. *Experimental Gerontology.* p111339.

Howlett, S.E., Grandy, S.A. and Ferrier, G.R. 2006. Calcium spark properties in ventricular myocytes are altered in aged mice. *American Journal of Physiology-Heart and Circulatory Physiology.* **290**(4), pp.H1566-H1574.

Huang, C.-k., Chen, B.-y., Guo, A., Chen, R., Zhu, Y.-q., Kutschke, W., Hong, J. and Song, L.-s. 2016. Sildenafil ameliorates left ventricular T-tubule remodeling in a pressure overload-induced murine heart failure model. *Acta Pharmacologica Sinica.* **37**(4), p473.

Huang, C., Ding, W., Li, L. and Zhao, D. 2006. Differences in the aging-associated trends of the monophasic action potential duration and effective refractory period of the right and left atria of the rat. *Circulation Journal.* **70**(3), pp.352-357.

Huang, X., Yang, P., Du, Y., Zhang, J. and Ma, A. 2007. Age-related down-regulation of HCN channels in rat sinoatrial node. *Basic research in cardiology.* **102**(5), pp.429-435.

Janczewski, A., Spurgeon, H. and Lakatta, E. 2002. Action potential prolongation in cardiac myocytes of old rats is an adaptation to sustain youthful intracellular Ca2+ regulation. *Journal of molecular and cellular cardiology.* **34**(6), p641.

Jeevaratnam, K., Chadda, K.R., Huang, C.L.-H. and Camm, A.J. 2018. Cardiac potassium channels: physiological insights for targeted therapy. *Journal of cardiovascular pharmacology and therapeutics.* **23**(2), pp.119-129.

Jeevaratnam, K., Chadda, K.R., Salvage, S.C., Valli, H., Ahmad, S., Grace, A.A. and Huang, C.L.H. 2017. Ion channels, long QT syndrome and arrhythmogenesis in ageing. *Clinical and Experimental Pharmacology and Physiology.* **44**, pp.38-45.

Jiang, M.-t. and Narayanan, N. 1990. Effects of aging on phospholamban phosphorylation and calcium transport in rat cardiac sarcoplasmic reticulum. *Mechanisms of ageing and development.* **54**(1), pp.87-101.

Jiang, M.T., Moffat, M.P. and Narayanan, N. 1993. Age-related alterations in the phosphorylation of sarcoplasmic reticulum and myofibrillar proteins and diminished contractile response to isoproterenol in intact rat ventricle. *Circulation research.* **72**(1), pp.102-111.

Johnson, W., Katugampola, S., Able, S., Napier, C. and Harding, S. 2012. Profiling of cAMP and cGMP phosphodiesterases in isolated ventricular cardiomyocytes from human hearts: comparison with rat and guinea pig. *Life sciences.* **90**(9-10), pp.328-336.

Jones, S.A., Boyett, M.R. and Lancaster, M.K. 2007. Declining into failure: the age-dependent loss of the L-type calcium channel within the sinoatrial node. *Circulation.* **115**(10), pp.1183-1190.

Jones, S.A., Lancaster, M.K. and Boyett, M.R. 2004. Ageing-related changes of connexins and conduction within the sinoatrial node. *The Journal of physiology.* **560**(2), pp.429-437.

Josephson, I., Sanchez-Chapula, J. and Brown, A. 1984. Early outward current in rat single ventricular cells. *Circulation Research.* **54**(2), pp.157-162.

Josephson, I.R., Guia, A., Stern, M.D. and Lakatta, E.G. 2002. Alterations in properties of L-type Ca channels in aging rat heart. *Journal of molecular and cellular cardiology.* **34**(3), pp.297-308.

Jost, N., Papp, J.G. and Varró, A. 2007. Slow delayed rectifier potassium current (IKs) and the repolarization reserve. *Annals of Noninvasive Electrocardiology.* **12**(1), pp.64-78.

Jost, N., Virág, L., Bitay, M., Takács, J., Lengyel, C., Biliczki, P., Nagy, Z., Bogáts, G., Lathrop, D.A. and Papp, J.G. 2005. Restricting excessive cardiac action potential and QT prolongation: a vital role for I Ks in human ventricular muscle. *Circulation.* **112**(10), pp.1392-1399.

Joukar, S. 2021. A comparative review on heart ion channels, action potentials and electrocardiogram in rodents and human: extrapolation of experimental insights to clinic. *Laboratory Animal Research.* **37**(1), pp.1-15.

Jourdon, P. and Feuvray, D. 1993. Calcium and potassium currents in ventricular myocytes isolated from diabetic rats. *The Journal of Physiology.* **470**(1), pp.411-429.

Jullien, T., Cand, F., Fargier, C. and Verdetti, J. 1989. Age-dependent differences in energetic status, electrical and mechanical performance of rat myocardium. *Mechanisms of ageing and development.* **48**(3), pp.243-254.

Kamada, R., Yokoshiki, H., Mitsuyama, H., Watanabe, M., Mizukami, K., Tenma, T., Takahashi, M., Takada, S. and Anzai, T. 2019. Arrhythmogenic β-adrenergic signaling in cardiac hypertrophy: The role of small-conductance calcium-activated potassium channels via activation of CaMKII. *European journal of pharmacology.* **844**, pp.110-117.

Kang, C., Badiceanu, A., Brennan, J., Gloschat, C., Qiao, Y., Trayanova, N. and Efimov, I. 2017. β-adrenergic stimulation augments transmural dispersion of repolarization via modulation of delayed rectifier currents I Ks and I Kr in the human ventricle. *Scientific reports.* **7**(1), p15922.

Katsube, Y., Yokoshiki, H., Nguyen, L. and Sperelakis, N. 1996. Differences in isoproterenol stimulation of Ca2+ current of rat ventricular myocytes in neonatal compared to adult. *European journal of pharmacology.* **317**(2-3), pp.391-400.

Keating, M.T., Sanguinetti, M.C. and Splawski, I. 2001. *Mutations in the KCNE1 gene encoding human minK which cause arrhythmia susceptibility thereby establishing KCNE1 as an LQT gene*. Google Patents.

Keller, K.M. and Howlett, S.E. 2016. Sex differences in the biology and pathology of the aging heart. *Canadian Journal of Cardiology.* **32**(9), pp.1065-1073.

Kilborn, M. and Fedida, D. 1990. A study of the developmental changes in outward currents of rat ventricular myocytes. *The Journal of physiology.* **430**(1), pp.37-60.

King, J.H., Huang, C.L. and Fraser, J.A. 2013. Determinants of myocardial conduction velocity: implications for arrhythmogenesis. *Frontiers in physiology.* **4**, p154.

Koch, W.J., Rockman, H.A., Samama, P., Hamilton, R., Bond, R.A., Milano, C.A. and Lefkowitz, R.J. 1995. Cardiac function in mice overexpressing the beta-adrenergic receptor kinase or a beta ARK inhibitor. *Science.* **268**(5215), pp.1350-1353.

Kong, C.H., Rog-Zielinska, E.A., Kohl, P., Orchard, C.H. and Cannell, M.B. 2018. Solute movement in the t-tubule system of rabbit and mouse cardiomyocytes. *Proceedings of the National Academy of Sciences.* **115**(30), pp.E7073-E7080.

Korhonen, T., Hänninen, S.L. and Tavi, P. 2009. Model of excitation-contraction coupling of rat neonatal ventricular myocytes. *Biophysical journal.* **96**(3), pp.1189-1209.

Koumi, S.-i., Backer, C.L., Arentzen, C.E. and Sato, R. 1995. beta-Adrenergic modulation of the inwardly rectifying potassium channel in isolated human ventricular myocytes. Alteration in channel response to beta-adrenergic stimulation in failing human hearts. *The Journal of clinical investigation.* **96**(6), pp.2870-2881.

Kuschel, M., Zhou, Y.-Y., Cheng, H., Zhang, S.-J., Chen, Y., Lakatta, E.G. and Xiao, R.-P. 1999. Gi protein-mediated functional compartmentalization of cardiac β2-adrenergic signaling. *Journal of Biological Chemistry.* **274**(31), pp.22048-22052.

Kwak, S.K. and Kim, J.H. 2017. Statistical data preparation: management of missing values and outliers. *Korean journal of anesthesiology.* **70**(4), pp.407-411.

Lakatta, E.G. 1993. Cardiovascular regulatory mechanisms in advanced age. *Physiological reviews.* **73**(2), pp.413-467.

Lakatta, E.G., Maltsev, V.A. and Vinogradova, T.M. 2010. A coupled SYSTEM of intracellular Ca2+ clocks and surface membrane voltage clocks controls the timekeeping mechanism of the heart's pacemaker. *Circulation research.* **106**(4), pp.659-673.

Lakatta, E.G. and Sollott, S.J. 2002. Perspectives on mammalian cardiovascular aging: humans to molecules. *Comparative Biochemistry and Physiology Part A: Molecular & Integrative Physiology.* **132**(4), pp.699-721.

Larson, E.D., Clair, J.R.S., Sumner, W.A., Bannister, R.A. and Proenza, C. 2013. Depressed pacemaker activity of sinoatrial node myocytes contributes to the age-dependent decline in maximum heart rate. *Proceedings of the National Academy of Sciences.* **110**(44), pp.18011-18016.

Layland, J., Solaro, R.J. and Shah, A.M. 2005. Regulation of cardiac contractile function by troponin I phosphorylation. *Cardiovascular research.* **66**(1), pp.12-21.

Leosco, D., Rengo, G., Iaccarino, G., Filippelli, A., Lymperopoulos, A., Zincarelli, C., Fortunato, F., Golino, L., Marchese, M. and Esposito, G. 2008. Exercise training and-blocker treatment ameliorate age-dependent impairment of-adrenergic receptor

signaling and enhance cardiac responsiveness to adrenergic stimulation. *Cardiovasc Res.* **78**(2), pp.385-394.

Li, J., McLerie, M. and Lopatin, A.N. 2004. Transgenic upregulation of I K1 in the mouse heart leads to multiple abnormalities of cardiac excitability. *American Journal of Physiology-Heart and Circulatory Physiology.* **287**(6), pp.H2790-H2802.

Liao, H., Li, Y. and Brooks, G. 2016. Outlier impact and accommodation methods: Multiple comparisons of Type I error rates. *Journal of Modern Applied Statistical Methods.* **15**(1), p23.

Lim, C.C., Liao, R., Varma, N. and Apstein, C.S. 1999. Impaired lusitropy-frequency in the aging mouse: role of Ca2+-handling proteins and effects of isoproterenol. *American Journal of Physiology-Heart and Circulatory Physiology.* **277**(5), pp.H2083-H2090.

Liu, D.-W., Gintant, G.A. and Antzelevitch, C. 1993. Ionic bases for electrophysiological distinctions among epicardial, midmyocardial, and endocardial myocytes from the free wall of the canine left ventricle. *Circulation research.* **72**(3), pp.671-687.

Liu, D. and Antzelevitch, C. 1995. Characteristics of the delayed rectifier current (IKr and IKs) in canine ventricular epicardial, midmyocardial, and endocardial myocytes. A weaker IKs contributes to the longer action potential of the M cell. *Circulation research.* **76**(3), pp.351-365.

Liu, J., Sirenko, S., Juhaszova, M., Sollott, S.J., Shukla, S., Yaniv, Y. and Lakatta, E.G. 2014. Age-associated abnormalities of intrinsic automaticity of sinoatrial nodal cells are linked to deficient cAMP-PKA-Ca2+ signaling. *American Journal of Physiology-Heart and Circulatory Physiology.* **306**(10), pp.H1385-H1397.

Liu, S.J., Wyeth, R.P., Melchert, R.B. and Kennedy, R.H. 2000. Aging-associated changes in whole cell K+ and L-type Ca2+ currents in rat ventricular myocytes. *American Journal of Physiology-Heart and Circulatory Physiology.* **279**(3), pp.H889-H900.

Liu, W., Yasui, K., Arai, A., Kamiya, K., Cheng, J., Kodama, I. and Toyama, J. 1999. β-Adrenergic modulation of L-type Ca2+-channel currents in early-stage embryonic mouse heart. *American Journal of Physiology-Heart and Circulatory Physiology.* **276**(2), pp.H608-H613.

Madamanchi, A. 2007. β-Adrenergic receptor signaling in cardiac function and heart failure. *McGill Journal of Medicine: MJM.* **10**(2), p99.

Manfra, O., Frisk, M. and Louch, W.E. 2017. Regulation of cardiomyocyte T-tubular structure: opportunities for therapy. *Current heart failure reports.* **14**(3), pp.167-178.

Maron, B.J. and Pelliccia, A. 2006. The heart of trained athletes: cardiac remodeling and the risks of sports, including sudden death. *Circulation.* **114**(15), pp.1633-1644.

Masuda, K., Takanari, H., Morishima, M., Ma, F., Wang, Y., Takahashi, N. and Ono, K. 2018. Testosterone-mediated upregulation of delayed rectifier potassium channel in cardiomyocytes causes abbreviation of QT intervals in rats. *The Journal of Physiological Sciences.* **68**(6), pp.759-767.

Mathers, C.D., Stevens, G.A., Boerma, T., White, R.A. and Tobias, M.I. 2015. Causes of international increases in older age life expectancy. *The Lancet.* **385**(9967), pp.540-548.

Mayourian, J., Ceholski, D.K., Gonzalez, D.M., Cashman, T.J., Sahoo, S., Hajjar, R.J. and Costa, K.D. 2018a. Physiologic, pathologic, and therapeutic paracrine modulation of cardiac excitation-contraction coupling. *Circulation research.* **122**(1), pp.167-183.

Mayourian, J., Sobie, E.A. and Costa, K.D. 2018b. An introduction to computational modeling of cardiac electrophysiology and arrhythmogenicity. *Experimental Models of Cardiovascular Diseases.* Springer, pp.17-35.

McCorry, L.K. 2007. Physiology of the autonomic nervous system. *American journal of pharmaceutical education.* **71**(4), p78.

Meschiari, C.A., Ero, O.K., Pan, H., Finkel, T. and Lindsey, M.L. 2017. The impact of aging on cardiac extracellular matrix. *Geroscience.* **39**(1), pp.7-18.

Meszaros, J., Coutinho, J., Bryant, S., Ryder, K. and Hart, G. 1997. L-type calcium current in catecholamine-induced cardiac hypertrophy in the rat. *Experimental Physiology: Translation and Integration.* **82**(1), pp.71-83.

Milanović, Z., Pantelić, S., Trajković, N., Sporiš, G., Kostić, R. and James, N. 2013. Age-related decrease in physical activity and functional fitness among elderly men and women. *Clinical interventions in aging.* **8**, p549.

Moghtadaei, M., Jansen, H.J., Mackasey, M., Rafferty, S.A., Bogachev, O., Sapp, J.L., Howlett, S.E. and Rose, R.A. 2016. The impacts of age and frailty on heart rate and sinoatrial node function. *The Journal of physiology.* **594**(23), pp.7105-7126.

Molina, C.E., Heijman, J. and Dobrev, D. 2016. Differences in left versus right ventricular electrophysiological properties in cardiac dysfunction and arrhythmogenesis. *Arrhythmia & electrophysiology review.* **5**(1), p14.

Morganroth, J., Maron, B.J., Henry, W.L. and Epstein, S.E. 1975. Comparative left ventricular dimensions in trained athletes. *Annals of internal medicine.* **82**(4), pp.521-524.

Najafi, A., Sequeira, V., Kuster, D.W. and van der Velden, J. 2016. β-adrenergic receptor signalling and its functional consequences in the diseased heart. *European journal of clinical investigation.* **46**(4), pp.362-374.

Nakano, S.J., Sucharov, J., Van Dusen, R., Cecil, M., Nunley, K., Wickers, S., Karimpur-Fard, A., Stauffer, B.L., Miyamoto, S.D. and Sucharov, C.C. 2017. Cardiac adenylyl cyclase and phosphodiesterase expression profiles vary by age, disease, and chronic phosphodiesterase inhibitor treatment. *Journal of cardiac failure.* **23**(1), pp.72-80.

Nakou, E., Parthenakis, F., Kallergis, E., Marketou, M., Nakos, K. and Vardas, P. 2016. Healthy aging and myocardium: A complicated process with various effects in cardiac structure and physiology. *International journal of cardiology.* **209**, pp.167-175.

Narayanan, N. and Derby, J.-A. 1982. Alterations in the properties of β-adrenergic receptors of myocardial membranes in aging: Impairments in agonist—receptor interactions and guanine nucleotide regulation accompany diminished catecholamine-responsiveness of adenylated cyclase. *Mechanisms of ageing and development.* **19**(2), pp.127-139.

Narayanan, N. and Tuckler, L. 1986. Autonomic interactions in the aging heart: age-associated decrease in muscarinic cholinergic receptor mediated inhibition of β-adrenergic activation of adenylate cyclase. *Mechanisms of ageing and development.* **34**(3), pp.249-259.

Natali, A., Wilson, L., Peckham, M., Turner, D., Harrison, S. and White, E. 2002. Different regional effects of voluntary exercise on the mechanical and electrical properties of rat ventricular myocytes. *The Journal of physiology.* **541**(3), pp.863-875.

Navaratnarajah, A. and Jackson, S.H. 2017. The physiology of ageing. *Medicine.* **45**(1), pp.6-10.

Niccoli, T. and Partridge, L. 2012. Ageing as a risk factor for disease. *Current biology.* **22**(17), pp.R741-R752.

Niederer, S. and Smith, N. 2012. At the heart of computational modelling. *The Journal of physiology.* **590**(6), pp.1331-1338.

Niederer, S.A., Lumens, J. and Trayanova, N.A. 2019. Computational models in cardiology. *Nature Reviews Cardiology.* **16**(2), pp.100-111.

Nio, A.Q., Stöhr, E.J. and Shave, R.E. 2017. Age-related differences in left ventricular structure and function between healthy men and women. *Climacteric.* **20**(5), pp.476-483.

Nishimura, M., Ocorr, K., Bodmer, R. and Cartry, J. 2011. Drosophila as a model to study cardiac aging. *Experimental gerontology.* **46**(5), pp.326-330.

Noble, D. 1962. A modification of the Hodgkin—Huxley equations applicable to Purkinje fibre action and pacemaker potentials. *The Journal of physiology.* **160**(2), pp.317-352.

O'Connell, T.D., Jensen, B.C., Baker, A.J. and Simpson, P.C. 2014. Cardiac alpha1-adrenergic receptors: novel aspects of expression, signaling mechanisms, physiologic function, and clinical importance. *Pharmacological reviews.* **66**(1), pp.308-333.

Ocorr, K., Reeves, N.L., Wessells, R.J., Fink, M., Chen, H.-S.V., Akasaka, T., Yasuda, S., Metzger, J.M., Giles, W. and Posakony, J.W. 2007. KCNQ potassium channel mutations cause cardiac arrhythmias in Drosophila that mimic the effects of aging. *Proceedings of the National Academy of Sciences.* **104**(10), pp.3943-3948.

Ogawa, T., Spina, R.J., Martin 3rd, W., Kohrt, W.M., Schechtman, K.B., Holloszy, J.O. and Ehsani, A.A. 1992. Effects of aging, sex, and physical training on cardiovascular responses to exercise. *Circulation.* **86**(2), pp.494-503.

Olgar, Y., Durak, A., Bitirim, C.V., Tuncay, E. and Turan, B. 2022. Insulin acts as an atypical KCNQ1/KCNE1-current activator and reverses long QT in insulin-resistant aged rats by accelerating the ventricular action potential repolarization through affecting the β3-adrenergic receptor signaling pathway. *Journal of Cellular Physiology.* **237**(2), pp.1353-1371.

Pan, B., Xu, Z., Xu, Y., Liu, L., Zhu, J., Wang, X., Nan, C., Zhang, Z., Shen, W. and Huang, X. 2016. Diastolic dysfunction and cardiac troponin I decrease in aging hearts. *Archives of biochemistry and biophysics.* **603**, pp.20-28.

Pandit, S.V., Clark, R.B., Giles, W.R. and Demir, S.S. 2001. A mathematical model of action potential heterogeneity in adult rat left ventricular myocytes. *Biophysical journal.* **81**(6), pp.3029-3051.

Parashar, R., Amir, M., Pakhare, A., Rathi, P. and Chaudhary, L. 2016. Age related changes in autonomic functions. *Journal of clinical and diagnostic research: JCDR.* **10**(3), pCC11.

Pare, G.C., Bauman, A.L., McHenry, M., Michel, J.J.C., Dodge-Kafka, K.L. and Kapiloff, M.S. 2005. The mAKAP complex participates in the induction of cardiac myocyte hypertrophy by adrenergic receptor signaling. *Journal of cell science.* **118**(23), pp.5637-5646.

Pathmanathan, P. and Gray, R.A. 2018. Validation and trustworthiness of multiscale models of cardiac electrophysiology. *Frontiers in Physiology.* **9**, p106.

Penner, R. 1995. A practical guide to patch clamping. *Single-channel recording.* Springer, pp.3-30.

Pinnell, J., Turner, S. and Howell, S. 2007. Cardiac muscle physiology. *BJA Education.* **7**(3), pp.85-88.

Pluim, B.M., Zwinderman, A.H., van der Laarse, A. and van der Wall, E.E. 2000. The athlete's heart: a meta-analysis of cardiac structure and function. *Circulation.* **101**(3), pp.336-344.

Pond, A.L., Scheve, B.K., Benedict, A.T., Petrecca, K., Van Wagoner, D.R., Shrier, A. and Nerbonne, J.M. 2000. Expression of distinct ERG proteins in rat, mouse, and human heart: relation to functional I Kr channels. *Journal of Biological Chemistry.* **275**(8), pp.5997-6006.

Rabkin, S.W., Cheng, X.-B.J. and Thompson, D.J. 2016. Detailed analysis of the impact of age on the QT interval. *Journal of geriatric cardiology: JGC.* **13**(9), p740.

Rajagopal, S. and Shenoy, S.K. 2018. GPCR desensitization: acute and prolonged phases. *Cellular signalling.* **41**, pp.9-16.

Randall, M. 2017. Overview of the UK population: July 2017. *UK Office for National Statistics (July 2017).*

Ravens, U. and Cerbai, E. 2008. Role of potassium currents in cardiac arrhythmias. *Europace.* **10**(10), pp.1133-1137.

Ravens, U. and Wettwer, E. 1998. Electrophysiological aspects of changes in heart rate. *Basic Research in Cardiology.* **93**(1), pp.s060-s065.

Reardon, M. and Malik, M. 1996. QT interval change with age in an overtly healthy older population. *Clinical Cardiology.* **19**(12), pp.949-952.

Regan, C.P., Cresswell, H.K., Zhang, R. and Lynch, J.J. 2005. Novel method to assess cardiac electrophysiology in the rat: characterization of standard ion channel blockers. *Journal of cardiovascular pharmacology.* **46**(1), pp.68-75.

Rengo, G., Perrone-Filardi, P., Femminella, G.D., Liccardo, D., Zincarelli, C., De Lucia, C., Pagano, G., Marsico, F., Lymperopoulos, A. and Leosco, D. 2012.

Targeting the β-Adrenergic Receptor System Through G-Protein–Coupled Receptor Kinase 2: A New Paradigm for Therapy and Prognostic Evaluation in Heart Failure: From Bench to Bedside. *Circulation: Heart Failure.* **5**(3), pp.385-391.

Rikli, R.E. and Jones, C.J. 1998. The reliability and validity of a 6-minute walk test as a measure of physical endurance in older adults. *Journal of aging and physical activity.* **6**(4), pp.363-375.

Roberts, B.N., Yang, P.-C., Behrens, S.B., Moreno, J.D. and Clancy, C.E. 2012. Computational approaches to understand cardiac electrophysiology and arrhythmias. *American Journal of Physiology-Heart and Circulatory Physiology.* **303**(7), pp.H766-H783.

Rochais, F., Vandecasteele, G., Lefebvre, F., Lugnier, C., Lum, H., Mazet, J.-L., Cooper, D.M. and Fischmeister, R. 2004. Negative feedback exerted by cAMP-dependent protein kinase and cAMP phosphodiesterase on subsarcolemmal cAMP signals in intact cardiac myocytes an in vivo study using adenovirus-mediated expression of cng channels. *Journal of Biological Chemistry.* **279**(50), pp.52095-52105.

Rodeheffer, R.J., Gerstenblith, G., Becker, L.C., Fleg, J.L., Weisfeldt, M.L. and Lakatta, E.G. 1984. Exercise cardiac output is maintained with advancing age in healthy human subjects: cardiac dilatation and increased stroke volume compensate for a diminished heart rate. *Circulation.* **69**(2), pp.203-213.

Roh, J., Rhee, J., Chaudhari, V. and Rosenzweig, A. 2016. The Role of Exercise in Cardiac Aging: From Physiology to Molecular Mechanisms. *Circulation research.* **118**(2), pp.279-295.

Saeed, Y., Temple, I.P., Borbas, Z., Atkinson, A., Yanni, J., Maczewski, M., Mackiewicz, U., Aly, M., Logantha, S.J.R. and Garratt, C.J. 2018. Structural and functional remodeling of the atrioventricular node with aging in rats: The role of hyperpolarization-activated cyclic nucleotide–gated and ryanodine 2 channels. *Heart rhythm.* **15**(5), pp.752-760.

Sakatani, T., Shirayama, T., Yamamoto, T., Mani, H., Shiraishi, H. and Matsubara, H. 2006. Cardiac hypertrophy diminished the effects of isoproterenol on delayed rectifier potassium current in rat heart. *The Journal of Physiological Sciences.* **56**(2), pp.173-181.

Sakmann, B. and Neher, E. 1984. Patch clamp techniques for studying ionic channels in excitable membranes. *Annual review of physiology.* **46**(1), pp.455-472.

Sala, L., Hegyi, B., Bartolucci, C., Altomare, C., Rocchetti, M., Váczi, K., Mostacciuolo, G., Szentandrássy, N., Severi, S. and Pál Nánási, P. 2017. Action potential contour contributes to species differences in repolarization response to β-adrenergic stimulation. *EP Europace.*

Sampson, K.J. and Kass, R.S. 2010. Molecular mechanisms of adrenergic stimulation in the heart. *Heart Rhythm.* **7**(8), pp.1151-1153.

Sankaranarayanan, R., Kistamás, K., Greensmith, D.J., Venetucci, L.A. and Eisner, D.A. 2017. Systolic [Ca2+] i regulates diastolic levels in rat ventricular myocytes. *The Journal of physiology.* **595**(16), pp.5545-5555.

Sankaranarayanan, R., Li, Y., Greensmith, D.J., Eisner, D.A. and Venetucci, L. 2016. Biphasic decay of the Ca transient results from increased sarcoplasmic reticulum Ca leak. *The Journal of physiology.* **594**(3), pp.611-623.

Santulli, G. and Iaccarino, G. 2013. Pinpointing beta adrenergic receptor in ageing pathophysiology: victim or executioner? Evidence from crime scenes. *Immunity & Ageing.* **10**(1), p10.

Santulli, G. and Iaccarino, G. 2016. Adrenergic signaling in heart failure and cardiovascular aging. *Maturitas.* **93**, pp.65-72.

Saucerman, J.J., Brunton, L.L., Michailova, A.P. and McCulloch, A.D. 2003. Modeling β-adrenergic control of cardiac myocyte contractility in silico. *Journal of Biological Chemistry.* **278**(48), pp.47997-48003.

Saucerman, J.J. and McCulloch, A.D. 2006. Cardiac β-Adrenergic Signaling: From Subcellular Microdomains to Heart Failure. *Annals of the New York Academy of Sciences.* **1080**(1), pp.348-361.

Scamps, F., Mayoux, E., Charlemagne, D. and Vassort, G. 1990. Calcium current in single cells isolated from normal and hypertrophied rat heart. Effects of beta-adrenergic stimulation. *Circulation Research.* **67**(1), pp.199-208.

Scarpace, P.J., Turner, N. and Mader, S.L. 1991. β-Adrenergic function in aging. *Drugs & aging.* **1**(2), pp.116-129.

Şengül Ayan, S., Sırcan, A.K., Abewa, M., Kurt, A., Dalaman, U. and Yaraş, N. 2020. Mathematical model of the ventricular action potential and effects of isoproterenol-induced cardiac hypertrophy in rats. *European Biophysics Journal.* **49**, pp.323-342.

Shigematsu, S., Kiyosue, T., Sato, T. and Arita, M. 1997. Rate-dependent prolongation of action potential duration in isolated rat ventricular myocytes. *Basic research in cardiology.* **92**(3), pp.123-128.

Shimizu, I. and Minamino, T. 2016. Physiological and pathological cardiac hypertrophy. *Journal of molecular and cellular cardiology.* **97**, pp.245-262.

Skeberdis, V.A. 2004. Structure and function of β³-adrenergic receptors. *Medicina.* **40**(5), pp.407-413.

Slack, J., Grupp, I., Dash, R., Holder, D., Schmidt, A., Gerst, M., Tamura, T., Tilgmann, C., James, P. and Johnson, R. 2001. The enhanced contractility of the phospholamban-deficient mouse heart persists with aging. *Journal of molecular and cellular cardiology.* **33**(5), pp.1031-1040.

Sorrentino, A., Signore, S., Qanud, K., Borghetti, G., Meo, M., Cannata, A., Zhou, Y., Wybieralska, E., Luciani, M. and Kannappan, R. 2016. Myocyte repolarization modulates myocardial function in aging dogs. *American Journal of Physiology-Heart and Circulatory Physiology.* **310**(7), pp.H873-H890.

Spadari, R.C., Cavadas, C., de Carvalho, A.E.T.S., Ortolani, D., de Moura, A.L. and Vassalo, P.F. 2018. Role of beta-adrenergic receptors and sirtuin signaling in the heart during aging, heart failure, and adaptation to stress. *Cellular and molecular neurobiology.* pp.1-12.

Spina, R.J., Turner, M.J. and Ehsani, A.A. 1998. β-Adrenergic-mediated improvement in left ventricular function by exercise training in older men. *American Journal of Physiology-Heart and Circulatory Physiology.* **274**(2), pp.H397-H404.

Steenman, M. and Lande, G. 2017. Cardiac aging and heart disease in humans. *Biophysical reviews.* **9**(2), pp.131-137.

Stevenson-Cocks, H.J. 2019. *Biophysical modelling of rat cardiac electrophysiology and calcium handling*. thesis, University of Leeds.

Strait, J.B. and Lakatta, E.G. 2012. Aging-associated cardiovascular changes and their relationship to heart failure. *Heart failure clinics.* **8**(1), pp.143-164.

Stratton, J.R., Cerqueira, M.D., Schwartz, R.S., Levy, W.C., Veith, R., Kahn, S.E. and Abrass, I.B. 1992. Differences in cardiovascular responses to isoproterenol in relation to age and exercise training in healthy men. *Circulation.* **86**(2), pp.504-512.

Stratton, J.R., Levy, W.C., Caldwell, J.H., Jacobson, A., May, J., Dale Matsuoka, C. and Madden, K. 2003. Effects of Aging on Cardiovascular Responses to Parasympathetic Withdrawal. *age.* **41**, pp.2077-2083.

Stratton, J.R., Levy, W.C., Cerqueira, M.D., Schwartz, R.S. and Abrass, I.B. 1994. Cardiovascular responses to exercise. Effects of aging and exercise training in healthy men. *Circulation.* **89**(4), pp.1648-1655.

Stuart, S.D.F., Wang, L., Woodard, W.R., Ng, G.A., Habecker, B.A. and Ripplinger, C.M. 2018. Age-related changes in cardiac electrophysiology and calcium handling in response to sympathetic nerve stimulation. *The Journal of physiology.* **596**(17), pp.3977-3991.

Sun, Z.Q., Thomas, G.P. and Antzelevitch, C. 2001. Chromanol 293B inhibits slowly activating delayed rectifier and transient outward currents in canine left ventricular myocytes. *Journal of cardiovascular electrophysiology.* **12**(4), pp.472-478.

Tanaka, H. and Seals, D.R. 2008. Endurance exercise performance in Masters athletes: age-associated changes and underlying physiological mechanisms. *The Journal of physiology.* **586**(1), pp.55-63.

Tande, P.M., Bjørnstad, H., Yang, T. and Refsum, H. 1990. Rate-dependent class III antiarrhythmic action, negative chronotropy, and positive inotropy of a novel Ik blocking drug, UK-68,798: potent in guinea pig but no effect in rat myocardium. *Journal of cardiovascular pharmacology.* **16**(3), pp.401-410.

Tellez, J.O., Mączewski, M., Yanni, J., Sutyagin, P., Mackiewicz, U., Atkinson, A., Inada, S., Beresewicz, A., Billeter, R. and Dobrzynski, H. 2011. Ageing-dependent remodelling of ion channel and Ca2+ clock genes underlying sino-atrial node pacemaking. *Experimental physiology.* **96**(11), pp.1163-1178.

Terrenoire, C., Clancy, C.E., Cormier, J.W., Sampson, K.J. and Kass, R.S. 2005. Autonomic control of cardiac action potentials: role of potassium channel kinetics in response to sympathetic stimulation. *Circulation research.* **96**(5), pp.e25-e34.

Tobise, K., Ishikawa, Y., Holmer, S.R., Im, M.-J., Newell, J.B., Yoshie, H., Fujita, M., Susannie, E.E. and Homcy, C.J. 1994. Changes in type VI adenylyl cyclase isoform expression correlate with a decreased capacity for cAMP generation in the aging ventricle. *Circulation research.* **74**(4), pp.596-603.

Trial, J. and Cieslik, K.A. 2018. Changes in cardiac resident fibroblast physiology and phenotype in aging. *American Journal of Physiology-Heart and Circulatory Physiology.*

Ungerer, M., Böhm, M., Elce, J., Erdmann, E. and Lohse, M. 1993. Altered expression of beta-adrenergic receptor kinase and beta 1-adrenergic receptors in the failing human heart. *Circulation.* **87**(2), pp.454-463.

van der Heyden, M.A., Wijnhoven, T.J. and Opthof, T. 2006. Molecular aspects of adrenergic modulation of the transient outward current. *Cardiovascular research.* **71**(3), pp.430-442.

Varró, A., Lathrop, D., Hester, S., Nanasi, P. and Papp, J. 1993. Ionic currents and action potentials in rabbit, rat, and guinea pig ventricular myocytes. *Basic research in cardiology*. **88**(2), pp.93-102.

Varshneya, M., Devenyi, R.A. and Sobie, E.A. 2018. Slow delayed rectifier current protects ventricular myocytes from arrhythmic dynamics across multiple species: a computational study. *Circulation: Arrhythmia and Electrophysiology*. **11**(10), pe006558.

Verkerk, A.O., Geuzebroek, G.S., Veldkamp, M.W. and Wilders, R. 2012. Effects of acetylcholine and noradrenalin on action potentials of isolated rabbit sinoatrial and atrial myocytes. *Frontiers in Physiology*. **3**, p174.

Vincent, J.-L. 2008. Understanding cardiac output. *Critical Care*. **12**, p174.

Vizgirda, V.M., Wahler, G.M., Sondgeroth, K.L., Ziolo, M.T. and Schwertz, D.W. 2002. Mechanisms of sex differences in rat cardiac myocyte response to β-adrenergic stimulation. *American Journal of Physiology-Heart and Circulatory Physiology*. **282**(1), pp.H256-H263.

Volders, P.G., Stengl, M., van Opstal, J.M., Gerlach, U., Spätjens, R.L., Beekman, J.D., Sipido, K.R. and Vos, M.A. 2003. Probing the contribution of I Ks to canine ventricular repolarization: key role for β-adrenergic receptor stimulation. *Circulation*. **107**(21), pp.2753-2760.

Wachter, S.B. and Gilbert, E.M. 2012. Beta-adrenergic receptors, from their discovery and characterization through their manipulation to beneficial clinical application. *Cardiology*. **122**(2), pp.104-112.

Wahler, G.M. 1992. Developmental increases in the inwardly rectifying potassium current of rat ventricular myocytes. *American Journal of Physiology-Cell Physiology*. **262**(5), pp.C1266-C1272.

Waldeyer, C., Fabritz, L., Fortmueller, L., Gerss, J., Damke, D., Blana, A., Laakmann, S., Kreienkamp, N., Volkery, D. and Breithardt, G. 2009. Regional, age-dependent, and genotype-dependent differences in ventricular action potential duration and activation time in 410 Langendorff-perfused mouse hearts. *Basic research in cardiology*. **104**(5), pp.523-533.

Walker, K., Lakatta, E. and Houser, S. 1993. Age associated changes in membrane currents in rat ventricular myocytes. *Cardiovascular research*. **27**(11), pp.1968-1977.

Walton, R.D., Jones, S.A., Rostron, K.A., Kayani, A.C., Close, G.L., McArdle, A. and Lancaster, M.K. 2015. Interactions of short-term and chronic treadmill training with

aging of the left ventricle of the heart. *Journals of Gerontology Series A: Biomedical Sciences and Medical Sciences.* **71**(8), pp.1005-1013.

Wang, H.-w., Yang, Z.-f., Zhang, Y., Yang, J.-m., Liu, Y.-m. and Li, C.-z. 2009. Beta-receptor activation increases sodium current in guinea pig heart. *Acta Pharmacologica Sinica.* **30**(8), pp.1115-1122.

Wang, X. and Fitts, R.H. 2017. Ventricular action potential adaptation to regular exercise: role of β-adrenergic and KATP channel function. *Journal of Applied Physiology.* **123**(2), pp.285-296.

Wang, X. and Fitts, R.H. 2020. Cardiomyocyte Slowly Activating Delayed Rectifier Potassium Channel: Regulation by Exercise and β-Adrenergic Signaling. *Journal of Applied Physiology.*

Watanabe, T., Delbridge, L.M., Bustamante, J.O. and McDonald, T.F. 1983. Heterogeneity of the action potential in isolated rat ventricular myocytes and tissue. *Circulation Research.* **52**(3), pp.280-290.

Wei, J.Y., Spurgeon, H.A. and Lakatta, E.G. 1984. Excitation-contraction in rat myocardium: alterations with adult aging. *American Journal of Physiology-Heart and Circulatory Physiology.* **246**(6), pp.H784-H791.

Wei, X., Yohannan, S. and Richards, J.R. 2020. Physiology, Cardiac Repolarization Dispersion and Reserve. *StatPearls [Internet]*.

Weiner, R.B. and Baggish, A.L. 2012. Exercise-induced cardiac remodeling. *Progress in cardiovascular diseases.* **54**(5), pp.380-386.

Welsh, T.M., Kukes, G.D. and Sandweiss, L.M. 2002. Differences of creatine kinase MB and cardiac troponin I concentrations in normal and diseased human myocardium. *Annals of Clinical & Laboratory Science.* **32**(1), pp.44-49.

Wessells, R.J. and Bodmer, R. 2007. Cardiac aging. In: *Seminars in cell & developmental biology*: Elsevier, pp.111-116.

White, M., Roden, R., Minobe, W., Khan, M., Larrabee, P., Wollmering, M., Port, J., Anderson, F., Campbell, D. and Feldman, A. 1994. Age-related changes in beta-adrenergic neuroeffector systems in the human heart. *Circulation.* **90**(3), pp.1225-1238.

Wilkins, E., Wilson, L., Wickramasinghe, K., Bhatnagar, P., Leal, J., Luengo-Fernandez, R., Burns, R., Rayner, M. and Townsend, N. 2017. European cardiovascular disease statistics 2017.

Winslow, R.L., Trayanova, N., Geman, D. and Miller, M.I. 2012. Computational medicine: translating models to clinical care. *Science translational medicine.* **4**(158), pp.158rv111-158rv111.

Wisløff, U., Loennechen, J.P., Falck, G., Beisvag, V., Currie, S., Smith, G. and Ellingsen, Ø. 2001. Increased contractility and calcium sensitivity in cardiac myocytes isolated from endurance trained rats. *Cardiovascular research.* **50**(3), pp.495-508.

Wittenberg, R., Hu, B. and Hancock, R. 2018. Projections of demand and expenditure on adult social care 2015 to 2040.

Xiao, R.-P., Spurgeon, H.A., O'connor, F. and Lakatta, E.G. 1994. Age-associated changes in beta-adrenergic modulation on rat cardiac excitation-contraction coupling. *The Journal of clinical investigation.* **94**(5), pp.2051-2059.

Xiao, R.-P., Tomhave, E.D., Wang, D.-J., Ji, X., Boluyt, M.O., Cheng, H., Lakatta, E.G. and Koch, W.J. 1998. Age-associated reductions in cardiac beta1-and beta2-adrenergic responses without changes in inhibitory G proteins or receptor kinases. *The Journal of clinical investigation.* **101**(6), pp.1273-1282.

Xu, A. and Narayanan, N. 1998. Effects of aging on sarcoplasmic reticulum Ca2+-cycling proteins and their phosphorylation in rat myocardium. *American Journal of Physiology-Heart and Circulatory Physiology.* **275**(6), pp.H2087-H2094.

Xu, H., Zhao, M., Liang, S., Huang, Q., Xiao, Y., Ye, L., Wang, Q., He, L., Ma, L. and Zhang, H. 2016. The effects of puerarin on rat ventricular myocytes and the potential mechanism. *Scientific reports.* **6**(1), pp.1-11.

Yang, H.-Q., Subbotina, E., Ramasamy, R. and Coetzee, W.A. 2016. Cardiovascular KATP channels and advanced aging. *Pathobiology of Aging & Age-related Diseases.* **6**(1), p32517.

Yang, J.H. and Saucerman, J.J. 2011. Computational models reduce complexity and accelerate insight into cardiac signaling networks. *Circulation research.* **108**(1), pp.85-97.

Yang, K.-C. and Nerbonne, J.M. 2016. Mechanisms contributing to myocardial potassium channel diversity, regulation and remodeling. *Trends in cardiovascular medicine.* **26**(3), pp.209-218.

Yang, T., Kanki, H. and Roden, D.M. 2003. Phosphorylation of the I Ks channel complex inhibits drug block: novel mechanism underlying variable antiarrhythmic drug actions. *Circulation.* **108**(2), pp.132-134.

Zhang, Q., Huang, A., Lin, Y.-C. and Yu, H.-G. 2009. Associated changes in HCN2 and HCN4 transcripts and If pacemaker current in myocytes. *Biochimica et Biophysica Acta (BBA)-Biomembranes.* **1788**(5), pp.1138-1147.

Zhengrong, H., Weihua, L. and Qiang, X. 2011. Studies on ionic mechanisms of the effects of isoproterenol on Brugada syndrome. *Heart.* **97**(Suppl 3), pp.A35-A35.

Zhou, K. and Hong, T. 2017. Cardiac BIN1 (cBIN1) is a regulator of cardiac contractile function and an emerging biomarker of heart muscle health. *Sci China Life Sci.* **60**, pp.257-263.

Zhou, Y.-Y., Lakatta, E.G. and Xiao, R.-P. 1998. Age-associated alterations in calcium current and its modulation in cardiac myocytes. *Drugs & aging.* **13**(2), pp.159-171.

Zhu, X., Altschafl, B.A., Hajjar, R.J., Valdivia, H.H. and Schmidt, U. 2005. Altered Ca2+ sparks and gating properties of ryanodine receptors in aging cardiomyocytes. *Cell Calcium.* **37**(6), pp.583-591.

Zou, S., Qiu, S., Su, S., Zhang, J., Sun, J., Wang, Y., Shi, C. and Xu, Y. 2021. Inhibitory G-protein–mediated modulation of slow delayed rectifier potassium channels contributes to increased susceptibility to arrhythmogenesis in aging heart. *Heart Rhythm.* **18**(12), pp.2197-2209.

Zouhal, H., Jacob, C., Delamarche, P. and Gratas-Delamarche, A. 2008. Catecholamines and the effects of exercise, training and gender. *Sports medicine.* **38**(5), pp.401-423.